SYNTHESIS AND CHARACTERIZATION OF NOVEL COPOLYMERS

A THESIS SUBMITTED TO THE

UNIVERSITY OF PUNE

FOR THE DEGREE OF

DOCTOR OF PHILOSOPHY

IN

CHEMISTRY

BY

PRERANA M. PATIL

POLYMER SCIENCE AND ENGINEERING DIVISION

NATIONAL CHEMICAL LABORATORY

PUNE 411 008, INDIA

DECEMBER 2009

CERTIFICATE

This is to certify that the work incorporated in the thesis entitled "Synthesis and characterization of novel copolymers" submitted by Ms. Prerana M. Patil was carried out under my supervision. Such material as has been obtained from other sources has been duly acknowledged in the thesis.

Date: 8/12/2009   **Dr. M. G. Kulkarni**

National Chemical Laboratory,   **(Research Guide)**

Pune 411008.

DECLARATION

I hereby declare that the thesis entitled **"Synthesis and characterization of novel copolymers"** submitted for Ph. D. degree to the University of Pune has been carried out under the supervision of **Dr. M. G. Kulkarni** at the Division of Polymer Science and Engineering, National Chemical Laboratory, Pune, India. The work is original and has not been submitted in part or full by me for any degree or diploma to this or any other University.

Date: 8/12/2009   **(Prerana M. Patil)**

National Chemical Laboratory,   **(Research Student)**

Pune 411008.

Acknowledgements

First and foremost, I would like to thank my research guide Dr. M. G. Kulkarni (Head, PSE). He gave me the opportunity to learn his approach to science and the value of pursuing important questions. I am very thankful to him for his valuable guidance in presentation skills and technical writing.

It is my pleasure to acknowledge Dr. S. Sivaram, Director, NCL, for permitting me to present this work in form of thesis.

I am grateful to Dr. G. N. Sastry and Mr. M. Nagaraju for their help for Molecular modeling simulation. My sincere thanks go to Dr. Rajmohanan, Mr. Thakar, Dr. Badiger and Dr. G. V. N. Rathna.

This page would be incomplete without the mention of my lab-mates who extended help throughout the tenure of my work at NCL. I thank them for useful scientific discussions and for being good teammates. I would like to thank Mr. Dhavale and Mr. Mahajan for all the help rendered by them.

Completion of this thesis would not have been possible without the support, faith and liberty to pursue career, bestowed by my husband, Umesh.

Finally, I thank my family, especially my parents. I find no words to express my feelings for their unconditional support and freedom for career. Their patience and sacrifice will remain my inspiration throughout my life. The infallible love and support offered by my brother, sister, niece and brother-in-law have always been my strength.

Prerana M. Patil

8/12/2009

Table of Contents

Chapter 6

Inclusion complexes of multivinyl monomers : Synthesis and characterization

List of Figures

Chapter 6

Inclusion complexes of hydrophilic crosslinkers : Synthesis and characterization

Chapter 7

Biodegradable nanogels for sustained and targeted release of macromolecular drugs

List of Tables

List of Schemes

Abbreviations and Symbols

AA	Acrylic acid
ACl	Acryloyl chloride
Aerosol-T	Sodium bis-2-ethylhexylsulfosuccinate (AOT)
AIBN	2, 2' Azo bis iso butyro nitrile
AM	Acrylamide
AMSD	Alpha methyl styrene dimer
AFCT	Addition fragmentation chain transfer
β - CD	β - Cyclodextrin
$CDCl_3$	Deuterated chloroform
CTA	Chain transfer agent
$CHCl_3$	Chloroform
Cys	L-cysteine
DMF	N, N' dimethyl formamide
D_2O	Deuterium oxide
$DMSOd_6$	Deuterated dimethyl sulfoxide
DM - β - CD	Dimethylated beta cyclodextrin
DMAEMA	2,. – dimethyl amino ethyl methacrylate
DSC	Differential scanning calorimetry
DSDMA	bis(2-methacryloyloxyethyl) disulfide
DTT	2, 3 dihydroxy 1, 4-butanethiol or dithiothreitol
DRS	Diffused reflectance spectroscopy
FITC-Dx	fluorescein isothiocyanate conjugated dextran
f	Functionality
FTIR	Fourier transform infra red spectroscopy
GPC	Gel permeation chromatography
GSH	Glutathione tripeptide (g-glutamyl-cysteinyl-glycine)
GSSG	glutathione disulfide
HEMA	2 – hydroxyl ethyl methacrylate
IC	Inclusion complex
MA	Methacrylic acid
MeCl	Methacryloyl chloride
MeOH	Methanol
MMA	Methyl methacrylate
M_n	Number average molecular weight
M_w	Weight average molecular weight
NaAMPS	2 – acrylamido 2 – methyl propane sulphonic acid sodium salt
NaSSA	Styrene sulphonic acid sodium salt
NMR	Nuclear magnetic resonance spectroscopy
NVP	N – vinyl pyrrolidone
N – 2 HPAM	N – 2 hydroxy propyl methacrylamide
N – 3 HPAM	N – 3 hydroxy propyl methacrylamide
P(AA)	Poly(acrylic acid)

P(AM)	Poly(acrylamide)
PD	Polydispersity
P(DMAEMA)	Poly(2 – dimethyl amino ethyl methacrylate)
P(DMA-co-NVP)	Poly(disulfide dimethacrylate-co-N vinyl pyrrolidone)
P(NaAMPS)	Poly(2 – acrylamido 2 – methyl propane sulphonic acid sodium salt)
P(NaSSA)	Poly(Styrene sulphonic acid sodium salt)
P(N– 2 HPAM)	Poly(N – 2 hydroxy propyl methacrylamide)
P(N– 3 HPAM)	Poly(N – 3 hydroxy propyl methacrylamide)
P(NVP)	Poly(N – vinyl pyrrolidone)
P(MA)	Poly(methacrylic acid)
P(MBAM-co-NVP)	Poly(methylene bisacrylamide-co-N-vinyl pyrrolidone)
P(STY)	Poly(styrene)
P(VP)	Poly(4 – vinyl pyridine)
$K_2S_2O_8$	Potassium persulphate
RES	Reticulo endothelial system
STY	Styrene
TEMED	N, N, N', N'' tetramethyl ethylenediamine
4 – VP	4 – vinyl pyridine
V 50	2, 2' azo bis amidino propane dihydrochloride
VPO	Vapour pressure osmometer
W_s	Weight of swollen polymer
W_d	Weight of dry polymer
XRD	X – ray diffraction

Chapter 1
Thesis Overview

1.1 Introduction

A variety of approaches for the synthesis of polymer architectures such as block, graft, star polymers and dendrimers are being developed by researchers in view of distinctive properties offered by these materials *vis a vis* random copolymers (Wohlrab et. al. 2001, Ito et. al. 1983). Graft copolymers containing hydrophobic and hydrophilic micro domains exhibit a variety of morphologies such as micelles and vesicles, which as carriers improve solubility, stability and bioavailability of drugs (Lo et. al. 2007). They are also used as compatibilizer to improve the mechanical properties of the polymers and as stabilizers during the synthesis of microspheres and microreactors.

For the synthesis of graft copolymers 'Grafting through' which involves the copolymerization of macromonomers with vinyl monomers is preferred over generating a radical on the polymer backbone followed by grafting the vinyl monomer on the backbone (Joshi et. al. 2007). Macromonomers can be prepared by a two step synthesis involving polymerization in the presence of functional initiators and functional chain transfer agents followed by the condensation of a methacryloyl unit with the end group (Yamashita et. al. 1982, Akashi et. al. 1989). A single step synthesis is obviously desirable.

Hydrogels are another class of materials which have applications in personal hygiene products, drug delivery, sensors etc. Generally these are prepared by copolymerization of water soluble monomers in the presence of crosslinkers such as methylene bis acrylamide (MBAM) and glutaraldehyde. It is known that traces of these unreacted monomers and crosslinkers left in the product are toxic and therefore the biological applications of these polymers are restricted. The unreacted monomer and crosslinker need to be removed completely from the gel network in an independent step.

Stimuli-responsive polymers, which undergo dissolution / degradation in response to environmental changes have been extensively investigated for biomedical applications especially in drug delivery. The stimulus could be pH (Hruby et. al. 2005, Lang et. al. 2006), UV light irradiation frequency (Ozlem et. al. 2004), temperature (Junya et. al. 2005) and reducing agent concentration (Zelikin et. al. 2006, Kakizawa et. al. 2001).

Biodegradable polymers in general and hydrogels in particular are widely used in a wide variety of therapeutic applications including tissue engineering (Langer and Vacanti 1993, Cohen 1993) and pharmaceutical applications such as controlled drug release (Kwon et. al. 2007, Peppas et. al. 1999, Vinogradov et. al. 2002). Gels can be degraded when crosslinked with degradable agents. The disulfide group is an example of biodegradable group which can be cleaved in the presence of reducing agents such as nucleophiles, electrophiles or photochemically. Some of the examples of reducing agent are dithiothreitol (DTT), glutathione (GSH), L-cysteine (Cys) and so on (Kakizawa Y. et. al. 1999, Li et. al. 2006, Lees et. al. 1993, Hisano et. al. 1998).

Reduction-sensitive biodegradable polymers are characterized by an excellent stability in the circulation and in extracellular fluids, whereas they undergo rapid degradation under a reductive environment present in intracellular compartments. The large difference in glutathione concentration between the intracellular and extracellular milieu can be exploited for triggered intracellular delivery of a variety of bioactive molecules. These polymers can be synthesized by incorporating disulfide linkage in the main chain, at the side chain or in the cross-linker.

This research describes two classes of water soluble copolymers synthesized using supramolecular chemistry of cyclodextrin. The graft copolymers of the first group comprise hydrophilic and / or hydrophobic grafts and pH sensitive segments. These copolymers exhibit pH dependent slow dissolution as compared to random copolymers of identical composition which dissolve instantaneously. The copolymers were synthesized from the macromonomers containing terminal unsaturation which in turn were obtained by the polymerization of monomers in the presence of host-guest complexes of cyclodextrin (CD) and α methyl styrene dimer (AMSD) which retained addition fragmentation chain transfer activity of the latter.

The copolymers of the second group are water soluble comprising pendant unsaturation and can be subsequently crosslinked either thermally or photochemically to obtain hydrogels. These copolymers were obtained from the inclusion complex (IC) of the crosslinker containing disulfide bonds where the complexation allows the polymerization of only one vinyl unsaturation while the other remains encapsulated

inside the CD cavity. In the second stage, the pendant unsaturation was crosslinked to obtain drug loaded nanogels. As the copolymers used for crosslinking are free from any unreacted monomer and crosslinker, the monomer and crosslinker toxicity can be avoided. Yields of drug loaded nanogels are enhanced and the release profile can be manipulated by the concentration of the disulfide containing crosslinker and reducing agent.

CD forms host – guest complexes with a variety of organic compounds and polymers. CD is a cyclic oligosaccharide composed of six (α), seven (β) or eight (γ) glucopyranose ring units, which are joined together through α (1–4) linkage forming torus shaped ring structure (Ritter and Tabatabai 2002). The primary hydroxyl groups of glucose ring are exterior to the cavity, which make it soluble in water whereas the hydrophobic interior cavity facilitates the formation of an inclusion complex by hydrophobic interactions. The ability of CD to form IC and hence suppression of the reactivity has been exploited in highly selective organic synthetic procedures. However, controlling the reactivity of the addition fragmentation chain transfer (AFCT) agent and crosslinker is not yet reported.

AFCT is being explored for the synthesis of macromonomers in view of the high reactivity of the chain transfer agents towards propagating radicals. Amongst various AFCT agents based on oligomers of α methyl vinyl monomers, AMSD has been found to be particularly efficient (Yamada et. al. 2004). Since AMSD is hydrophobic, the technique is primarily restricted to macromonomers soluble in organic solvents. Thus, there is a need to synthesize either new water–soluble AFCT agent, which can impart terminal unsaturation or to modify the existing AFCT agents so that they can be used in polymerizations in aqueous media. Prior research efforts (Hirano 2003, McHale 2005) reveal that incorporation of bulkier substituents in the monomer as well as the chain transfer agent results in higher addition fragmentation efficiency and enhanced terminal unsaturation content.

If AMSD formed an IC with CD derivatives, the increase in steric hindrance would lead to enhanced addition fragmentation efficiency and macromonomers of methyl methacrylate (MMA) having terminal unsaturation could be obtained. Further, if the IC

were water soluble, it could be further used to synthesize water–soluble macromonomers. We found that inclusion complexation of AMSD with β–CD leads to increase in addition fragmentation chain transfer efficiency during the polymerization of MMA. Further, complexation with dimethylated β–cyclodextrin (DM–β–CD) enhanced the solubility of AMSD in water and enabled the synthesis of macromonomers of 2-dimethyl amino ethyl methacrylate (DMAEMA), acrylamide (AM), N–vinyl pyrrolidone (NVP) and methacrylic acid (MAA) in aqueous medium. The macromonomers were further copolymerized with pH sensitive monomers to yield graft copolymers.

The control of the reactivity of divinyl monomers so as to form water soluble polymers comprising pendant unsaturation through inclusion complexation of CD is not yet reported in the literature. Ritter et. al. have reported the CD inclusion complexes to enhance the solubility of hydrophobic molecules or as emulsifier in the emulsion polymerization of acrylates.

In the present investigation, CD ICs were used to control the reactivity of the crosslinker during polymerization to yield water soluble copolymers comprising pendant unsaturation. Crosslinker forms an inclusion complex with the cyclodextrin so that only one unsaturation site is exposed to polymerization while other remains entrapped in the cavity yielding water–soluble polymers. The polymerization of crosslinkers with vinyl monomers through supramolecular inclusion complex approach enables removing the traces of the unreacted crosslinkers in the first stage i.e. prior to crosslinking. The water–soluble copolymers obtained by this approach contain pendant unsaturation which can be used to yield drug loaded nanogels. When biodegradable crosslinker are used for the synthesis of nanogels it gives burst release of drug in the presence of reducing agent; otherwise it gives the sustained release. The release can be manipulated by the concentration of the crosslinker and reducing agent.

The chapter 2 highlights the objective and scope of the work carried out. The main objective of this study was to synthesize graft copolymers obtained from terminally unsaturated macromonomers and water soluble copolymers comprising pendant unsaturation exploiting supramolecular chemistry of CD.

For aqueous systems, AFCT agents which yield terminally unsaturated macromonomer in a single step are not yet reported. The literature review revealed that thiol functionalized macromonomers were synthesized in the first step which had then to be thermolyzed in the second step to obtain terminally unsaturated macromonomers. Hence, new water soluble AFCT agents which can yield terminally unsaturated macromonomers in a single step need to be developed. Alternatively, solubility of the existing AFCT agents in water has to be enhanced.

The objective of this study was to synthesize inclusion complex of AMSD with DM–β-CD which enhances its water solubility and enables its application in aqueous system to yield water soluble macromonomers in a single step. Yet another objective of the investigation was to synthesize macromonomers which have functionality ('*f*') close to unity and copolymerize with pH sensitive monomers to yield pH sensitive graft copolymers.

Incorporation of bulkier substituents in the side chain enhances the addition fragmentation chain transfer efficiency of 2–substituted 1–allyl compounds. An objective of the study was also to study the influence of the complexation on the addition fragmentation chain transfer activity of AMSD during polymerization of MMA and to synthesize terminally unsaturated poly(MMA) macromonomers having '*f*' close to unity. These macromonomers were further copolymerized to obtain pH sensitive graft copolymers.

The traces of unreacted toxic crosslinker in the gel network restrict its use in biological applications such as drug delivery and enzyme immobilization. Thus, there is a need for a polymeric matrix which will be soluble in the first stage and can be crosslinked in the subsequent step. This has been achieved through inclusion complexation of the crosslinkers using cyclodextrin. It is possible to get rid off unreacted toxic crosslinker after polymerization is completed. The inclusion complexation of the crosslinker results in encapsulation of one of the vinyl unsaturation in CD cavity and hence suppresses its polymerization. Thus, IC comprising crosslinker and CD behaves as a monovinyl monomer and leads to water soluble polymer comprising pendant unsaturation. The

polymer containing pendant unsaturation further could be used to entrap drug or enzyme and then crosslinked to yield macro / nano particles.

In view of the abovementionted limitations of the synthetic methodologies, the objectives of the proposed research work were

1. Synthesis of AMSD–β–CD and AMSD–DM–β–CD complexes and their characterization using techniques such as FTIR, NMR, TGA and molecular modeling

2. Chain transfer constant and functionality ('f') evaluation for AMSD, AMSD–β–CD and AMSD–DM–β–CD during the polymerization of MMA

3. Synthesis of Poly (MMA) macromonomer having 'f' close to unity and composition determination by ^{1}H NMR

4. Copolymerization of Poly(MMA) macromonomer with pH sensitive vinyl monomers to yield graft copolymers

5. Chain transfer constant and 'f' evaluation for AMSD–DM–β–CD during the polymerization of DMAEMA, AM, NVP and MAA in aqueous medium

6. Synthesis of water–soluble macromonomers having 'f' close to unity viz: Poly(DMAEMA), Poly(AM), Poly(NVP) and Poly(MAA) using AMSD–DM–β–CD complex and their characterization for terminal unsaturation content by ^{1}H NMR

7. Copolymerization of Poly(AM), Poly(NVP) with pH sensitive vinyl monomers to yield graft copolymers

8. Synthesis of inclusion complexes of crosslinker and their characterization by FTIR, NMR, XRD and molecular modeling

9. Synthesis of copolymers containing pendant unsaturation from crosslinker inclusion complexes, their composition determination and thermal / photopolymerization

10. Evaluation of copolymers containing pendant unsaturation for drug encapsulation

The chapter 3 starts with a discussion on mechanism of AFCT, reaction conditions and the parameters affecting the addition fragmentation efficiency. Substitution is known to enhance the addition fragmentation chain transfer activity of 2-substituted 1-allyl

compounds. To evaluate the influence of the steric hindrance caused by CD on addition fragmentation chain transfer activity, AMSD was complexed with β-CD and DM-β-CD. AMSD forms a complex with β-CD and DM–β-CD as confirmed by various analytical techniques and molecular modeling simulations. The synthesis of AMSD–β-CD and AMSD-DM–β-CD IC and their structural characterization is discussed. The effect of steric hindrance on addition fragmentation chain transfer is discussed in chapter 4.

In FTIR analysis, OH stretching of the glucose ring of CD showed a shift of -21 cm^{-1} (3370 to 3349 cm^{-1}) in AMSD-β-CD IC whereas in AMSD-DM–β-CD IC it was -24 cm^{-1} (3408 to 3384 cm^{-1}). The shift towards lower value indicated the disruption of intramolecular hydrogen bonding in native β-CD (C_2-OH group of one glucopyranoside unit forms a hydrogen bond with C_3-OH group of adjacent glucopyranose unit) and hence the insertion of AMSD inside the CD cavity.

^{1}H NMR analysis confirms that the stoichiometry of the complex is 1:1 and also that the two methyl groups of the cumyl ring of AMSD are in different environment. 500 MHz ^{1}H NMR of AMSD-β-CD and AMSD-DM–β-CD in D_2O showed peak splitting for methyl protons of AMSD due to its inclusion inside the CD cavity. The separation for methyl signals was 24 Hz in case of AMSD-DM–β-CD while it was 3.9 Hz in case of AMSD-β–CD. The higher magnitude of separation in case of AMSD-DM–β-CD was attributed to the stronger complexation as compared to that in β-CD. The stability of both the ICs in D_2O was evaluated by NMR which showed that the separation between the methyl groups decreased from 19 to 8.1 Hz in case of AMSD-DM–β-CD as the temperature was raised from room temperature to 90°C whereas the methyl signal yielded a single peak at 35°C in AMSD-β-CD IC. Thus, AMSD-DM–β-CD IC is more stable compared to inclusion complex comprising AMSD and β-CD.

Molecular modeling analysis revealed that cumyl ring of AMSD is inside the CD cavity in case of both the complexes. Deeper insertion of the allyl group was seen in case of AMSD–β-CD IC than AMSD-DM–β-CD IC. It also confirmed that the stoichiometry of the IC was 1:1.

The decrease in chain transfer activity of AFCT agent (AMSD) during free radical polymerization has been demonstrated in the chapter 4. The substitution enhances the

addition fragmentation efficiency of AFCT agent in a manner similar to that observed in case of oligomers. In this chapter, the effect of complexation with β–CD and DM–β–CD on the chain transfer constant of AMSD during the polymerization of MMA was evaluated.

Inclusion complexation decreases the chain transfer constant and enhances the addition fragmentation chain transfer efficiency due to the steric hindrance rendered by the CD cavity. The chain transfer constants for AMSD, AMSD–β–CD and AMSD–DM–β–CD IC in the polymerization of MMA in N, N' dimethyl formamide were calculated using Mayo's method. The chain transfer activity of AMSD decreased after complexation.

The chain transfer constants were in the order AMSD > AMSD–β–CD > AMSD–DM–β–CD which was due to the limited availability of allylic CH_2 for fragmentation after complexation. The functionality '*f*' close to unity was obtained using AMSD-β–CD IC which was attributed to the enhanced steric hindrance caused by the β–CD cavity as compared to DM–β–CD which increased its fragmentation rate. The enhanced steric hindrance in AMSD-β–CD IC was due to the deeper insertion of the allyl group of AMSD inside β–CD cavity as compared to DM–β-CD cavity. In the formation of terminally unsaturated macromonomers the addition fragmentation chain transfer dominated over disproportionation and combination.

The chapter 5 describes the chain transfer activity of AMSD–DM–β–CD complex in aqueous polymerization. For aqueous systems, AFCT agents which yield terminally unsaturated macromonomer in a single step are not yet reported. Hence, new water-soluble AFCT agents need to be developed. Alternatively, solubility of the existing AFCT agents in water has to be enhanced. In the earlier chapter, we showed that the solubility of AMSD in water is enhanced after complexation with DM–β-CD.

In chapter 5, we evaluated the use of AMSD-DM–β-CD IC as AFCT agent in the synthesis of water-soluble macromonomers (WSM). This approach presents a method for the synthesis of terminally unsaturated water-soluble macromonomers which have been used in the synthesis of comb copolymers. The advantage of this approach was that the macromonomers were synthesized in a single step. The chain transfer constants

and functionality '*f*' for 2-dimethyl aminoethyl methacrylate (DMAEMA), acrylamide (AM), N-vinyl pyrrolidone (NVP) and methacrylic acid (MAA) were evaluated using Mayo's method. The chain transfer constant decreased in the order DMAEMA>NVP>AM>MAA and was attributed to the relative reactivity of the propagating radical with the monomer and the inclusion complex.

The highest '*f*' value (1.05) was obtained for Poly(DMAEMA) where captodative effect plays an important role in AFCT mechanism. Due to high fragmentation rate of AMSD in DMAEMA, very low molecular weight macromonomers having '*f*' value close to unity were obtained. As fragmentation rate increased with temperature; '*f*' values tended to unity at higher temperature for all macromonomers. Thus, by a judicious choice of AMSD concentration and temperature, macromonomers having functionality close to unity could be obtained. The kinetic analysis of all the macromonomers showed that the polymerization takes place in a controlled manner. Poly(NVP) and Poly(AM) macromonomers were used to synthesize the graft copolymers with pH sensitive monomers such as 4 – vinyl pyridine (4 – VP), DMAEMA and MAA. These copolymers exhibited pH dependent slow dissolution as compared to random copolymers of identical composition which dissolved instantaneously.

The inclusion complexes of multivinyl monomers are illustrated in the chapter 6. The prior efforts reported in the literature for synthesis of soluble polymers containing free unsaturation and their advantages and limitations have been described. The aim of the present research work was to control the reactivity of multivinyl monomers via IC mediated polymerization. The synthesis of inclusion complexes of methylene bis acrylamide (MBAM) and disulfide dimethacrylate (DSDMA) by solvent evaporation / precipitation method and characterization by different instrumental methods. The inclusion complexation was also validated by molecular modeling simulation is illustrated.

In the FTIR spectrum of MBAM-β-CD IC, OH peak of CD shifted from 3370 cm^{-1} to 3303.8 cm^{-1}, MBAM–DMCD IC showed the shift from 3413.8 cm^{-1} to 3404 cm^{-1} and DSDMA--β-CD IC showed a shift from 3370 cm^{-1} to 3335cm^{-1}. This indicates the disruption of intramolecular hydrogen bonding in native CD (C$_2$-OH group of one

glucopyranoside unit forms a hydrogen bond with C_3-OH group of adjacent glucopyranose unit) due to the insertion of crosslinker inside the CD cavity. NMR data reveals complex formation in 1:1 ratio. The amorphous nature of the complex was confirmed by XRD which is also reflected in its increased water solubility. The molecular modeling data confirms the encapsulation of one of the double bond of the crosslinker in the CD cavity and formation of the complex in 1:1 ratio.

The synthesis of water soluble copolymers containing pendant unsaturation and their application sustained / burst delivery of macromolecular drug is demonstrated in the chapter 7. The inclusion complexes of the crosslinker were copolymerized to obtain water soluble polymers containing pendant unsaturation. This new method allows the complete removal of the unreacted crosslinker and monomer from the polymer prior to crosslinking.

Biodegradable nanogels ($\sim$ 50 nm diameter) were obtained by crosslinking droplets comprising aqueous solutions of Poly(Methylene bis acrylamide–co–N vinyl pyrrolidone) i.e. Poly(MBAM–co–NVP) and Poly(Disulfide dimethacrylate-co-NVP) i.e. Poly(DSDMA-co-NVP) and fluorescein isothiocyanate conjugated dextran (FITC-Dx) dispersed in n-hexane. The encapsulation efficiency of FITC-Dx as well as yield of the nanogels exceeded 90 % *vis a vis* values of 84 and 25 % reported in the literature for the inverse emulsion technique. FITC-Dx was released from nanogels containing DSDMA in presence of dithiothreitol (DTT) as a result of degradation of the disulfide link and was a function of crosslinker content and DTT concentration. The biodegradable nanogels would find applications for sustained / targeted intracellular delivery of macromolecular drugs.

The chapter 8 concludes and gives recommendations for the further work.

References

1. Wohlrab S. and Kuckling D. J. Polym. Sc. Part A Polymer chemistry **2001**, 39 (21), 3797. (b) Ito K.; Masuda Y.; Shintani T.; Kitano T.; Yamashita Y. Polymer J. **1983**, 15 (6), 443.

2. Lo C.; Huang C.; Lin K.; Hsiue G. Biomaterials **2007**, 28 (6), 1225.

3. Joshi J.; Sinha V. Carbohydrate polymers **2007**, 67 (3), 427.

4. (a) Yamashita Y.; Ito K.; Mizuno H.; Okada K. Polym. J. **1982**, 14, 255. (b) Akashi M.; Yanagi T.; Yashima E. and Miyauchi N. J. Polym. Sc. Part A **1989**, 27 (10), 3521.

5. Hruby M., Konak C., Ulbrich K. J. Controlled Release **2005**, 103, 137.

6. Lang Y., Li M., Pan S., Zheng Y. J. Drug Delivery Sci. Tech. **2006**, 16, 65.

7. Ozlem C., Vasif H. J. Controlled Release **2004**, 96, 85.

8. Junya F., Yasuo Y., Etsuo Y., Katsuhide T. J. Controlled Release **2005**, 102, 49.

9. Zelikin N., Quinn F., Caruso F. Biomacromolecules **2006**, 7, 27.

10. Langer R., Vacanti P., Science **1993**, 260, 920.

11. Cohen S., Bano C., Linda G., Cima G., Allcock R., Vacanti P., Vacanti A., Langer R., Clin. Mater. **1993**, 13, 3.

12. Kwon J., Siegwart D., Lee H., Sherwood G., Peteanu L., Hollinger J., Kataoka K., Matyjaszewski K., J. Am. Chem. Soc. **2007**, 129, 5939.

13. Peppas N., Keys K., Torres-Lugo M., Lowman A., J. Controlled Release **1999**, 62, 81.

14. Kakizawa Y., Harada A., Kataoka K. J. Am. Chem. Soc. **1999**, 121, 11247.

15. Li C., Madsen J., Armes S., Lewis A. Angew. Chem. Int. Ed. **2006**, 45, 3510.

16. Lees W., Whitesides G. J. Org. Chem. **1993**, 58, 642.

17. Ritter H.; Tabatabai M. Prog. Polym. Sci. **2002**, 27, 1713.

18. Yamada B., Oku F., Harada T. J. Polym. Sci. Part A: Polym. Chem. **2003**, 41(5), 645.

19. Hirano T., Yamada B. Polymer **2003**, 44, 347.

20. McHale R., Aldabbagh F., Carroll W., Yamada B. Macromol. Chem. and phy. **2005**, 206, 2054.

Chapter 2

Objectives & Scope of Work

Cyclodextrin (CD) host-guest chemistry has been used in variety of applications in organic chemistry, polymer chemistry, pharmaceutical chemistry, analytical separations, cosmetics and agricultural industry. In organic chemistry, CD has been used to control the reactivity of included guest molecule. In polymer science, CD has been exploited mainly to solubilize the hydrophobic monomers in water and mediate their polymerization in aqueous media.

Addition fragmentation chain transfer (AFCT) is being explored for the synthesis of macromonomers in view of the high reactivity of the chain transfer agents towards propagating radicals. Amongst various AFCT agents based on oligomers of α methyl vinyl monomers, α- methyl styrene dimer (AMSD) has been found to be particularly efficient. Since AMSD is hydrophobic, the technique is primarily restricted to macromonomers soluble in organic solvents. Thus, there is a need to synthesize either new water–soluble AFCT agent, which can impart terminal unsaturation or to modify the existing AFCT agents so that they can be used in polymerizations in aqueous media. Prior research efforts reveal that incorporation of bulkier substituents in the monomer as well as the chain transfer agent results in higher addition fragmentation efficiency and enhanced terminal unsaturation content. However, controlling the reactivity of AFCT agent through inclusion complexation with CD is not yet reported.

Our objective was to estimate the effect of inclusion complexation on the addition fragmentation chain transfer activity of AMSD. Inclusion complexation of AMSD with DM-β-CD would enhance its water solubility. Thus, another objective of the present investigation was to evaluate the utility of AMSD-DM-β-CD inclusion complex for the synthesis of water soluble macromonomers. Yet another objective of the investigation was to synthesize macromonomers which have functionality ('f') close to unity and investigate their copolymerization with pH sensitive monomers to yield pH sensitive graft copolymers.

Generally, gels are prepared by copolymerization of water soluble monomers in the presence of crosslinkers such as methylene bis acrylamide (MBAM) and glutaraldehyde. It is known that residual traces of these unreacted monomers and crosslinkers in the product are toxic and therefore the biomedical applications of these

polymers are restricted. The unreacted monomer and crosslinker need to be removed completely from the gel network in an independent step. This is often cumbersome, time consuming and expensive. Thus, there is a need for a polymeric matrix which will be soluble in the first stage so that it enables the removal of the unreacted crosslinker and can be crosslinked in the subsequent step.

The homo and copolymerization of a divinyl compound usually results in crosslinked polymers because of the uncontrolled or random propagation of the growing radical of both double bonds. Almost, no selective radical polymerization of crosslinker is known. A possible solution for the highly selective polymerization is to alter the reactivity of one of the vinyl groups by either chemical or physical methods.

The soluble polymers containing pendant double bond from ethylene glycol dimethacrylate (EGDMA) have been reported in the literature. However, the control of the reactivity of divinyl monomers so as to form water soluble polymers comprising pendant unsaturation through inclusion complexation of CD is not yet investigated. Our aim was to demonstrate synthesis of such polymers through inclusion complexation of the water soluble crosslinker. The polymer containing pendant unsaturation further could be used to entrap drug or enzyme and then crosslinked to yield nanogels. The copolymerization of N- vinyl pyrrolidone (NVP) with the inclusion complex of the biodegradable crosslinker and further its crosslinking in the presence of macromolecular drugs may lead to the formation of biodegradable nanogels. The nanogels would find applications for sustained / targeted intracellular delivery of macromolecular drugs.

The objectives and scope of the work is described below

I. Inclusion complexes of AFCT agent

- Synthesis of inclusion complex of hydrophobic AFCT agent, AMSD with cyclodextrin
- Structural characterization of the inclusion complex using NMR, XRD and thermal stability measurement by NMR and TGA
- Molecular modeling analysis of inclusion complex to predict the disposition of allyl group of AFCT agent

II.   Effect of complexation on addition fragmentation activity

• Elucidation of the effect of steric hindrance caused by complexation on AFCT activity of AMSD during methyl methacrylate (MMA) polymerization

• Synthesis of P(MMA) macromonomer having functionality '*f*' ~ unity

III. Synthesis of water soluble macromonomers and their graft copolymers

• Synthesis of terminally unsaturated water soluble macromonomers with '*f*' ~ unity viz: (Poly(2- dimethyl aminoethyl methacrylate, Poly(acrylamide), Poly(N-vinyl pyrrolidone), Poly(methacrylic acid)) from inclusion complex of hydrophobic AMSD in aqueous medium

• Copolymerization of the macromonomers with pH sensitive vinyl monomers to synthesize graft copolymers

• Structural characterization of macromonomers and their copolymers using NMR, GPC and DSC

IV. Inclusion complexes of crosslinker

• Synthesis of inclusion complexes of divinyl monomers MBAM, disulfide dimethacrylate (DSDMA) and their detailed characterization to evaluate stoichiometry

• Molecular modeling analysis of inclusion complexes to determine their conformation

V. Synthesis of water-soluble polymers comprising pendant unsaturation and their application in encapsulation of hydrophilic drugs

• Polymerization of inclusion complexes of MBAM and DSDMA with NVP

• Structural validation of the polymers comprising pendant unsaturation by FTIR and NMR.

• Synthesis of FITC-Dx loaded nanogels and their characterization

• Degradation study of the crosslinked polymer and nanogels

• Sustained / burst release study of the drug loaded nanogels

Chapter 3

AMSD inclusion complexes :

Synthesis and characterization

3.1 Introduction

Cyclodextrin (CD) host-guest chemistry has been extensively used in organic, polymer and pharmaceutical chemistry because of its easy availability and complex formation ability with a variety of organic compounds (Szejtli 1998). The physical properties such as solubility, reactivity, stability and volatility of the guest molecule included are modified without affecting its chemical structure.

In polymer chemistry CD has been mainly used to carry out the polymerization of the hydrophobic monomers in water, as a surfactant in emulsion polymerization and to form polymer architectures such as polyrotaxanes or pseudorotaxanes. The solubilization is effected by complexation of the hydrophobic monomers within the hydrophobic cavity of CD. It was found that reactivity ratios of complexed monomer in water differ significantly from those of uncomplexed monomers. Molecular weights of polymers obtained from complexed monomers are higher than those obtained from uncomplexed monomers (Glockner et. al. 1999).

Highly hydrophobic monomers cannot be readily incorporated into the copolymer by emulsion polymerization. The use of a catalytic amount of CD facilitates the incorporation of highly hydrophobic monomers. In this case, CD acts as a phase transport catalyst continuously complexing and solubilizing the hydrophobic monomers and releasing them to the polymer particles (Lau et. al. 2000).

Harada and coworkers (Harada et al., 1996) evaluated the formation of polyrotaxane containing hydrophilic and hydrophobic polymers as well as inorganic polymers either by *insitu* polymerization or by threading of CDs on the preformed polymers. Rusa et al., (2000, 2001) investigated the formation of polyrotaxane between the CD and high molecular weight polymers. The complex formation between the CD and the polymer chain strongly depends on the nature of the polymer i.e. hydrophilic or hydrophobic, molecular weight of the guest polymer, the functional groups on the polymer backbone and the size of the CD cavity (Harada, 1996, Okumura et al., 2000).

The reactivity of the monomers and chain transfer agents is significantly altered on complexation with CD (Glockner et. al. 2000). Kollisch et. al. (2006) reported RAFT polymerization of styrene- dimethylated-β-cyclodextrin (St-DM-β-CD) IC using 3-

Benzyl sulfanyl thiocarbonyl sulfanyl propionic acid as AFCT agent. Incorporation of bulkier substitutents in AFCT agent enhances addition fragmentation efficiency and terminal unsaturation content (Sato et. al. 2004, McHale et. al. 2005). McHale et. al. (2005) described the macromonomer synthesis by polymerization of acrylic acid (AA) and tert-butyl acrylate (tBA) in the presence of the addition fragmentation chain transfer (AFCT) agents, ethyl α-(bromomethyl) acrylate (EBMA) and tert-butyl α-(bromomethyl) acrylate (BBMA). The authors concluded that in case of BBMA addition fragmentation is favored over propagation because of the bulkier of the poly(tBA) main chain. Hirano et. al. (2003) observed that the larger α-substituent of methyl acrylate trimer radical facilitates the β-fragmentation as compared to the methyl acrylate dimer. The greater steric hindrance of α substitutent of the AFCT agent decreases the level of retardation and increases the functionality of the macromonomer (Sato et. al. 2004).

In view of the above investigations, α-methyl styrene dimer- β-cyclodextrin (AMSD–β-CD) and α-methyl styrene dimer- dimethylated-β-cyclodextrin (AMSD-DM-β-CD) inclusion complexes (ICs) were synthesized to evaluate the effect of steric hindrance caused by inclusion complexation on its chain transfer activity. If AMSD formed an IC with CD derivatives, the increase in steric hindrance would lead to enhanced addition fragmentation efficiency and macromonomers having terminal unsaturation. Further, if the IC were water soluble, macromonomers such as poly(dimethyl amino ethyl methacrylate), poly(N-vinyl pyrrolidone), poly(acrylamide) and poly(methacrylic acid) could be directly synthesized in aqueous medium.

In this chapter, we will discuss the CDs in general, mechanism and evidences of complex formation as well as their applications in different fields. Synthesis of AMSD-β-CD and AMSD-DM- β-CD ICs and their characterization is described. The effect on the chain transfer activity of AMSD will be discussed in the next chapter.

3.2 Cyclodextrins

3.2.1 History of cyclodextrins

Cyclodextrins were called "cellulosine" when first described by Villiers in 1891 (Villiers 1891). Schardinger identified three naturally occurring form of CDs viz: α, β,

and γ. These compounds were therefore referred to as "Schardinger sugars" (1911). Pringsheim (1932) demonstrated that CDs formed stable aqueous complexes with many other chemicals. By the mid 1970's, CDs were structurally and chemically characterized and many more complexes were studied. Since the 1970s, extensive work has been conducted by Szejtli and others exploring encapsulation by CDs and their derivatives for industrial and pharmacological applications (Szejtli 1988).

3.2.2 Structure of cyclodextrins

Cyclodextrins are non-reducing cyclic glucose oligosaccharides obtained by degradation of starch (cyclomaltodextrin) in the presence of glucanotransferase. Their structures have been reviewed by Saenger et. al. (1980).

There are three forms of CDs with six, seven or eight D-glucopyranonsyl residues (α, β, and γ CD respectively) linked by α-1, 4 glycosidic bonds (figure 3.1A). The glucose residues have the $^4C_1$ (chair) conformation. All three CDs have similar structures (that is, bond lengths and orientations) apart from the structural requirement of accommodating a different number of glucose residues. They present a bottomless bowl shaped (truncated cone) molecule stiffened by hydrogen bonding between the C_3-OH and C_2-OH groups around the outer rim.

The cavities have different diameters depending on the number of glucose units (empty diameters between anomeric oxygen atoms given in the figure 3.1C). The side rim depth is the same for all three (about 0.8 nm). The flexible C_6-OH groups are also capable of forming hydrogen bonds around the bottom rim but these are destabilized by dipolar effects, easily dissociated in solution and not normally found in CD crystals. The hydrogen bonding is all C_3-OH (donor) and C_2-OH (acceptor) in α-CD but flips between this and all C_3-OH (acceptor) and C_2-OH (donor) in β and γ-CDs.

Cyclodextrin rings are amphipathic with the wider rim showing the C_2-OH and C_3-OH groups and the narrower rim showing C_6-OH group on its flexible arm (figure 3.1B). These hydrophilic groups are on the outside of the molecular cavity whereas the inner surface is hydrophobic lined with the ether like anomeric oxygen atoms and the C_3-H

and C_5-H hydrogen atoms. In aqueous solution, this hydrophobic cavity contains about 3 (α-CD), 7 (β-CD) or 9 (γ-CD) poorly held and easily displaceable water molecules.
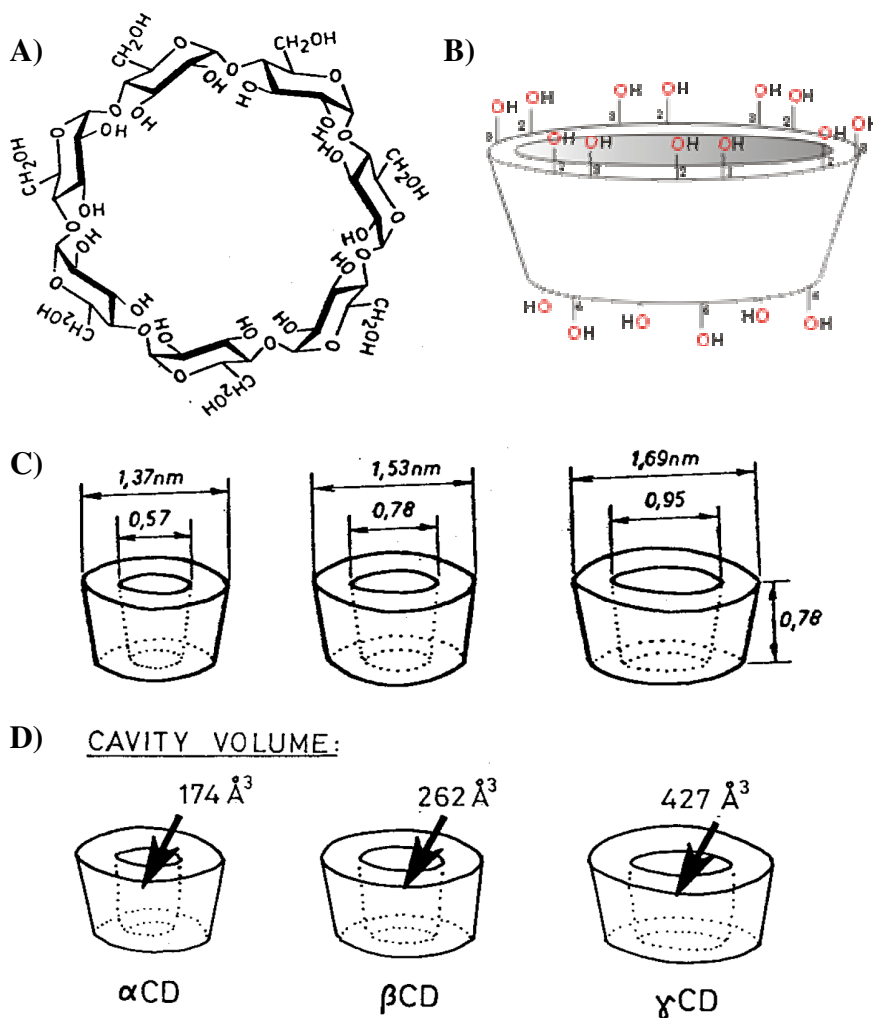
Figure 3.1 Structure of CD A) β-CD, B) OH positions in CD (Sabadini 2006), C) Inner and outer diameter of α, β and γ CD, D) Cavity volumes of α, β and γ CD, (Szejtli 1998)

Water in the cavities has low density as the cavities are large enough to accommodate several more molecules. Thus, the hydrophilic CD molecules may bind non-polar suitably sized aliphatic and aromatic compounds such as aroma compounds and lipophilic drugs. They may bind in 1:1, 2:1 and 1:2 ratios depending on the size of the molecules involved. The complexation is driven by the enthalpic and entropic gain on

the release of water molecules from the cavity to the bulk phase. Such binding also allows CDs to be used to increase the water solubility of normally hydrophobic compounds or minimize undesirable properties such as odor or taste in certain food additives. The CDs are non-toxic additives.

3.2.3 Synthesis of cyclodextrins

The production of CDs is relatively simple and involves treatment of ordinary starch with enzymes. Commonly CD glycosyltransferase (CGTase) is employed along with α-amylase. First starch is liquified either by heat treatment or using α-amylase, then CGTase is added for the enzymatic conversion. CGTases can be used to synthesize all forms of CDs. The conversion results in a mixture of cyclodextrins in ratios that are strictly dependent on the enzyme used. Each CGTase leads to a characteristic ratio α:β:γ.

Purification of CDs is done on the basis of the different water solubility of the molecules. β-CD which is very poorly water soluble (18.5 g/l or 16.3 mM) can be easily retrieved through crystallization while the more soluble α and γ-CDs (145 and 232 g/l respectively) are usually purified by chromatography techniques. As an alternative a "complexing agent" can be added during the enzymatic conversion step. Such agents (usually organic solvents like toluene, acetone or ethanol) form a complex with the desired CD which subsequently precipitates. The complex formation drives the conversion of starch towards the synthesis of the precipitated CD which enriches its content in the final product mixture. The precipitated CD is easily retrieved by centrifugation and is later separated from the complexing agent.

3.2.4 Derivatives of cyclodextrin

The hydroxyl groups may be derivatized to modify the specificity, physical and chemical properties of the CDs. The limited water solubility of β-CD led to the development of the alkylated and hydroxyalkylated derivatives of β-CD having higher water solubility. The C_6-OH groups are most easily derivatized. The degree of substitution expresses the number of hydroxyl groups in glucose units that are substituted. Therefore, this number can be 1 or 2 or 3.

According to Pitha (1998), the CDs can be derivatized in two ways i.e. vertical (axial) and horizontal cavity modification. Horizontal modification is generally carried out by producing CGTase enzymes yielding natural α-, β-, γ- and larger CDs. Vertical cavity modification is carried out by chemical substitutions. This usually elongates the CD torus in an axial direction by introducing larger substituents. The author further concluded that an extension of the cavity would be rigid since the cavity itself was rigid.

Industrially important water soluble cyclodextrin derivatives

Methylated derivatives of β-CD

2-hydroxypropylated β and γ-CDs

Sulfobutylated β-CDs

Branched CDs (glucosyl and maltosyl-β-cyclodextrins)

Acetylated β and γ-CDs

3.2.4.1 Methylated cyclodextrins
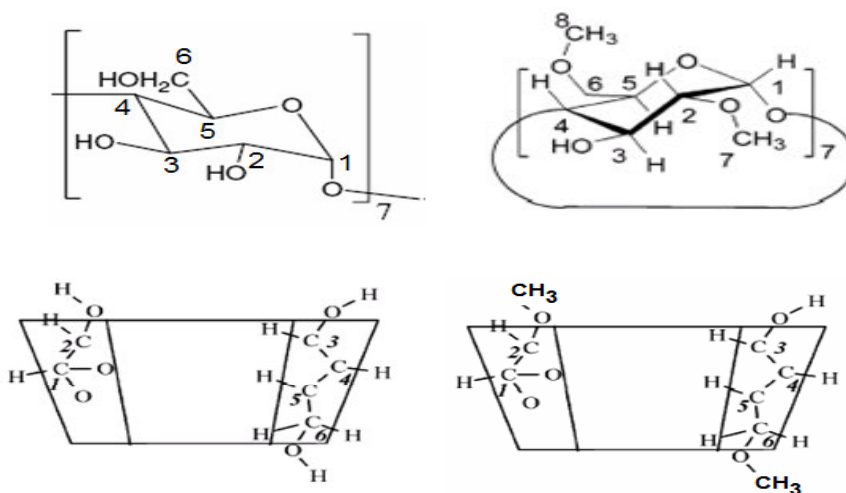
Figure 3.2 C_2 and C_6 OH positions in β-CD and 2, 6 Dimethylated β-CD

The introduction of the methyl substituent into the parent β-CD at C_2 and C_6 positions (figure 3.2) dramatically improves the water solubility of the derivative compared to the parent β-CD. The aqueous solubility increases as the number of methyl groups reaches around 13–14 and then decreases as methylation approaches 21 methoxy groups per β-CD molecule.

Methylation can be performed in different ways as follows.

1. Kuhn-Trischmann methylation (Takeo 1976)

2. Wacker's industrial method using methyl chloride under pressure

3. Hakamori methylation using methyl halogenide and sodium hydride (Rao 1991)

The first two technologies are used to produce randomly methylated CD mixture and to provide more than 50% isomeric purity heptakis 2, 6-di-O-methylated products. Hakamori methylation can yield a fully methylated heptakis 2, 3, 6 tri-O- methylated CDs, which however are not of industrial significance and are expensive.

Systematic comparative studies suggest that the most appropriate form of commercially viable, pharmaceutically useful methylated β-CD is the randomly methylated product (RAMEB) produced by Wacker Chemie. This compound has an average degree of methylation of 1.8 per anhydroglucose unit (Aman et. al. 1995). The material has a very good aqueous solubility, high binding capacities for most of poorly soluble drugs.

3.2.4.2 Hydroxypropyl cyclodextrins

Hydroxypropyl CD is obtained by reaction of CD with propylene oxide in alkaline aqueous solution which results in substitution of CD hydroxyls by 2-hydroxypropyl groups (Pitha et. al. 1987).

3.2.4.3 Sulfoalkylated cyclodextrins

Stella and Rajewski (1991) described the preparation of series of sulfoalkylated CDs from sulfoethyl to sulfohexyl derivatives of the cyclodextrins. Reaction of CD in alkaline aqueous solution with propane-sultone and butane-sultone yields soluble sulfopropyl-CD and sulfobutyl-CD respectively.

3.2.5 IC formation mechanism

Several hypotheses have been proposed to explain the mechanism of IC formation. These include a relief from conformational strain, release of cavity bound water, hydrophobic interaction, dipole-dipole and hydrogen bonding interactions as well as induction and dispersion forces (Szejtli 1988, Connors 1997). It is believed that hydrophobic interactions, dipole-dipole interactions and dispersion forces are the major factors in IC formation (Connors 1997). However, the size of the guest molecule and

CD cavity play an important role in the formation of strong ICs. Wide CD cavities would be unable to hold small guest molecules and to prevent dissociation of the complex. On the other hand, a guest molecule which is too large will not be able to enter the CD cavity and thus a strong complex will not be formed (Szejtli 1988, Connors 1997). Water is the preferred solvent for complexation and plays a key factor in the formation of IC. It acts as a driving force for the hydrophobic interaction of the guest with the cavity of the CD. In some cases, water is required to stabilize the ICs, since water molecules can form a bridge between the hydroxyl groups of adjacent molecules of CD to form a cage structure (Hedge 1998).

ICs can be prepared using co-precipitation, slurry, paste, dry mixing and solvent evaporation methods. Among these the co-precipitation is the most commonly used method to prepare the ICs of native CDs, whereas the solvent evaporation methodology is utilized to obtain the ICs of CD derivatives.
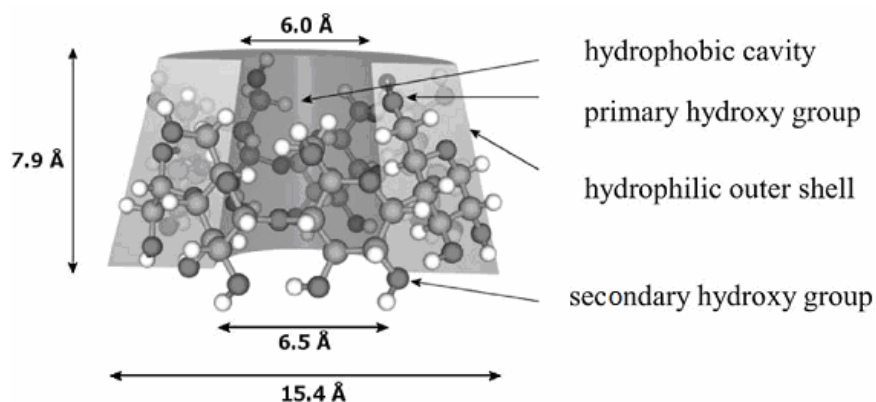
Figure 3.3 Hydrophobic cavity of CD (Tabatabai and Ritter 2002)

The most stable three dimensional structure of CDs is a toroid with the larger and smaller openings presenting hydroxyl groups to the external environment and mostly hydrophobic functionality lining the interior of the cavity (figure 3.3). It is this unique configuration that gives CDs their interesting properties and creates the thermodynamic driving force needed to form host-guest complexes with apolar molecules and functional groups. The conformation of the glucose units in the CD places the hydrophilic hydroxyl groups at the top and bottom of the three dimensional ring and the hydrophobic glycosidic groups on the interior.

Energetically favorable interactions responsible for complex formation (figure 3.4) are

1. The displacement of polar water molecules from the apolar CD cavity

2. The increased number of hydrogen bonds formed as the displaced water returns to the large pool

3. Reduction of the repulsive interactions between the hydrophobic guest and the aqueous environment

4. Increase in the hydrophobic interactions as the guest inserts itself into the apolar CD cavity
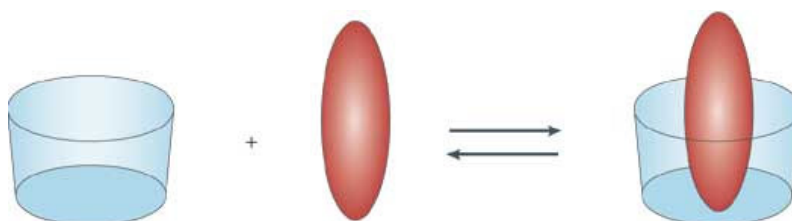
Figure 3.4 IC formation (Davis 2004)

3.2.6 IC formation evidences

3.2.6.1 X ray diffractometry (XRD)
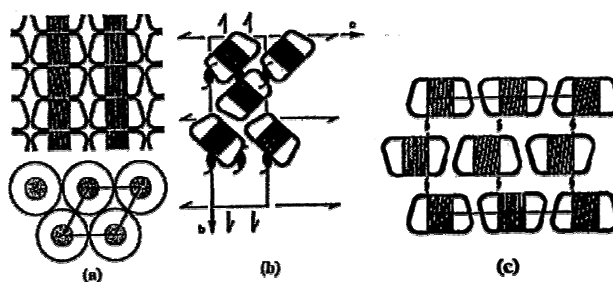
Figure 3.5 Schematic of a. channel type, b. cage herringbone type, c. cage brick type crystal structures formed by crystalline ICs (Rusa et al., 2001)

XRD has been used to determine the structure of IC. Crystals of β-CD are categorized into two types, cage type and channel type (figure 3.5). In cage-type structure, β-CD molecules are arranged in a herringbone fashion, and both ends of the β-CD cavity are blocked by adjacent molecules (Harata 2002). The channel-type structure is formed by

the linear stack of β-CD rings. The column-like structure can include molecules that are longer than the depth of the β-CD cavity and penetrating two or more β-CD rings.

3.2.6.2 Fourier transform infrared (FTIR) spectroscopy

FTIR is a useful tool to prove the presence of both guest and host components in their ICs (Jiao 2001). The most distinct peak in the spectrum of CD is due to the OH stretching of the glucose ring appearing at 3370 cm^{-1}. At equilibrium, β-CD contains 11-12 water molecules. The FTIR spectrum of β-CD shows the peak at 1650 cm^{-1} due to OH bending of water molecules within the CD cavity. During IC formation, these water molecules are replaced by the guest molecule. Thus, both the peaks at 3370 and 1650 cm^{-1} can be used to monitor the formation of complex.

3.2.6.3 Nuclear magnetic resonance (NMR) spectroscopy

^{1}H NMR

NMR is the technique most widely used to provide evidence for the formation and composition of IC in solution. Since complexation affects the proton environment in both the host and guest it is reflected in chemical shift variations of protons (Jiang 2007). The spectra for crosslinker in the presence of CD are compared with the spectra for the individual components.

3.2.6.4 Solid state ^{13}C CP/MAS NMR spectroscopy

The formation of the ICs should change the conformation and the electromagnetic environment of both the host CDs and the guest molecules. So, the inclusion behavior should be reflected in the ^{13}C CP/MAS NMR spectra. It is well known that CD molecules have less symmetrical conformation in the crystalline state (Gidley and Bociek 1988, Harada 1993) and would show resolved carbon resonances from each of the glucose units, reflected by strong splitting for all C_1–C_6 resonances.

3.2.7 Applications of cyclodextrin inclusion complexes

3.2.7.1 Organic chemistry

The formation of an IC alters the reactivity and selectivity of included guest molecules (Takahashi 1998). Breslow and Campbell (1969) demonstrated that complexation of

anisole with α-CD suppressed the reaction at the 'o' position and enhanced the p/o ratio of the chlorinated product from 1.48 to 21.6 %.

3.2.7.2 Polymer science

CDs are well known cyclic oligosaccharides that can solubilize hydrophobic compounds in aqueous media (Wenz 1994). The solubility is affected by complexation of the hydrophobic molecules within the hydrophobic cavity of CD. The use of CD to dissolve suitable monomers in water or to alter the reactivity of the chain transfer agents has been described in the literature (Ritter 2002). Some patents describe the use of CD preferably in catalytic amounts in order to improve emulsion polymerization yields. (US Patent 6,225,299, US Patent 5,521,266).

3.2.7.3 Pharmaceutical science

In pharmaceutical industry, CDs are used for different applications such as to enhance bioavailability, reduce irritation, improve patient compliance by reducing unpleasant odors, stabilize drugs against oxidation and hydrolysis, to prevent drug-drug or drug-additive interactions. CDs are also utilized to enhance the solubility of poorly soluble drug without any chemical modification. CDs may act as protecting agent for certain drug molecules by forming complex and thus prevent their premature metabolism.

Both β-CD and DM-β-CD remove cholesterol from cultured cells. The methylated form DM-β-CD was found to be more efficient than β-CD. The water-soluble DM-β-CD is known to form soluble ICs with cholesterol, thereby enhancing its solubility in aqueous solution. DM-β-CD is employed for the preparation of cholesterol-free products the bulky and hydrophobic cholesterol molecule easily enters inside CD rings which are then removed.

3.2.7.4 Analytical separation

In analytical chemistry application, CD is used mainly in chromatographic methods such as thin layer chromatography, gas chromatography, capillary electrophoresis and high pressure liquid chromatography (HPLC). CDs are used as complexing agent for the analytes under study. The presence of CDs or their derivatives in the mobile phase or as chemical bonded to the stationary phase improve the separation efficiency and the

speed of analysis and thus lead to the separations of isomers as well as closely related compounds. This is a low cost alternative to the HPLC separation of enantiomer using expensive chiral columns.

3.2.7.5 Food and flavor industry

Cyclodextrins are used in food industry because of their high temperature stability during food processing. Complexation of expensive flavor of oils and spices, such as apple, citrus, cinnamon, garlic, ginger, and menthol with CDs reduces the loadings needed to achieve the required flavor strength. The inclusion of flavor protects it from oxidation, photochemical degradation, thermal decomposition or loss by sublimation etc. Complexation of volatile oils with CDs converts them into the fine powder thus reduces their handing, packaging and storage costs as well as reduces their microbial contaminations. CDs are also utilized to selectively remove cholesterol from the products like milk, butter and eggs.

3.2.7.6 Agricultural applications

In agriculture, CDs are used to encapsulate the herbicides, pesticides, insecticides, fungicides, repellant, growth regulators etc. The inclusion increases their stability as well as water solubility.

3.2.7.7 Cosmetics, personal care and toiletry

The main advantages of ICs of CD in this field are to improve the process after conversion of liquid ingredient into the solid form, their stabilization and odor control. The applications include toothpaste, skin creams, liquid and solid fabric softeners, and deodorant etc.

3.3 Experimental

3.3.1 Materials

Alpha methyl styrene dimer (AMSD) was purchased from Aldrich. β-cyclodextrin (β-CD) was purchased from Hi media laboratories and dimethylated-β-CD (DM-β-CD) from Wacker Chemie (Germany). HPLC grade chloroform ($CHCl_3$) was obtained from

s. d. fine. The solvents methanol and petroleum ether were used after distillation. Deionized water was obtained from Millipore system.

The deuterated solvents D_2O and MeOD were purchased from Aldrich.

3.3.2 Methods

X-Ray diffractograms of CD and its IC were recorded at room temperature using a Rigaku X-ray diffractometer. The measurements were carried out using the parameters given below : target Cu K_α; filter Ni; voltage 40 kV; current 30 mA; slit 0.2 nm; scanning speed 2° per min., $2\theta = 5°-50°$. The XRD of CD and its IC were compared. Thermogravimetric measurements of the IC and CD were carried out at a heating rate of 10°C min.$^{-1}$ under inert atmosphere of nitrogen on a Perkin-Elmer 7 instrument. FTIR spectra were recorded on Perkin–Elmer spectrum one. ICs and polymers were properly mixed with KBr and the spectra were recorded at frequencies from 4000 to 450 cm^{-1}. The resolution was 4 cm^{-1}. Bruker AV 400 and AV 500 NMR spectrometers were used to record the ^1H NMR spectra of IC and macromonomers. The spectra of IC were recorded in D_2O and D_2O-MeOD mixture and those of macromonomers were recorded in CDCl$_3$. The proton-proton interactions between AMSD and CD in solution were studied at room temperature by ROESY and NOESY experiments at 500 MHz. The thermal stability of both IC was studied by high temperature NMR experiments. Variable temperature ^1H NMR experiments were carried out in the range 27-90°C on AV 400 NMR spectrometer. The solid state ^{13}C CP/MAS NMR spectra of ICs were recorded at 75 MHz on a Bruker AV 300 spectrometer at a sample spinning rate of 8 KHz at room temperature using a standard 4 mm triple resonance MAS probe.

3.3.3 Molecular modeling : Computational methodology

3.3.3.1 Conformational search

The geometry of β-CD was obtained from its crystallographic structure as determined by X-ray diffraction and deposited in the Cambridge databank. Conformational analysis was done for AMSD molecule using Monte Carlo Multiple Minimum Torsional sampling (Torsional sampling MCMM) method implemented in Macro Model 9.0 (Schrodinger 2005) module of the program Schrödinger package using parameters

described below : MM2* force field, Number of steps 3000, gradient method was used for minimization using following parameters, maximum iterations 1000, convergence threshold 0.05 kcal/mol. These conformations were optimized at B3LYP /6-31G level of theory using Gaussian 03 program (Frisch 2004). Amongst the structures possessing the shortest and longest end-end distances in the exhaustive conformational sampling carried out, two representative structural conformations exhibiting maximum stability were chosen. (figure 3.6) To the optimized geometry obtained at B3LYP /6-31G level, single point energies were calculated with various force fields and optimized at AM1, PM3, HF /6-31G, and MP2 /6-31G level of theory.

Bent conformation   Stretched conformation
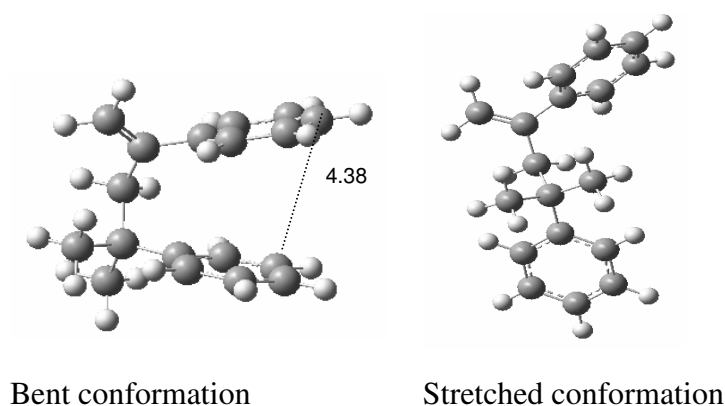
Figure 3.6 Bent and stretched conformations of AMSD at MP2/6-31G optimized geometry
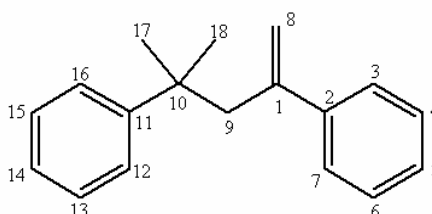
Figure 3.7 Atom numbering of AMSD in AMSD–β–CD and AMSD–DM-β-CD IC

3.3.3.2 Docking studies

Initial conformation of AMSD molecule was taken from the optimized geometry obtained at B3LYP /6-31G level of theory and geometry of β-CD was obtained from its

crystallographic structure. Polar hydrogens were added to β-CD and Gasteiger-Marsili charges were assigned to both AMSD and β-CD using sibyl 6.9 program (SYBYL 6.9). Rigid Docking calculations were performed using Lamarckian Genetic algorithm implemented in AUTODOCK 3.0.5 program (Morris 1998). Parameters used in docking protocols were: energy evolutions 1.5×10^6, population size 50, GA runs 30, grid points $60 \times 60 \times 60$ in X, Y, Z directions and grid spacing 0.315 Å.

3.3.3.3 MD simulations

Parameters for AMSD molecules were taken from GAFF force field and for β-CD, DM-β-CD molecules glycam 04 force field was used. Missing force field parameters were estimated using ff03 database. Partial charges for the AMSD molecule were calculated using the RESP procedure on optimized geometry obtained at HF /6-31G* level using Gaussian 03. The lowest energy docked conformation was taken as starting conformation in MD-simulation. System was solvated with TIP3P water model using buffer radius of 6.0 Å. System was minimized to 1000 steps and equilibrated to 500 ps time scale by gradual heating to 300 K. Production run was carried out initially with 2 ns time scale and conformations were saved for every 25 ps. Further the MD runs were extended to 10 ns and the conformational samplings as well as the lowest energy conformation obtained were virtually identical to those obtained with 2 ns. Thus, it could be concluded that the system had reached a conformational equilibrium and the time scale employed in the MD simulations was appropriate. Long-range interactions were treated using the Particle Mesh Ewald (PME) method. The PME charge grid spacing was ~1.0 Å and the charge grid was interpolated using a cubic B-spline of fourth order, a direct sum tolerance of 1×10^{-5}, and an 8 Å direct space cut off. Constant temperature and pressure were maintained throughout the simulations using the Berendsen scaling algorithm (Berendsen 1984) with a time constant of 1.0 ps. All bond lengths were constrained using the SHAKE algorithm. A time step of 1 fs was used to integrate the equations of motion. All calculations were done with AMBER 8.0 program (Case 2004).

3.3.3.4 Reactivity of -CH=CH₂ group

The reactivity of -CH=CH$_2$ group was analyzed in two ways (I) from the observation of trajectory generated by molecular dynamics simulation (II) calculating the quantum chemical descriptors.

3.3.4 IC synthesis

3.3.4.1 AMSD-β-CD IC preparation by precipitation method

9.6186 g (8.4×10^{-3} moles) β-CD was dissolved in 425 mL of water with continuous magnetic stirring. 2 g (8.4×10^{-3} moles) AMSD was added to above solution. The resulting complex started precipitating within 10 min. Stirring was continued for 24 h. The precipitated complex (Scheme 3.1) was filtered and washed with water and petroleum ether to remove uncomplexed β–CD and AMSD respectively.

3.3.4.2 AMSD-DM-β-CD IC preparation by solvent evaporation method

11.2828 g (8.4×10^{-3} moles) DM-β-CD was dissolved in chloroform with continuous magnetic stirring. 2 g (8.4×10^{-3} moles) AMSD was added. Stirring was continued for 24 h. The complex obtained was soluble in chloroform. The solution was concentrated using rota-vapour. The solid complex obtained (Scheme 3.1) was dried at room temperature, washed with petroleum ether to remove uncomplexed AMSD. Finally, it was dried under vacuum and characterized further.

The formation of both ICs was confirmed by instrumental techniques such as NMR, FTIR, XRD, TGA and molecular modeling.
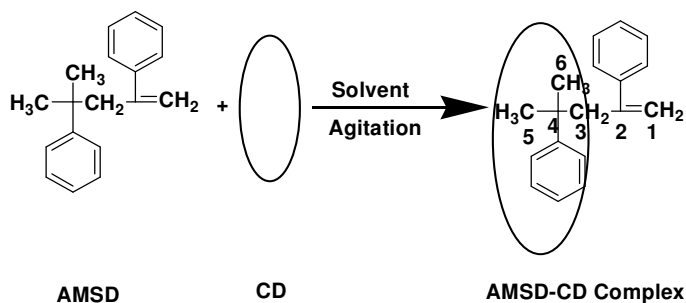
Scheme 3.1 AMSD inclusion complex synthesis

3.4 Results and discussion

3.4.1 IC Synthesis and characterization

ICs comprising AMSD-β-CD and AMSD-DM-β-CD were prepared in water and chloroform respectively by precipitation and solvent evaporation techniques. A job plot was made to confirm that both β-CD and DM-β-CD formed 1 : 1 IC with AMSD. (figure 3.8) The structure of the IC is shown schematically in Scheme I. AMSD-β-CD is insoluble in water while AMSD-DM-β-CD is water soluble. Cholesterol and prazosin hydrochloride which have limited solubility in water, formed a water soluble complex with HP-β–CD (Williams 1998, Liu 2006). Butyl methacrylate, isobornyl methacrylate and styrene also formed water soluble complexes with DM-β-CD (Casper 2000).
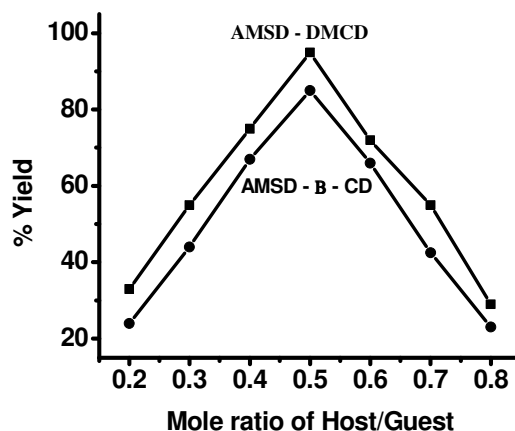
Figure 3.8 Job plot for AMSD inclusion complexes

In the following sections, the formation of the IC was established by a variety of characterization techniques. Complex formation can result from van der Waal interactions, hydrophobic interactions, hydrogen bonding and electrostatic interactions between the guest molecule and CD. In addition, the steric considerations play an important role in governing the stability of ICs. The complexation involves insertion of the less polar portion of the guest into the CD cavity from the wider side.

3.4.2 X-Ray diffractometry (XRD)

XRD has been extensively used to characterize the structure of ICs comprising CD. AMSD is liquid and hence does not contribute to XRD. The XRD pattern of β-CD shows a crystalline structure and DM-β-CD shows amorphous structure. The XRD

pattern of AMSD-β-CD IC reveals that the peaks at 2θ=18.88°, 19.6°, 22.72° observed for native β-CD have disappeared whereas new peaks at 2θ=5.7°, 7.24°, 23.87° and 26.07° have appeared, which confirms the formation of an IC. DM-β-CD shows only two broad peaks at 10^0 and 17^0 while in AMSD-DM-β-CD new peaks at 2θ=6.62°, 8.93°, 10.32°, 11.56°, 17.71° have appeared (figure 3.9). The absence of peaks at 2θ=20° and 7.6° in both ICs confirms that the IC has a cage type rather than a channel type structure. It may be noted that the formation of a 1:1 IC indicated by the job plot does not necessarily imply a cage type structure. Channel type structures are normally formed when molecules larger than the depth of the CD cavity are involved and penetrate into two or more β-CD rings. Liu and Zu (2007) reported that prazosin hydrochloride formed a channel type 1:1 IC comprising β-CD and the furan ring as well as the neighbouring carbonyl group of prazosin hydrochloride. α-CD and isosorbide dinitrate formed a 2:1 channel type IC (Harata 2002).
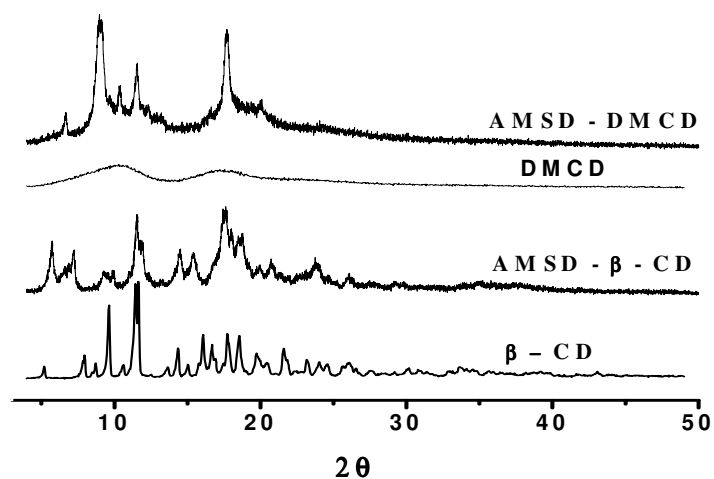
Figure 3.9 XRD of inclusion complexes

3.4.3 Thermogravimetric analysis (TGA)

Thermal stabilities of the ICs were evaluated by TGA (figure 3.10).

The initial decomposition temperature of β-CD is enhanced on complexation with a guest molecule, when the IC is stabilized by hydrogen bonding. However, when the complexation involves weaker hydrophobic interaction, stabilization is poor. It is further reported that when the conformation and electromagnetic environment of β-CD

become more symmetrical, the steric congestion and geometric distortion render the IC less stable (Li et. al. 2007). In the present study, we found that the initial decomposition temperature of β-CD (302°C) is actually lowered to 274°C on complexation with AMSD. Our findings are consistent with those reported earlier (Li et. al. 2007). The molecular modeling analysis shows that the penetration of the 4-phenyl ring of AMSD is greater in β-CD than in the case of DM-β-CD. We therefore expect the stability of β-CD to be lower than that of DM-β-CD in the presence of AMSD. This is again substantiated by the higher decomposition temperature of AMSD-DM-β-CD IC to 316°C as compared to that of DM-β-CD (288°C). NMR analysis further confirmed enhanced interactions in the AMSD-β-CD IC over those in AMSD-DM-β-CD IC.
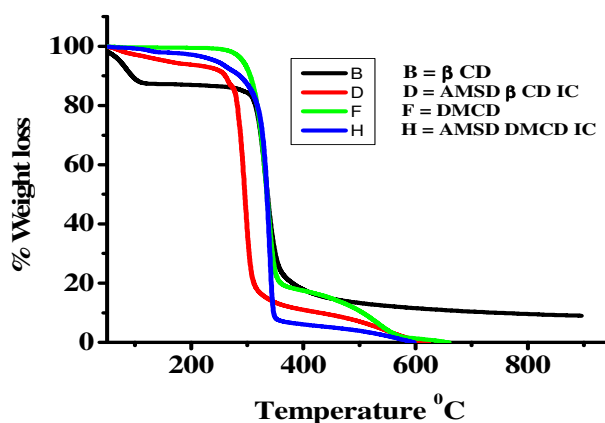
Figure 3.10 Thermal stability of inclusion complexes

3.4.4 FTIR analysis

The frequency shifts of native β-CD and its IC with AMSD are shown in figure 3.11.

The most distinct peak in the spectrum of CD is due to the OH stretching of the glucose ring appearing at 3370 cm^{-1}. This peak shows a shift of -21 cm^{-1} (3349 cm^{-1}) in AMSD-β-CD IC, indicating disruption of intramolecular hydrogen bonding in native β-CD (C$_2$-OH group of one glucopyranoside unit forms a hydrogen bond with C$_3$-OH group of adjacent glucopyranose unit). This peak shift cannot be attributed to hydrogen bonding, as AMSD lacks groups favoring hydrogen bonding. In the past, a shift of -59 cm^{-1} for OH stretching band of β-CD (3370 cm^{-1} to 3311 cm$^{-1)}$ for TMPTMA-β-CD IC was reported by Satav et. al. (2007). Comparatively weaker shift observed in the present

study indicates weaker hydrophobic forces driving complexation between AMSD and β-CD. Diclofenac sodium contains a carbonyl group which can participate in hydrogen bonding with β-CD and a phenyl ring which can participate in bonding through weaker hydrophobic binding. The weak shifts from 3387 to 3367 cm^{-1} for OH stretching peak were attributed to complex formation being driven by hydrophobic binding rather than hydrogen bonding (Bratu 1998). These results support that hydrophobic binding drives the complexation between AMSD and β-CD.
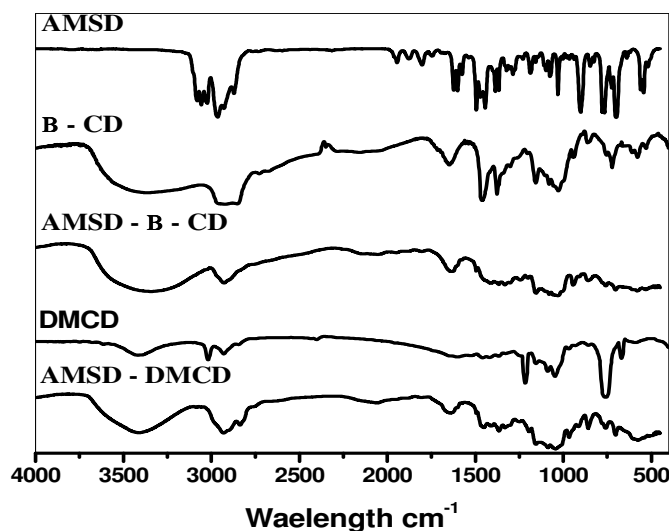
Figure 3.11 FTIR of AMSD inclusion complexes

At equilibrium, β-CD contains 11-12 water molecules. The FTIR spectrum of β-CD shows the peak at 1650 cm^{-1} due to OH bending of water molecules within the CD cavity. During IC formation, these water molecules are replaced by the guest molecule. Thus, this peak can be used to monitor the formation of complex. AMSD contains an aromatic ring and vinyl unsaturation. As a result, the peaks in this region become broad and accurate estimation of the shifts in this region becomes little difficult. After complex formation the intensity of this peak is reduced and it is shifted to 1642 cm^{-1} (Table 3.1). The shift towards lower wavelength supports the IC formation.

37

Table 3.1 FTIR frequency shifts of AMSD–β–CD inclusion complex

Sr. No.	Peak position cm^{-1} Constituent	Peak position cm^{-1} IC	Remarks
1.	3370 (OH stretching in β–CD	3349	Disruption of intramolecular H bonding in β–CD
2.	2964 (CH stretching in AMSD)	2927	Sterically hindered AMSD
3.	2924 (CH stretching in β – CD)	2927	
4.	1650 (OH bending of β – CD)	1642	Replacement of water molecules of β–CD by AMSD
5.	1623 (C=C of AMSD) 1600 (aromatic CH stretching of AMSD)	Merged with OH bending peak of β – CD at 1642 cm^{-1}	AMSD and β–CD peaks overlap
6.	755 (Pyranose ring of β – CD)	759	
7.	698 (Monosubstituted benzene ring of AMSD)	702	Steric hindrance for 4 phenyl ring of AMSD due to penetration inside the CD cavity

Table 3.2 FTIR frequency shifts of AMSD–DM-β-CD inclusion complex

Sr. No.	Peak position cm^{-1} Constituent	Peak position cm^{-1} IC	Remarks
1.	3408 (OH stretching in DM-β-CD	3384	Disruption of intramolecular H bonding in DM-β-CD
2.	2964 (CH stretching in AMSD)	2930	Sterically hindered AMSD
3.	2920 (CH stretching in DM-β-CD)	2930	
4.	1623 (C=C of AMSD)	1620	Sterically hindered AMSD
5.	756 (Pyranose ring of DM-β-CD)	758	
6.	698 (Monosubstituted benzene ring of AMSD)	702	Steric hindrance for 4-phenyl ring of AMSD due to penetration inside the CD cavity

The peak at 698 cm^{-1} characteristic of monosubstituted benzene ring of AMSD is shifted to 702 cm^{-1} on complexation. This change may be due to the penetration of 4

phenyl ring. Similar frequency shifts were also seen in AMSD-DM-β-CD IC (Table 3.2). These were further investigated by the molecular modeling analysis and NMR analysis discussed in subsequent section.

3.4.5 NMR analysis

3.4.5.1 ^{1}H NMR

The ^{1}H NMR spectra of the ICs are compared with those of free host and guest molecules (figure 3.12). Since, there are no chemical bonds formed between host and guest during complexation, the difference in chemical shifts is very small (Jiang et. al. 2007).
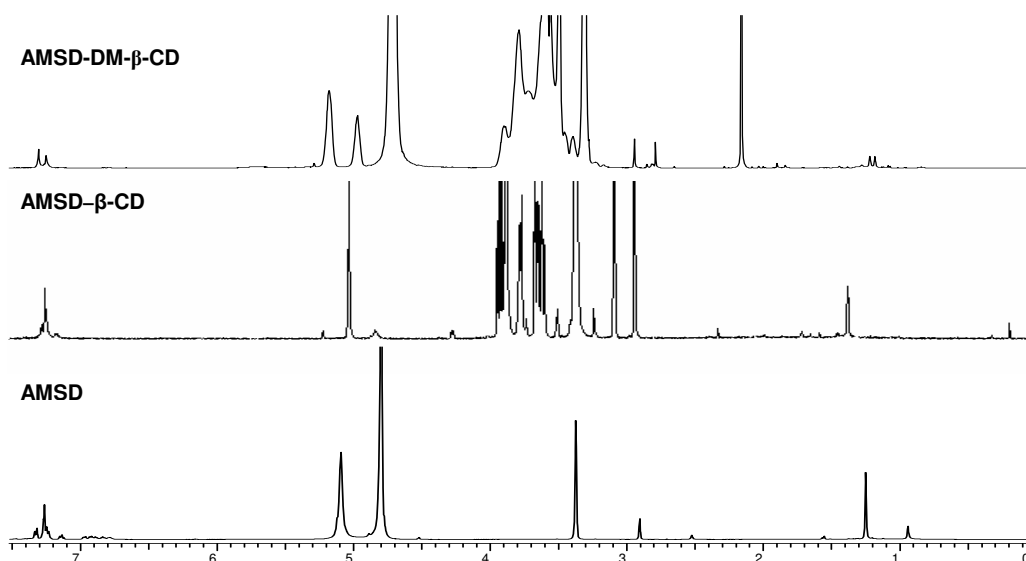
Figure 3.12 500 MHz ^{1}H NMR of AMSD inclusion complexes

500 MHz ^{1}H NMR of AMSD-β-CD and AMSD-DM-β-CD in D_2O showed peak splitting for methyl protons of AMSD at 1.26 δ. The separation for methyl signals was 24 Hz in case of AMSD-DM-β-CD while it was 3.9 Hz in case of AMSD-β-CD as shown in figure 3.13. If, the environment for both the methyl attached to the carbon having phenyl ring were same; it would yield only one peak as seen in neat AMSD. But, in complex form, the methyl signal was seen at two different ppm values which indicate that the two methyl groups are in different environment. The greater magnitude of separation in case of AMSD-DM-β-CD was attributed to the stronger

complexation as compared to that in β-CD. This is also supported by TGA data. The CH_2 protons of AMSD-DM-β-CD IC were also not equivalent and hence appeared as an AB quartet with a geminal coupling constant of 13.65 Hz. The methylene protons of the β-CD IC were broad and were not equivalent under the measurement conditions (25^0C).
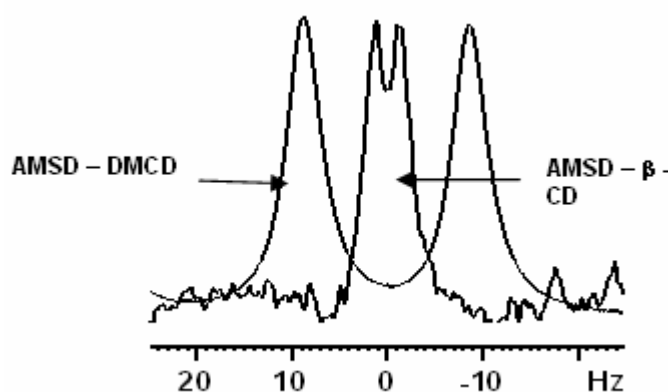
Figure 3.13 500 MHz ^{1}H NMR spectrum of methyl region of AMSD in inclusion complexes

AMSD-β-CD : ^{1}H NMR (D_2O + MeOD 1:2) δ [ppm]: 1.26 CH_3 of AMSD, 2.88 (broad) CH_2 of AMSD, 7.37 aromatic protons of AMSD, 3.56-3.92 C_2-C_6 protons of β-CD, 5.1 C_1 proton of β-CD.

AMSD–DM-β-CD : ^{1}H NMR (D_2O) δ [ppm]: 1.24, 1.28 CH_3 of AMSD, 2.86 (quartet) CH_2 of AMSD, 7.35-7.41 aromatic protons of AMSD, 3.39-3.98 C_2-C_6 protons of DM-β-CD, 5.06, 5.27 C_1 proton of DM-β-CD.

3.4.5.2 ^{13}C Solid state NMR

The solid state ^{13}C resonances of C_1 and C_4 of CD elucidate the conformation of glycosidic linkages and the packing state (Okada 1999). Solid state NMR spectra of the IC of AMSD-β-CD confirm inclusion of AMSD into the CD cavity (Harada 1993).
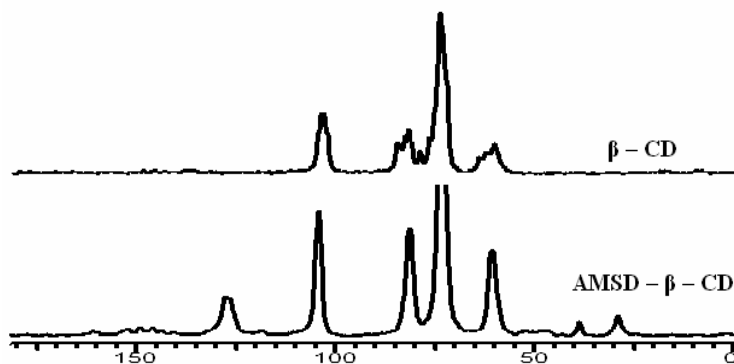
Figure 3.14 ^{13}C CP/MAS of AMSD-β–CD inclusion complex
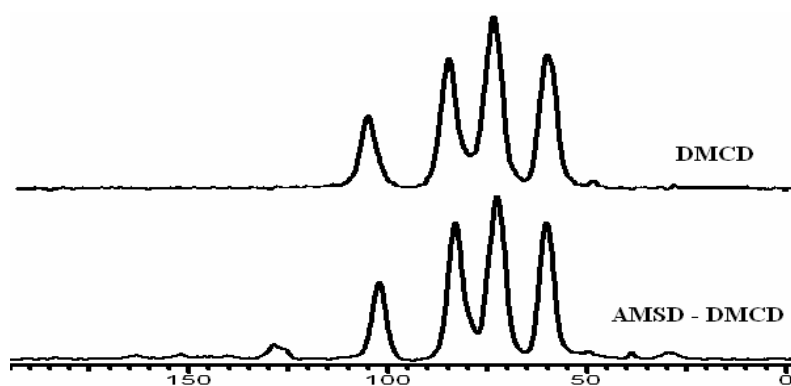
Figure 3.15 ^{13}C CP/MAS of AMSD-DM-β-CD inclusion complex

CP/MAS solid state ^{13}C NMR spectrum of AMSD-β-CD IC displayed well resolved, single peaks for each carbon of all glucose units. The peaks at 78.6 and 101 ppm corresponding to C_1 and C_4 (figure 3.14), adjacent to conformationaly strained glycosidic linkage disappeared. This indicates symmetrical conformation of glycosidic linkage due to the inclusion of AMSD within the cavity of β-CD.

In case of free DM-β-CD (figure 3.15), C_1 peak at 101.91 ppm is broad indicating that DM-β-CD is asymmetric. In AMSD-DM-β-CD IC it shifts to 102.14 ppm. However, multiplicity is not affected. These results are consistent with those reported by Hall et. al. (Hall 1986).

3.4.5.3 Thermal stability of inclusion complexes
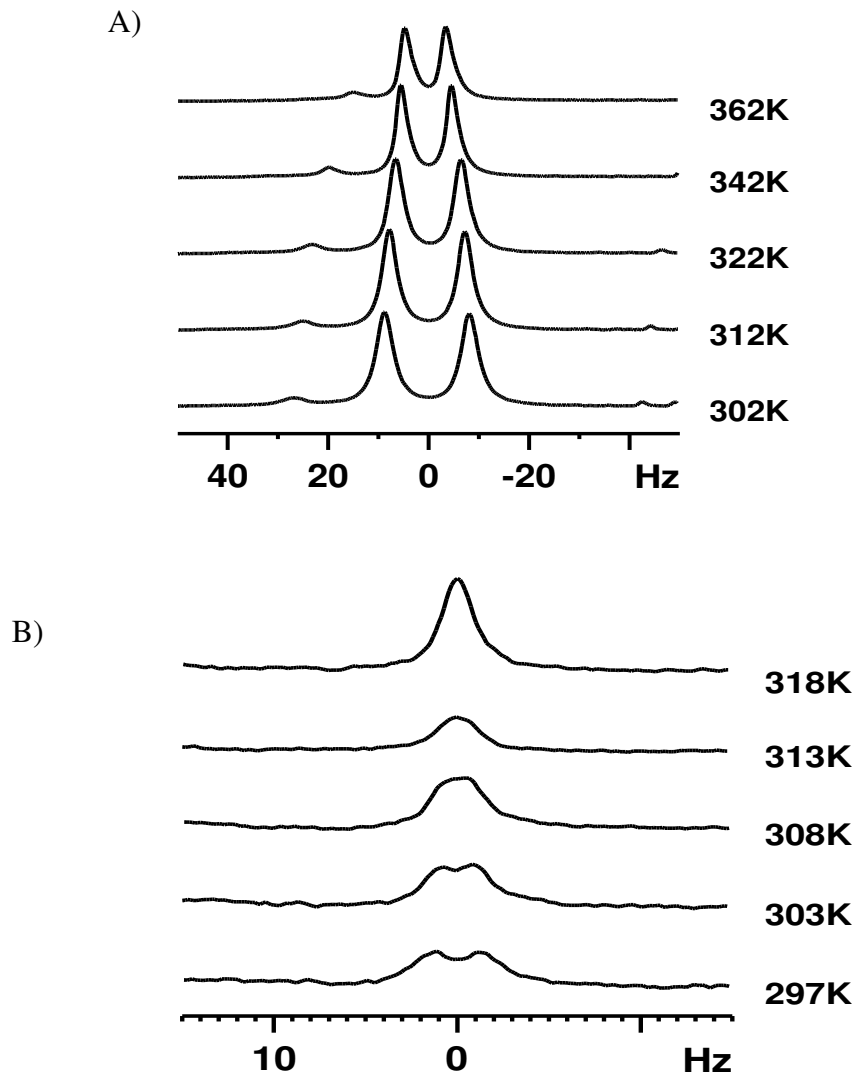
Figure 3.16 400 MHz ^{1}H VT Spectrum in D_2O + MeOD: Me Region of inclusion complexes: A) AMSD-DM-β-CD inclusion complex, B) AMSD–β-CD inclusion complex

The stability of both the ICs in D_2O was evaluated by NMR by scanning the sample from room temperature to 90°C. The methyl signal of AMSD in AMSD-DM-β-CD IC was found to split into two peaks at 1.21 and 1.26 ppm corresponding to 24 Hz on a 500 MHz spectrometer. In case of AMSD-β-CD IC the splitting of methyl signal was also seen but on the same spectrometer the separation was 3.9 Hz only. The splitting of methyl signal was attributed to the complex formation as discussed in ^{1}H NMR section.

On a 400 MHz spectrometer, the separation between the methyl groups was found to be 19 Hz and 2.4 Hz respectively for the AMSD-DM-β-CD and AMSD-β-CD IC. The separation decreased from 19 to 8.1 Hz in case of AMSD-DM-β-CD as the temperature was raised from room temperature to 90°C whereas the methyl signal yielded a single peak at 35°C in AMSD-β-CD IC (figure 3.16). However, for AMSD-DM-β-CD IC, the splitting remained intact even at 90°C. This further substantiates our earlier findings by TGA analysis indicating greater stability of AMSD-DM-β-CD IC over AMSD–β-CD IC.

3.4.5.4 Elucidating interactions within the inclusion complexes: ROESY / COSY experiments

A)   B)
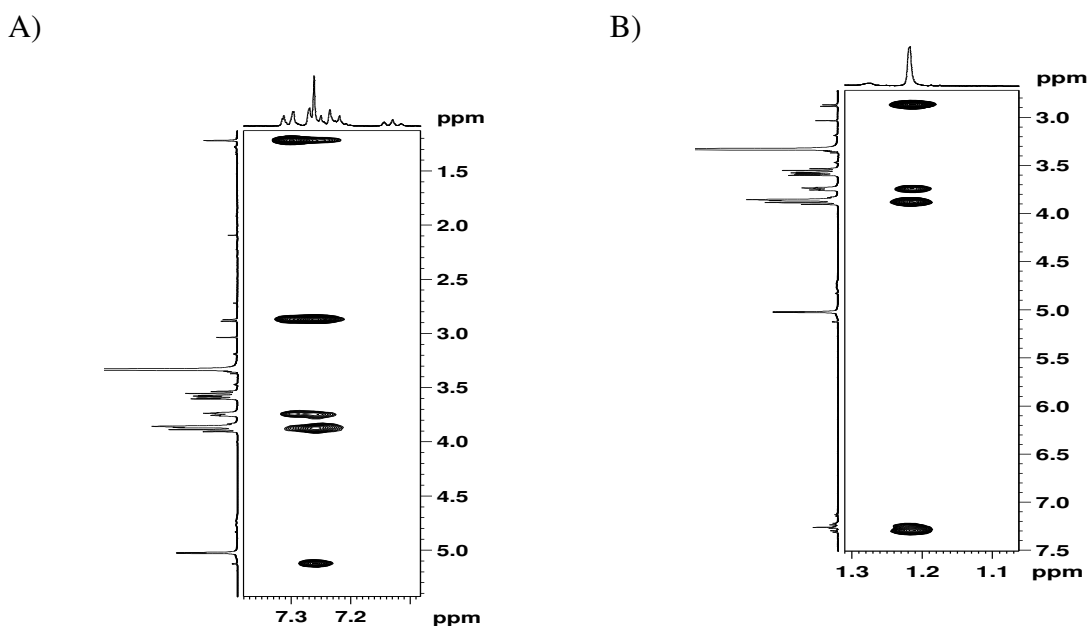
Figure 3.17 NOESY of AMSD–β–CD inclusion complex in D₂O + CD₃OD: A) aromatic region of AMSD, B) methyl region of AMSD

A)

B)

C)
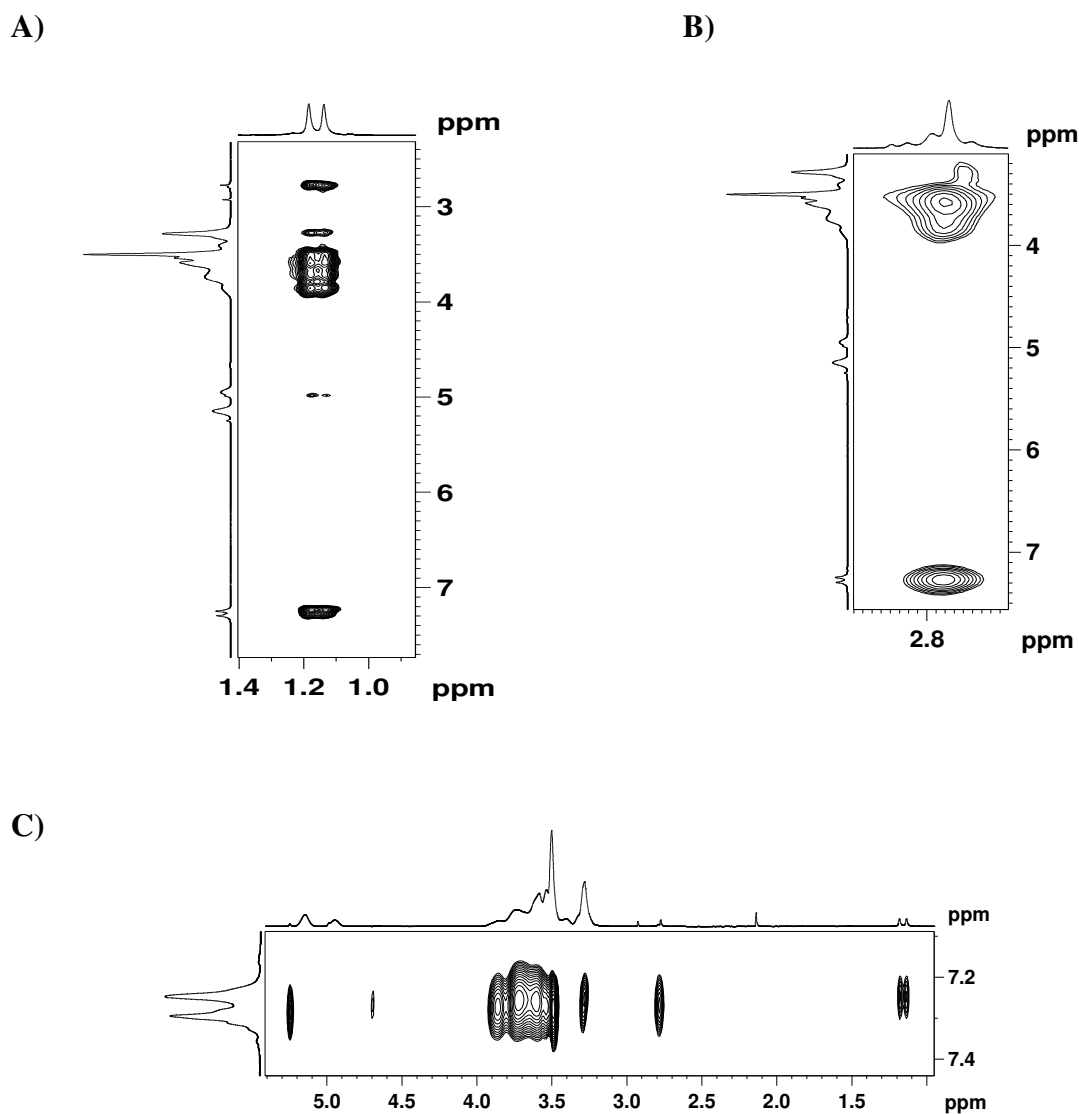
Figure 3.18 NOESY of AMSD–DM-β-CD inclusion complex in D$_2$O A) Methyl region of AMSD, B) Methylene region of AMSD C) Aromatic region of AMSD

In order to obtain information about the geometry and orientation of the guest in the cavity, two dimensional ROESY experiments were performed. The presence of NOE crosspeaks between protons from both species indicates separation closer than 0.4 nm in space. Also, the relative intensities of crosspeaks depend on the distance between the corresponding protons.

In both the cases, the NOESY spectrum showed positive crosspeak between proton of the host (DM-β-CD, β-CD) and the guest (AMSD). The presence of the crosspeaks

clearly demonstrates that AMSD indeed forms IC with both β-CD and DM-β-CD as it acquires longer correlation time of the host due to the complex formation. In the long correlation regime, at the mixing times employed for the measurement, the NOESY peak intensity does not correspond to the internuclear distance due to the presence of spin diffusion. The ROESY spectrum confirmed the NOE contacts, wherein the dipolar contacts leading to NOE appeared as negative ROE crosspeaks.

NOESY spectrum of AMSD in D_2O-MeOD mixture shows all negative crosspeaks because of its shorter correlation time associated with its smaller size. But, in both ICs it shows positive crosspeaks indicating that correlation time has increased on complexation. This increase in τ_0 is due to the increase in its effective size after complexation. Thus, NOESY spectrum shows that AMSD in complex form does not behave as a single entity but has acquired correlation time of CD. This implies that AMSD is bound to CD cavity. Due to the spin diffusion, crosspeaks between AMSD and CD are seen as positive. In the ROESY experiments the spatially coupled spins by NOE appear as negative crosspeaks and the intensity / volume ratio of crosspeaks can be considered as a measure of spatial proximity. Allylic CH_2 from both AMSD-DM-β-CD and AMSD-β-CD ICs show NOE crosspeaks with the sugar units of CD revealing that they are within the distance of 0.4 nm. Also, the aromatic ring peaks of AMSD from both the ICs show NOE crosspeaks to CD (figure 3.17 and 3.18). Both ICs do not show NOE to the peak at 3.27 ppm which is characteristic peak of C_6 of CD. This is expected because this proton lies out side the CD cavity and hence is far from AMSD. All other protons of both the CDs show NOE to methyl and methylene protons of AMSD. AMSD shows NOE to C_3 and C_5 protons of CD which are placed inside the cavity. Thus, ROESY data confirm that AMSD is placed inside the cavity of both the CDs as predicted by molecular modeling.

3.4.6 Molecular modeling

The conformational analysis of AMSD, its complexation with β-CD, DM-β-CD was analyzed by computational studies. Conformational analysis reveals that stretched conformation is more stable than bent conformation. Semi-empirical methods (AM1, PM3), Hartree Fock methods (at 6-31G level), DFT methods (with 6-31G basis set) and

MP2 methods (at 6-31G level) revealed that the stretched conformation is more stable than bent one by 8-10 kJ/mol (Table 3.3). The complexation of AMSD with β-CD was analyzed by docking, quantum chemical and molecular dynamics simulations using Autodock 3.0.5, Gaussian 03 and AMBER 8.0 programs respectively. The lowest energy complex, obtained from the Autodock calculation, was taken as initial structure for MD simulations. TIP3P water models were used as solvent and equilibration was performed for 500 ps and MD simulation was carried for 2ns. Conformations of these molecules in MD simulation are shown in figure 3.19 and 3.20.

Table 3.3 Conformational energies of AMSD at various level of theory

Methods	Conformation of AMSD molecules				Relative energy(kJ/mol)	
	Bent		Stretch			
	Energy (in hartrees)	End–end distance Å)	Energy (in hartrees)	End–end distance(Å)	Bent	Stretch
AM1	0.0822	5.51	0.0808587	9.31	3.75	0
PM3	0.0771	5.21	0.0749346	9.18	5.72	0
HF/6-31G	-693.0072	5.10	-693.0082906	9.44	2.65	0
B3LYP/6-31G	-697.7876	5.11	-697.7890361	9.51	3.71	0
MP2/6-31G	-692.9912	4.38	-692.9946395	9.53	8.87	0

Computations were also carried out to ascertain if AMSD could bind to a second β-CD and DM-β-CD. This was necessary since Harata and Kawano (2002) reported that isosorbide dinitrate formed a 2:1 channel type IC with α CD. Docking studies and the subsequent binding energies evaluated at B3LYP/6-31G level of theory revealed that the complexation of AMSD with the first β-CD resulted in substantial stabilization of the order of 15-20 kJ /mol and with first DM-β-CD of the order of 10-15 kJ/mol; while the addition of second β-CD and DM-β-CD does not provide substantial stabilization.

AMSD-bent conformation	AMSD-stretch conformation	AMSD-bent conformation	AMSD-stretch conformation
Docked Energy in kcal/mol: **-8.27**	Docked Energy in kcal/mol: **-7.39**	Docked Energy in kcal/mol: **-9.56**	Docked Energy in kcal/mol: **-9.13**
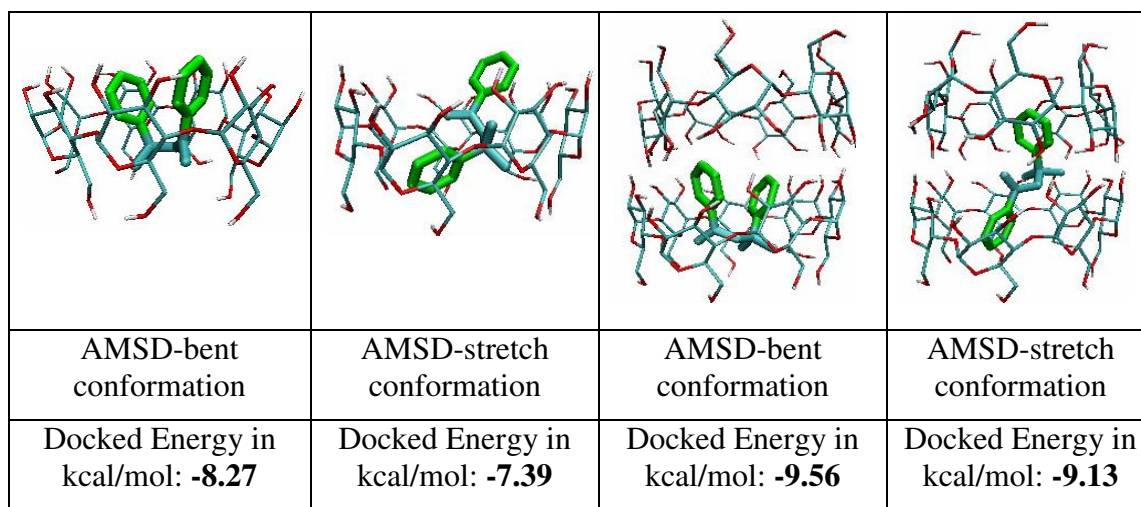
Figure 3.19 Conformations of AMSD molecule with one and two β-CDs

AMSD-bent conformation	AMSD-stretch conformation	AMSD-bent conformation	AMSD-stretch conformation
Docked Energy in kcal/mol: **-8.39**	Docked Energy in kcal/mol: **-7.45**	Docked Energy in kcal/mol: **-8.65**	Docked Energy in kcal/mol: **-7.85**
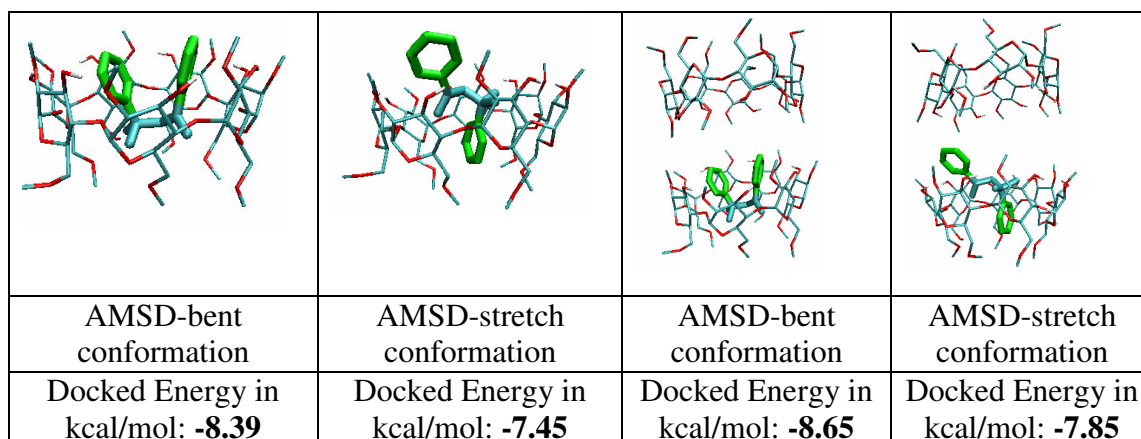
Figure 3.20 Conformations of AMSD molecule with one and two DM-β-CDs

Lowest energy complex was taken from MD simulations and single point energy was calculated at AM1, PM3, HF/6-31G and B3LYP /6-31G level of theory for AMSD molecule. Interaction energy (in kcal/mol) was given in Table 3.4 and 3.5 for AMSD molecule with one and two β-CDs, as well as with DM-β-CDs respectively. Conformations obtained from MD-simulations were given in Figure 3. 21.

The interaction energy for complex was computed as follows:

$$E_{int} = E_{com} - (E_{βcd/DM-β-CD} + E_{lig})$$

Where E_{int} – Interaction energy, E_{com} – energy of complex, $E_{βcd/DM-β-CD}$ – energy of β-CD (or) DM-β-CD, E_{lig} –energy of AMSD.

Lowest energy complex was taken from MD simulations and energies evaluated on the equilibrium geometries obtained at AM1, PM3, HF /6-31G and B3LYP /6-31G level of theory using Gaussian 03 suite of programs.

Table 3.4 Interaction energy of AMSD molecule with one and two β-CDs

Molecules	Methods	Energy of system in hartrees			Interaction Energy in kcal/mol
		Complex	Only β-CDs	AMSD	
One β-CD	AM1	-2.14202	-2.27431	0.1330	-0.43
	PM3	-1.89069	-1.9955	0.1188	-8.81
	HF/6-31G	-4941.9893	-4249.0283	-692.9559	-3.16
	B3LYP/6-31G	-4971.3034	-4273.5426	-697.7470	-8.67
Two β-CDs	AM1	-4.3608	-4.5254	0.1653	-0.42
	PM3	-3.8612	-3.9863	0.1453	-12.71
	HF/6-31G	-9191.0607	-8498.1260	-692.9402	3.50
	B3LYP/6-31G	-9244.9203	-8547.1803	-697.7260	-8.73

Table 3.5 Interaction energy of AMSD molecule with one and two DM-β-CDs

Molecules	Methods	Energy of system in hartrees			Interaction Energy in kcal/mol
		Complex	Only DM-β-CDs	AMSD	
ONE DM-β-CD	AM1	-1.9113	-2.0636	0.1539	-1.00
	PM3	-1.6909	-1.8199	0.1425	-8.43
	HF/6-31G	-5487.9204	-4794.9974	-692.9273	2.70
	B3LYP/6-31G	-5521.2861	-4823.5540	-697.7240	-5.06
TWO DM-β-CDs	AM1	-3.8778	-4.0324	0.1523	1.43
	PM3	-3.4636	-3.5850	0.1375	-10.13
	HF/6-31G	-10282.8510	-9589.9211	-692.9403	6.47
	B3LYP/6-31G	-10344.8027	-9647.0656	-697.7301	-4.35

The distance between $CH=CH_2$ group of AMSD and centroid of DM-β-CD, as well as between $CH=CH_2$ group and centroid of 2° hydroxyl group was calculated to find the expose of $CH=CH_2$ out side the CD cavity. After analyzing 40 conformations in AMSD-β-CD IC, it was found that 12 conformations were outside the CD cavity whereas in the case of DM-β-CD IC 32 conformations were exposed out side the CD cavity. The corresponding distances are given in Table 3.6 and 3.7. This shows that

CH=CH$_2$ group of AMSD is more exposed to out side in case of DM-β-CD compared to that in case of β-CD. Thus, CH=CH$_2$ group in AMSD-DM-β-CD IC is more accessible for chain transfer reaction as compared to that in AMSD-β-CD IC. The trends observed in the chain transfer constant may thus be rationalized based on the NPA, NBO and Fukui functions analysis methods. Charge distribution on CH=CH$_2$ group present in AMSD, AMSD-β-CD and AMSD-DM-β-CD ICs was calculated using NPA method to correlate the reactivity of CH=CH$_2$ group in respective complexes. As shown in Table 3.8, more charge is located on AMSD-β-CD IC, followed by AMSD-DM-β-CD and least for AMSD.

The polarization coefficients and hybridization of CH=CH$_2$ groups was calculated using NBO method. The π bond polarization coefficients of carbon atom of CH$_2$ are more in AMSD-β-CD, followed by AMSD and AMSD-DM-β-CD ICs (Table 3.9). The average hybridization of p-orbital in π bond for C-atom of CH$_2$ is 93.62, 75.62, 84.66 and that of C-atom of R-CH is 89.91, 88.22, 89.56 in AMSD, AMSD-β-CD and AMSD-DM-β-CD ICs respectively. The polarization coefficients and hybridization show that activity of double bond is in the order AMSD > AMSD-DM-β-CD > AMSD-β-CD. From Fukui function values (Table 3.10) it can be seen that the reactivity of C atom of CH$_2$ is greater than that of C atom of R-CH in R-CH=CH$_2$ group.
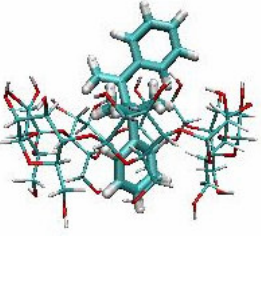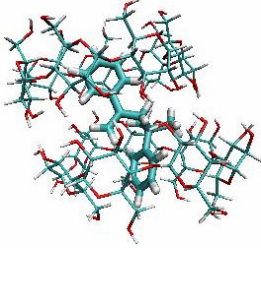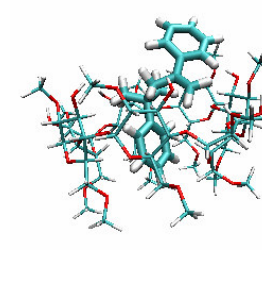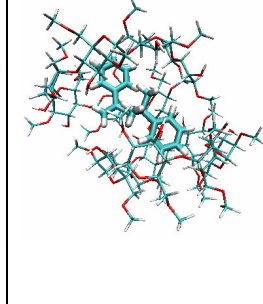
AMSD-one β-CD	AMSD-two β-CDs	AMSD-one DM-β-CD	AMSD two DM-β-CDs
Interaction energy: **-8.67**kcal/mol	Interaction energy: **-8.73**kcal/mol	Interaction energy: **-5.06** kcal/mol	Interaction energy: **-4.35** kcal/mol

Figure 3.21 Conformations of AMSD molecules obtained in MD simulations with one and two β-CDs as well as with DM-β-CDs

Table 3.6 Distance between CH=CH$_2$ group of AMSD and centroid of β-CD

Conformations	Distance between centroid CD and CH=CH$_2$ of AMSD(Å)	Distance between centroids of 2° hydroxyl group and CD(Å)	Distance between centroid of 2° hydroxyl group and CH=CH$_2$of AMSD(Å)
1	2.45	4.29	2.36
2	3.50	5.45	2.29
3	3.54	5.54	2.35
4	3.58	5.75	2.47
5	2.62	4.45	2.45
6	3.17	5.17	2.43
7	2.63	4.74	2.45
8	1.88	3.28	2.53
9	2.25	2.57	2.49
10	1.74	3.18	2.39
11	1.80	3.00	2.43
12	2.11	4.03	2.44
13	3.36	5.40	2.47
14	3.14	5.25	2.51
15	1.53	2.51	2.50
16	2.22	3.45	2.47
17	2.22	3.48	2.47
18	1.60	2.75	2.48
19	1.88	3.18	2.46
20	2.11	3.57	2.47
21	4.61	2.61	2.25
22	4.97	3.20	2.43
23	4.61	2.86	2.45
24	4.45	2.91	2.43
25	4.59	2.69	2.34
26	3.91	2.34	2.46
27	3.92	2.21	2.42
28	4.22	2.54	2.41
29	3.68	2.78	2.48
30	3.31	2.48	2.45
31	4.26	2.25	2.49
32	4.13	2.71	2.41
33	4.60	2.44	2.48
34	2.33	2.53	2.46
35	2.46	1.73	2.44
36	2.40	1.91	2.67
37	2.53	1.78	2.41
38	2.34	1.90	2.44
39	2.45	2.32	2.48
40	2.34	2.22	2.35

Table 3.7 Distance between CH=CH$_2$ group of AMSD and centroid of DM-β-CD

Conformations	Distance between centroid CD and CH=CH$_2$ of AMSD(Å)	Distance between centroids of 2° hydroxyl group and CD(Å)	Distance between centroid of 2° hydroxyl group and CH=CH$_2$ of AMSD(Å)
1	2.39	2.03	2.64
2	2.43	2.56	2.58
3	4.26	2.26	2.46
4	5.35	3.12	2.40
5	4.71	3.14	2.63
6	4.11	2.27	2.67
7	4.52	2.60	2.48
8	4.80	2.76	2.56
9	4.62	2.70	2.49
10	4.81	2.79	2.57
11	4.45	2.81	2.43
12	3.61	2.00	2.57
13	4.80	2.95	2.53
14	3.65	1.96	2.53
15	3.61	1.97	2.68
16	3.74	1.68	2.61
17	4.13	2.34	2.50
18	4.16	2.33	2.66
19	4.67	2.91	2.63
20	4.22	2.60	2.61
21	5.18	3.04	2.47
22	4.18	2.26	2.63
23	4.70	2.98	2.50
24	4.01	2.52	2.60
25	4.80	2.85	2.60
26	4.62	2.99	2.59
27	2.75	2.08	2.65
28	3.54	2.10	2.61
29	3.03	1.82	2.52
30	4.45	2.28	2.64
31	2.73	1.90	2.55
32	3.24	1.91	2.59
33	4.04	2.68	2.61
34	4.84	2.87	2.60
35	5.33	3.20	2.45
36	4.23	2.27	2.61

37	5.07	2.79	2.52
38	4.79	2.63	2.66
39	4.67	3.04	2.46
40	4.63	3.04	2.43

Table 3.8 NPA charges of CH=CH$_2$ group in AMSD, AMSD–β–CD and AMSD–DM-β-CD complexes at HF/3–21G level

Method/Complexes	No. of sets	NPA charges on R–CH=CH$_2$ group	
		R–CH	**CH$_2$**
AMSD	**1**	–0.03254	–0.41517
AMSD–β–CD	**a**	–0.02962	–0.43712
	b	–0.03706	–0.41785
AMSD–DM-β-CD	**a**	–0.05013	–0.42158
	b	–0.04074	–0.41315

Table 3.9 NBO analysis of occupancy and energies of CH=CH$_2$ group in AMSD, AMSD-β-CD and AMSD-DM-β-CD complexes at HF/ 3-21G level

Property	Sets	Bond	Polarization Coefficient		Hybridization		Occupancy
			R-CH	**CH$_2$**	**R-CH**	**CH$_2$**	
AMSD	**a**	σ	0.7204	0.6936	sp1.73	sp1.68	1.98374
		π	0.6990	0.7152	sp89.91	sp93.62	1.95158
AMSD-β-CD	**a**	σ	0.7223	0.6915	sp1.73	sp1.67	1.98078
		π	0.6949	0.7191	sp91.08	sp76.58	1.95188
	b	σ	0.7221	0.6918	sp1.75	sp1.66	1.98136
		π	0.6974	0.7167	sp 85.37	sp74.67	1.95254
AMSD-DM-β-CD	**a**	σ	0.7226	0.6913	sp1.75	sp1.68	1.98100
		π	0.7040	0.7102	sp79.14	sp69.33	1.95289
	b	σ	0.7222	0.6917	sp1.72	sp1.61	1.98069
		π	0.6995	0.7146	sp99.99	sp99.99	1.94916
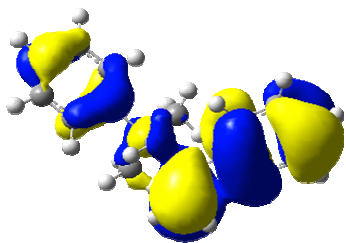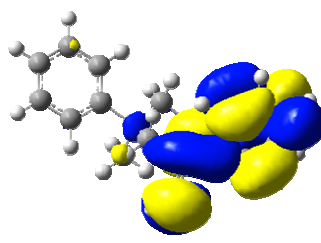
AMSD-HOMO   AMSD-LUMO   AMSD-β-CD-HOMO
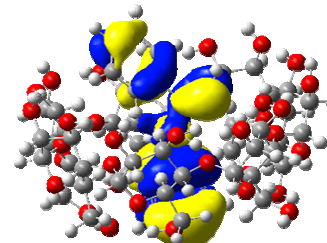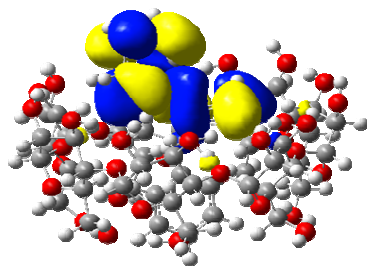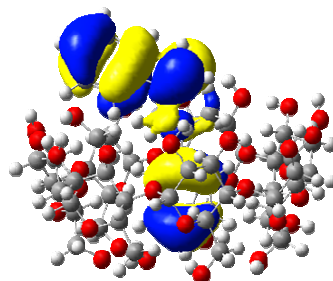
AMSD- β-CD-LUMO   AMSD-β-CD-HOMO   AMSD-β-CD-LUMO
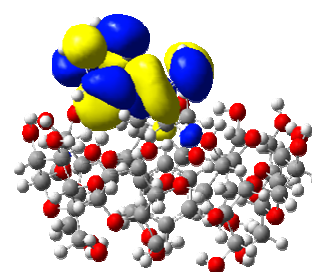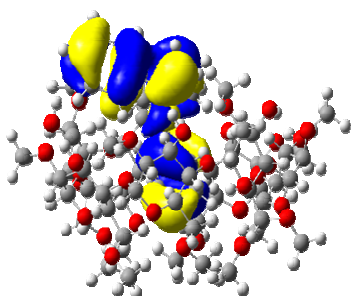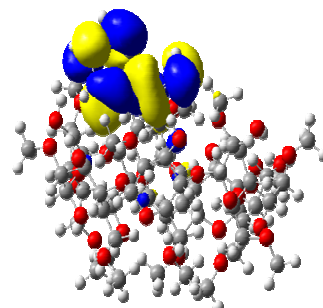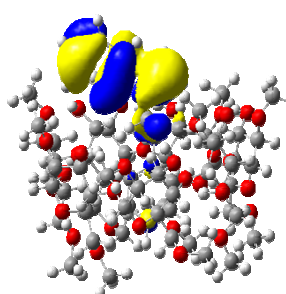
AMSD-DM-β-CD-HOMO   AMSD-DM-β-CD-LUMO   AMSD-DM-β-CD-HOMO
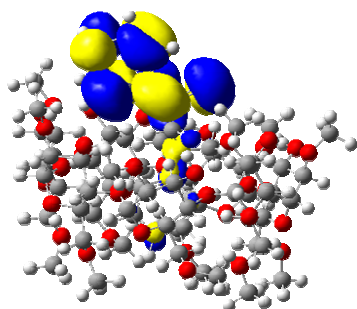
AMSD-DM-β-CD-LUMO

Figure 3.22 HOMO-LUMO of AMSD, AMSD-β-CD and AMSD-DM-β-CD

inclusion complexes

Table 3.10 Fuki functions of CH=CH$_2$ group in AMSD, AMSD-β-CD and AMSD-DM-β-CD inclusion complexes HF/3-21G level

Method/Complexes	No. of sets	Charge is -1 unit on molecule		Charge is 1 unit on molecule		Calculated fuki function	
		R-CH	CH$_2$	R-CH	CH$_2$	R-CH	CH$_2$
AMSD	1	-0.0652	-0.2161	-0.0019	0.2926	0.0632	0.5087
AMSD-β-CD	a	-0.0478	-0.194	-0.0388	0.0560	0.0089	0.2500
	b	-0.0653	-0.1945	-0.0223	0.2009	0.0429	0.3954
AMSD-DM-β-CD	a	-0.0632	-0.1379	-0.0326	0.2144	0.0305	0.3524
	b	-0.055	-0.2094	0.0370	0.3266	0.0923	0.5360

Reactivity of R-CH=CH$_2$ group can be explained based on interaction energy between Lewis and non-Lewis natural bonding orbital. In AMSD molecule, π-electrons of R-CH=CH$_2$ group are stabilized by anti-bonding π orbital (π*-orbital) of C$_2$-C$_7$ bond and σ* anti-bonding orbital of C$_9$-C$_{10}$ bond, stabilization energies are 9.50, 6.00 kcal/mol respectively. Figure 3.22 depicts the alteration of frontier orbital shapes in free AMSD and AMSD IC. In AMSD-β-CD IC, π-electrons of R-CH=CH$_2$ group stabilized by π*-orbital of C$_{175}$-C$_{176}$ (for set b, C$_{175}$-C$_{184}$) with the stabilization energies in the range of 8.34- 9.02 kcal/mol. In case of AMSD-DM-β-CD IC, the stabilization energy of π-electrons is of the order of 8.01-10.93 kcal/mol with the anti-bonding π*-orbital of C$_{217}$-C$_{218}$. This stabilization energy indicates that reactivity of R-CH=CH$_2$ group is in the order, AMSD > AMSD-DM-β-CD > AMSD-β-CD IC.

3.5 Conclusions

AMSD forms IC with β-CD and DM-β-CD. AMSD-DM-β-CD IC has greater thermal stability at higher temperature as shown by NMR data and thermogravimetric analysis. The low water solubility of AMSD-β-CD IC and high water solubility of AMSD-DM-β-CD IC was attributed to their crystalline and amorphous nature respectively which was confirmed by XRD analysis. Allylic CH$_2$ of AMSD remains inside the cavity in case of AMSD-β-CD IC whereas it remains outside the cavity in AMSD-DM-β-CD as shown by molecular modeling analysis. The extent of insertion of AMSD in both the complexes inside the CD cavity also affects its reactivity. The reactivity of R-CH=CH$_2$ group in the order, AMSD > AMSD-DM-β-CD > AMSD-β-CD IC was explained on

the basis of NPA, NBO methods, Fuki functions and interaction energy between Lewis and non-Lewis natural bonding orbital. Water soluble AMSD-DM-β-CD IC could be used for the synthesis of water soluble macromonomers in aqueous media. This has been described in chapter 5.

3.6 References

1. Szejtli J. Cyclodextrin Technology, Kluwer Academic Publisher, Dordrecht, 1988, 450.

2. Glockner P., Ritter H. Macromol. Rap. Comm., 1999, 20(11), 602.

3. Lau W. Macromol. Symp. 2000, 182, 283.

4. Harada A. Coordination Chemistry Reviews 1996, 148, 115.

5. Rusa C., Tonelli A. Macromolecules 2000, 33, 5321.

6. Rusa C., Luca C, Tonelli A. Macromolecules 2001, 34, 1318.

7. Okumura H., Okada M., Kawaguchi Y., Harada A. Macromolecules, 2000, 33(12), 4297.

8. (a) Glockner P., Ritter H. Macromol. Chem. and Phys. 2000, 201 (17), 2455. (b) Glockner P., Metz N., Ritter H. Macromolecules 2000, 33 (11), 4288.

9. Kollisch H., Barner–Kowollik C., Ritter H. Macromol. Rap. Commun. 2006, 27, 848.

10. Sato E., Zetterlund P., Yamada B. Macromolecules 2004, 37 (7), 2363.

11. McHale R., Aldabbagh F., Carroll W., Yamada B. Macromol. Chem. and phy. 2005, 206, 2054.

12. Hirano T., Yamada B. Polymer 2003, 44, 347.

13. Villiers A. Compt. Rend. 1891, 112, 536.

14. Schardinger F. Zentralbl. Bakteriol. Parasintenk Abt. 1911, 29, 188.

15. Pringsheim H. Chemistry of the saccharides, McGraw-Hill, New York, 1932, 280.

16. Szejtli J. Cyclodextrin Technology, Kluwer Academic Publisher, Dordrecht, 1988, 450.

17. Sabadini E., Cosgrovea T., Egídio F. Carbohydr. Res. 2006, 341, 270.

18. Saenger W. Angew. Chem. Int. Ed. Engl. 1980, 19, 344.

19. Pitha J., Cyclodextrin derivatives with enhanced solubility power and lower toxicity, Proc. of 9th Int. Symposium on Cyclodextrins, Santiago de Compostela, 1998.

20. Takeo K., Kuge T., Starch / Starke 1976, 28 (7), 226.

21. Rao T., Pitha J. Carbohydr. Res. 1991, 200, 209.

22. Aman M., Reuscher H., Wimmer T., Hirsenkorn R., Rational design of cyclodextrin derivatives benefits that pay off in applications, 209th ACS National Meeting, Anaheim CA, 1995.

23. Stella V., Rajewski R., 1991, WO 9111172.

24. Connors A. Chem. Rev. 1997, 97 (5), 1325.

25. Hedge A. Chem. Rev. 1998, 98, 2035.

26. Davis M., Brewster M. Nature reviews: Drug discovery 2004, 3, 1023.

27. Harata K., Kawano K. Carbohydrate research 2002, 337 (6), 537.

28. Jiao H., Goh S., Valiyaveettil S. Macromolecules 2001, 34, 8138.

29. Jiang H., Sun H., Zhang S., Hua R., Xu Y., Jin S., Gong H., Li L. Journal of inclusion phenomena and macrocyclic chemistry, 2007, 58 (1-2), 133.

30. Gidley M., Bociek S. J. Am. Chem. Soc., 1988, 110, 3820.

31. Harada A., Li J., Kamachi M. Macromolecules 1993, 26, 5698.

32. Takahashi K. Chem. Rev. 1998, 98, 2013.

33. Breslow R, Campbell P. J. Am. Chem. Soc. 1969, 91, 3085.

34. Wenz G. Angew. Chem. 1994, 106, 851.

35. Ritter H., Tabatabai M. Prog. Polym. Sci. 2002, 27, 1713.

36. Lau Willie May 1996, US Patent 5,521,266.

37. Golbs S., Oettel M., Dittgen M., Graser T., Luders S. May 2001 US Patent 6,225,299.

38. MacroModel, version 9.0, Schrodinger, LLC, New York, NY, 2005.

39. Frisch M., Trucks G., Schlegel H., Scuseria G., Robb M., Cheeseman J., Montgomery Jr. J., Vreven, T.; Kudin, K. N.; Burant, J. C.; Millam, J. M.; Iyengar, S. S.; Tomasi, J.; Barone, V.; Mennucci, B.; Cossi, M.; Scalmani, G.; Rega, N.; Petersson, G. A.; Nakatsuji, H.; Hada, M.; Ehara, M.; Toyota, K.; Fukuda, R.; Hasegawa, J.; Ishida, M.; Nakajima, T.; Honda, Y.; Kitao, O.; Nakai, H.; Klene, M.;

Li, X.; Knox, J. E.; Hratchian, H. P.; Cross, J. B.; Adamo, C.; Jaramillo, J.; Gomperts, R.; Stratmann, R. E.; Yazyev, O.; Austin, A. J.; Cammi, R.; Pomelli, C.; Ochterski, J. W.; Ayala, P. Y.; Morokuma, K.; Voth, G. A.; Salvador, P.; Dannenberg, J. J.; Zakrzewski, V. G.; Dapprich, S.; Daniels, A. D.; Strain, M. C.; Farkas, O.; Malick, D. K.; Rabuck, A. D.; Raghavachari, K.; Foresman, J. B.; Ortiz, J. V.; Cui, Q.; Baboul, A. G.; Clifford, S.; Cioslowski, J.; Stefanov, B. B.; Liu, G.; Liashenko, A.; Piskorz, P.; Komaromi, I.; Martin, R. L.; Fox, D. J.; Keith, T.; Al-Laham, M. A.; Peng, C. Y.; Nanayakkara, A.; Challacombe, M.; Gill, P. M. W.; Johnson, B.; Chen, W.; Wong, M. W.; Gonzalez, C.; Pople, J. A.; Gaussian 03, Revision C.02; Gaussian, Inc., Wallingford CT, 2004.

40. SYBYL 6.9. Tripos Inc., 1699 Hanley Road, St. Louis, MO 63144.

41. Morris M., Goodsell S., Halliday S., Huey R., Hart E., Belew K., Olson J. J. Comput. Chem. 1998, 19 (14), 1639.

42. Berendsen C., Postma M., Gunsteren V., DiNola W., and Haak R., J. Chem. Phys., 1984, 81 (8), 3684.

43. Case A., Pearlman A., Caldwell W., Cheatham E. III, Wang J., Ross S., Simmerling L., Darden A., Merz M., Stanton V., Cheng L., Vincent J., Crowley M., Tsui V., Gohlke H., Radmer J., Duan Y., Pitera J., Massava I., Seibel L., Singh C., Weiner K., Hornak V., Cui G., Schafmeister C., Gohlke J., Kollman A. AMBER8.0, University of California: San Francisco, CA, 2004.

44. Williams R., Mahaguna V., Sriwongjanya M. Eur. J. of pharm. and biopharm. 1998, 46 (3), 355.

45. Liu l., Zhu S. J. of pharm. and biomed. analysis 2006, 40 (1), 122.

46. Casper P., Glockner P., Ritter H. Macromolecules, 2000, 33 (12), 4361.

47. Liu L., Zhu S. Carbohydrate polymers 2007, 68 (3), 472.

48. Harata K., Kawano K. Carbohydrate research 2002, 337 (6), 537.

49. Li N., Liu J., Zhao X., Gao Y., Zheng L., Zhang J., Yu L. Colloids and surfaces A : Physicochem. Eng. Aspects 2007, 292 (2-3), 196.

50. Satav S., Karmalkar R., Kulkarni M., Mulpuri N., Sastry N. Macromolecules 2007, 40 (6), 1824.

51. Bratu I. Astilean S., Ionesc C., Indrea E., Huvenne J., Legrand P. Spectrochimica Acta Part A 1998, 54 (1), 191.

52. Okada M., Kamachi M., Harada A. Macromolecules 1999, 32 (21), 7202.

53. Harada A., Li J., Kamachi M. Macromolecules 1993, 26 (21), 5698.

54. Hall D., Lim K. J. Am. Chem. Soc. 1986, 108 (10), 2503.

Chapter 4

Chain transfer activity of AMSD and its complex in the polymerization of MMA

4.1 Introduction

A variety of approaches for the synthesis of polymer architectures such as block, graft, star polymers and dendrimers are being developed by researchers in view of distinctive properties offered by these materials *vis a vis* random copolymers (Wohlrab 2000, Ito 1983). Branching in polymers is a useful structural variable which can be used to modify the processing characteristics and properties of the polymers such as crystallinity, glass transition temperature and viscoelasticity (Dlubek 2002). Grafting is a very useful technique to introduce branching in polymers.

Graft copolymers containing hydrophobic and hydrophilic micro domains exhibit a variety of morphologies such as micelles and vesicles, which as carriers improve solubility, stability and bioavailability of drugs (Lo 2007). They are also used as compatibilizers to improve the mechanical properties of the polymers and as stabilizers during the synthesis of microspheres. They are also very useful in membrane separation science (Bhattacharya 2004) and exhibit thermotropic smectic mesophases with mesogenic groups that do not generate mesophases with other types of main chains (Gallot 1996). They give the highest binding ability with the oligonucleotide (Deshpande 2002) and applied in cartilage and bone tissue engineering (Wang 2003).

Graft copolymers are generally prepared by three general methods 'grafting onto', 'grafting from' and 'grafting through' (Pistikalis 1998). The 'grafting onto' method involves a coupling reaction between the backbone and the branches which are prepared separately by a living polymerization mechanism. In 'grafting from' method, active sites are generated along the main chain backbone which can initiate the polymerization of the second monomer and results in the formation of branches and the final graft copolymer. In 'grafting through' method, polymer chain having polymerizable end group known as macromonomers are copolymerized with another monomer so as to obtain graft copolymers (Ito 1998). For the synthesis of graft copolymers 'Grafting through' which involves the copolymerization of macromonomers with vinyl monomers is preferred over generating a radical on the polymer backbone followed by grafting the vinyl monomer on the backbone (Joshi 2007).

Macromonomers bearing unsaturated end groups i.e. 2–substituted 2–propenyl end groups have attracted considerable attention as useful precursors for the synthesis of graft copolymers. (Cacioli 1986), (Yamada 1992, 1993), (Kobatake 1997), (Nair 1999), (Yamada 2003). Macromonomers can be prepared by different methods such as carrying out polymerization in the presence of initiator, (Ishizu 1990) chain transfer agents (Kobayashi 1989), (Kennedy and Hiza 1983), (Kitayama 1991), (Yamashita 1982), (Akashi 1989) or by end capping method, (Milkovich 1980), (Rempp 1984), (Rao 1984), (Asami 1986) living radical polymerization (Vergas 1980), (Uryu 1986), (Aoshima 1985) and using addition–fragmentation chain transfer (AFCT) agents. Macromonomers can be prepared by a two step synthesis involving polymerization of vinyl monomers in the presence of functional initiators and functional chain transfer agents followed by the condensation of a methacryloyl unit with the end group (Yamashita 1982, Akashi 1989, Ito 1983). A single step synthesis is obviously desirable. But, these methods do not provide good control over molecular weight and functionality. This can also be achieved by living polymerization methods such as anionic or cationic or atom transfer radical polymerization However, these methods are restricted to few monomers and require stringent reaction conditions.

Among all the above methods, AFCT has received considerable attention because the chain transfer agents available have sufficiently high reactivity towards propagating radicals and hence can efficiently introduce ω–unsaturated chain ends. Also, it can be applied to a wide range of vinyl monomers and can be carried out in organic as well as aqueous medium. In AFCT mechanism (figure 4.1), polymer radical adds to the terminal double bond of AFCT agent and then the adduct radical undergoes fragmentation to give a polymer with a terminal double bond.

Hirano et. al. (2003) and McHale (2005) have described the effect of sterically hindered monomer and AFCT agent on the addition fragmentation chain transfer mechanism of ethyl methacrylate, cyclohexyl methacrylate and styrene. The authors concluded that efficient macromonomer synthesis could be achieved in AFCT polymerization of methacrylates by manipulating steric hindrance of the AFCT agents.

The reactivity of the monomers and chain transfer agents is significantly altered on complexation with cyclodextrin (CD) (Glockner et. al. 2000). Higher chain transfer constant values were obtained for complexed monomers (C_s for methyl methacrylate (MMA)-dimethylated (DM)-β-CD IC = 1.7± 0.3 and C_s for Styrene-DM-β-CD = 2.6 ± 0.3) as compared to the polymerization of uncomplexed monomers (C_s for MMA = 0.7± 0.1 and C_s for Styrene = 0.7± 0.1) in organic solvent. The values of the CTC of dodecanethiol in the polymerization of MMA and Styrene in DMF / water were 3.1 and 3.4. The corresponding values for DM-β-CD complexes of MMA, Styrene and dodecanethiol in aqueous medium were 0.5 and 2.2.

A study of structure performance relationship of oligomers of α methyl vinyl monomers revealed that incorporation of bulkier substitutents in the chain transfer agent resulted in enhanced addition fragmentation efficiency and terminal unsaturation content. In this chapter, the investigation was undertaken to explore if the same result is achieved by enhancing the effective size of the AFCT agent as a result of inclusion complexation α-methyl styrene dimer (AMSD) with β-CD and DM-β-CD. If so, the approach could be explored for the synthesis of macromonomers containing terminal unsaturation. The chain transfer constants of AMSD and its inclusion complex in the polymerization of MMA were evaluated using Mayo's method and are explained on the basis of the disposition of the allylic CH$_2$ inside the CD cavity. We concluded that though IC formation lowers the CTC of AMSD in the polymerization of MMA, it results in macromonomers containing terminal unsaturation with functionality equal to unity. Further, these macromonomers were copolymerized to obtain graft copolymers. The resulting graft copolymers exhibited pH dependent swelling rather than dissolution exhibited by random copolymers of identical composition. This chapter starts with the brief overview of AFCT, its mechanism, different chain transfer agents and favorable experimental conditions followed by the implications of AMSD ICs for the macromonomer synthesis and their graft copolymers.

4.2 Addition fragmentation chain transfer polymerization

4.2.1 History

Reversible addition-fragmentation chain transfer (RAFT) polymerization has been the focus of intensive research over the past few years. This is because it helps to tailor macromolecules with complex architectures including block, graft, comb and star structures with predetermined molecular weight, terminal functionality and narrow molecular weight distribution. The first report of the radical addition fragmentation process appeared in early 1970s (Giese 1986, Motherwell 1992) such as the Keck reaction [Keck 1985] and the Bartone McCombie deoxygenation process with xanthates [Barton 1975]. The first report of the use of addition fragmentation chain transfer agents to control radical polymerization appeared in the late 1980s (Meijs 1988, Cacioli, 1986). Reversible addition fragmentation chain transfer polymerization discovered by researchers at CSIRO in the late 1990s (Chiefari 1998, Mayadunne 1999, Hawthorne 1999, Chong 1999, Moad 2000).

AFCT agents and their applications to control molecular weight and end group functionality have been exclusively reviewed (Rizzardo 1995, Colombani 1999, Yamada 1994, Moad 2008).

4.2.2 Addition-fragmentation chain transfer polymerization

Addition-fragmentation transfer agents and mechanisms whereby these reagents provide addition-fragmentation chain transfer during polymerization are shown in figure 4.1.

Unsaturated compounds of general structure 1 or 4 can act as transfer agents by a two-step addition-fragmentation mechanism. In these compounds C=X should be a double bond that is reactive towards radical addition. X is most often CH_2 or S. Z is a group chosen to give the transfer agent an appropriate reactivity towards propagating radicals and confer appropriate stability to the intermediate radicals (2 or 5, respectively).

Examples of A are CH_2, $CH_2=CHCH_2$, O or S. R is a homolytic leaving group and R· should be capable of efficiently reinitiating polymerization. Since functionality can be introduced to the products 3 or 6 in either or both the transfer (typically from Z) and

reinitiation (from R) steps, these reagents offer a route to a variety of end-functional polymers including telechelics.
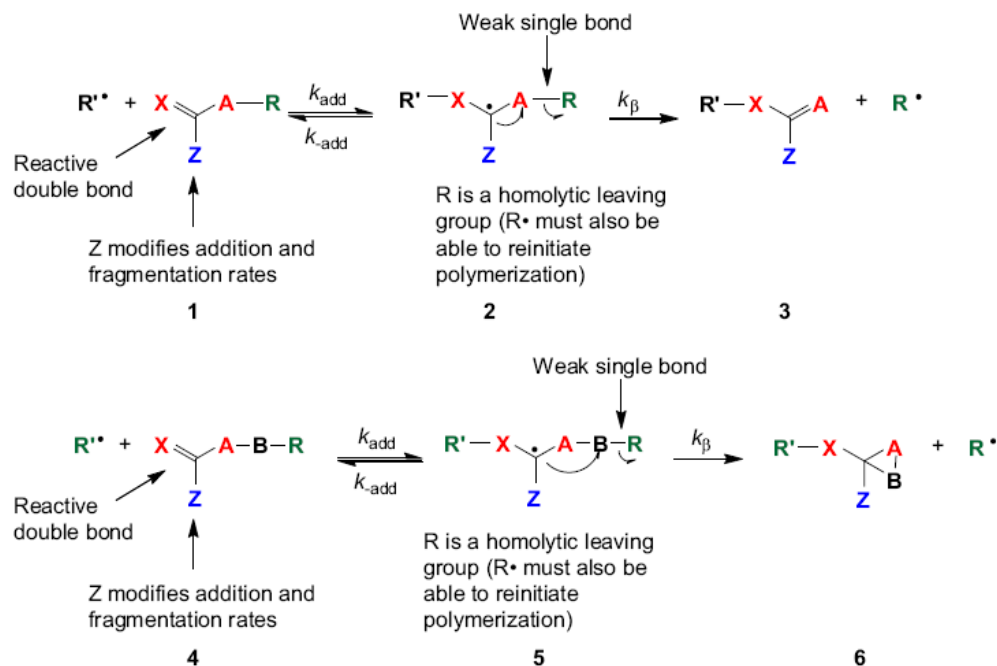
Figure 4.1 Mechanism for addition fragmentation chain transfer (Moad 2008)

Rates of addition to transfer agents 1 and 4 with $X=CH_2$ are determined by the same factors that determine rates of addition to monomer. Thus, substituents at A (i.e. R, B-R) have only a minor influence on reactivity, consequently the double bonds of the transfer agents 1 and 4 with $X=CH_2$ have a reactivity towards radical addition that is similar to that of the common monomers they resemble. Thus, with efficient fragmentation, transfer constants (C_{tr}) can be close to unity. A C_{tr} of unity has been called 'ideal' since the transfer agent and monomer are consumed at the same rate and, as a consequence, the molecular weight should remain essentially constant with monomer conversion [Corner 1984].

Efficient transfer requires that the radical intermediates formed by addition undergo facile β-scission (for 1) or rearrangement (for 4) to form a new radical that can reinitiate polymerization. The radical intermediates 2 and 5 typically have low reactivity towards further propagation and other intermolecular reactions because of steric crowding about the radical centre.

The driving force for fragmentation of the intermediate radical is provided by cleavage of a weak A-R or B-R bond and / or formation of a strong C=A bond (for 1). If both addition and fragmentation are rapid and irreversible with respect to propagation the polymerization kinetics differ little from those seen in polymerization with conventional chain transfer. If the overall rate of β-scission is slow relative to propagation then retardation is a likely result. If fragmentation is slow, adducts (2 or 5) also have a greater potential to undergo side reactions by addition to monomer (copolymerization of the transfer agent) or radical-radical termination. Retardation is often an issue with high k_p monomers such as vinyl acetate (VAc) and methacrylic acid (MAA). In designing transfer agents and choosing an R group, a balance must also be achieved between the leaving group ability of R and reinitiation efficiency of $R^\bullet$ since, as with conventional chain transfer, the rate constant for reinitiation by $R^\bullet$ should be $\geq k_p$. If fragmentation leads preferentially back to starting materials the transfer constants are low.

The design of transfer agents that give reversible addition-fragmentation chain transfer (RAFT) has provided one of the more successful approaches to living radical polymerization and is described in the next section.

4.2.3 Reversible addition fragmentation chain transfer (RAFT) polymerization

The reverse pathway can also be blocked by choice of A. For example, when A is oxygen (e.g., vinyl ethers, thionoesters) or bears a substituent (e.g., A = CH-CH$_3$), the product is rendered essentially unreactive to radical addition.

'Macromonomers' have been known as potential reversible transfer agents in radical polymerization since the mid 1980s [Cacioli 1986].

In 1995, it was reported that polymerizations of methacrylic monomers in the presence of methacrylic macromonomers (7, X = CH$_2$, Z = CO$_2$R) under monomer-starved conditions display many of the characteristics of living polymerization [Krstina 1995, Krstina 1996]. These systems involve the RAFT mechanism (figure 4.2).
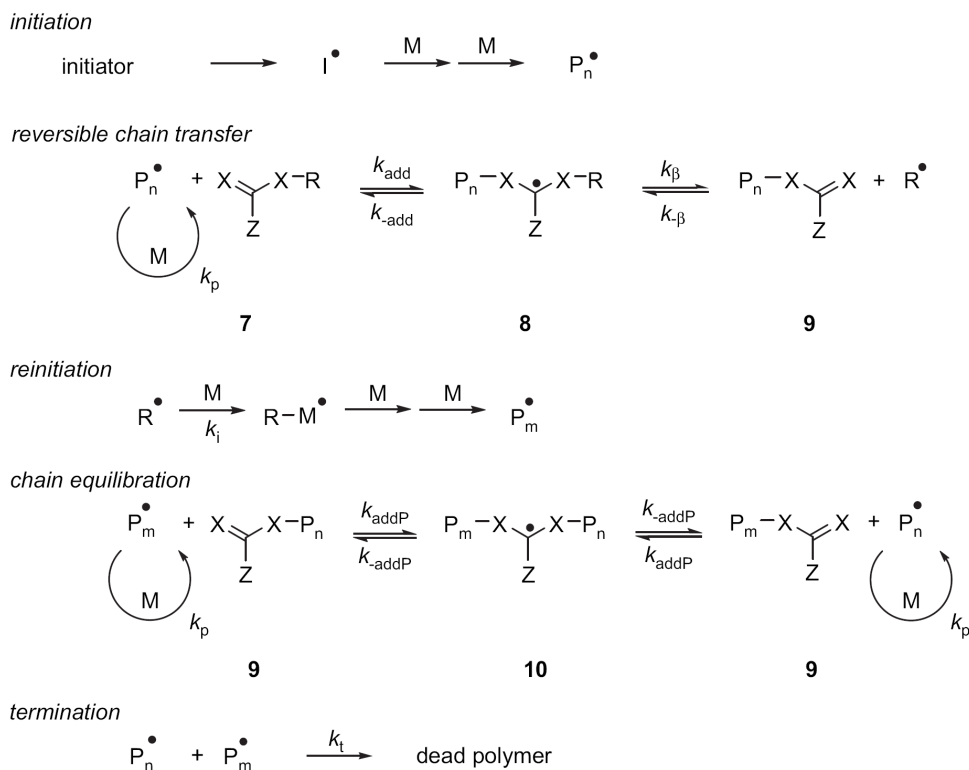
Figure 4.2 Mechanism of RAFT Polymerization (Moad 2008)

4.2.4 Addition-fragmentation chain transfer agents (figure 4.3)

4.2.4.1 Vinyl ethers

The vinyl ethers (1, X = CH$_2$, A =O) are very effective addition-fragmentation chain transfer agents [Meijs 1988, Rizzardo 1995, Meijs 1990, Dais 1993]. The driving force for fragmentation is provided by formation of a strong carbonyl double bond. It is also important that R is a good radical leaving group. The examples with an R = benzyl are appropriate for use in S or (meth)acrylate ester polymerization but give retardation in polymerization of VAc and related monomers because benzyl radical is slow to initiate these polymerizations. Even traces of acidic impurities in the monomer or the polymerization medium can catalyze decomposition of the vinyl ethers and hence are not suitable for the acidic monomers.
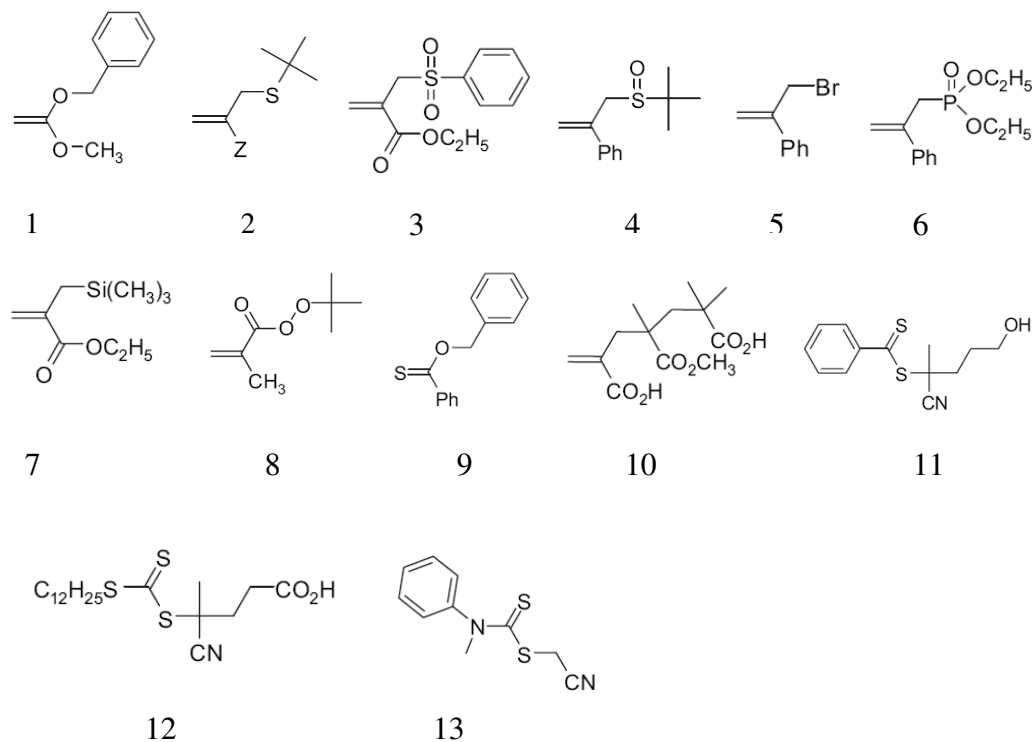
Figure 4.3 AFCT and RAFT agents 1. Benzyl vinyl ethers, 2. Allyl sulfides, 3. Allyl sulfones, 4. Sulfoxides, 5. Allyl halides, 6. Phosphonates, 7. Silanes, 8. Allyl peroxides, 9. Thionoesters, 10. MMA trimer, 11. Dithioesters, 12. Trithiocarbonate, 13. Dithiocarbamates

4.2.4.2 Allyl sulfides, sulfones, halides, phosphonates, silanes

Allyl transfer agents (1, X = CH_2, A = CH_2) include allyl sulfides [Meijs 1988, Meijs 1991, Mathias 1992], allyl sulfones [Meijs 1990] and sulfoxides [Meijs 1990, Sato 1995], and allyl halides [Meijs 1990, Yamada 1994, 1991, 1990, 1992, 1991, 1993], phosphonates [Meijs 1990], silanes [Meijs 1990]. Allyl bromides give predominantly chain transfer whereas the chlorides undergo copolymerization as well as chain transfer [Meijs 1990, Yamada 2003]. The silanes too copolymerize and as well as acts as chain transfer agents [Meijs 1990]. Allyl ethers (1, R = alkoxy, X = A = CH_2) may give degradative chain transfer by hydrogen abstraction.

4.2.4.3 Thionoester and related transfer agents

Thione derivatives [Meijs 1991, 1991, 1992] also are very effective as addition-fragmentation chain transfer agents.

4.2.4.4 Allyl peroxides

In the case of allyl peroxides (4, X = CH_2, A = CH_2, B = O, R = O-alkyl) [Meijs 1992, Shanmugananda 1996, Colombani 1994, 1994, 1995], intramolecular homolytic substitution on the O-O bond gives an epoxy end group (1,3-S_Hi mechanism). They may, however, be thermally unstable at higher temperatures.

4.2.5 Reversible addition-fragmentation chain transfer agents

A wide variety of macromonomer (7, X = CH_2) and thiocarbonylthio RAFT agents (7, X = S) have been reported.

4.2.5.1 Macromonomers

Macromonomers (7, X = CH_2, R = polymer chain) can react by a RAFT mechanism. The most reported transfer agents of this class are the methacrylate macromonomers (figure 4.4). The macromonomer chain end is also identical in structure to the unsaturated chain end formed by termination by disproportionation [Tanaka 1989]. Some examples of block copolymers synthesized by macromonomer RAFT polymerization are reported by Moad et. al. [Moad 2006].
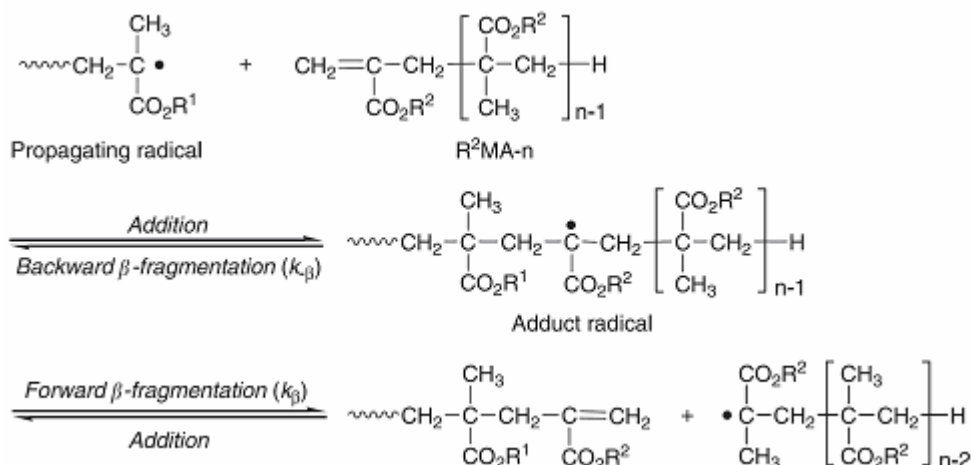
Figure 4.4 Reactions of poly(methacrylate R^1 ester) radical and unsaturated oligomer of methacrylate R^2 ester and fragmentation of adduct radical (Bon 2000)

4.2.5.2 Thiocarbonylthio compounds

Thiocarbonylthio RAFT agents include certain dithioesters, trithiocarbonates, xanthates, dithiocarbamates and other compounds. The use of bis- and multi-RAFT agents permits

the synthesis of polymers with complex architectures. Symmetrical trithiocarbonates can also be considered as a member of the class of bis-RAFT agents.

4.2.5.3 Dithioesters

A wide range of dithioester RAFT agents have been reported. Examples of unprotected functionality that have been incorporated into the 'R' fragment of dithiobenzoate RAFT agents include hydroxyl, carboxylic acid/carboxylate, sulfonic acid/sulfonate, azide, olefin and siloxane.

Dithiobenzoates and similar dithioesters with Z = aryl are amongst the most active RAFT agents and with appropriate choice of 'R' have general applicability in the polymerization of (meth)acrylic and styrenic monomers [Moad 2005, Moad 2006]. However, their use can give retardation, particularly when used in high concentrations and with high k_p monomers (acrylates, acrylamides). They are also more sensitive to hydrolysis and decomposition by Lewis acids [Rizzardo 2007] than other RAFT agents.

4.2.5.4 Trithiocarbonates

The utility of trithiocarbonate RAFT agents was disclosed in the first RAFT patent [Le 1998]. A wide range of trithiocarbonate RAFT agents have now been reported, two classes are distinguished. Non-symmetrical trithiocarbonates have only one good homolytic leaving group. The other S-substituent is typically primary alkyl. Symmetrical trithiocarbonates have two good homolytic leaving groups and the trithiocarbonate group remains in the centre of the structure.

4.2.5.5 Dithiocarbamates

N, N' Dialkyl dithiocarbamates and O-alkyl xanthates are most suited for polymerization of vinyl acetate (VAc), N-vinyl pyrrolidone (NVP) and related vinyl monomers where the propagating radical is a poor homolytic leaving group.

4.2.5.6 Xanthates

RAFT polymerization with xanthates is sometimes called MADIX (macromolecular design by interchange of xanthate). O-Alkyl xanthates have been widely exploited for RAFT polymerization of VAc, NVP where the propagating radical is a relatively poor homolytic leaving group. They are generally less effective (have low transfer constants)

in polymerization of styrenic and acrylic monomers and offer no control for methacrylic polymers.

4.2.5.7 Other RAFT Agents

Dithiophosphinate esters have been shown to provide some control over styrene polymerization and they have been used to prepare polystyrene-b-PVAc [Gigmes 2003].

4.2.6 Structural requirements for fragmentation
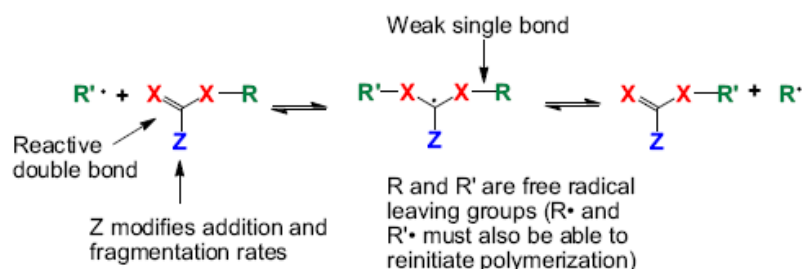
Figure 4.5 Structural requirements for AFCT agent (Moad 2005)

4.2.6.1 Z group

The Z group mainly influences the transfer rate. It should activate the double bond so that the addition rate can compete with the propagation rate, while stabilizing the intermediate radical (IR) as little as possible to favor a high fragmentation rate. However, the more Z activates the double bond, the more it stabilizes the IR. In the case of a monomer corresponding to a poorly stabilized propagating radical (e.g. vinyl acetate), a complete inhibition of the polymerization can be observed in the presence of dithiobenzoates.

4.2.6.2 R group

The R group mainly influences the fragmentation reaction selectivity and the re-initiation step. Above all, $R^\bullet$ should be a better leaving group (figure 4.6) than the propagating radical considering equilibrium (I) of the reversible addition-fragmentation reaction (Moad 2000, Favier 2002).

To obtain a fast and quantitative initiation step, equilibrium (I) should be strongly displaced in favor of the fragment radical $R^\bullet$. However, $R^\bullet$ should not be too stabilized

to ensure a fast and efficient initiation of new chains. In general, the better the leaving group R slower is the re-initiation rate. Although the fragment radicals $R^\bullet$ of the usual CTA are able to rapidly add monomer units, (Moad 2002) they can add preferentially to a CTA rather than to a monomer unit, thus they contribute to the retardation phenomenon (Chong 2003) and probably to an induction period. To avoid such problems, fast propagating $R^\bullet$ should be preferred.
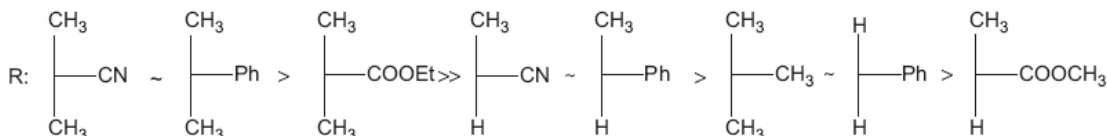
Figure 4.6 Order of R group leaving ability in RAFT

4.2.6.3 Nature and size of the labile fragment

The driving force for fragmentation has to be high enough to compete with propagation. Either the steric hindrance can be increased in the intermediate free adduct radical to inhibit almost totally the possibility of copolymerization or a small strain can be introduced in the transient radical in order to force its fragmentation. The intramolecular process may also be favored by the formation of a more stable radical than the adduct radical formed through addition or more simply by choosing higher polymerization temperatures. The elimination of a stable molecule is an important driving force for the fragmentation reaction.

4.2.6.4 Relief of strain

The relief of strain is often claimed to be one of the main factors affecting the competition between fragmentation and propagation reactions.

4.2.6.5 Stereoelectronic factors

In strained structures, the molecular flexibility needed for adopting an appropriate conformation for the intramolecular reaction leading to fragmented structures which cannot be obtained in the presence of some rigid groups. In the fragmentation of a C–C bond adjacent to a radical center, the bond which can meet the maximum degree of coplanarity with the semi-occupied p orbital of the radical is stereoelectronically favored to break the transition state. (Favier 2006)

The addition rate coefficient (k_{add}) depends on the reactivity of the radical and of the CTA, which involves resonance, polar, and steric effects. According to Moad and Solomon (1995), the substituents that bear a p-orbital (e.g. phenyl) induce an increase in k_{add} by resonance, in comparison with substituents that bear an atom with a lone pair (e.g., halogens, –OR, –NR$_2$, –SR). Concerning the polar effects, the electron-withdrawing substituents (e.g., halogens, –COOR, –CN) lead to an increase in k_{add}, since the attacking radicals are mostly nucleophilic.

The fragmentation rate depends on the intermediate radical (IR) substituents as well as on the experimental conditions. The fragmentation reaction is an intramolecular reaction, thus favoured over the other reactions (intermolecular) when the IR is sterically hindered and when monomer concentration is low, temperature is high and pressure is low (Moad 1995, Colombani 1999).

4.2.6.6 Influence of the monomer

The nature of the monomer has a strong influence on the addition and the fragmentation rates. Generally, a more stabilized and sterically hindered propagating radical requires the use of a CTA with a more activated thiocarbonyl function, more stabilized and sterically hindered R. Considering dormant chains (macroCTA), the substitutents on the monomer, P_n also has a great influence on the fragmentation rate. The more stabilized and sterically hindered the P_n substituent, the weaker the S–P_n bond and the higher the fragmentation rate.

Two major cases that lead to a low polymerization control can be distinguished: i) Z sufficiently activates the C=S relative to the reactivity of $P_n^\bullet$ but R is a poor leaving group [Otsu 2000] and ii) Z does not sufficiently activate the C=S relative to the reactivity of $P_n^\bullet$ but R is a good leaving group (Favier 2002).

When Z is a poor C=S activating group [Grignard 2007] or when R is a very poor leaving group relative to the monomer [Klemm 1993], the polymerization is definitively not controlled.

4.2.7 Influence of experimental conditions

4.2.7.1 Influence of temperature and pressure

In addition-fragmentation reaction, an increase in temperature favors the fragmentation reaction in comparison with intermolecular reactions (Colombani 1999) in the cases where IRs are well stabilized, a reduced retardation and an improvement of the molecular weight control can be obtained (Favier 2004). RAFT process, the addition and the fragmentation rates are thus expected to increase and decrease, respectively, with increasing pressure (Arita 2004). This is because the rate of decomposition of the initiator decreases and the rate of propagation increases with increase in pressure.

4.2.7.2 Influence of the concentration of the polymerization medium

The viscosity of the polymerization medium influences both the kinetics and MWD control. First, the polymerization rate increases with concentration (Favier 2004). Second, a high viscosity induces a decrease in the rate of the diffusion controlled reactions (like termination, Trommsdorff effect and, probably, addition of active chains onto dormant chains), which favors an acceleration of the polymerization rate, reduces the number of active/dormant cycles and thus broadens the MWD (Wang 2003). On the contrary, dilution favors intramolecular reactions, such as fragmentation and transfer to polymer (backbiting), as well as transfer to solvent (Lowe 2007).

Some α-(substituted methyl) acrylates e.g. α-(alkylthiomethyl) acrylate (Meijs 1988, Meijs 1990, Yamada 1992, Bon 2000, Sato 1995) function as AFCT agents during polymerization of conjugated monomers such as MMA, St, Ma and cyclohexyl acrylate but not in the case of non conjugated monomers such as VAc (Sato 1995, Meijs F., 1991, Rizzardo 1995).

Certain α-(substituted methyl) acrylates undergo AFCT through carbon–carbon bond homolysis, resulting in the carbalkoxypropenyl o-end-groups (Cacioli 1986). The effects of MMAD, MMA-3, MMA-4, and higher oligomers (MMA-n, 13) on MMA polymerization have been studied in detail (Moad 1996) HEMA-2, the trimers of nBMA and methacrylic acid (MAA), the mixed trimer of HEMA–MMA, and HEMA oligomer were used as AFCT agents in MMA polymerization (Hutson 2004) MeSt

dimer ($CH_2=C(C_6H_5)CH_2C(CH_3)_2C_6H_5$, AMSD), which is a low reactivity monomer in copolymerization at 100°C or below acts as an effective AFCT agent at 140°C (Yamada 1994, Watanabe 1993). It undergoes β-fragmentation of the adduct radical to generate a cumyl radical and a phenyl propenyl o-end-group bound to poly(St). The β-fragmentation reaction becomes increasingly significant with increasing temperature as a result of the activation energy of fragmentation being higher than that of the bimolecular reaction.

Among the dimers, those bearing the alpha methyl styrene moiety in the alpha substituent are noted as highly reactive chain transfer agents. The chain transfer constant for AMSD during polymerization of methyl methacrylate at 110°C was found to be 0.13. (Yamada 1994) Alpha methyl styrene dimer (AMSD) is known as an addition fragmentation agent for organic system (Watanabe 1993). It regulates the molecular weight and also introduces the terminal unsaturation in the polymer.

Watanabe et. al. (1993) (figure 4.7) proposed the chain transfer mechanism of AMSD through addition fragmentation polymerization. In this mechanism, polymer radical adds to the terminal double bond of AMSD and then the adduct radical undergoes fragmentation to give a cumyl radical and a polymer with a terminal double bond. This is due to the greater stability of the cumyl radical being tertiary radical as compared to polymer radical, which is secondary radical.
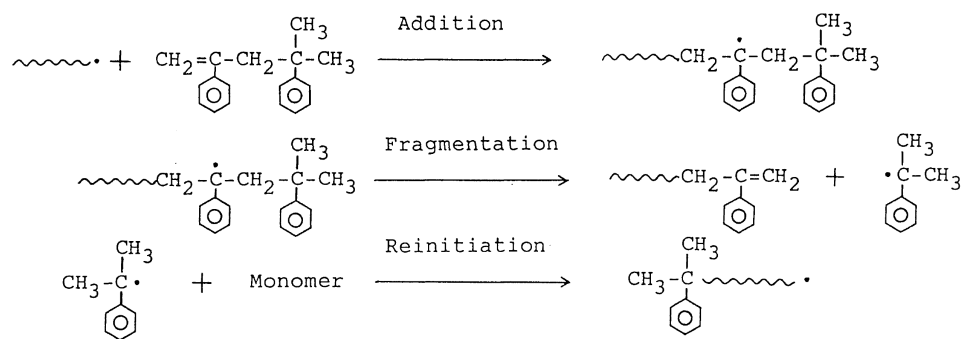
Figure 4.7 Addition fragmentation chain transfer mechanism in AMSD (Watanabe 1993)

Hirano (2003) and (McHale 2005) described the effect of sterically hindered monomer and AFCT agent on the addition fragmentation chain transfer of ethyl methacrylate,

cyclohexyl methacrylate and styrene. The authors concluded that efficient macromonomer synthesis could be achieved in AFCT polymerization of methacrylates by manipulation of the level of steric hindrance of the AFCT agents.

The use of equimolar amounts of cyclodextrins to dissolve hydrophobic monomers in water and the free radical polymerization of such host-guest complexes has been investigated by Ritter et. al. (Ritter and Tabatabai 2002). The solubility of hydrophobic monomers in water is enhanced as a result of the formation of host-guest ICs of these monomers with CD.

Kollisch et. al. (Kollisch 2006) applied RAFT polymerization during polymerization of DM-β-CD complexed styrene in aqueous medium. The effect of complexation on the chain transfer activity of dodecanethiol and N–acetyl L–cysteine in free radical solution polymerization was reported by Glockner et. al. (2000). The chain transfer activity of the inclusion complex decreases in case of dodecanethiol while it increases in case of N–acetyl L-cysteine. This is because dodecanethiol was used as CTA in the form of the complex to render it water soluble whereas N–acetyl L–cysteine was used as such.

So far, there is no report on the effect of complexation of AFCT agent with CD on its addition fragmentation chain transfer mechanism.

4.3 Experimental section

4.3.1 Materials

Methyl methacrylate (MMA) was obtained from Aldrich and used after distillation. Alpha methyl styrene dimer (AMSD) was purchased from Aldrich. *β-* cyclodextrin (*β-CD*) was purchased from Hi media laboratories and dimethylated-*β-CD* (DMCD) from Wacker Chemie (Germany). HPLC grade chloroform (CHCl$_3$) was obtained from s. d. fine. 2, 2' azo bis isobutyro nitrile (AIBN) was purchased from local supplier.

The solvents N, N' dimethyl formamide (DMF), acetone, methanol, petroleum ether were used after distillation. Deionized water was obtained from Millipore system.

The deuterated solvents D$_2$O, CDCl$_3$ and MeOD were purchased from Aldrich.

4.3.2 Methods

FTIR spectra were recorded on Perkin–Elmer spectrum one. Polymers were mixed with KBr and the spectra were recorded at frequencies from 4000 to 450 cm^{-1}. The resolution

was 4 cm^{-1}. Bruker AV 400 and AV 500 NMR spectrometers were used to record the ^{1}H NMR spectra of macromonomers. The spectra of macromonomers were recorded in CDCl$_3$. Molecular weights of macromonomers were determined at 25°C using Waters alliance model 660 equipped with styragel columns using tetrahydrofuran at a flow rate 1 ml min^{-1}. The columns were calibrated using Poly(MMA) standards. Molecular weights of the graft copolymers were determined in chloroform using Knauer vapour pressure osmometer (VPO) K–7000. Benzil was used as standard for the calibration of the instrument. Differential scanning calorimetric (DSC) measurements were performed under nitrogen at a flow rate of 50 ml min^{-1} on a differential scanning calorimeter (TA instruments, model Q–10). Polymer sample was heated from -80 to 250°C at 10°C min^{-1} and scanned to calculate the glass transition temperature (T_g) of the polymer in subsequent heating cycles.

4.3.3 Synthesis

4.3.3.1 Synthesis of ICs

Synthesis of ICs of AMSD i.e. AMSD–β–CD, AMSD–DM-β–CD and characterization of the inclusion complexes is described in detail in the previous chapter.

4.3.3.2 Polymerization of MMA in presence of AFCT agents
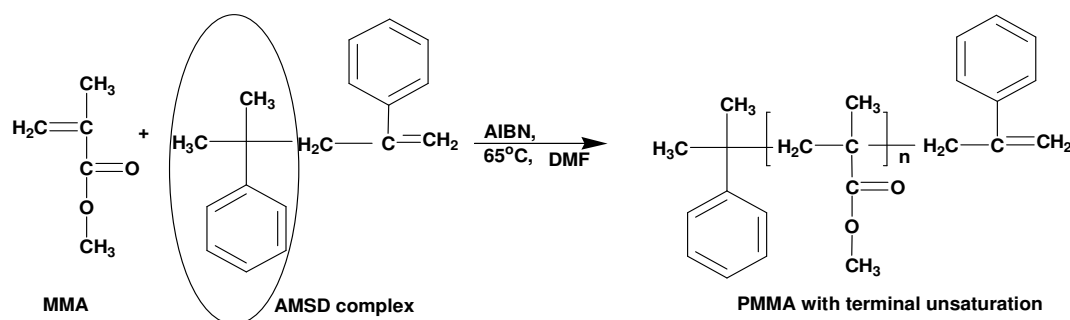
Scheme 4.1 Macromonomer synthesis

MMA and AIBN were dissolved in DMF. The chain transfer agent to be evaluated (varying mole % of AMSD) was added. Nitrogen was purged through the reaction mixture. The polymerization was carried out at 65°C for 18 h. The reaction time was monitored such that the conversion remained below 10 %. The polymer solution was precipitated in water. The precipitate obtained was filtered, dried and washed with

methanol to remove the unreacted AMSD. After drying the polymer (Scheme 4.1) under vacuum, it was characterized by ^{1}H NMR for the unsaturation content.

4.3.3.3 Polymerization of P(MMA) macromonomer with comonomers

P(MMA) macromonomer, DMAEMA and AIBN were dissolved in DMF. Nitrogen was purged through the reaction mixture. The copolymerization was carried out at 65°C for 18 h. The polymer solution was precipitated in water. The precipitate obtained was filtered, dried and washed with pet ether to remove unreacted comonomer and dried under vacuum. The copolymer composition (Scheme 4.2) was determined by ^{1}H NMR.
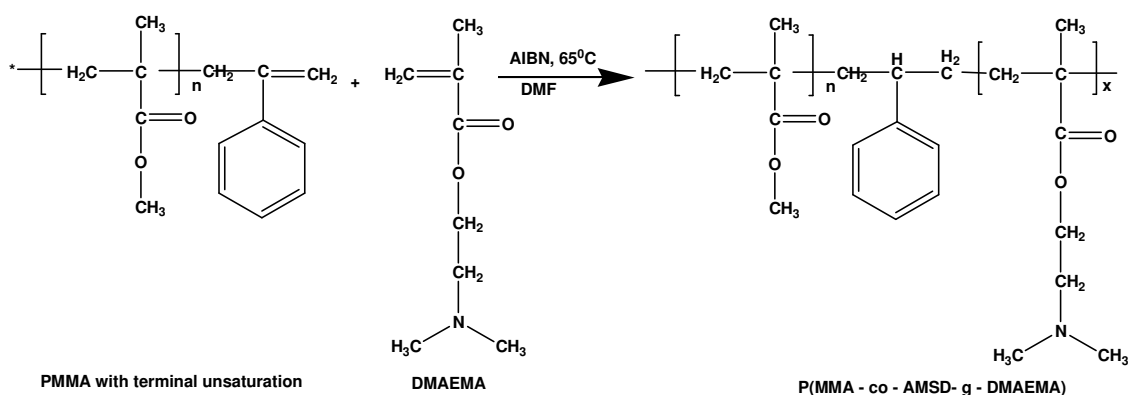
Scheme 4.2 Copolymer synthesis

4.4 Results and discussion

4.4.1 Chain transfer constant : Effect of complexation

Macromonomers bearing terminal unsaturation have been synthesized using radical addition fragmentation chain transfer agents or catalytic chain transfer agents using cobalt complexes. Meijs (1988) reported that *α*-benzyloxy styrene acts as addition fragmentation chain transfer agent in the polymerization of St and MMA. Watanabe et. al. (1993) reported synthesis of macromonomers containing terminal unsaturation using AMSD as the chain transfer agent and showed that the chain transfer involved addition fragmentation mechanism. During this process, the polymer radical adds to the terminal double bond of AMSD and the adduct radical undergoes fragmentation to yield a cumyl radical and a macromonomer bearing a terminal double bond. This is attributed to the stability of the tertiary cumyl radical over the polymer radical, which is secondary. Amongst a number of addition fragmentation chain transfer agents investigated; AMSD

was reported to be the most efficient (Yamada 1994). The efficiency of addition fragmentation was reportedly enhanced with increasing steric hindrance of α substituents (Sato 2004). AMSD–β-CD and AMSD–DMCD ICs were investigated to compare the effect of steric hindrance caused by inclusion complexation on the chain transfer and addition fragmentation efficiency of AMSD.

Polymerization of MMA in DMF was carried out in the presence of 0 to 2 mole % AMSD, AMSD–β-CD and AMSD–DMCD using AIBN initiator (Scheme 4.2). Since AMSD-β-CD IC is soluble only in DMF and DMSO; polymerization could be carried out in these two solvents only. However, the IC is reported to be unstable in DMSO (Zhao 2003). Hence, polymerization was carried out in DMF. Under these conditions, the chain transfer due to DMF and CD derivatives may be neglected ($C_s \sim 0$) (Glockner 2000, Berger 1989). After isolation, the degree of polymerization was determined by GPC using Poly(MMA) standards (Table 4.1). The chain transfer constants were calculated using Mayo's method (Odian 2004). Typical Mayo plots are shown in Figure 8, 9 and 10. The chain transfer constants (figure 4.8, 4.9 and 4.10) obtained were AMSD (5.49), AMSD–DMCD (0.97) and AMSD-β-CD (0.096). Thus, the chain transfer constant of AMSD is significantly lowered on complexation with DMCD and furthermore so on complexation with β-CD.

The value of chain transfer constant of N-acetyl L-cysteine for MMA and St in DMF/ water mixture was 0.7, whereas the corresponding values for DMCD complexes in water were 1.7 and 2.6. In DMF-water medium, the propagation involved reaction between the growing radical and the monomer. In the aqueous medium, the growing radical was the phenyl ring of St or methacrylate group of MMA included in the DMCD cavity. Propagation involved reaction of this growing radical with monomers which formed ICs with DMCD. The chain transfer constant involved reaction with the water soluble chain transfer agent which unlike the monomer was not sterically hindered. As a result propagation was suppressed over chain transfer, resulting in enhanced chain transfer constant in aqueous medium.

The values of the chain transfer constant of dodecanethiol in the polymerization of MMA and St in DMF-water were 3.1 and 3.4. The corresponding values for DMCD

complexes of all the species in aqueous medium were 0.5 and 2.2. In this case, the chain transfer in aqueous medium too involved the reaction between the growing radical species and the DMCD complex of dodecanethiol. This reaction was suppressed over the propagation reaction as compared to the reaction in DMF-water medium wherein none of the species were involved in complexation and were therefore not sterically hindered.

Table 4.1 Chain transfer constant evaluation for AMSD and inclusion complexes

Sr. no.	[S]/[M] mole ratio	AMSD		AMSD-β-CD IC		AMSD–DMCD IC	
		M_n	f	M_n	f	M_n	f
1.	0.0200	1,113	0.21	13,502	1.14	4,515	0.65
2.	0.0133	2,175	0.21	14,380	1.05	7,969	0.98
3.	0.0100	3,358	0.33	15,424	1.07	9,713	0.88
4.	0.0080	6,475	0.64	15,724	1.06	9,931	0.76
5.	0.0067	11,989	0.33	16,509	1.06	13,084	0.85
6.	0.0057	15,255	0.42			15,052	0.92
7.	0.0050	20,035	0.56				

[S] : AMSD   [M] : MMA f : functionality = M_n GPC / M_n NMR

In the present case, the growing methacrylate radical can more readily react with AMSD. In contrast, the reaction with AMSD-β-CD as well as AMSD–DMCD IC is hindered because of the presence of the bulkier β-*CD* or DMCD torus which includes AMSD. It is therefore not surprising that the chain transfer constant of AMSD in the polymerization of MMA is suppressed due to the formation of ICs.

Chain transfer constant of AMSD-β-CD IC is lower than that of AMSD–DMCD IC. This is because the double bond of AMSD in AMSD-β-CD IC is buried deeper into the β-CD cavity than in DMCD, wherein it is more exposed and is more readily available for participation in chain transfer reaction. In case of β-CD, there is no steric hindrance at the wider rim of cavity for the entry of the guest. Thus, AMSD is inserted deeper within the cavity while in case of DMCD, methyl groups of C_2 and C_6 hinder the

penetration of AMSD inside the cavity. During addition fragmentation, AMSD is cleaved at allylic CH_2, generating cumyl radical. If this allylic CH_2 resides within the β-CD cavity, it can not readily participate in addition fragmentation process and hence AMSD-β-CD IC exhibits lower chain transfer constant than AMSD–DMCD IC.
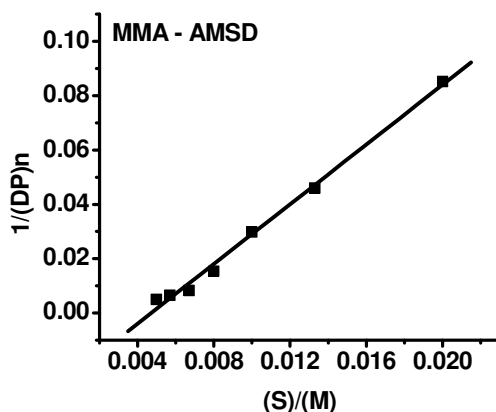
Figure 4.8 Mayo plot for AMSD CD
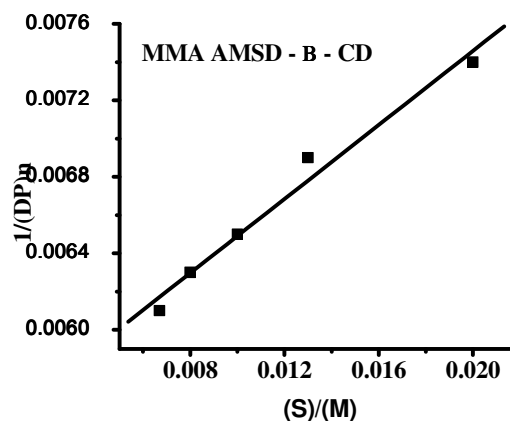
Figure 4.9 Mayo plot for AMSD–β– inclusion complex
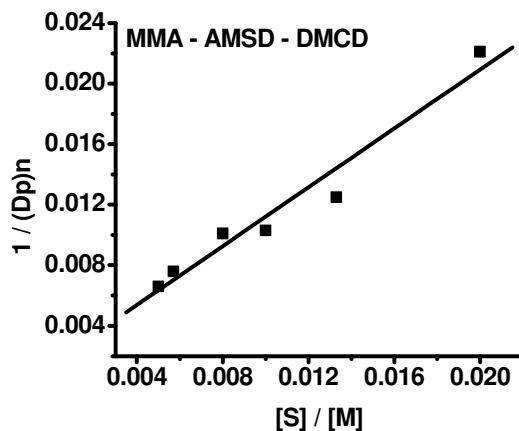
Figure 4.10 Mayo Plot for AMSD – DMCD inclusion complex

4.4.2 Structural analysis of P(MMA) macromonomer

4.4.2.1 FTIR analysis

FTIR spectra of P(MMA) macromonomers (figure 4.11) synthesized from AMSD as well as its CD ICs show the presence of unsaturation at 1625 cm^{-1}, phenyl ring at 1573, 1604 cm^{-1} and the ester peak at 1735 cm^{-1}.
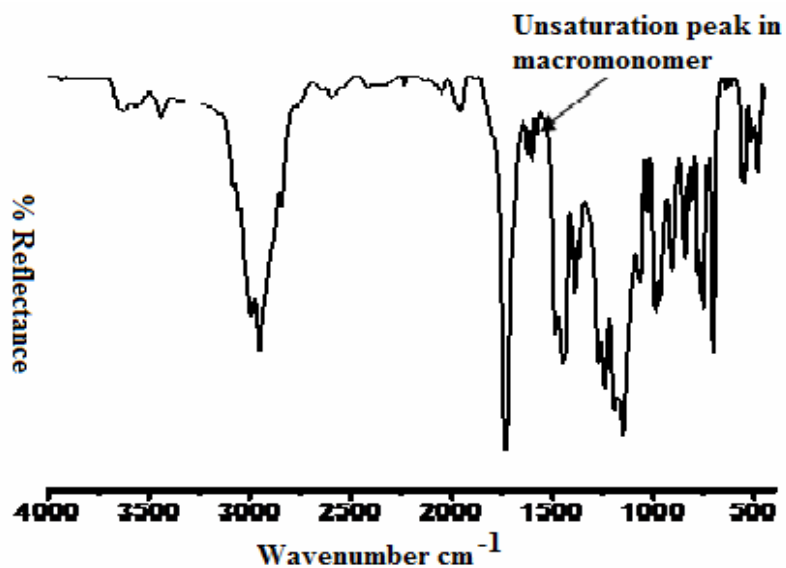
Figure 4.11 FTIR spectrum of P(MMA) macromonomer from AMSD–DMCD inclusion complex

4.4.2.2 NMR analysis

^{1}H NMR spectra of the P(MMA) macromonomers show the peaks corresponding to terminal unsaturation at 4.78 and 5.13 ppm (figure 4.12). The aromatic protons and methylene of AMSD at 7.25 and 2.83 ppm respectively are also seen. (Table 4.2)
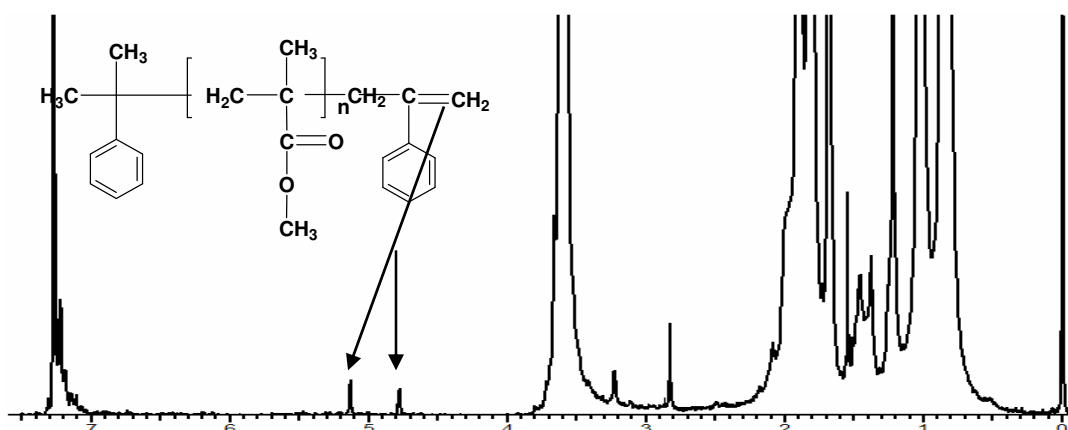
Figure 4.12 ^{1}H NMR of P(MMA) macromonomer

Table 4.2 ^{1}H NMR assignments of P(MMA) macromonomer

Sr. no.	Peak δ [ppm]	Remarks
1.	0.84 CH$_3$ of MMA	Atactic P(MMA)
2.	1.02 CH$_3$ of MMA	Syndiotactic (PMMA)
3.	1.22 CH$_3$ of AMSD and CH$_3$ of MMA	Isotactic (PMMA)
4.	1.7 CH$_2$ of MMA	Atactic P(MMA)
5.	1.82 CH$_2$ of MMA	Syndiotactic (PMMA)
6.	1.89 CH$_2$ of MMA	Isotactic (PMMA)
7.	2.83 CH$_2$ of AMSD	
8.	3.6 OCH$_3$ of MMA	
9.	4.78 C=CH$_2$ of AMSD	Macromonomer terminal unsaturation resulting from AFCT mechanism (1 mole %)
10.	5.13 C=CH$_2$ of AMSD	Macromonomer terminal unsaturation resulting from AFCT mechanism (1 mole %)
11.	5.6 C=CH$_2$ of MMA	Macromonomer terminal unsaturation resulting from disproportionation mechanism (0.016 mole %)
12.	6.1 C=CH$_2$ of MMA	Macromonomer terminal unsaturation resulting from disproportionation mechanism (0.016 mole %)
13.	7.25 Aromatic protons of AMSD	

4.4.3 Chain transfer during MMA polymerization

4.4.3.1 Disproportionation

The terminal unsaturation seen in the macromonomer could result from disproportionation and / or addition fragmentation. Disproportionation is dominant in methacrylate polymerizations which yields terminal MMA and the corresponding NMR peaks appear in the region 5.6~6.1 ppm. On the contrary, addition fragmentation yields terminal double bond followed by α substituted styrene. Since, this double bond is attached to the electron rich benzene ring, it appears more downfield i.e. at 4.78 and 5.13 ppm. The maximum unsaturation obtained as a result of disproportionation was 0.016 % (Table 4.2).

Since, the peaks resulting from disproportionation which are expected at around 5.5 and 6.2 ppm, are absent in all the macromonomers obtained in this work, we concluded that

the unsaturation obtained in all the macromonomers is due to the addition fragmentation mechanism and not by disproportionation. This confirms that the terminally unsaturated macromonomers are formed as a result of AFCT brought about by AMSD.

4.4.3.2 Chain transfer due to AMSD and its inclusion complexes

When AMSD was used as AFCT agent, the molecular weight decreased from 20,035 to 1,113 as [S]/[M] increased from 0.005 to 0.02. In case of AMSD-β-CD, the molecular weight decreased from 16,509 to 13,502 as [S]/[M] varied from 0.0067 to 0.02. For AMSD–DMCD the molecular weight decrease was from 15,052 to 4,515 as [S]/[M] varied from 0.005 to 0.02. Thus, the effective chain transfer was in the order AMSD > AMSD–DMCD > AMSD-β-CD. The reasons are discussed in the following section.

4.4.3.3 Effect of steric hindrance on chain transfer activity

Moad et. al. (1996) concluded that steric effects govern the preferred fragmentation pathway. In the fragmentation process, steric compression is relieved as the β-carbon moves from tetrahedral (sp^3) hybridization to planar (sp^2) hybridization, thus allowing the attached substituents to move further apart from each other. Thus, amongst the MMA oligomers evaluated, MMA trimer yielded the highest chain transfer constant.

Amongst the chain transfer agents investigated in this work, AMSD–DMCD IC is the bulkiest since the methyl group at C_6 position of CD points outwards. As a result, AMSD can penetrate deeper into the cavity of β-CD. In case of AMSD–DMCD, the steric hindrance due to methyl groups of C_2 limits the penetration of AMSD inside the cavity as confirmed by NMR measurement and modeling calculations. During addition fragmentation, AMSD fragments at allylic CH_2 generating cumyl radical. Since this allylic CH_2 is buried deep within β-CD cavity, it is not readily available for addition fragmentation and hence AMSD-β-CD IC is less effective chain transfer agent than AMSD–DMCD IC. In the case of AMSD–DMCD IC, the methyl group at the C_2 position in DMCD hinders the penetration of the allylic CH_2 into the cavity. As a result, this IC is more effective as an AFCT agent.

4.4.3.4 End functionality calculations

In order that a macromonomer can be copolymerized with a monomer to yield a graft copolymer it is essential that each macromonomer obtained by AFCT has a terminal

unsaturation. Although the need to quantify unsaturation in macromonomers has been emphasized in the literature, not many attempts have been made to quantify the same. Since the mechanistic aspects of addition fragmentation are similar to those in RAFT polymerization M_n theoretical was evaluated using the equation suggested by Rizzardo et. al. (Moad 1996).

$M_n(Theo) = (M_M. [M]_0.x)/[AFCT]_0 + M_{AFCT}$

Where M_M and M_{AFCT} are the molecular weights of Monomer and AFCT agent, x is the conversion and $[M]_0$ and $[AFCT]_0$ are the initial concentrations of monomer and AFCT agent.

We calculated the functionality *f* of the macromonomer, which represents the nature of unsaturated end group per polymer according to the formula

$f = M_n(GPC) / M_n(theoretical)$

For polymerization in presence of AMSD-β-CD IC, the functionality '*f*' obtained was close to unity at all concentrations, while the values were very low in case of polymerization in the presence of AMSD (Table 4.1).

4.4.3.5 Effect of steric hindrance on functionality

There is no hindrance for AMSD participation in chain transfer. The chain transfer activity of β-CD and DMCD ICs is lowered as a result of steric hindrance caused by the CD cavity. AMSD is inserted deeper into the β-CD cavity than in the DMCD cavity due to the presence of the methyl group at C_2 position in the latter. This favors addition fragmentation in AMSD-β- CD IC over that in case of AMSD–DMCD IC. The greater steric hindrance in AMSD-β-CD results in higher fragmentation rate comparable to propagation rate and results in '*f*'→1 which is crucial for the synthesis of macromonomers containing terminal unsaturation.

4.4.4 Graft copolymer synthesis

To check whether the unsaturated end groups of the macromonomer undergo copolymerization, polymerization was also carried out with pH sensitive comonomer 4 – vinyl pyridine (4-VP) and 2 - dimethyl amino ethyl methacrylate (DMAEMA) in different compositions. The molecular weight of the copolymers increased with increase

in DMAEMA concentration. GPC chromatogram showed a single peak corresponding to copolymer and no peak corresponding to the parent macromonomer was seen. Thus, it can be concluded that there was no unreacted macromonomer present. DSC study of the copolymers showed two T_g peaks at 107°C and 29°C corresponding to MMA and DMAEMA whereas 108°C and 158°C corresponding to MMA and 4 – VP segments of P(MMA-co-AMSD-co- 4-VP) and P(MMA-co-AMSD-co- DMAEMA) respectively. It may be noted that copolymerization of MMA and DMAEMA leads to a random copolymer having a single T_g depending on the monomer composition whereas in the present case the T_g values characteristic of each homopolymer are obtained regardless of monomer composition. This behaviour is similar to the lower critical solution temperature behaviour of graft vs. random copolymers reported by Wohlrab et. al. (2001).

Unlike the random copolymer of identical composition, which dissolves rapidly at pH 1.2 to yield clear solutions, the 'Graft through' copolymers synthesized herein swell as the hydrophobic grafts which are insoluble act as virtual crosslinks and prevent dissolution of the 4-VP and DMAEMA segments.

Table 4.3 P(MMA-co-AMSD-4-VP) synthesis and properties

Sr. no.	MMA g	4-VP g	Composition ^{1}H NMR Mole %	P(MMA-AMSD-4 – VP) M_n	Solubility at pH 1.2	T_g °C
1.	0.1	0.9462	15.9: 84.1	7,094	Soluble in 1 hr	107 and 158
2.	0.2	0.8411	27 : 73	6,128	Soluble in 1.5 hr	
3.	0.3	0.7359	36.1: 63.9	5,376	Soluble in 1.5 hr	
4.	0.4	0.6308	46.1 : 53.9	4,558	Insoluble	
5.	0.6	0.4205	67.1 : 32.9	4,126	Insoluble	
6.	0.8	0.2103	90.8 : 9.2	4,076	Insoluble	

Initiator (AIBN) : 0.0328 (2 mole % based on total moles of monomer), Solvent (DMF) : 10 ml ([M] = 10 %), Molecular weight of P(MMA) macromonomer = 3800

Table 4.4 P(MMA-co-AMSD-DMAEMA) synthesis and properties

Sr. no.	MMA g	DMAEMA g	Composition Mole %	P(MMA-AMSD-DMAEMA) M_n	Solubility at pH 1.2	T_g °C
1.	0.4144	0.5856	26.7 : 70.3	20,088	365 % swelling	
2.	0.6142	0.3857	41.0 : 59.0	16,776	169 % swelling	108 and 27
3.	0.2144	0.7855	50.4 : 40.6	12,535	150 % swelling	
4.	0.298	0.7019	64 : 33.3	10,255	43 % swelling	
5.	0.4886	0.5114	70.8 : 26.2	7,655	Insoluble	
6.	0.7181	0.2819	80.8 : 16.2	5,890	Insoluble	

Initiator (AIBN) : (2 mole % based on total moles of monomer), Solvent (DMF) : 10 ml ([M] = 10 %), Molecular weight of P(MMA) macromonomer = 3,504

*[1]Composition determined by ^{1}H NMR.

$$*[2]\text{Swelling ratio} \quad = \quad \frac{\text{(Weight of swollen polymer - Weight of dry polymer)}}{\text{(Weight of dry polymer)}}$$
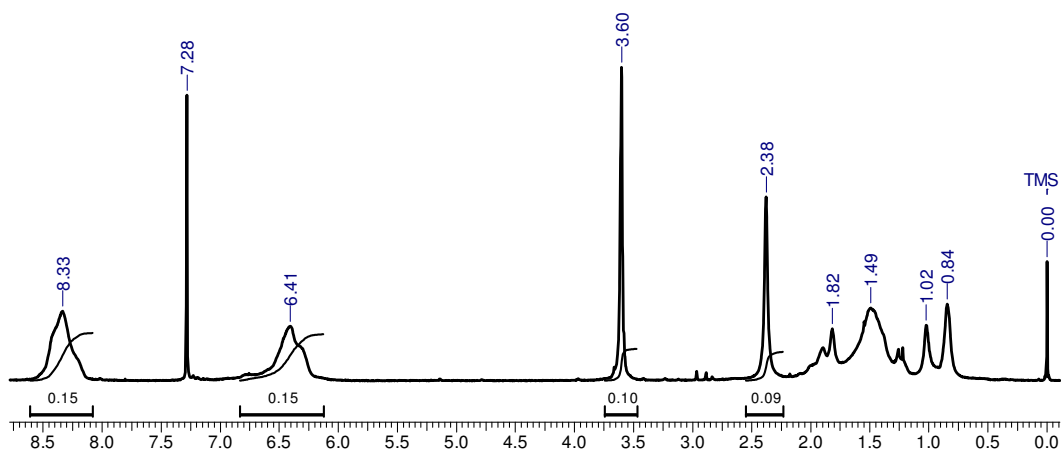
Figure 4.13 ^{1}H NMR of P(MMA-co-AMSD-co-4 VP) (66.63:1:32.36 mole %)
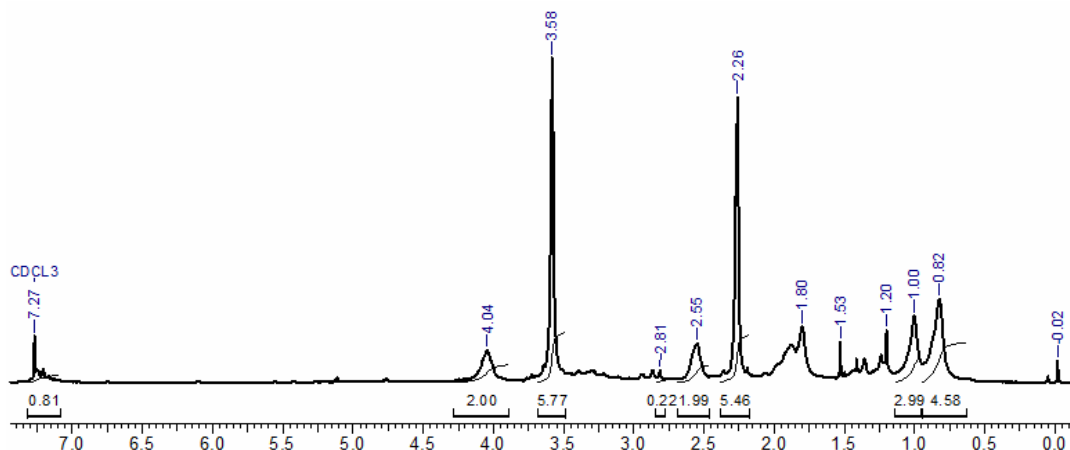
Figure 4.14 ^{1}H NMR of P(MMA-co-AMSD-co-DMAEMA) (64.04:2.66:33.29 mole%)

4.5 Conclusions

Substitution is known to influence the addition fragmentation chain transfer activity of 2-substituted 1-allyl compounds. We demonstrate that the IC formation with β-CD and DMCD influences the addition fragmentation chain transfer activity of AMSD in a similar manner, although the cyclodextrins are not chemically conjugated. The observed order of chain transfer constant in the polymerization of MMA viz. AMSD > AMSD-DMCD > AMSD-β-CD is governed by the disposition of the allylic group in the CD cavity as shown by molecular modeling simulations and NMR spectroscopy. The deeper insertion of allyl group in the β-CD cavity results in enhanced addition fragmentation efficiency of AMSD resulting in macromonomer containing terminal unsaturation as reflected in $f \rightarrow 1$. The macromonomers so synthesized have been copolymerized with DMAEMA to yield graft copolymers which exhibits distinctly different thermal and dissolution characteristics as compared to random copolymers of identical composition. Since, AMSD–DMCD IC is water soluble, this can be used for the synthesis of water soluble macromonomers in a single step which has so far not been possible. Copolymerization of this macromonomer with hydrophobic monomer leads to graft copolymers which exhibit diverse morphologies which will be discussed in the next chapter.

4.6 References

1.   Wohlrab S. and Kuckling D. J. Polym. Sc. Part A: Polym. Chem. **2001**, 39 (21), 3797. (b) Ito K., Masuda Y., Shintani T., Kitano T., Yamashita Y. Polymer J. **1983**, 15 (6), 443.

2.   Dlubek G., Bamford D., Rodriguez-Gonzalez A., Bornemann S., Stejny J., Schade B., Alam M., Arnold M. J. Polym. Sc. Part B: Polym. Phys. **2002**, 40, 434.

3.   Lo C., Huang C., Lin K., Hsiue G. Biomaterials **2007**, 28 (6), 1225.

4.   Bhattacharya A., Misra B. Prog. Polym. Sci. **2004**, 29, 767.

5.   Gallot B., Monnet F. Eur. Polym. J. **1996**, 32, 147.

6.   Deshpande M., Garnett M., Vamvakaki M., Bailey L., Armes S., Stolniket S. Journal of Controlled Release **2002**, 81, 185.

7.   Wang D., Williams C., Li Q., Sharma B., Elisseeff J. Biomaterials **2003**, 24, 3969.

8.   Pistikalis M., Pispas S., Mays J., Hadjichristidis N. Adv. Poly. Sc. **1998**, 135, 1.

9.   Ito K. Prog. Poly. Sc. **1998**, 23, 581.

10. Joshi J., Sinha V. Carbohydrate polymers **2007**, 67 (3), 427.

11. Cacioli P., Hawthorne D., Laslett R., Rizzardo E. and Solomon D. J. Macromol. Sc. Chem. **1986**, A 23, 839.

12. Yamada B., Kobatake S. Polym. J. **1992**, 24, 281.

13. Yamada B., Kobatake S., Aoki S. Polym. Bull. **1993**, 31, 263.

14. Yamada B., Kobatake S., Aoki S. Macromolecules **1993**, 26, 5099.

15. Kobatake S., Yamada B. Macromol. Chem. Phys. **1997**, 198, 2825.

16. Nair C., Chaumont P., Charmot D. J. Polym. Sc. Part A: Polym. Chem. **1999**, 37, 2511.

17. Yamada B., Oku F., Harada T. J. Polym. Sci. Part A: Polym. Chem. **2003**, 41(5), 645.

18. Ishizu K. J. Polym. Sci. Part A : Polym. Chem. **1990**, 28, 1887.

19. Kobayashi S., Masuda E., Shoda S., Shimano Y. Macromolecules **1989**, 22, 2878.

20. Kennedy and Hiza M. J. Polym. Sci. Part C: Polym. Chem. **1983,** 21, 1033.

21. Kitayama T., Kishiro S., Hatada K. Polym. Bull. **1991**, 25, 161.

22. Yamashita Y., Ito K., Mizuno H., Okada K. Polym. J. **1982**, 14, 255.

23. Akashi M., Yanagi T., Yashima E., Miyauchi N. J. Polym. Sc. Part A: Polym. Chem. **1989**, 27, 3521.

24. Milkovich R. ACS Polym. Prepr. **1980**, 21, 40.

25. Rempp P., Lutz P., Masson P., Franta E. Makromol. Chem., Suppl. **1984**, 8, 3.

26. Rao P., Masson P., Lutz P., Neinert G., Rempp P. Poly. Bull. **1984**, 11, 115.

27. Asami R., Takaki M., Moriyama Y. Polym. Bull. **1986**, 16, 125.

28. Vergas J., Zilliox J., Rempp P., Franta E. Polym. Bull. **1980**, 3, 83.

29. Uryu T., Yamanaka M., Date M., Ogawa M., Hatanaka K. Macromolecules **1986**, 21, 1916.

30. Aoshima S., Ebara K., Higashimura T. Polym. Bull. **1985**, 14, 425.

31. (a) Yamashita Y., Ito K., Mizuno H., Okada K. Polym. J. **1982**, 14, 255. (b) Akashi M., Yanagi T., Yashima E., Miyauchi N. J. Polym. Sc. Part A: Polym. Chem. **1989**, 27 (10), 3521.

32. Ito K., Masuda Y., Shintani T., Kitano T., Yamashita Y. Polymer J. **1983**, 15 (6), 443.

33. Meijs G., Rizzardo E., Thang S., Macromolecules **1988**, 21, 3122.

34. Meijs G., Rizzardo E. Makromol. Chem. **1990**, 191, 1545.

35. Meijs G., Morton T., Rizzardo E., Thang S. Macromolecules **1991**, 24, 3689.

36. Hirano T., Yamada B. Polymer **2003**, 44, 347.

37. McHale R., Aldabbagh F., Carroll W., Yamada B. Macromol. Chem. and phy. **2005**, 206, 2054.

38. Glockner P., Ritter H. Macromol. Chem. & Phys **2000**, 201, 2455.

39. Glockner P., Metz N., Ritter H. Macromolecules, **2000**, 33, 4288.

40. Giese B. Radicals in organic synthesis:formation of carbon-carbon bonds, Oxford, Pergamon press, **1986**.

41. Motherwell B., Crich D. Free radical chain reactions in organic synthesis, London, Academic press, **1992**.

42. Keck G., Enholm E., Yates J., Wiley M. Tetrahedron **1985**, 41, 4079.

43. Barton D., McCombie S. J. Chem. Soc. Perkin Trans **1975**, 1, 1574.

44. Chiefari J., Chong K., Ercole F., Krstina J., Jefery J., Le T. Macromolecules **1998**, 32, 5559.

45. Mayadunne A., Rizzardo E., Chiefari J., Chong K., Moad G., Thang H. Macromolecules **1999**, 32, 6977.

46. Hawthorne G., Moad G., Rizzardo E., Thang H. Macromolecules **1999**, 32, 5457.

47. Chong K., Le T., Moad G., Rizzardo E., Thang H. Macromolecules **1999**, 32, 2071.

48. Moad G., Chiefari J., Chong K., Krstina J., Mayadunne A., Postma A. Polym. Int. **2000**, 49, 993.

49. Moad L., Moad G., Rizzardo E., Thang H. Macromolecules **1996**, 29, 7717.

50. Rizzardo E., Meijs G., Thang S. Macromol. Symp. **1995**, 98, 101.

51. Colombani D. Prog. Polym. Sci. **1999**, 24, 425.

52. Yamada B., Kobatake S. Prog. Polym. Sci. **1994**, 19, 1089.

53. Moad G., Rizzardo E., Thang S. Polymer **2008**, 49, 1079.

54. Corner T. Adv. Polym. Sci. **1984**, 62, 95.

55. Krstina J., Moad G., Rizzardo E., Winzor C., Berge C., Fryd M. Macromolecules **1995,** 28, 5381.

56. Krstina J., Moad C., Moad G., Rizzardo E., Berge C., Fryd M. Macromol. Symp. **1996**, 111, 13.

57. Dais V., Priddy D., Bell B., Sikkema K., Smith P. J. Polym. Sci. Part A: Polym Chem **1993,** 31, 901.

58. Mathias L., Thompson R., Lightsey A. Polym Bull (Berlin) **1992**, 27, 395.

59. Sato T., Seno M., Kobayashi M., Kohna T., Tanaka H., Ota T. Eur. Polym. J. **1995,** 31, 29.

60. Yamada B., Otsu T. Die Makromol. Chem, **1991,** 192, 333.

61. Yamada B., Kato E., Kobatake S., Otsu T. Polym Bull (Berlin) **1991**, 25, 423.

62. Yamada B., Otsu T. Die Makromol. Chem. Rap. Commun. **1990**, 11, 513.

63. Meijs G., Rizzardo E., Le T. Polym. Int. **1991**, 26, 239.

64. Meijs G., Rizzardo E. Polym Bull (Berlin) **1991**, 26, 291.

65. Meijs G., Rizzardo E., Le T., Chong Y. Macromol. Chem. Phys. **1992**, 193, 369.

66. Shanmugananda M., Kishore K. J. Polym. Sci. Part A: Polym. Chem. **1996**, 34, 1415.

67. Colombani D., Chaumont P. J. Polym. Sci. Part A: Polym. Chem. **1994**, 32, 2687.

68. Colombani D., Chaumont P. Macromolecules **1994**, 27, 5972.

69. Colombani D., Chaumont P. Polymer **1995**, 36, 129.

70. Tanaka H., Kawa H., Sato T., Ota T. J. Polym. Sci. Part A: Polym. Chem. **1989**, 27, 1741.

71. Moad G., Solomon D. The chemistry of radical polymerization. 2nd ed. Oxford: Elsevier; **2006**, 501.

72. Bon F., Morseley R., Waterson C., Haddleton M. Macromolecules, **2000**, 33, 5819.

73. Moad G., Rizzardo E., Thang S. Aust. J. Chem. **2005**, 58, 379.

74. Rizzardo E., Chen M., Chong B., Moad G., Skidmore M., Thang S. Macromol. Symp. **2007,** 248, 104.

75. Le T., Moad G., Rizzardo E., Thang S. **1998**, WO 9801478.

76. Gigmes D., Bertin D., Marque S., Guerret O., Tordo P. Tetrahedron Lett. **2003**, 44, 1227.

77. Favier A., Charreyre M., Chaumont P., Pichot C. Macromolecules **2002**, 35, 8271.

78. Moad G., Chiefari J., Mayadunne R., Moad C., Postma A., Rizzardo E., Thang S., Macromol. Symp. **2002**, 182, 65.

79. Chong B., Krstina J., Le T., Moad G., Potsma A., Rizzardo E., Thang S. Macromolecules **2003**, 36, 2256.

80. Favier A, Charreyre M-T. Macromol. Rap. Commun. **2006**, 27, 653.

81. Moad G., Solomon D. The chemistry of radical polymerization. 2nd ed. Oxford: Elsevier; **2006**, 194.

82. Otsu T. J. Polym. Sci. Part A: Polym. Chem. **2000**, 38, 2121.

83. Grignard B., Jerome C., Calberg C., Detrembleur C., Jerome R. J. Polym. Sci. Part A: Polym. Chem. 45, **2007,** 1499.

84. Klemm E., Schulze T. Makromol. Chem. 194, **1993**, 2087.

85. Favier A., Ladaviere C., Charreyre M., Pichot C. Macromolecules **2004,** 37, 2026.

86. Arita T., Buback M., Janssen O., Vana P. Macromol. Rap. Commun. **2004,** 25, 1376.

87. Wang Z., He J., Tao Y., Yang L., Jiang H., Yang Y. Macromolecules **2003**, 36, 7446.

88. Lowe A., McCormick C. Prog. Polym. Sci. **2007,** 32, 283.

89. Hutson L., Krstina J., Moad C., Moad G., Morrow G., Postma A. Macromolecules **2004**, 37, 4441.

90. Kollisch H., Barner–Kowollik C., Ritter H. Macromol. Rap. Commun. **2006**, 27, 848.

Chapter 5

Chain transfer activity of AMSD–DM–β–CD complex in aqueous polymerization

5.1 Introduction

Graft and block copolymers are used as surfactants, compatibilizers and pigment dispersants. The interest in the synthesis of double hydrophilic block copolymers is increasing in view of their applications in drug delivery including gene therapy (Kabanova 1998), switchable amphiphiles (Butun 1998), mineralization templates (Antonietti 1998) and crystal growth modifiers (Colfen 1998), etc.

Graft copolymers are generally prepared by three methods; 'grafting onto', 'grafting from', 'grafting through' (Pistikalis 1998, Hadjichristidis 2002). In grafting through approach, macromonomers are copolymerized with a monomer (Ito 1998). For the synthesis of the macromonomer, a monomer is polymerized in the presence of functional initiator or functional chain transfer agent followed by end capping (Yamashita 1982, Akashi 1989). Unfortunately, the approach does not yield precise control over molecular weight and functionality. Anionic or cationic polymerization approaches are restricted to monomers such as methyl methacrylate and styrene and require stringent reaction conditions. ATRP can not be adapted for the polymerization of monomers such as N-vinyl pyrrolidone (NVP) and acrylic acid (AA) since the polar lactam group present in NVP and carboxyl groups in AA complex with the metal catalyst used during polymerization (Devasia 2005, Patten 1998). There is therefore a need for a method which will yield macromonomers containing terminal unsaturation which can be extended to a wide range of water soluble monomers.

Reversible addition fragmentation chain transfer (RAFT) polymerization in aqueous medium has been explored as it can be carried out under mild reaction conditions and can be applied to a wide range of vinyl monomers. Chain transfer agents such as dithioesters (Chiefari 1998), trithiocarbonates and dithiocarbamates (Mayadunne 2000), xanthates (Taton 2001, Francis 2000, Ladaviere 2001) have been used. However, commonly used dithioesters are known to undergo aminolysis by 1° and 2° amines and are susceptible to hydrolysis (Thomas 2003, 2004) leading to poor control on end functionality and efficiency as AFCT agents. The thiol end group obtained needs to be thermolyzed at higher temperature to obtain terminal unsaturation which may not be always desirable (Postma 2006, Postma 2006). In any case, the synthesis of unsaturated

macromonomers involves two steps. For aqueous systems, AFCT agents which yield terminally unsaturated macromonomer in a single step are not yet reported. Hence, new water-soluble AFCT agents need to be developed. Alternatively, solubility of the existing AFCT agents in water has to be enhanced.

Amongst various AFCT agents based on oligomers of α methyl vinyl monomers, α methyl styrene dimer (AMSD) was found to be the most efficient during polymerization of styrene, which yielded terminal unsaturation in a single step (Watanabe 1993, Yamada 1994). However, AMSD cannot be used in aqueous system because of its hydrophobic nature. Ritter et. al. (Ritter 2002) reported that the solubility of the hydrophobic monomers such as methyl methacrylate (MMA) and styrene (Sty) in water could be enhanced by complexation with methylated cyclodextrin (DMCD) enabling polymerization in aqueous medium. Kollisch et. al. (Kollisch 2006) reported RAFT polymerization of styrene-DMCD inclusion complex (IC) using 3-Benzyl sulfanyl thiocarbonyl sulfanyl propionic acid as AFCT agent. Incorporation of bulkier substitutents in AFCT agent enhances addition fragmentation efficiency and terminal unsaturation content (Sato 2004, McHale 2005). The complexation of AMSD serves two purposes: i) enhances the water solubility of AMSD and ii) increases steric hindrance by inclusion complexation.

In this chapter, we demonstrate the use of AMSD-DMCD IC as AFCT agent in the synthesis of water-soluble macromonomers (WSM). Poly(NVP) and Poly(AM) macromonomers having 'f' close to unity were obtained and further copolymerized to yield pH sensitive polymers. This approach presents a method for the synthesis of terminally unsaturated water-soluble macromonomers which can be used for the synthesis of comb copolymers.

5.2 Aqueous addition fragmentation chain transfer polymerization

History of AFCT, its mechanism and favourable reaction conditions are discussed in the previous chapter. This chapter highlights the application of RAFT agents to the synthesis of water-soluble macromonomers and their copolymers in aqueous medium. Limitations of aqueous RAFT are also discussed.

5.2.1 Aqueous addition fragmentation chain transfer agents

The AFCT agents available for organic system are mainly based on the α - substituted methyl acrylates or the dimers, trimers of the monomer which introduces the terminal unsaturation (Moad 2008). They cannot be applied for the aqueous system because of their limited solubility. The commonly used aqueous RAFT agents include thiocarbonylthio species (figure 5.1 and 5.2) belonging to one of the following general families of compounds i.e. dithioesters, xanthates, dithiocarbamates and trithiocarbonates (Le 1998, Corpart 1998, Lai 2006, Mayadunne 1999, Corpart 1999, Lai 2006, Schilli 2002, Liu 2004, Stenzel 2002, Lai 2002, Mayadunne 2000, Wang 2005). These AFCT agents introduce S=S group in the macromonomer and not the C=C group. The macromonomers obtained from aqueous AFCT agents need to be thermolyzed further in order to yield the terminally unsaturated macromonomers.

Z= aryl,alkyl   y = aryl, alkyl   R = R' or R= R'

       A   **B**   **C**   **D**
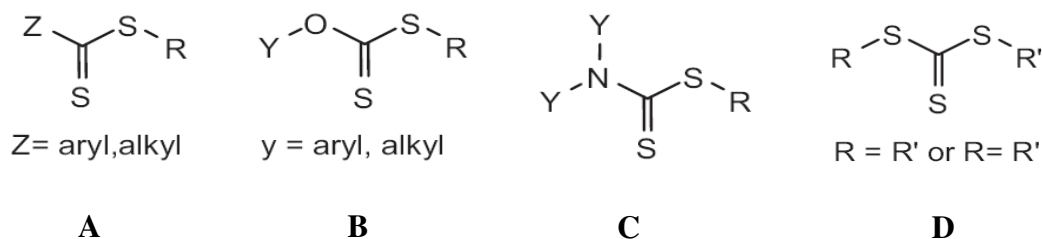
Figure 5.1 General structures of common thiocarbonylthio RAFT agents A) Dithioesters, B) Xanthates, C) Dithiocarbamates and D) Trithiocarbonates

Dithioesters (A) are the most susceptible to radical addition (have the highest chain transfer constants) especially when Z = phenyl. On the other hand, radical species add less readily to the C=S bond of both xanthates (B) and dithiocarbamates (C). Dithiocarbamates in which Y is a simple alkyl species such as ethyl groups are not effective RAFT agents for common monomers such as styrenics, (meth)acrylates and (meth)acrylamides but they are very effective for non-conjugated monomer substrates such as vinyl acetate. One of the reasons for their lower efficacy as RAFT agents is their zwitterionic canonical structures contributing to the overall resonance hybrid. These canonical forms reduce the double bond character of the C=S species making it less susceptible to radical addition. The same is also true of xanthates. The efficiency of

RAFT agent depends on the stability and steric hindrance of the propagating radical (figure 5.3).
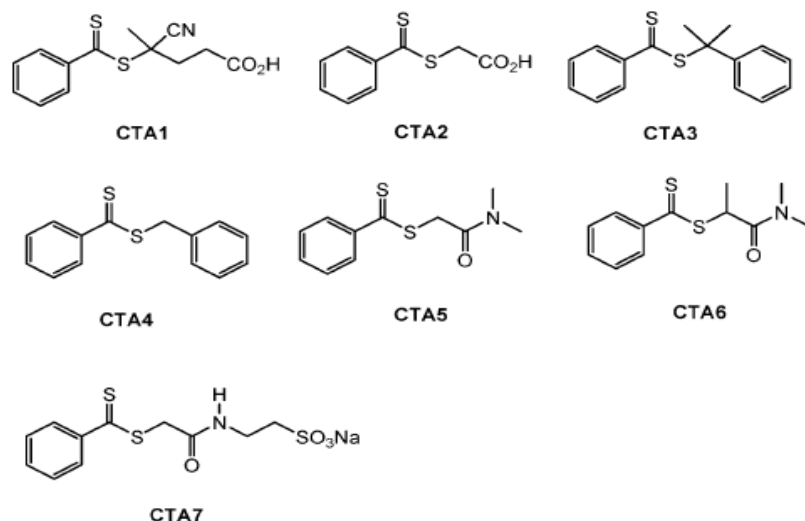
Figure 5.2 Chain transfer agents used in aqueous RAFT polymerization CTA 1 sodium 4-cyanopentanoic acid dithiobenzoate, CTA 2 carboxymethyl dithiobenzoate, CTA 3 cumyl dithiobenzoate, CTA 4 benzyl benzodithioate, CTA 5 (dimethyl carbamoyl) methyl benzodithioate, CTA 6 1-(dimethyl carbamoyl) ethyl benzodithioate, CTA 7 2-(2-thiobenzoylsulfonylproponylamino) ethanesulfonic acid
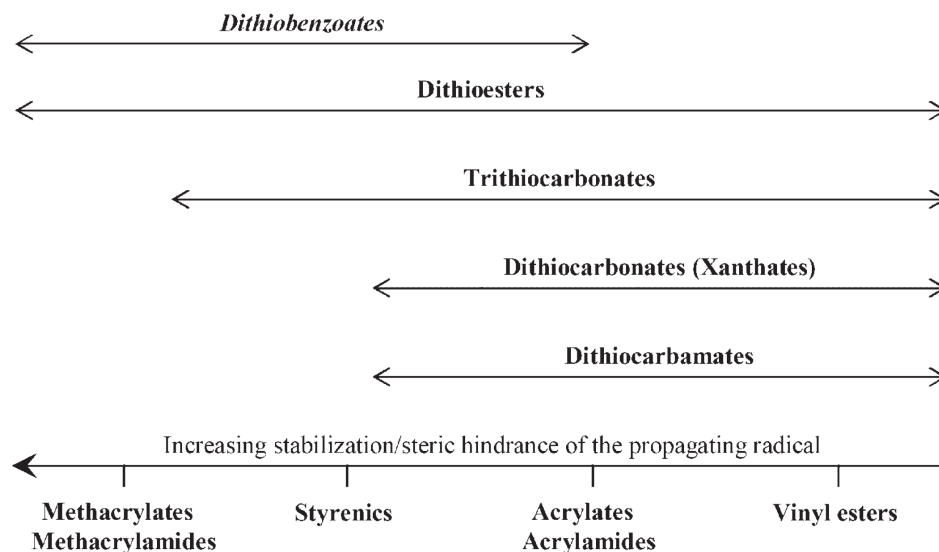
Figure 5.3 Efficiency range of various CTAs for different monomers (Favier 2006)

5.2.2 Monomers in aqueous addition fragmentation chain transfer polymerization
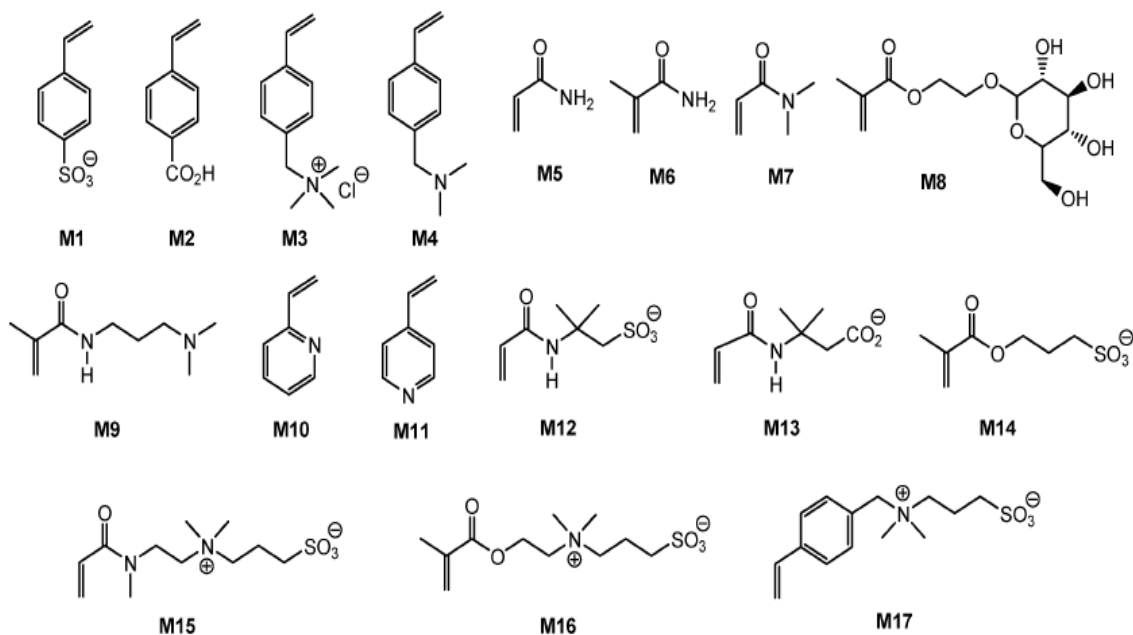
Figure 5.4 Hydrophilic monomers amenable to aqueous RAFT polymerization M_1 Sodium salt of 4-styrene sulfonate, M_2 4-vinyl benzoic acid, M_3 Vinyl benzyl trimethyl ammonium chloride, M_4 N, N' dimethyl benzyl vinyl amine, M_5 Acrylamide, M_6 Methacrylamide, M_7 N, N' dimethyl acrylamide, M_8 2-methacryloxyethyl glucoside, M_9 N-3 dimethyl amino propyl methacrylamide, M_{10} 2-vinyl pyridine, M_{11} 4-vinyl pyridine, M_{12} 2-acrylamido 2-methyl propane sulphonic acid, M_{13} 3-acrylamido 3-methyl butanoate, M_{14} Acrylamido sulfobetaine, M_{15} Methacrylamido sulfobetaine, M_{16} styrenic sulfobetaine

The first successful aqueous RAFT polymerization was reported by the Australian CSIRO group in December of 1998. (Chiefari 1998) Sodium salt of 4-styrenesulfonate (NaSS) was polymerized at 70 °C in the presence of the water-soluble CTA sodium 4-cyanopentanoic acid dithiobenzoate in the presence of 4, 4' azobis(4-cyanopentanoic acid) obtaining a homopolymer with M_n = 8000 and a polydispersity index (PDI) of 1.13.

The first RAFT experiments with a variety of water-soluble monomers indicated that in order to have any success it is necessary to (a) control relative selectivity of propagating

radicals for the thiocarbonylthio groups and monomer, (b) consideration of intermediate chain scission and reinitiation rates with more reactive monomers and (c) elimination or reduction of hydrolysis of thiocarbonylthio groups. Later, it was found that even low degrees of hydrolysis of monomer side-chain functionality could be fatal to RAFT if not controlled or eliminated. Mitsukami (2001) conducted preliminary hydrolysis experiments clearly demonstrating that lowering pH could reduce hydrolysis in two dithioester CTAs, sodium 4-cyanopentanoic acid dithiobenzoate and carboxymethyl dithiobenzoate. Since NaSS is soluble over the entire useful pH range, it was possible to adjust pH to significantly retard CTA hydrolysis and yet maintain initiator and CTA solubility, both critical to reaction control.

Sumerlin (2001, 2003) reported the RAFT polymerization of 2-acrylamido 2 methyl propane sulphonic acid (AMPS, M_{12}) in water at 70°C, pH ≈ 9.6 using sodium 4-cyanopentanoic acid dithiobenzoate with a CTA : Initiator molar ratio 5:1. Linear pseudo-first-order rate plots were obtained after an initial induction / retardation period of ~60 min. M_w / M_n increased with conversion at pH 9.6 but decreased with conversion at pH 7.0 (figure 5.5). The difference was attributed to the CTA hydrolysis. The hydrolysis was minimum at the lower pH.
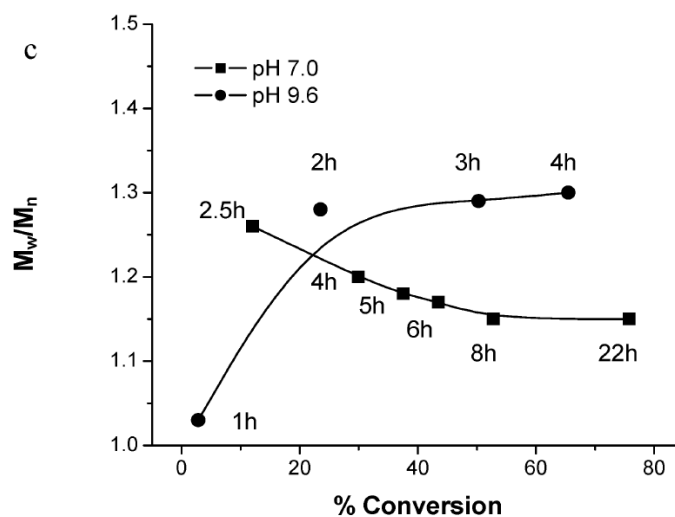
Figure 5.5 Homopolymerization of AMPS : M_w/M_n Vs % Conversion at pH 7 and 9.6

To study the hypothesized pH-induced self-assembly, series of well-defined AB diblock and statistical copolymers of M_{12} and 2-acrylamido 2 methyl butanoate (AMBA, M_{13}) were prepared. At pH values below 5, the carboxylate functionality in M_{13} is protonated, rendering it hydrophobic. In contrast, the M_{12} units remain hydrophilic at both low and high pH. NMR spectroscopy, dynamic light scattering and fluorescence measurements confirmed reversible pH-induced micelle formation. Hydrodynamic diameters of the unimers and multimeric micelles were in the range 6-28 nm. The sequestration / release potential of these stimuli-responsive micelles was demonstrated by observing relative fluorescence intensity of the I_1 and I_3 bands of pyrene added to the aqueous solutions at low and high pH (Sumerlin 2003).

Sumerlin and Donovan explored the RAFT polymerization of N, N' dimethyl acrylamide (DMAM) in organic, aqueous, and mixed N, N' dimethylformamide (DMF) / water mixtures (Donnovan 2002, Donnovan 2002). Sodium 4-cyanopentanoic acid dithiobenzoate (CTA_1) and 1-(dimethyl carbamoyl) ethyl benzodithioate (CTA_6) for the RAFT polymerization of DMAM having R groups structurally and electronically similar to the propagating chain end of DMAM were designed and synthesized. The effectiveness of CTA_1 and CTA_6 in controlling the polymerization of DMA was studied at CTA / initiator ratio of 5:1 at 60, 70 and 80 °C in water or DMF / water solution. It was found that elevated temperature and a cosolvent (DMF) are needed to solvate and assist in the production of the $R^\bullet$ fragment necessary for controlling the RAFT process for CTA_6 whereas, the radical from fragmentation of CTA_1 addition in water at lower temperature is readily solubilized and sufficiently energetic for monomer addition. However, the experimental molecular weights were still higher than the predicted one.

The main disadvantage of these aqueous AFCT agents is that in aqueous media they undergo hydrolysis at longer reaction times and aminolysis with 1^0 and 2^0 amines. (Thomas et. al. 2003, 2004) Hence, they cannot be applied for acrylamide. Thomas et. al (2003, 2004) studied the effect of hydrolysis and aminolysis in aqueous RAFT polymerizations of acrylamide.

Thomas et. al. (2004) was successful in controlling the synthesis of poly(acrylamide) (PAM) homopolymers and block copolymers in water which required not only

appropriate choice of CTA, but careful selection of reaction conditions. The homopolymerization was successfully performed in an aqueous acetic acid / sodium acetate buffer (pH = 5.0) utilizing 2-(2-thiobenzoylsulfonylproponylamino) ethanesulfonic acid (STPE) CTA_7. This CTA was designed such that it was soluble over a wide pH range and had desired steric and electronic characteristics for facile fragmentation. However, it was observed that the molecular weights experimentally determined were almost 50% higher than the predicted ones. The polymerization was very slow and reached ~ 30 % conversion in 24 h. These observations prompted to think of side reactions such as hydrolysis of monomer and/or CTA or aminolysis of monomer and initiated a further study of the stability of CTA and macro-CTA.

The magnitude of the apparent rate constant of hydrolysis, k_{hyd}, for CTA_1 increases by nearly an order of magnitude from 2.5×10^{-5} to 15×10^{-5} s^{-1} as the pH increases from 7.0 to 10.0. Also, very little change in k_{hyd} was observed as the pH was lowered from 7.0 to 2.0 demonstrating the enhanced stability of the dithioesters at low pH. At pH ~ 7.0 and higher, the loss of CTA_1 due to both hydrolysis and aminolysis occurred as dithioesters are known to be readily attacked by both 1° and 2° amines, whereas at pH ~ 5.5 any loss could be attributed solely to hydrolysis. This reinforced the conclusion that maintenance of neutral pH to minimize hydrolysis and acidic pH to minimize aminolysis is crucial for the controlled RAFT polymerization of AM.

MAA can be polymerized only by free radical polymerization as the COOH functionality is not suitable for the cationic and anionic propagating chain ends. Chong et. al. (1999) reported the copolymerization of benzyl methacrylate macromonomer with MAA in DMF which resulted in the oligomeric block of MAA. Sprong et. al. (2002) used RAFT technique for the synthesis of random and block copolymers of MMA, MAA and a hydrophobic macromonomer which exhibited associative behaviour and reported its rheological properties. There is no report on the RAFT homopolymerization of MAA in water. However, Loiseau et. al. (2003) reported retardation in the RAFT polymerization of acrylic acid in aqueous medium due to the formation of a stable adduct radical.

Xiong et. al. (2004) reported the polymerization of DMAEMA with narrow PD (1.04-1.35) in aqueous medium using 4- cyanopentanoic acid as RAFT agent. You et. al. (2007) reported the RAFT polymerization of DMAEMA in THF having PD 1.4.

Being nonconjugative, NVP produces a highly reactive radical. It is very difficult to maintain the fast interconversion between these highly reactive radical and dormant species in living polymerization methods. ATRP of NVP was not possible since the polar lactam group present in NVP complexes with the metal catalyst used during polymerization.

Wan et. al (2005) investigated the polymerization of NVP in the presence of xanthates and dithioesters in fluroalcohols at 20, 60 and 120^{0}C. Induction period was observed for polymerization at 20^{0}C and 60^{0}C but more at 120^{0}C. This was a result of uncontrolled polymerization at high temperature due to side reaction at high concentration of the radical species and poor reinitiating ability of benzylic radicals. At lower temperature the decreased concentration of the radical species minimized the side reaction and led to better molecular weight control. The PD observed by this approach was in the range 2.3 – 4.8 and increased with temperature. Polymerization carried out at 60^{0}C yields linear graph for yield Vs molecular weight and yield Vs PD.

Devasia et. al. (2005) reported the RAFT polymerization of NVP in dioxane in the presence of diphenyl dithiocarbamate of diethyl malonate as RAFT reagent. The effect of ratio of [I] / [CTA] on conversion and PDs was investigated. The PD control was good at lower concentration of initiator which decreased the side reaction due to lower concentration of initiator radicals. However, the conversion was very low. The higher molecular weight obtained compared to the theoretical one could be due to the bimolecular termination. The PDs obtained were in the range 1.2–2.3 which were very low compared to the conventional radical polymerization in which PD was 8.4.

Postma et. al. (2006) reported that O–Ethyl S-(Phthalimidylmethyl) xanthate was efficient during the RAFT polymerization of NVP. At lower concentrations, molecular weights obtained were lower than expected and also PDs were broader, whereas, at higher concentrations PDs were lower and the molecular weights were consistent with the calculated one.

Bilalis et. al. (2006) found that with increasing [NVP] / [CTA] molar ratio the conversion decreases and PD is narrowed. When polymerization was carried in water polymers with high PD (2.1) was obtained which shows that termination reactions are taking place during the polymerization, whereas, when THF was used as a solvent PDs obtained were narrower (1.5).

The problem of spontaneous polymerization often observed in polar solvents for vinyl pyridine monomers was overcome by carrying out its polymerization in bulk rather than in solution (Convertine 2003). The polymerization of 2- and 4-vinylpyridine utilizing 2, 2' azobis isobutyro nitrile (AIBN) as the source of free radicals and cumyl dithiobenzoate (CTA_3) as the RAFT CTA using a molar ratio of 1:4.75 at 60 °C was demonstrated.

To date, relatively very few examples of aqueous RAFT have been reported, probably due to difficulties in preparing appropriate water-soluble CTAs and improper selection of monomers, solvent and other conditions. A water soluble AFCT agent which can yield unsaturated macromonomers is not yet synthesized. Among all the dimers reported AMSD was found to be most efficient AFCT agent. (Yamada B., 1994) Glockner et. al. (2000) reported that the complexation of hydrophobic monomers as well as the chain transfer agent i.e. dodecanethiol with dimethyl cyclodextrin increased the solubility of both species in water. The efficiency of AMSD–DMCD IC as an AFCT agent for water soluble monomers was evaluated.

5.3 Experimental

5.3.1 Materials

Dimethylated β-cyclodextrin (DMCD) was obtained from Wacker-Chemie GmbH, Germany and had an average degree of methylation of about 1.8 per glucose unit. Alpha methyl styrene dimer (AMSD) was purchased from aldrich. Acrylamide (AM) and 2, 2' azo bis 2–amidinopropane dihydrochloride were obtained from Aldrich. Methacrylic acid (MAA), 2–dimethyl amino ethyl methacrylate (DMAEMA) and N–vinyl pyrrolidone (NVP) were obtained from Aldrich and used after vacuum distillation. The deuterated solvents $DMSOd_6$, D_2O and $CDCl_3$ were also purchased from Aldrich.

The solvents acetone, methanol and petroleum ether were used after purification by distillation. Distilled water was obtained from Millipore system.

5.3.2 Methods

FTIR spectra were recorded on Perkin–Elmer spectrum one. IC and polymers were mixed with KBr and the spectra were recorded at frequencies from 4000 to 450 cm^{-1} using diffused reflectance spectroscopy (DRS) mode. The resolution was 4 cm^{-1}. Bruker AV 400 NMR spectrometers were used to record the ^1H NMR spectra of macromonomers. The macromonomer spectrum was recorded in D_2O and $CDCl_3$. Molecular weights of macromonomers and their copolymers were determined at 25 °C using aqueous size exclusion chromatography equipped with TSK-GEL columns using 0.2 M $NaNO_3$ at a flow rate 1 mL min^{-1}. The columns were calibrated using Poly(AM) standards. Differential scanning calorimetric (DSC) measurements were performed under nitrogen at a flow rate of 50 mL min^{-1} on TA instruments, model Q–10. The samples were scanned from -80 to 250 °C at 10 °C min^{-1}. The conversions during polymerizations were determined gravimetrically.

5.3.3 Synthesis

5.3.3.1 Synthesis of AMSD-DMCD IC by solvent evaporation
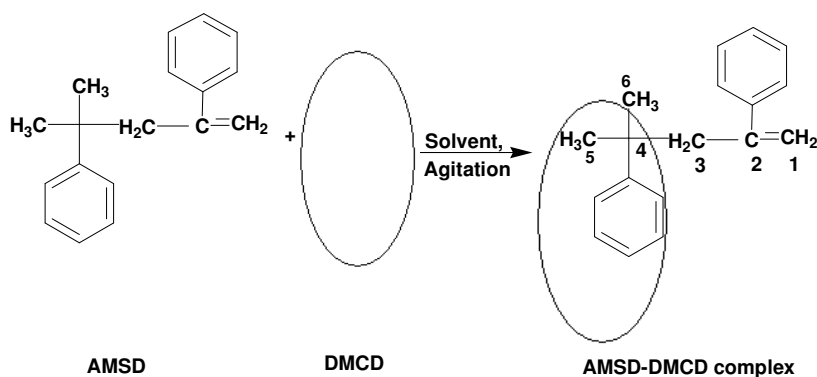
Scheme 5.1 Synthesis of AMSD-DMCD IC

The synthesis of AMSD-DMCD IC (Scheme 5.1) is described in the previous chapter.

The formation of IC was confirmed by instrumental techniques such as NMR, FTIR, XRD, TGA and molecular modeling as described in this chapter.

5.3.3.2 Synthesis and characterization of WSM
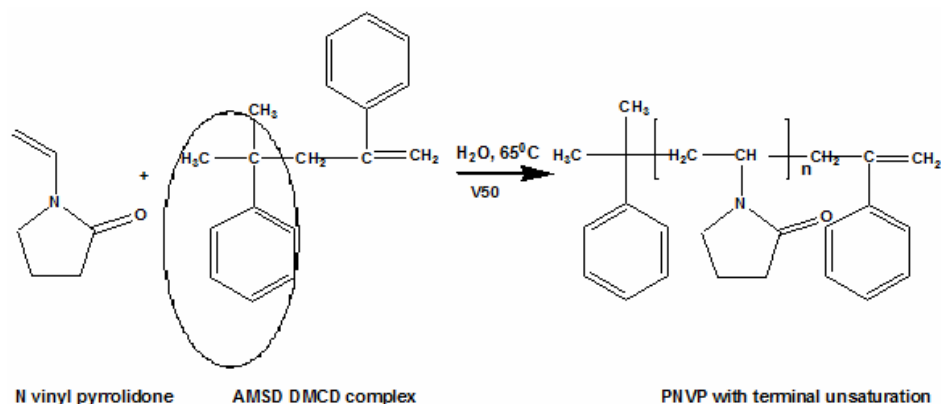
Scheme 5.2 WSM Synthesis

A representative procedure for macromonomer synthesis (Scheme 5.2) is described below.

1 g (0.009 mole) NVP, 0.010 g 2, 2' azo bis amidinopropane dihydrochloride (1 wt % based on monomer) and 0.1129 g AMSD–DMCD IC (Monomer : complex mole ratio 125:1) were dissolved in 10 mL distilled water. The reaction mixture was purged with nitrogen gas and polymerization was carried out at 65 °C so as to maintain the conversion below 10 %. The polymer solution was precipitated in acetone, filtered and washed repeatedly with petroleum ether to eliminate unreacted monomer and AMSD respectively and then dried. Macromonomers of AM, DMAEMA and MAA were similarly prepared.

5.3.3.3 Synthesis of graft copolymers from macromonomers

The macromonomers were copolymerized with monomers such as 4–VP, DMAEMA and MAA in different ratios to yield graft copolymers.

A representative procedure for copolymerization (Scheme 5.3) is described below.

0.9 g (0.0081 mole) Poly(NVP) macromonomer having M_n 4404, 0.0409 g potassium persulphate (2 mole % based on macromonomer and comonomer) and 0.0669 g (0.0004 mole) DMAEMA (Macromonomer : DMAEMA 95:5 mole ratio) were dissolved in 9.7 ml distilled water. The reaction mixture was purged with nitrogen gas and polymerization was carried out at 65 °C for 12 h. The resultant solution was precipitated in acetone to remove unreacted NVP, DMAEMA and homopolymers formed if any,

filtered and washed with tetrahydrofuran to remove unreacted Poly(NVP). Similarly, other graft copolymers i.e. Poly(NVP-co-MA), Poly(NVP-co-4-VP), Poly(AM-co-MA), Poly(AM-co-DMAEMA) and Poly(AM-co-4-VP) were prepared.

PNVP with terminal unsaturation   **DMAEMA**   **P(NVP - co - DMAEMA)**
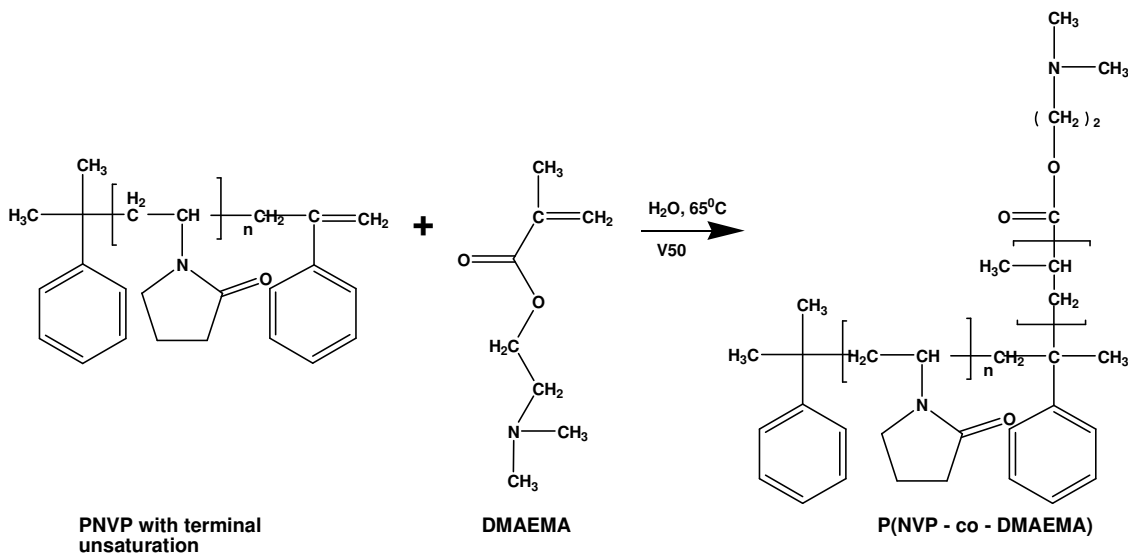
Scheme 5. 3 Graft copolymer synthesis

5.4 Results and discussion

5.4.1 IC synthesis and characterization

AMSD-DMCD IC was prepared in chloroform by solvent evaporation technique as described earlier. The complex formation was confirmed by the thermogravimetric analysis, ^{1}H NMR and molecular modeling analysis. The use of AMSD-DMCD IC as AFCT agent for the synthesis of water-soluble macromonomer (WSM) was explored. The steric hindrance caused by the presence of DMCD in the complex at the radical center and stability of the propagating radical govern the addition fragmentation efficiency of AMSD IC. The functionality '*f*' of the macromonomers could be manipulated by varying temperature and AFCT agent concentration. Poly(NVP) and Poly(AM) macromonomers having '*f*' close to unity were further copolymerized with pH sensitive monomers to yield graft copolymers which exhibited slow dissolution as compared to random copolymers of identical composition, which dissolved instantaneously.

5.4.2 Evaluation of CTC

α-substituted methyl acrylates and their oligomers which act as AFCT agents, cannot be used in the aqueous media because of lack of solubility. The AFCT agents traditionally used for the aqueous system are dithioesters, trithiocarbonates and dithiocarbamates which introduce S=S group rather than the C=C group in the macromonomer and need to be thermolyzed further to obtain the terminally unsaturated macromonomers. They also undergo hydrolysis and aminolysis with 1^0 and 2^0 amines in aqueous media and cannot be used for acrylamide unless neutral pH is maintained to minimize hydrolysis and acidic pH to minimize aminolysis (Thomas et. al. 2003, 2004).

Water soluble AFCT agents which can yield unsaturated macromonomers are not yet known. Glockner et. al. (2000) reported that the complexation of hydrophobic monomers and the chain transfer agent dodecanethiol increases solubility of both in water and showed that the chain transfer activity of dodecanethiol decreases. Amongst all the dimers evaluated as AFCT agents, AMSD was found to be most efficient (Yamada 1994). The efficiency of AMSD–DMCD IC as an AFCT agent for water soluble monomers was therefore investigated.

Watanabe et. al. (1993) reported AMSD as the AFCT agent in the synthesis of Sty macromonomer. The growing polymer chain radical adds to the double bond in AMSD and the adduct radical undergoes fragmentation to produce a cumyl radical and a macromonomer bearing a terminal double bond, since the tertiary cumyl radical is more stable than the secondary polymer radical.

5.4.2.1 Effect of monomer structure and temperature on CTC

The major factors which govern the efficiency of the addition fragmentation are steric hindrance at the radical centre, reactivity of the propagating radical and the stability of the radical formed (Colombani 1999). The reactivity of the radical is governed by the polar, inductive and resonance effects. The competition between fragmentation and propagation is critical during AFCT polymerization. The reported reactivities of DMAEMA, MAA, AM and NVP with sty are summarized in table 5.1.

Table 5.1 Reactivities of monomers

Monomer (r_1)	r_1	Sty (r_2)
DMAEMA (Bulk)	0.37	0.53
MAA	0.55	0.21
AM	0.58	1.17
NVP	0.057	17.2

DMAEMA has electron withdrawing carbonyl and electron donating methyl group attached to the vinyl radical. This results in preferred attack of electron rich monomer such as styrene on the growing DMAEMA radical. This is reflected in lower value of r_1 in copolymerization of DMAEMA with Sty. For similar reason, the attack of AMSD-DMCD IC on DMAEMA is preferred which results in highest chain transfer constant for DMAEMA amongst the monomers investigated herein (Table 5.6). The molecular weights of DMAEMA macromonomers were comparable with the values calculated (Rizzardo et. al. Table 5.2). The captodative effect in DMAEMA also results in the incorporation of highest percent unsaturation (32 %) in the resulting macromonomer.

In the case of NVP, the presence of electron withdrawing carbonyl group attached to the vinyl radical through nitrogen lowers the probability of radical formation. Although the monomer is electron deficient, the attack of AMSD-DMCD IC is less favored as a result of steric hindrance caused by the bulky pyrrolidone group. This results in lower chain transfer constant. On the other hand the increased steric hindrance results in enhanced fragmentation efficiency and hence the terminal unsaturation content of the resulting NVP macromonomer is higher (McHale et. al. 2005). The experimental molecular weights of NVP macromonomer were comparable to the theoretical ones especially at higher concentrations of AMSD-DMCD IC (Table 5.3).

Table 5.2 Role of AMSD-DMCD as CTA in polymerization of DMAEMA

AMSD mole% by ^{1}H NMR at °C			% Conv. at °C[a]			M_n (Theo)[b] at °C			M_n (GPC)[c] at °C			PD[d] at °C			$f = M_n$(GPC) / M_n(Theo) at °C		
50	65	75	50	65	75	50	65	75	50	65	75	50	65	75	50	65	75
3.85	4.0	4.9	8.3	9.5	9.4	32813	31510	28878	51200	33245	6575	2.18	2.21	1.86	1.56	1.05	0.73
1.96	2.7	3.7	6.7	9.3	9.6	52830	48988	39463	59807	38536	8976	2.05	2.17	1.78	1.13	0.78	0.45
1.32	2.2	3.1	7.5	9.6	8.8	88547	67237	43422	65095	45278	11932	1.87	2.14	1.73	0.73	0.67	0.33
0.99	1.8	2.6	7.6	8.9	8.5	119568	76466	50228	73322	48425	14367	1.80	2.06	1.58	0.61	0.63	0.23
0.65	1.3	2.1	7.9	8.8	9.1	189811	105131	66840	77877	52232	17899	1.69	2.02	1.51	0.41	0.49	0.13
0.40	0.70	0.50	8.1	9.1	9.9	316889	202907	102301	86566	53989	21105	1.65	1.99	1.48	0.27	0.26	0.06

[Monomer] : 0.90 mol L^{-1}, Initiator [V-50] : 0.0037 mol L^{-1}, Solvent : Water

[a.] Measured gravimetrically, b. M_n(Theo) = (M_M. [M]$_0$.x)/[AFCT]$_0$ + M_{AFCT} where M_M and M_{AFCT} are the molecular weights of Monomer and AFCT agent, x is the conversion and [M]$_0$ and [AFCT]$_0$ are the initial concentrations of monomer and AFCT agent. (Le 1998) c. M_n(GPC) calculated by aqueous size exclusion chromatography (RI detector), d. PD = M_w/M_n

Table 5.3 Role of AMSD-DMCD as CTA in polymerization of NVP

AMSD mole% by ^{1}H NMR at °C			% Conv. at °C[a]			M_n (Theo)[b] at °C			M_n (GPC)[c] at °C			PD[d] at °C			$f=M_n(GPC) / M_n(Theo)$ at °C		
65	75	85	65	75	85	65	75	85	65	75	85	65	75	85	65	75	85
1.75	1.98	2.7	6.5	6.9	7.2	40794	38199	29073	28677	26676	22333	2.18	2.21	1.86	0.70	0.70	0.77
1.35	1.73	2.1	5.4	6.7	7.3	44091	42534	38059	31100	29010	25466	2.05	2.17	1.78	0.70	0.68	0.67
1.17	1.4	1.6	5.3	6.3	6.9	49992	49548	47398	33423	31,233	29739	1.87	2.14	1.73	0.62	0.63	0.63
0.85	1.17	1.3	4.9	6.5	6.5	63760	61258	55083	34555	33544	31899	1.80	2.06	1.58	0.52	0.55	0.58
0.64	0.96	0.9	5.8	5.4	6.3	100312	62152	77333	37878	35466	33722	1.69	2.02	1.51	0.34	0.57	0.43
0.41	0.75	0.7	5.4	6.9	6.8	146015	101717	107444	41234	39843	36194	1.65	1.99	1.48	0.26	0.39	0.33

[Monomer] : 0.90 mol L^{-1}, Initiator [V-50] : 0.0037 mol L^{-1}, Solvent : Water

a. Measured gravimetrically, b. M_n(Theo) = (M_M. [M]$_0$.x)/[AFCT]$_0$ + M_{AFCT} where M_M and M_{AFCT} are the molecular weights of Monomer and AFCT agent, x is the conversion and [M]$_0$ and [AFCT]$_0$ are the initial concentrations of monomer and AFCT agent. (Le 1998) c. M_n(GPC) calculated by aqueous size exclusion chromatography (RI detector), d. PD = M_w/M_n

Table 5.4 Role of AMSD-DMCD as CTA in polymerization of AM

AMSD mole% by ^{1}H NMR at °C			% Conv. at °C[a]			M_n (Theo)[b] at °C			M_n (GPC)[c] at °C			PD[d] at °C			$f=M_n$(GPC) / M_n(Theo) at °C		
65	75	85	65	75	85	65	75	85	65	75	85	65	75	85	65	75	85
3.29	3.63	3.84	9.8	8.7	9.8	20689	16634	17659	49536	46534	26638	1.85	1.91	2.19	2.39	2.8	1.50
1.65	1.87	1.96	9.2	8.4	8.9	39170	31532	31843	70024	56565	36605	1.78	1.87	1.93	1.78	1.79	1.15
0.97	1.20	1.31	8.9	9.6	8.9	64748	56354	47840	94697	65469	44345	1.69	1.88	1.89	1.46	1.16	0.92
0.82	0.90	0.99	9.5	8.6	9.6	81817	67469	68402	95589	71423	50455	1.59	1.83	1.80	1.16	1.05	0.74
0.62	0.71	0.79	9.2	9.3	9.9	104937	92575	88507	98422	77709	61024	1.52	1.60	1.71	0.94	0.84	0.69
0.51	0.62	0.66	8.2	9.0	8.6	113810	102661	92140	104232	86767	66989	1.50	1.61	1.67	0.91	0.84	0.73
0.35	0.48	0.57	7.8	9.6	7.9	157910	141554	98078	109495	96948	74572	1.46	1.54	1.61	0.69	0.68	0.76

[Monomer] : 1.41 mol L^{-1}, Initiator [V-50] : 0.0037 mol L^{-1}, Solvent : Water

a. Measured gravimetrically, b. M_n(Theo) = (M_M. $[M]_0$.x)/$[AFCT]_0$ + M_{AFCT} where M_M and M_{AFCT} are the molecular weights of Monomer and AFCT agent, x is the conversion and $[M]_0$ and $[AFCT]_0$ are the initial concentrations of monomer and AFCT agent. (Le 1998) c. M_n(GPC) calculated by aqueous size exclusion chromatography (RI detector), d. PD = M_w/M_n

Table 5.5 Role of AMSD-DMCD as CTA in polymerization of MAA

AMSD mole% by ^{1}H NMR at °C			% Conv. at °C^a			M_n (Theo)^b at °C			M_n (GPC)^c at °C			PD^d at °C			$f=M_n$(GPC) / M_n(Theo) at °C		
65	75	85	65	75	85	65	75	85	65	75	85	65	75	85	65	75	85
1.9	2.2	2.7	8.5	8.9	8.7	37978	34261	27198	29888	27788	23040	2.23	2.15	2.06	0.78	0.81	0.85
1.7	2.0	2.3	8.6	9.3	9.1	43002	39426	33479	33687	31257	27877	2.15	2.07	1.99	0.78	0.79	0.83
1.4	1.6	1.8	9.7	9.2	9.6	58987	48894	45277	45785	37766	37070	2.03	1.98	1.88	0.77	0.77	0.82
1.1	1.3	1.5	9.8	9.2	8.9	76011	60306	50497	58090	46566	47656	1.95	1.86	1.81	0.76	0.77	0.94
0.7	0.9	1.2	8.9	9.1	9.2	108813	86408	65378	81470	54780	50788	1.81	1.76	1.72	0.75	0.63	0.77
0.5	0.65	0.8	9.1	8.9	9.4	155973	117224	100477	85333	62233	63945	1.75	1.67	1.61	0.55	0.60	0.63

[Monomer] : 1.16 mol L^{-1}, Initiator [V-50] : 0.0037 mol L^{-1}, Solvent : Water

a. Measured gravimetrically, b. M_n(Theo) = (M_M. [M]$_0$.x)/[AFCT]$_0$ + M_{AFCT} where M_M and M_{AFCT} are the molecular weights of Monomer and AFCT agent, x is the conversion and [M]$_0$ and [AFCT]$_0$ are the initial concentrations of monomer and AFCT agent. (Le 1998) c. M_n(GPC) calculated by aqueous size exclusion chromatography (RI detector), d. PD = M_w/M_n
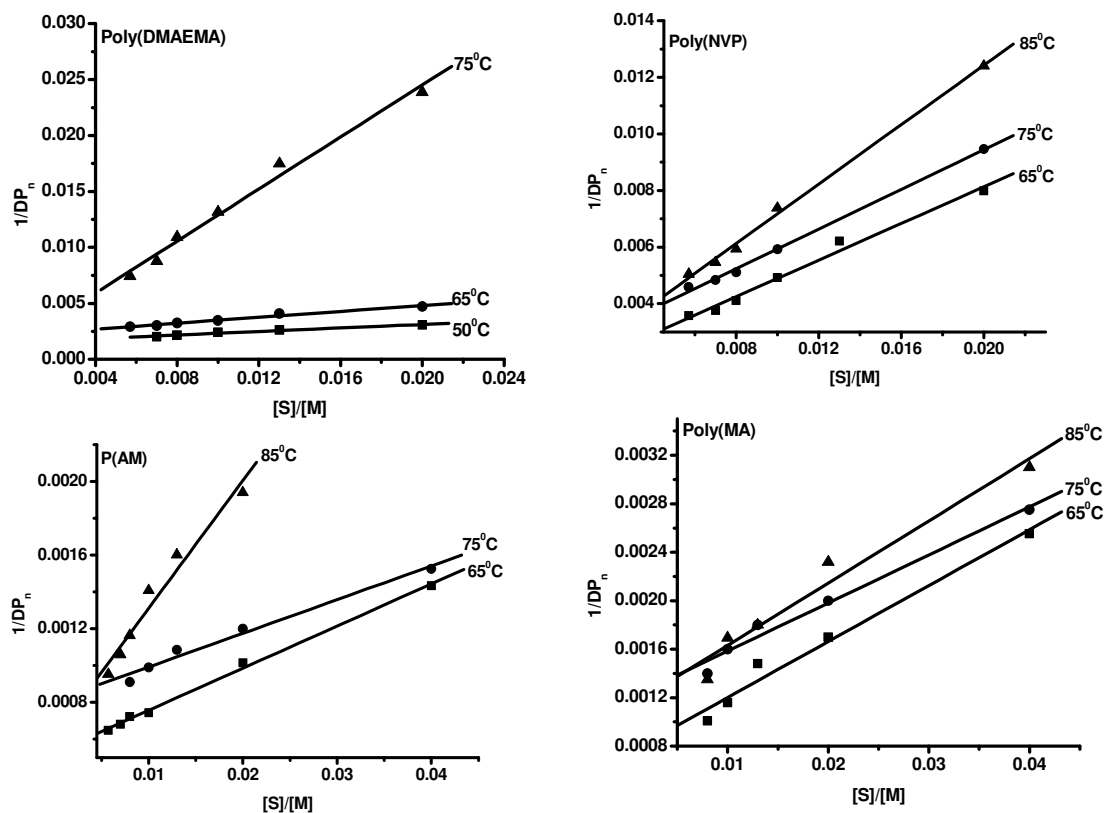
Figure 5.6 Mayo Plots for Poly(DMAEMA), Poly(NVP), Poly(AM) and Poly(MAA)

In AM radical, presence of electron withdrawing carbonyl group makes it less electron rich centre, and favors attack of AMSD on the AM radical. However, the chain transfer constant is lower than in case of DMAEMA and NVP because of the absence of the captodative effect and steric hindrance. The theoretical molecular weights of AM macromonomer were close to the experimental values at lower concentrations of AMSD-DMCD IC (Table 5.4).

MAA radical is attached to the electron donating CH_3 group and electron withdrawing carbonyl group. Though captodative effect operates, the stability of the adduct radical formed does not favor fragmentation. Loiseau (2003) too reported that AA forms stable adduct radical which is less susceptible to fragmentation. The propagation of MAA dominates over fragmentation and the chain transfer constant is lowered. Also, the propagation is favored over fragmentation; the difference between the theoretical and experimental molecular weights is hence significant (Table 5.5). The chain transfer

constants (CTCs) were evaluated by Mayo's method (Odian 1991). Typical Mayo plots are shown in figure 5.6 and the values of CTC are summarized in Table 5.6.

Table 5.6 Chain transfer constants of macromonomers

Sr. no.	Macromonomer	Chain transfer constant			
		50°C	65°C	75°C	85°C
1.	Poly(AM)	-	0.023	0.018	0.069
2.	Poly(NVP)	-	0.32	0.35	0.52
3.	Poly(DMAEMA)	0.08	0.13	1.16	-
4.	Poly(MAA)	-	0.05	0.04	0.05

5.4.3 Kinetics

A series of polymerizations were carried out wherein the concentration of the AFCT agent was kept constant and the reaction time was varied (Tables 5.7-10). In all cases, conversion increased with time. No induction period / retardation were observed. Further, the molecular weight of all the macromonomers increased linearly with conversion, which proves the living nature of polymerization (figures 5.7-10 A). Polydispersities (PDs) remained almost constant with time (1.46-2.1) (figures 5.7-10 (B-D)). We therefore conclude that AMSD-DMCD acts as AFCT agent. Kollisch et. al. (2006) reported PDs in the range 1.23-2.36 for the RAFT polymerization of Sty-DMCD IC in water. The broader PDs were attributed to the heterogeneity of the medium during polymerization. In the present case too, the PDs are high, and can be ascribed to the heterogeneity of the medium as reported by Kollisch.

Table 5.7 Polymerization of AM

Time Min.	% Conv. at °C			M_n at °C			PD at °C		
	65	75	85	65	75	85	65	75	85
10	9.8	10.7	11.5	49536	47756	30656	1.85	1.93	2.1
15	22.3	24.3	26.5	51989	49879	38767	1.83	1.9	2.08
20	45.6	47.6	49.8	53888	52444	42345	1.82	1.92	2.09
25	55.8	58.9	61.3	56787	55899	46755	1.84	1.92	2.1
30	67.6	70.1	74.5	59878	58766	51243	1.88	1.93	1.98
35	78.5	81.2	83.6	63455	61233	57646	1.89	1.89	1.9
40	83.4	86.7	89.8	67654	64566	61245	1.89	1.8	1.89
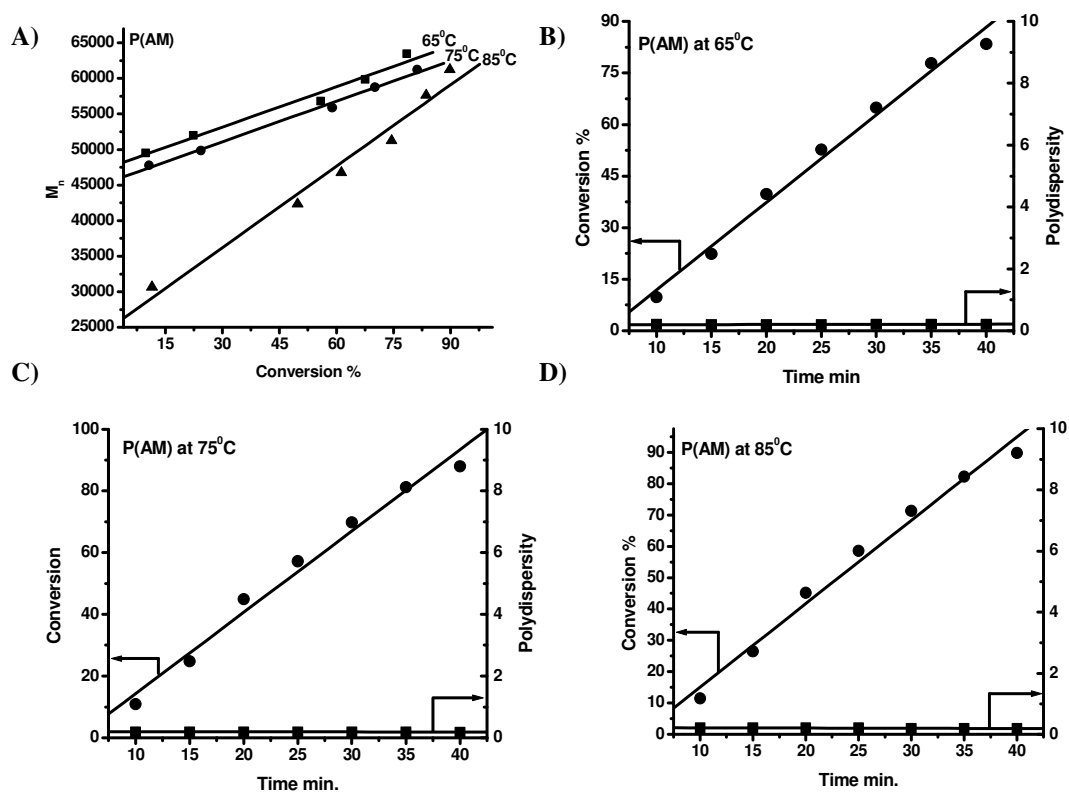
Figure 5.7 A) Conv. Vs M_n 65, 75 and 85°C and Time Vs Conv. and PD for P(AM) macromonomer at B) 65, C) 75 and D) 85°C

Table 5.8 Polymerization of NVP

Time Min.	% Conv. at °C			M_n at °C			PD at °C		
	65	75	85	65	75	85	65	75	85
10	4.5	5.2	6	25435	24583	20500	1.9	1.97	1.98
20	9.9	10.8	11.9	28713	27980	24658	1.85	1.97	1.98
30	16.7	17.5	18.7	31243	30785	28765	1.81	1.95	1.96
40	28.4	29.3	30.6	35676	34555	31245	1.79	1.9	1.94
60	48.4	49.7	50.9	42345	41356	37654	1.72	1.81	1.84
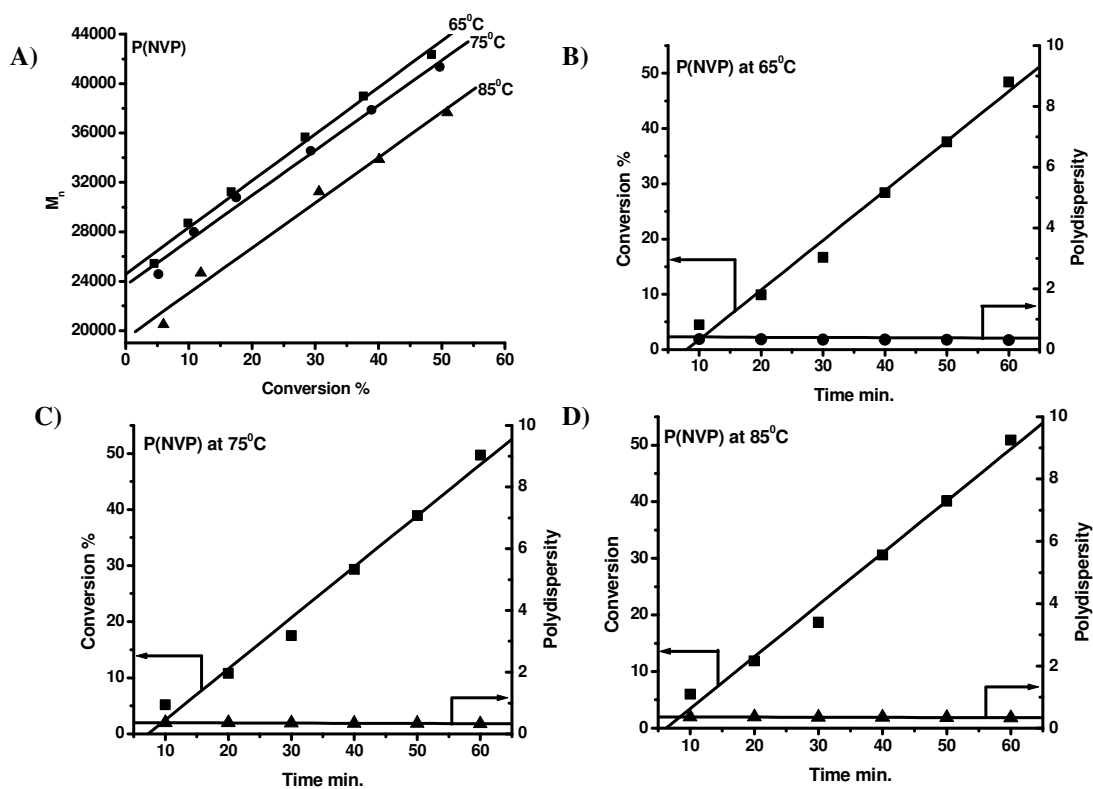
Figure 5.8 A) Conv. Vs M_n 65, 75 and 85°C and Time Vs Conv. and PD for P(NVP) macromonomer at B) 65, C) 75 and D) 85°C

Table 5.9 Polymerization of DMAEMA

Time	% Conv. at °C			M_n at °C			PD at °C		
Min.	50	65	75	50	65	75	50	65	75
10	9.3	9.8	10.8	52366	34855	7394	1.98	2.00	1.97
20	12.4	13.2	14.1	54333	39896	13434	1.97	2.00	1.95
30	16.5	17	17.8	57485	45676	19425	1.97	1.95	1.90
40	21.2	22.3	23.1	60981	51243	23675	1.95	1.95	1.93
50	25.6	26.9	27.8	64294	57100	28755	1.95	1.98	1.91
60	29.4	30.8	31.7	67354	61987	33985	1.94	1.90	1.87
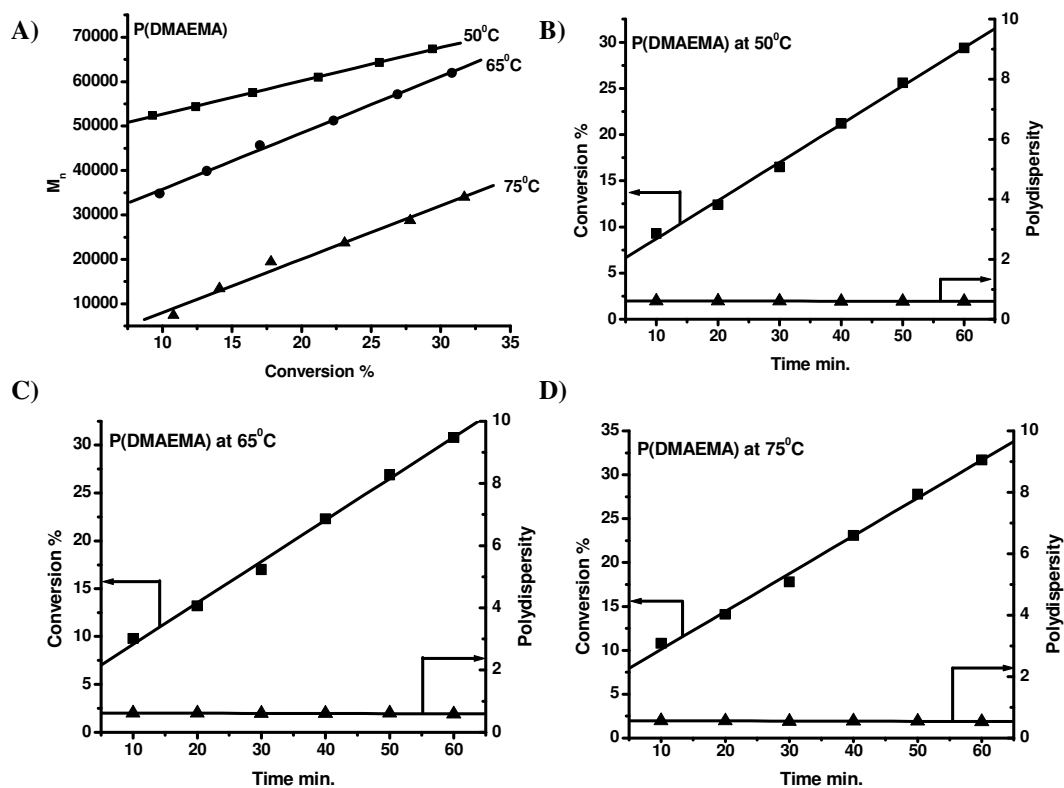
Figure 5.9 A) Conv. Vs M_n 50, 65 and 75°C and Time Vs Conv. and PD for P(DMAEMA) macromonomer at B) 50, C) 65 and D) 75°C

Table 5.10 Polymerization of MAA

Time Min.	% Conv. at °C			M_n at °C			PD at °C		
	65	75	85	65	75	85	65	75	85
10	7.3	8.5	9.7	28121	27850	25455	2.10	2.2	2.3
20	10.5	11.1	11.8	32455	30927	28974	2.10	2.2	2.3
30	12.9	13.4	14	36788	34215	31960	2.00	2.2	2.1
40	15.6	16.2	16.8	40291	38184	34765	1.97	2.1	2.2
50	18.4	19.1	19.9	44987	41975	37834	1.89	2.1	2.1
60	22.1	22.9	23.7	49878	45897	41210	1.86	2.1	2.1
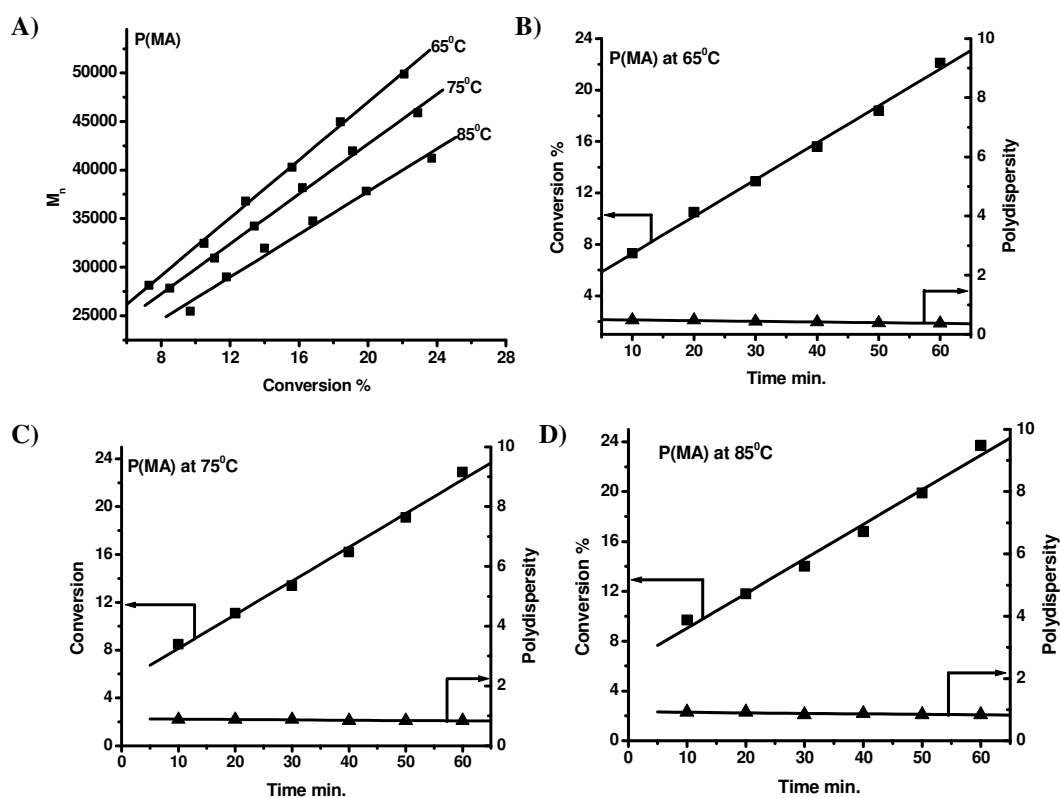
Figure 5.10 A) Conv. Vs M_n 65, 75 and 85°C and Time Vs Conv. and PD for P(MA) macromonomer at B) 65, C) 75 and D) 85°C

5.4.4 Structural analysis of macromonomer

Watanabe et. al. (1993) proposed that the chain transfer activity of AMSD is a result of addition fragmentation. The same mechanism can be expected to operate in the polymerization of water soluble monomers when AMSD-DMCD IC is used as an AFCT agent. The existence of vinyl groups in the macromonomer as evident from ^{1}H NMR confirms that the addition fragmentation chain transfer activity of AMSD is retained after inclusion complexation.
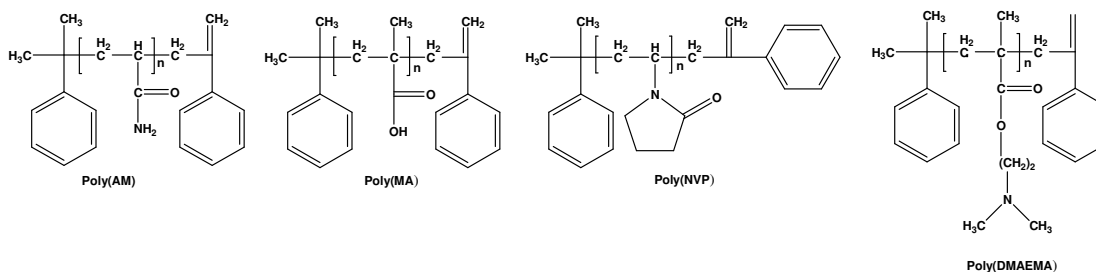
Figure 5.11 Structures of water soluble macromonomers

The terminal unsaturation in free radical polymerization can also result from the termination by disproportionation. If termination takes place by disproportionation the double bond will be attached directly to the monomer itself and will appear at 4.8-7 δ. Addition fragmentation will result in the attachment of the double bond to electronegative phenyl ring and hence the corresponding peaks will shift downfield and will appear at 4.7-5.6 δ. In all macromonomers the peaks due to unsaturation appeared in the region 4.7 to 5.6 δ (Figures 5.12-15 and Table 5.11). This confirms that terminally unsaturated WSMs result from the addition fragmentation chain transfer activity of AMSD-DMCD IC.
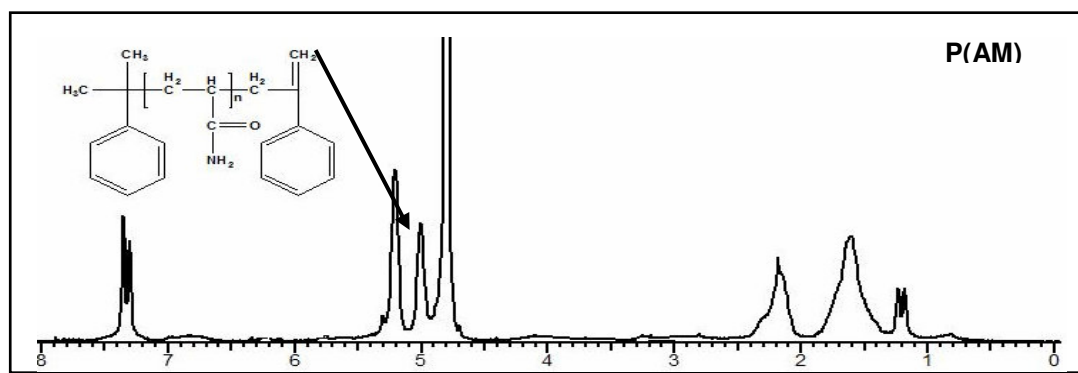
Figure 5.12 ^{1}H NMR of Poly(AM) macromonomer in D₂O
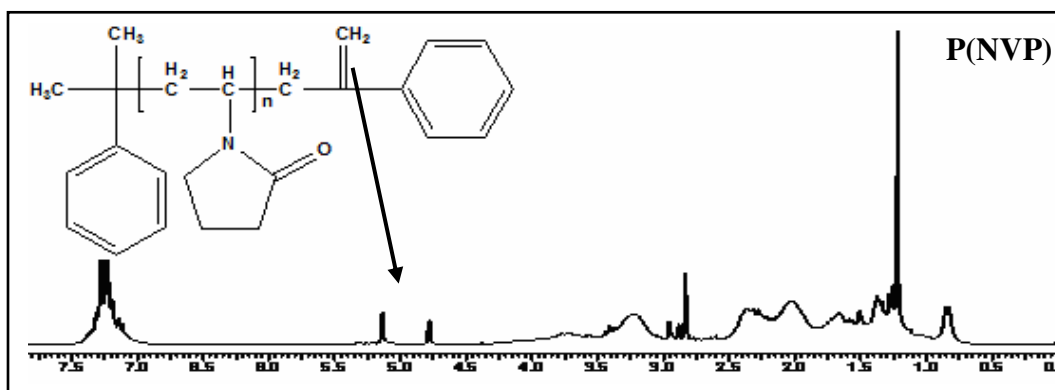
Figure 5.13 ^{1}H NMR of Poly(NVP) macromonomer in CDCl$_3$
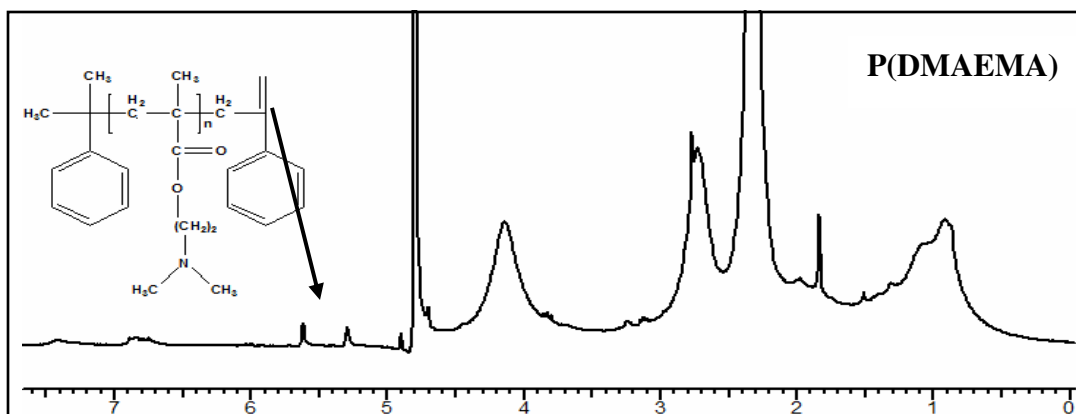
Figure 5.14 ^{1}H NMR of Poly(DMAEMA) macromonomer in D$_2$O
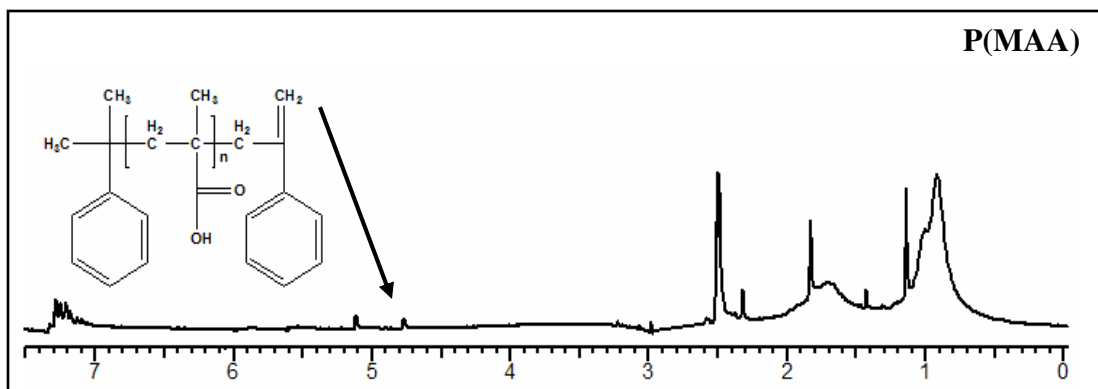
Figure 5.15 ^{1}H NMR of Poly(MAA) macromonomer in DMSOd$_6$

121

Table 5.11 ^{1}H NMR values of unsaturated peaks in macromonomers

macromonomers	vinyl peaks (δ ppm) resulting from	
	AFCT	Disproportionation
Poly(AM)	5 and 5.2	6.4 and 6.8
Poly(DMAEMA)	5.3 and 5.6	6.84
Poly(NVP)	4.7 and 5.3	4.8 and 6.8
Poly(MAA)	4.8 and 5.1	7.07

5.4.5 Evaluation of *f*

In the preceding section, the presence of terminal unsaturation in the macromonomers synthesized was established and shown to result from addition fragmentation rather than disproportionation. A graft copolymer can result from macromonomer only when each macromonomer has a terminal unsaturation. Very few reports attempt to quantify the unsaturation in macromonomers. The mechanistic aspects of addition fragmentation are similar to those in RAFT polymerization and hence $M_{n(theoretical)}$ was calculated using the following equation suggested by Le et. al. (1998).

$M_{n(Theo)} = (M_M.[M]_0.x / [AFCT]_0 + M_{AFCT}$

Where M_M and M_{AFCT} are the molecular weights of monomer and AFCT agent, x is the conversion and $[M]_0$ and $[AFCT]_0$ are the initial concentrations of monomer and AFCT agent.

We evaluated the functionality *f*, which represents the number of unsaturated end group per macromonomer according to the formula,

$f = M_{n(GPC)} / M_{n(theoretical)}$

Typical values of *f* are summarized in table 5.12. The details for each macromonomer synthesized are provided in tables 5.2-5.5.

Addition fragmentation chain transfer involves the reaction of the growing radical chain with the AFCT agent to yield an adduct radical which undergoes forward β-fragmentation to yield an ω unsaturated macromonomer and a small radical which reinitiates polymerization by reacting with a monomer. On the other hand, it can also undergo backward β-fragmentation to regenerate the AFCT agent and the propagating radical. The lower *f* value at lower concentrations of AMSD-DMCD IC could be

attributed to the lower concentration of the adduct comprising the growing radical chain and the AFCT agent. In contrast, the growing radical chain can react with the initiator fragment, other growing chains and radical generated by the forward fragmentation of the adduct to yield a dead polymer containing no terminal unsaturation.

Table 5.12 *f* values for macromonomers

Macromonomer	[S]/[M]	Temp. ^{0}C	*f*
Poly(DMAEMA)	0.013	50	1.13
	0.02	65	1.05
Poly(AM)	0.008	65	0.94
	0.01	75	1.05
	0.013	85	0.92
Poly(NVP)	0.02	65	0.7
	0.02	75	0.7
	0.02	85	0.77
Poly(MA)	0.04	75	0.81
	0.04	85	0.85

f = $M_{n(GPC)}$/ $M_{n(theoretical)}$ where $M_{n(Theo)}$ =(M_M.$[M]_0$.x / $[AFCT]_0$ + $M_{AFCT,}$ where M_M and M_{AFCT} are the molecular weights of monomer and AFCT agent, x is the conversion and $[M]_0$ and $[AFCT]_0$ are the initial concentrations of monomer and AFCT agent.

f approaches unity with increase in temperature. This is because the rate of fragmentation increases with temperature and dominates over propagation. At any given AFCT concentration adduct formation would be preferred at higher temperature because of higher energy of activation for the step involving reaction of the growing chain with AMSD-DMCD IC as compared to the addition of the monomer. Thus, with the proper choice of the concentration of AFCT agent and polymerization temperature macromonomers having *f* value close to unity could be obtained.

In some cases, *f* values greater than unity are observed. There are no similar reports in the literature since very few researchers reported *f* values. This could be explained as follows. The molecular weight of the macromonomer increases with decreasing temperature. At the same time, the conversion is still higher. Since the monomer is consumed in the propagation step; this results in a smaller increase in $M_{n(theoretical)}$ as compared to $M_{n(experimental)}$ i.e. $M_{n(GPC)}$ resulting in *f* values beyond unity.

An increase in inclusion complex concentration increases the adduct concentration, the fragmentation of which leads to the macromonomer containing terminal unsaturation. For instance, in case of NVP increase in temperature upto 85^0C still limits $f \approx 0.8$. The choice of NVP: AMSD mole ratio of 30:1 or 20:1 would be expected to lead to values approaching unity.

5.4.6 Graft copolymer synthesis

The macromonomers having functionality close to unity i.e. Poly(NVP) and Poly(AM) and molecular weights 4,404 and 5,614 were copolymerized with pH sensitive monomers i.e. 4–VP, DMAEMA and MAA. Poly(NVP) macromonomer was copolymerized with 4–VP, MAA and DMAEMA in water in the presence of potassium persulphate to yield Poly(NVP–co–4 VP), Poly(NVP–co–MAA) and Poly(NVP–co–DMAEMA). The molecular compositions of the graft copolymers were estimated by ^{1}H NMR. The shifting of the retention time of the formed copolymer towards the shorter retention time in GPC chromatogram confirms the copolymer formation. The absence of the peak corresponding to Poly(NVP) macromonomer further shows that no free macromonomer is present.

Devasia et. al. copolymerized Poly(NVP) macromonomer with styrene and butyl acrylate by RAFT method. This technique led to the formation of styrene / butyl acrylate blocks with Poly(NVP) macromonomer as a result of incorporation of the individual monomer into the adduct comprising the RAFT agent and the macromonomer. At any feed composition the content of the comonomer into the polymer was lower than that in the feed.

In contrast, the present approach leads to a random copolymer containing the comonomer and the Poly(NVP) macromonomer. The incorporation of the comonomer is quantitative. Although, the copolymer formed is random, the higher reactivity of the comonomer *vis a vis* Poly(NVP) macromonomer, results in blocks of comonomer in the main chain. The copolymer thus exhibits T_g corresponding to the homopolymer and T_g of the side chain viz. For example, Poly(NVP). In Poly(NVP-co-MAA), the copolymer also exhibits T_g corresponding to the T_g of MAA and Poly(NVP).

Table 5.13 Characteristics of graft copolymers

polymer	composition[1]	mol. wt. of macromonomer	mol. wt. of graft copolymer (M_n)	dissolution behavior	PD	T_g
Poly(NVP-co-DMAEMA)	94.0 : 6.0	4,404	10,846	15 min[2]	2.2	159 and 29
	89.5 : 10.5		14,139	35 min[2]	2.3	
Poly(NVP-co-4 VP)	84.3 : 14.7	4,404	6,515	5 min[2]	2.9	158
Poly(NVP-co-MAA)	67.3 : 32.7	4,404	8,060	Insoluble[3]	2.6	159 and 220
Poly(AM-co-4 VP)	93 : 7[4]	5,614	Insoluble	100[5]	-	150
	81.9 : 18.1[4]		Insoluble	600[5]	-	
Poly(AM-co-DMAEMA)	91.3 : 8.7	5,614	15,610	80 min[2]	2.6	156 and 27
	87.1 : 12.9		29,245	300[5]	2.5	
Poly(AM-co-MAA)	57.3 : 42.7	5,614	39,560	300% swelling upto 6h and then dissolves	2.7	149 and 223

[1]Composition determined by solution state ^{1}H NMR, [2]Soluble, [3]Dissolution study at pH 7.4, [4] Composition determined by solid state ^{1}H NMR, [5] % Swelling ratio.

AMSD content in Poly(NVP) and Poly(AM) macromonomer was 0.5 % and 1.8 % respectively.

In case of Poly(NVP–co–DMAEMA), with increasing concentration of DMAEMA from 6 to 26.3 mole % molecular weight increased from 10,846 to 18,596. The dissolution time of the polymer at pH 1.2 increased from 15 min to 40 min. When NVP macromonomer was copolymerized with 4–VP in mole ratio of 14.7 to 41.3 mole % the molecular weight increased from 6,515 to 11,230. The dissolution time was almost same for all the compositions. This was probably because the 4-VP content was already too high. Surprisingly, the graft copolymer comprising Poly(NVP) macromonomer and MAA (32.7 mole %) was insoluble at pH 7.4. This observation can not be explained at the moment.

All Poly(AM-co-4-VP) polymers were found to be insoluble in water, THF and chloroform since Poly(4-VP) is insoluble in water whereas Poly(AM) is insoluble in THF and chloroform. The compositions of these polymers were determined using ^{13}C solid state NMR. Poly(AM-co-DMAEMA) containing 8.7 mole % DMAEMA (Molecular weight 15,610) dissolved in 80 min. while those containing 12.9 mole % DMAEMA (Molecular weight 29,245) swelled 300 % at pH 1.2. Poly(AM–co-MAA) containing 42.7 mole % MAA (Molecular weight 39,560) swelled 300 % in first 6 h and then slowly dissolved. The random copolymers of the same composition dissolved immediately at same pH. DSC analysis of these graft copolymers showed that T_gs of the individual polymer segments were retained (Table 5.13) which is not surprising in view of the graft structure of the copolymers.

5.5 Conclusion

Though AMSD is hydrophobic in nature, complexation with DMCD enhances its water solubility. AMSD-DMCD IC with enhanced water solubility enables the macromonomer synthesis of DMAEMA, AM, NVP and MAA in water. The advantage of this approach is that the macromonomers could be synthesized in a single step. The highest '*f*' value (1.05) was obtained for Poly(DMAEMA) and Poly(AM) macromonomers where captodative effect plays an important role in AFCT mechanism. Due to the high fragmentation rate of AMSD in DMAEMA it gives very low molecular weight polymers and '*f*' values near to unity. As fragmentation rate increases with temperature; at higher temperature '*f*' values were closer to unity in all macromonomers. It is reported that AA forms a stable adduct radical and the propagation rate is high as compared to fragmentation. In case of MAA, the low control on molecular weight and poor '*f*' values at 85 $^{\circ}$C may be attributed to this. The kinetic analysis of all the macromonomers showed that the polymerization takes place in a controlled manner. The macromonomers were further copolymerized with pH sensitive vinyl monomers. Poly(NVP) and Poly(AM) macromonomers were used to synthesize the graft copolymers with pH sensitive monomers such as 4–VP, DMAEMA and MAA. The copolymers show the different dissolution characteristics than the random copolymers of the same composition. Thus, this approach makes possible to prepare double hydrophilic copolymers in a single step.

5.6 References

1. Kabanova A., Kabanov V. Adv. Drug Delivery Rev. **1998**, 30, 49.

2. Butun V., Billingham N., Armes S. J. Am. Chem. Soc. **1998**, 120, 11818.

3. Antonietti M., Breulmann M., Göltner C., Cölfen H., Wong K., Walsh D., Mann S. Chem. Eur. J. **1998**, 4, 2493.

4. Colfen H., Antonietti H. Langmuir **1998**, 14, 582.

5. Pistikalis M., Pispas S., Mays J., Hadjichristidis N. Adv. Poly. Sci. **1998**, 135, 1.

6. Hadjichristidis N., Latrou H., Pispas S., Pistikalis M. Curr. Org. chem., **2002**, 6, 155.

7. Ito K. Prog. Poly. Sci., **1998**, 23, 581.

8. Yamashita Y., Ito K., Mizuno H., Okada K. Polym. J. **1982**, 14, 255.

9. Akashi M., Yanagi T., Yashima E., Miyauchi N. J. Polym. Sc. Part A: Polym. Chem. **1989**, 27, 3521.

10. Devasia R., Bindu R., Borsali R., Mougin N., Gnanou Y. Macromol. Symp. **2005**, 229, 8.

11. Patten E., Matyjaszewski K. Adv. Mater. (Weinheim Ger.), **1998**, 10, 901.

12. Chiefari J., Chong Y., Ercole F., Krstina J., Jeffery J., Le T., Mayadunne R., Meijs G., Moad C., Moad G., Rizzardo E., Thang S. Macromolecules **1998**, 31, 5559.

13. Mayadunne R., Rizzardo E., Chiefari J., Krstina J., Moad G., Postma A., Thang S., Macromolecules **2000**, 33, 243.

14. Taton D., Wilczewska A., Destarac M. Macromol. Rap. Commun. **2001**, 22, 1497.

15. Francis R., Ajayaghosh A. Macromolecules **2000**, 33, 4699.

16. Ladaviere C., Dorr N., Claverie J. Macromolecules **2001**, 34, 5370.

17. Thomas D., Sumerlin B., Lowe A., McCormick C. Macromolecules **2003**, 36, 1436.

18. Thomas D., Convertine A., Hester R., Lowe A., McCormick C. Macromolecules **2004**, 37, 1735.

19. Postma H., Davis T., Evans R., Li G., Moad G., O'Shea M. Macromolecules **2006**, 39, 5293.

20. Postma A., Davis T., Li G., Moad G., O'Shea M., Macromolecules **2006**, 39, 5307.

21. Watanabe Y., Ishigaki H., Okada H., Suyama S. Chemistry letters **1993**, 22, 1089.

22. Yamada B., Tagashira S., Aoki S. J. Poly. Sci. Part A: Polymer chemistry **1994**, 32, 2745.

23. Ritter H., Tabatabai M., Prog. Polym. Sci. **2002**, 27, 1713.

24. Kollisch H., Barner–Kowollik C., Ritter H. Macromol. Rap. Comm. **2006**, 27, 848.

25. Sato E., Zetterlund P., Yamada B. Macromolecules **2004**, 37, 2363.

26. McHale R., Aldabbagh F., Carroll W., Yamada B. Macromol. Chem. and phys. **2005**, 206, 2054.

27. Moad G., Rizzardo E., Thang S. Polymer **2008,** 49, 1079.

28. Le T., Moad G., Rizzardo E., Thang S. WO 98/01478, **1998**.

29. Corpart P., Charmot D., Biadatti T., Zard S., Michelet D. WO 98/58974, **1998**.

30. Lai J., Shea R. J. Polym. Sci. Part A: Polym. Chem. **2006**, 44, 4298.

31. Mayadunne R., Rizzardo E., Chiefari J., Chong Y., Moad G., Thang S. Macromolecules **1999**, 32, 6977.

32. Corpart P., Charmot D., Zard S., Franck X., Bouhadir G. WO 99/35177, **1999**.

33. Lai J., Shea R., J. Polym. Sci. Part A: Polym. Chem. **2006**, 44, 4298.

34. Schilli C., Lanzendorfer M., Muller A. Macromolecules **2002,** 35, 6819.

35. Liu J., Hong C-Y, Pan C-Y. Polymer **2004**, 45, 4413.

36. Stenzel M., Davis T. J. Polym. Sci. Part A: Polym. Chem. **2002**, 40, 4498.

37. Lai J., Filla D., Shea R. Macromolecules **2002**, 35, 6754.

38. Mayadunne R., Rizzardo E. Macromolecules **2000**, 33, 243.

39. Favier A., Charreyre M. Macromol. Rapid Commun. **2006**, 27, 653.

40. Chiefari J., Chong, Y., Ercole F., Krstina J., Jeffery J., Le T., Mayadunne R., Meijs G., Moad C., Moad G., Rizzardo E., Thang S. Macromolecules **1998**, 31, 5559.

41. Mitsukami Y., Donovan M., Lowe A. and McCormick C. Macromolecules **2001**, 34 (7), 2248.

42. Sumerlin B., Donovan M., Mitsukami Y., Lowe A. McCormick C. Macromolecules **2001**, 34, 6561.

43. Sumerlin B., Lowe A., Thomas D., McCormick C. Macromolecules **2003**, 36, 5982.

44. Donovan M., Lowe A., Sumerlin B., McCormick C. Macromolecules **2002**, 35, 4123.

45. Donovan M., Sanford T., Lowe A., Sumerlin B., Mitsukami Y., McCormick C. Macromolecules **2002**, 35, 4570.

46. Chong Y., Le T., Moad G., Rizzardo E., Thang S. Macromolecules **1999**, 32, 2071.

47. Sprong E., Wet–Roos D., Tonge M., Sanderson R. J. Poly. Sci. Part A: Polym. Chem. **2003**, 41, 223.

48. Loiseau J., Doerr N., Suau J., Egraz J., Llauro M., Ladavie`re C., Claverie J. Macromolecules **2003**, 36, 3066.

49. Xiong Q., Ni P., Zhang F., Yu Z. Polymer Bulletin **2004**, 53, 1.

50. You Y., Manickam D., Zhou Q., Oupický D. J. of Controlled Release **2007**, 122, 217.

51. Wan D., Satoh K., Kamigaito M., Okamoto Y. Macromolecules **2005**, 38, 10397.

52. Devasia, R., Bindu R., Borsali R., Mougin N., Gnanou Y. Macromol. Symp. **2005**, 229, 8.

53. Bilalis P., M. Pitsikalis M., Hadjichristidis N. J. Poly. Sci. Part A: Poly. Chem. **2006**, 44, 659.

54. Convertine A., Sumerlin B., Thomas D., Lowe, A., McCormick C. Macromolecules **2003**, 36, 4679.

55. Wang R., McCormick C., Lowe A. Macromolecules **2005**, 38, 9518.

56. Okumura H., Kawaguchi Y., Harada A., Macromolecules **2003**, 36, 6422.

57. Li N., Liu J., Zhao X., Gao Y., Zheng L., Zhang J., Yua L. Colloids and Surfaces A: Physicochem. Eng. Aspects **2007**, 292, 196.

58. Jiang H., Sun H., Zhang S., Hua R., Xu Y., Jin S., Gong H., Li L. J. inclusion phenomena and macrocyclic chemistry, **2007**, 58 (1-2), 133.

59. Harata K., Kawano K. Carbohydrate research **2002**, 337 (6), 537.

60. (a) Glockner P., Ritter H. Macromol. Chem. and Phys. **2000**, 201 (17), 2455. (b) Glockner P., Metz N., Ritter H. Macromolecules **2000**, 33 (11), 4288.

61. Odian G. Principles of polymerization, 3rd ed.; J. Wiley & Sons: New York, **1991**, 640f.

62. Colombani D. Prog. Polym. Sci. **1999**, 24, 425.

63. Mironychev V., Mogilevich M., Smirnov B., Shapiro Y., Golikov Y., Polymer Science U.S.S.R **1986**, 28 (9), 2103.

64. Loiseau J., Doerr N., Suau J., Egraz J., Llauro M., Ladavie`re C., Claverie J., Macromolecules **2003**, 36, 3066.

65. Le T., Moad G., Rizzardo E., Thang S., **1998**, PCT. Int. Appl. WO 9801478.

Chapter 6

Inclusion Complexes of Multivinyl Monomers :
Synthesis and Characterization

6.1 Introduction

Crosslinked polymers obtained by simultaneous polymerization / crosslinking of monomers containing multiple double bonds find a wide range of applications such as ion exchange resins, adsorbents, molecularly imprinted polymers, supports for reagents in organic synthesis, enzyme immobilization and drug delivery systems (Zhu 1993). A sequential approach wherein a soluble linear polymer is first synthesized, converted into desirable form and then crosslinked, offers significant advantages in most of these applications (Liu et. al. 2001, Koo et. al. 2002, Li et. al. 2005, Mecerreyes et. al. 2001, Nagelsdiek et. al. 2004).

A number of attempts have been made to synthesize soluble polymers containing unsaturation. The strategies employed were polymerization in the presence of chain transfer agents (Guan 2002, Fukutomi et. al. 1982) or long chain alkyl groups (Matsumoto et. al. 1991), formation of vinyl group containing polymers by chloromethylation, followed by conversion into their phosphonium salts and finally by a Wittig reaction (Percec and Auman 1984, Neumann and Peterseim 1993, Farrall et. al. 1983). Anionic (Tsuruta, 1985) or group transfer polymerization and polymerization of crosslinkers in the presence of lewis acids are some of the examples of linear and pendant unsaturation containing polymers. Synthesis of reactive microgel by polymerization of divinyl benzene was carried out by Funke et. al. (Funke 1977).

A number of studies on the selective radical cyclopolymerization of divinyl compounds have been reported (Butler 1992, Butler 2000 and Kodaira 2000). Most of these studies were directed to diallylammonium, dialkyl methacrylamide or related divinyl compounds, the common feature of which is that the corresponding monovinyl compounds do not efficiently homopolymerize due to the stability of the allyl radicals or due to the bulkiness of the dialkyl methacrylamide monomer.

The homo and copolymerization of a divinyl compound usually results in crosslinked insoluble polymers due to the uncontrolled or random propagation of the growing radical of both double bonds. Almost, no selective radical polymerization of crosslinker is known which leads to linear soluble polymers with one of the two vinyl groups remaining unreacted. A possible solution for the highly selective polymerization is to

change the reactivity of the two vinyl groups or to alter the selectivity of the derived radical species using some additives that can give drastic effects on them.

Cyclodextrins (CD), because of their polar hydrophilic outer shell and hydrophobic cavity form host-guest complexes by inclusion of suitable molecules. The formation of these complexes leads to significant changes of the solubility and reactivity of the guest molecules without any chemical modification.

CD inclusion complexes (ICs) were exploited in organic chemistry to manipulate the selectivity of the reactions (Takahashi 1998). Selective chlorination of anisole at 'p' position was described by Breslow and Campbell (1969). Similarly, oxidation, reduction, hydrolysis, addition and photochemical reactions were also controlled by the use of CD ICs (Takahashi 1998).

In polymer chemistry, CD ICs were used as surfactants in emulsion polymerization of acrylates and methacrylates (Lau 1996). Chen et al., (2006) explored the use of CD in the condensation polymerization of 1-(2-aminoethyl) piperazine-CD IC and divinylsulfone to yield linear polymers, which otherwise yields hyperbranched structures. Sarvothaman and Ritter (2004) reported ICs comprising diacrylate and dimethacrylate and CD to obtain supramolecular architectures such as interlocked polyrotaxanes. The ICs comprising hydrophobic monomer and CD have been used to enhance solubility of monomers in aqueous media which enables their polymerization in water (Ritter and Tabatabai 2002). It was observed that the reactivity ratios of the methylated cyclodextrin (DMCD) complexed monomers isobornyl acrylate and n-butyl acrylate differ significantly from the reactivity ratios of the corresponding uncomplexed monomers (Glockner and Ritter 1999).

Crosslinker forms an inclusion complex with CD so that only one unsaturation site is exposed to polymerization while the other remains entrapped in the cavity yielding water–soluble polymers. The polymerization of crosslinker with vinyl monomers through supramolecular inclusion complex approach enables removing the traces of the unreacted crosslinkers in the first stage i.e. prior to crosslinking. Satav et. al. (2006) reported the selective polymerization of hydrophobic divinyl and trivinyl monomers to

yield soluble and pendant unsaturation containing polymers. However, these polymers cannot be used in the applications where water soluble polymers are required.

The water soluble copolymers obtained by this approach contain pendant unsaturation and can be used further for thermal or photocrosslinking to yield insoluble products. These polymers found applications in drug delivery, enzyme immobilization, photoresists based on water soluble polymers, etc.

We have demonstrated synthesis of water soluble polymers containing pendant unsaturation through selective polymerization of methylene bisacrylamide (MBAM), and bis(2-methacryloyloxyethyl) disulfide (DSDMA) via their inclusion complexes of CD. In this chapter, we will discuss the synthesis and characterization of ICs of MBAM and DSDMA with cyclodextrin derivatives. The details of structural investigation of these ICs i.e. stoichiometry of the complex by NMR and the insertion of the guest molecule inside the CD cavity by molecular modeling are also described. Before that we will discuss the prior efforts taken to synthesize linear polymers containing pendant unsaturation and peculiar characteristics of CD. The next chapter deals with the synthesis of copolymers of ICs and their application in sustained and burst delivery of macromolecular drugs.

6.2 Soluble polymers with pendant vinyl groups : Prior approaches and their limitations

Soluble and pendant vinyl group containing polymers from crosslinkers can be obtained by **c**opolymerization in the presence of chain transfer agent to retard the gel point or by emulsion polymerization by favouring intramolecular rather than intermolecular crosslinking (Hoffmann 1974, Obrecht et. al. 1974, Obrecht et. al. 1975, Obrecht et. al. 1976, Funke 1977). Chen et. al. (1984) found that the chain transfer agent prefers to suppcress the intermolecular crosslinks rather than the intramolecular crosslinks. Guan (2002) obtained soluble hyperbranched polymers of ethylene glycol dimethacrylate (EGDMA) in the presence of cobalt chain transfer catalyst which exhibit very low solution viscosities at high solid concentration. Matsumoto et. al. (1991) reported that the occurrence of intermolecular crosslinking leading to gelation is suppressed by the

steric effect of long chain alkyl groups. This provides a new way for the preparation of novel self crosslinkable polymers with pendant vinyl groups.
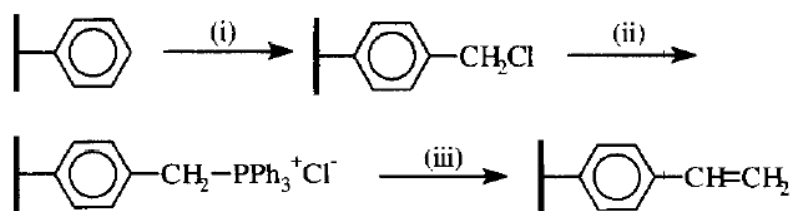
Figure 6.1 Modification of polystyrene matrix to form pendant vinyl groups (Neumann and Peterseim 1993) (i) SO$_2$Cl$_2$, ClSO$_3$H (CH$_3$O)CH$_2$ or ClH$_2$CO C$_8$H$_{17}$, CHCl$_3$, SnCl$_4$ (ii) PPh$_3$ (iii) CH$_2$0, NaOH

One of the popular routes to prepare polymers bearing pendant vinyl groups is by multistep conversion of the styrene to vinyl styrene by chloromethylation, followed by conversion into phosphonium salts and finally by a Wittig reaction (figure 6.1) (Percec and Auman 1984, Neumann and Peterseim 1993, Farrall et. al. 1983).

Farall and coworker (1983) synthesized polystyrene bearing pendant vinyl groups by an alternative method which involves lithiation, conversion to the aldehyde by reaction with N, N' dimethyl formamide, followed by reaction with methyl triphenyl phosphonium bromide and potassium tert-butoxide to form the vinyl groups.

Frechet and Schuerch (1971) synthesized polystyrene with pendant allyl acid, allyl ester and allyl alcohol groups from chloromethylated polystyrene to the aldehyde which was then converted to allyl acid, allyl ester and then allyl alcohol.

Polystyrene containing pendant vinyl groups were prepared by Farall et. al. (1983) from PSt-CH$_2$Cl or Pst-CHO via Wittig reactions. These polymers were used to prepare a negative photoresist in which absorbed light initiated a free radical crosslinking reaction. An alternative to chloromethylated polystyrene was the use of meta (1, 2 dibromoethyl) styrene as a monomer which was then copolymerized with styrene or meta divinylbenzene (figure 6.2) (Yamamizu et. al. 1985).
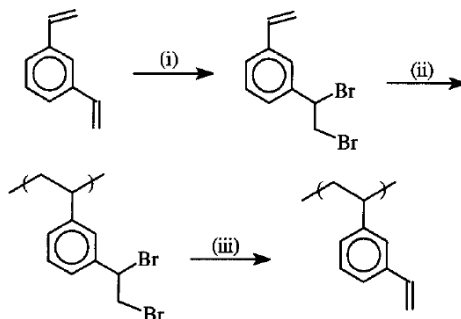
Figure 6.2 Preparation of polymer bearing pendant vinylbenzene groups (Yamamizu et. al. 1985) (i) Pyridinium hydrobromide perbromide (ii) copolymerization with styrene or divinylbenzene (iii) NaI

Tsuruta (1985) prepared soluble poly(para divinyl benzene) of varying molecular weights by anionic polymerization. Nagasaki et. al. (1986) studied further the reaction mechanism and ^{13}C NMR spectral peak assignments for this linear poly(para-divinyl benzene). Hasegawa and Higashimura (1980) polymerized cationically a mixture of meta and para divinyl benzene using oxy acids such as CF_3SO_3H, $AcCLO_4$, p-$CH_3C_6H_4SO_3H$ or BF_3-OEt_2 as catalytic initiators using benzene or 1,2 dichloroethane as solvent. Except for BF_3-OEt_2 and dichloroethane, linear polymers were formed. The best system was benzene as a solvent and CF_3SO_3H, $AcCLO_4$, p-$CH_3C_6H_4SO_3H$ as catalyst and low monomer concentrations. Molecular weights upto 25,000 were attained and the polymer was soluble in various solvents. Poly(1,4 phenylenevinylene) was prepared by metathesis of para-divinyl benzene (Kumar and Eichinger 1992). A metal-carbene complex was reacted with one of the vinyl groups to form a new metal-carbene complex followed by reaction with another monomer and elimination of the metal-carbene. The number average degree of polymerization was between 5 and 8.

Synthesis of reactive microgel by polymerization of divinyl benzene was carried out by Funke et. al. (1977). Seeded polymerization technique was used by Okubo and Nakagawa (1982) to synthesize micron size monodisperse polymers bearing pendant vinyl groups. The macroporous styrene-divinyl benzene copolymers with pendant vinyl groups were prepared by controlling time and temperature. (Jin et. al. 1992)

Earlier, it was reported that soluble polymers of vinyl methacrylate (VMA) can be obtained by the radical polymerization. But, the disadvantage of this approach was the conversions were low (< 20%), highly dilute solutions were used and mixed structures of both vinyl ester and methacryloyl groups in addition to the cyclic structures were obtained (Fukuda et. al. 1972). A possible solution for the highly selective polymerization is to alter the reactivity of the two vinyl groups or to alter the selectivity of the derived radical species. Anionic and group transfer polymerization can generate linear polymers retaining vinyl ester groups intact. The vinyl ester group remains intact during anionic polymerization and requires stringent conditions such as a low temperature and anhydrous conditions (Fukuda et. al. 1972, Kawaguchi et. al. 2004, Takahashi 2007, Lu et. al. 1997).
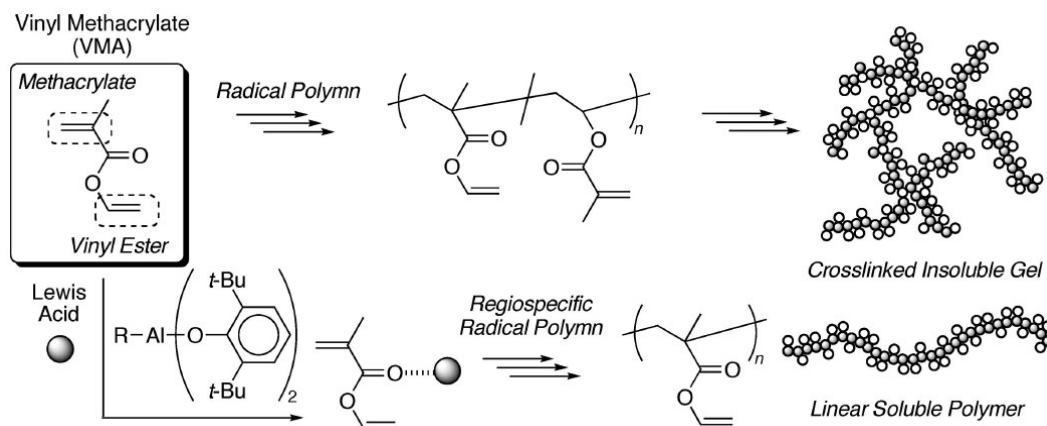
Figure 6.3 Radical polymerization of vinyl methacrylate in the presence of lewis acids (Fukuda et. al. 1972)

The polymerization of VMA in the presence of aluminium based lewis acids gave soluble polymers (figure 6.3). The bulky aluminum phenoxides afford the linear soluble polymers of VMA with complete retention of the vinyl ester groups, yields high molecular weights ($M_n > 10^4$) and quantitative conversions (>90%). Ruthenium-catalyzed living radical polymerization also generated soluble polymers bearing controlled molecular weights.

6.2.1 Soluble linear polymers and pendant group functionalization

This methodology involves the synthesis of linear, soluble copolymers containing pendant hydroxyl functionality and its subsequent modification. e.g. the free radical co-polymerization of 2-hydroxyethyl methacrylate (HEMA) or silyl protected HEMA i.e. HEMA-TMS with various co-monomers such as glycidyl methacrylate (GMA), methyl methacrylate (MMA), t-butyl methacrylate (t-BMA), n-butyl acrylate (n-BA), t-butyl methacrylate (t-BMA), acrylic acid (AA) was carried out over a range of co-monomer feed ratios (figure 6.4). The pendant hydroxyl groups of these co-polymers were then functionalized using methacryloyl / acryloyl chloride or methacrylic anhydride to obtain polymers containing pendant double bonds. These polymers were shown to be useful as a positive photoresist (Liu et. al., 2001), in wave-guide applications (Koo et. al., 2002), for the synthesis of functional self cross-linked nanoparticles (Mecerreyes et. al., 2001; Jiang and Thayumanavan 2005) and as molecularly imprinted polymers (Li et. al., 2005), etc.
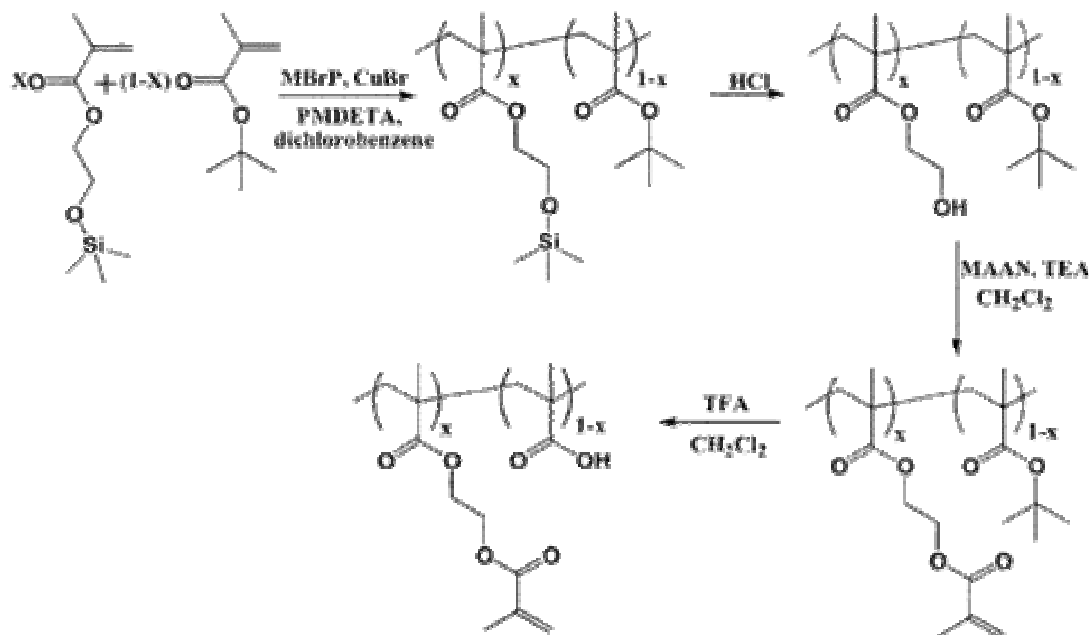
Figure 6.4 Synthesis of poly (HEMA-*co*-t-BMA) and post functionalization (Li et. al. 2005)
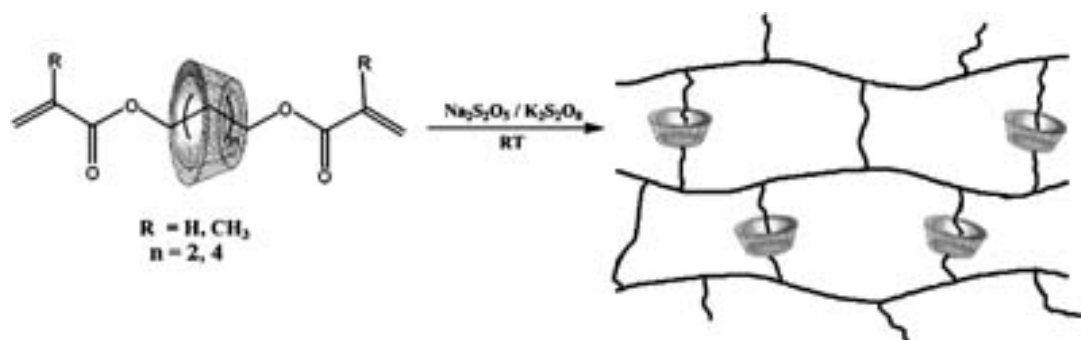
Figure 6.5 Interlocked crosslinked polymers from IC of divinyl monomers (Sarvothaman and Ritter 2004)

Recently, Sarvothaman and Ritter (2004) reported the IC mediated polymerization of dimethacrylate and diacrylate to develop a new class of mutually interlocked molecules (figure 6.5). The author aimed at the synthesis of polyrotaxane structures having different physical and mechanical properties because of different topology as compared to the classical polymers. Diacrylate and dimethacrylate of 1, 4 butane diol and 1, 6 hexane diol were complexed with methylated cyclodextrin (DM-β-CD) as well as α-CD. Diacrylate formed a true inclusion complex in which CD was completely threaded on the diacrylate molecule whereas dimethacrylate showed the partial inclusion in CD where the CD sits at the terminal position. Aqueous polymerization of these complexes resulted in the formation of interlocked polymer architectures because of dethreading of CD ring and cross-linking of the exposed double bonds (figure 6.5). The FTIR and thermal analysis of these polymers showed the evidence for the presence of polyrotaxane architecture.

Chen et al. (2006) explored the use of CD to control polymer topology in the condensation polymerization (figure 6.6). The polycondensation reaction of 1-(2-aminoethyl) piperazine, a BB'_2 monomer and divinylsulfone, an A_2 monomer resulted into the formation of hyperbranched structures by monomer coupling methods. This was due to the difference in reactivity between primary amino and secondary amino groups of 1-(2-aminoethyl) piperazine monomer which form an $AabB'_2$-type intermediate and further polymerization yields hyperbranched poly (sulfone-amine) (PSA). 1-(2-aminoethyl) piperazine formed stable complex with β-CD because of the presence of intermolecular hydrogen bonding interactions between the amino and

hydroxyl groups of 1-(2-aminoethyl) piperazine and β-CD respectively. Polymerization of 1-(2-aminoethyl) piperazine-β-CD IC and divinylsulfone yielded linear polymers having higher decomposition temperature than pure poly (sulfone-amine). The higher stability of polymer chain was attributed to the presence of complexed β-CD rings.
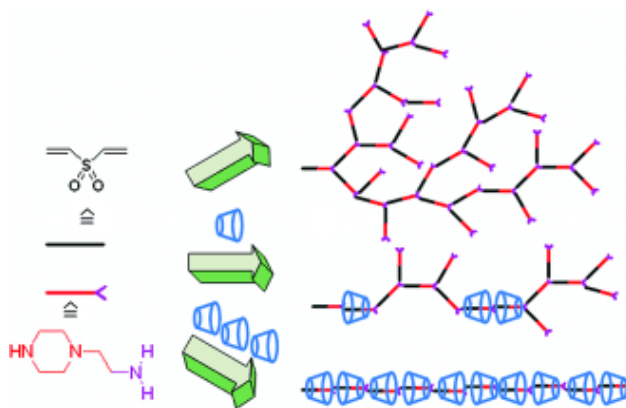
Figure 6.6 Inclusion complex mediated controlled polymerization (Chen et al. 2006)

The computational analysis revealed that the 1-(2-aminoethyl) piperazine molecule after encapsulating into the CD cavity, behaves as a bifunctional monomer during polymerization to yield a linear polymer with divinyl sulfone.

6.2.2 Atom transfer radical polymerization (ATRP)

In this method, the polymerization of divinyl monomer containing the double bonds differing in reactivity e.g. allyl methacrylate (AMA) was carried out. Soluble polymers were synthesized by adjusting the degree of polymerization of AMA using appropriate monomer / initiator ratio, which is the crucial parameter governing crosslinking reaction. Nagelsdiek et. al. (2004) reported the synthesis of various homopolymers and copolymers of AMA by this method.

6.2.3 Transition metal mediated polymerization

Guan (2002) reported a new approach to control polymer topology through transition metal mediated radical polymerization (figure 6.7). In this approach, hyperbranched polymers of EGDMA were synthesized using free radical polymerization by controlling the competition between propagation and chain transfer catalyst.
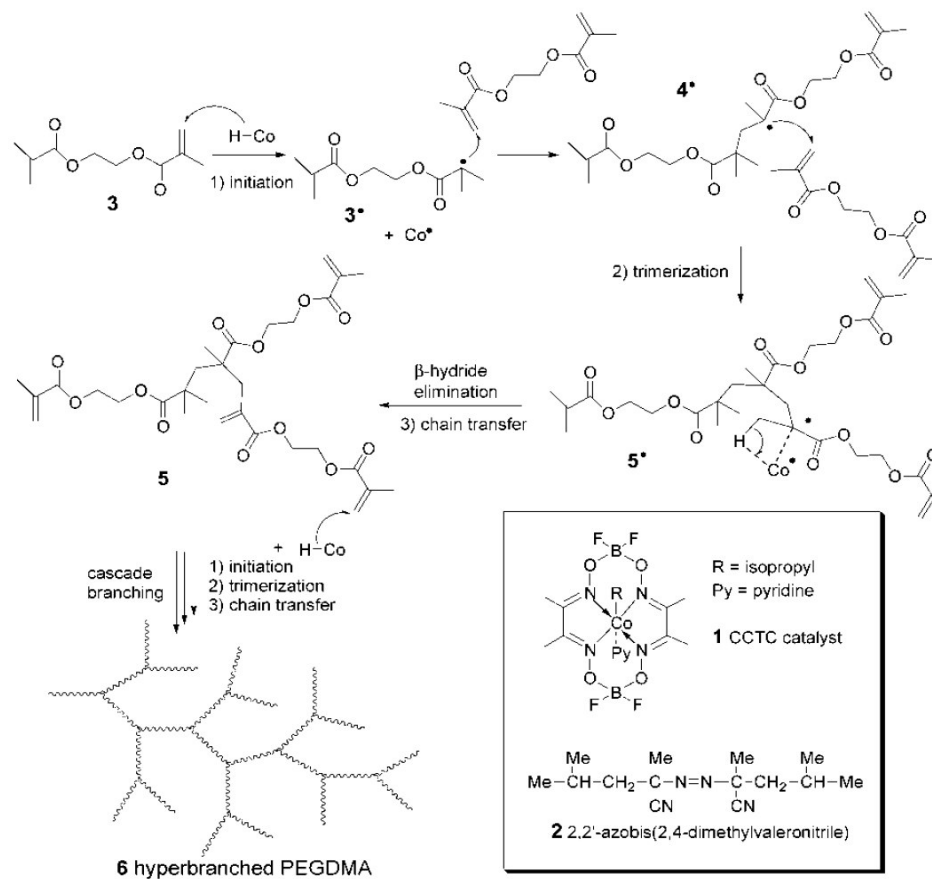
Figure 6.7 Cobalt mediated polymerization of EGDMA (Guan 2002)

In this study, a cobalt chain transfer catalyst (CCTC) was used to control the propagation of free radical polymerization of divinyl monomer. The cobalt complexes bind reversibly to the growing radical centers and this leads to β-hydride abstraction to terminate the propagating chains while generating cobalt-hydride species to reinitiate new propagating chains. If a dimethacrylate monomer is used and if the CCTC is chosen at the concentration for termination of methacrylate at the trimer stage, the repetitive trimerization of a dimethacrylate monomer leads to hyperbranched polymer.

6.2.4 Group transfer radical polymerization (GTP)

Isaure et. al. (2004) reported a facile, generic and cost effective route to branched vinyl polymers via conventional free radical polymerization using a multi-functional vinyl co-monomer as the branching species. In this case, the presence of chain transfer agent or catalytic chain transfer agent inhibited gelation. With appropriate choice of reaction

conditions, copolymerization of methyl methacrylate and EGDMA using Cu based ATRP or GTP methodologies yields soluble branched polymers in facile one pot reactions.

6.2.5 Initiator fragment incorporation radical copolymerization

Free radical polymerization of divinyl monomers yields crosslinked materials because of infinitely high molecular weight of the polymers. In the conventional radical polymerization, an increase in initiator concentration causes a decrease in the molecular weight of the polymer because of enhanced termination rate. Thus, the use of higher initiator concentration in the polymerization of divinyl monomer results in decrease in the polymer molecular weight and resulting polymer becomes soluble.

Sato et. al. (2004) reported a methodology to obtain soluble hyperbranched copolymers from divinyl monomer EGDMA using high concentration of initiator. In this case, the copolymerization of EGDMA with monomers such as N-methyl methacrylamide, 1,1-diphenylethylene, di α-ethyl β-N- (α'-methylbenzyl) itaconamates (RS- and S-EMBIs) derived from (RS)- and (S)-α- methylbenzylamines was conducted at 70 and 80 ^{0}C using dimethyl 2, 2' azobis isobutyrate as an initiator at concentration as high as 0.35 to 0.70 moles lit^{-1}. The use of large amount of initiator results in its incorporation in copolymer through initiation and primary radical termination and yields the soluble hyperbranched polymers**.**

The limitations of the techniques described above are summarized below.

- Percentage of double bonds available for further modification is low.

- Vinyl content from 6 to 42 % could be obtained depending on the reaction conditions (Neumann 1993, Farall 1983, Frechet 1982).

- Require extreme reaction conditions

- The synthesis of linear Poly(DVB) gives polymers with 95 to 98 % vinyl content, but it involves very stringent and hazardous reaction conditions and requires very pure reagents.

- The steps are time consuming and involve multi-step reactions thus limiting large scale applications.

- Incorporation of high concentration of chain transfer agents or initiator in polymer structure changes the properties of the final polymers.

- Methacryloylation using methacryloyl chloride

  The results of pendant group functionalization are not consistent and the product which varied in nature from a free flowing powder to a contaminated sticky solid was difficult to isolate (Koo et al., 2002).

- Methacryloylation using methacrylic anhydride

  Methacrylic anhydride is less reactive than methacryloyl chloride and is suitable for the preparation of esters only under mild conditions (Koo et al., 2002).

- In both methacryloylation using methacryloyl chloride and methacrylic anhydride stabilizers e.g. *p*-benzoquinone needed to add during the reaction to inhibit the crosslinking. But, there are problems in removing the stabilizer. Also, the presence of stabilizers lowers the rate of polymerization.

- Incomplete conversion of pendant groups, homo polymerization of modifier as well as crosslinking of the already functionalized polymers may also take place.

These limitations highlight the need to develop simple methodology to control the reactivity of multivinyl monomer in free radical polymerization independent of choice of multivinyl monomers.

The pendant vinyl groups can be used to graft another monomer or for crosslinking purpose. We have prepared the soluble homopolymers and copolymers of the crosslinkers containing pendant unsaturation through their inclusion complexes with cyclodextrin (CD) by free radical solution polymerization. CD encapsulates one of the vinyl group of the crosslinker which does not take part in polymerization. This methodology offers a single step approach towards the synthesis of unsaturated polymers using mild reaction conditions and without affecting the polymer properties.

6.3 Experimental

6.3.1 Materials

β-cyclodextrin (β-CD) was obtained from Himedia Laboratories, Mumbai, India. Dimethylated β-cyclodextrin (DMCD) was obtained from Wacker-Chemie GmbH, Germany and had an average degree of methylation of about 1.8 per glucose unit. Methylene bis acrylamide (MBAM), γ-cyclodextrin hydrate (γ - CD), α-cyclodextrin (α - CD), hydroxy propyl β-cyclodextrin (HP-β-CD) were purchased from Aldrich. Potassium persulphate AR grade was purchased from S. d. fine – chem Ltd, India. The solvents N, N' dimethyl formamide (DMF), chloroform ($CHCl_3$), acetone and methanol were used after distillation.

The deuterated solvents $DMSOd_6$, D_2O and $CDCl_3$ were purchased from Aldrich.

Methacryloyl chloride was synthesized in the laboratory. Disulfide dimethacrylate (DSDMA) was synthesized as per the procedure described before (Li et. al. 2005).

6.3.2 Methods

FTIR spectra were recorded on Perkin–Elmer spectrum one. CD, IC and crosslinker were mixed with KBr and the spectra were recorded at frequencies from 4000 to 450 cm^{-1} using diffused reflectance spectroscopy (DRS) mode. The resolution was 4 cm^{-1}. ^1H NMR spectra of crosslinker, cyclodextrin derivative as well as ICs were recorded using a Brucker DRX 200 and MSL 300 NMR spectrometer. The spectra were recorded in D_2O or $DMSOd_6$. The solid state ^{13}C CP/ MAS NMR spectra of ICs were recorded at 125.76 MHz on a Brucker DRX 500 spectrometer. X–Ray powder diffraction patterns were obtained at room temperature using a Rigaku X-ray diffractometer. The measurements were carried out using the parameter given below : target Cu K_α; filter Ni; voltage 40kV; current 30mA; slit 0.2nm; scanning speed 2° per min., 2θ = 5°–50°. Approximately, 20 mg samples were weighed into aluminium sample holders. The XRD traces of crosslinker, CD derivative and ICs were compared with respect to peak position.

6.3.3 Inclusion complex synthesis

Solvent evaporation method

MBAM-β-cyclodextrin IC by solvent evaporation method

11.35 g (0.01 moles) β-cyclodextrin was dissolved in 500 mL distilled water at room temperature. To this, 1.54 g (0.01 moles) MBAM was added and the mixture was stirred using a magnetic stirrer for 24 h at room temperature. A water soluble inclusion complex (IC) was obtained. The complex was isolated by evaporating the water at room temperature, dialyzed to remove unreacted crosslinker and then freeze dried. The yield was in the range 95%.

Similarly, the ability of MBAM to form inclusion complexes with different derivatives of cyclodextrin i.e. α, β, methylated β-CD, hydroxypropyl β-CD was checked.
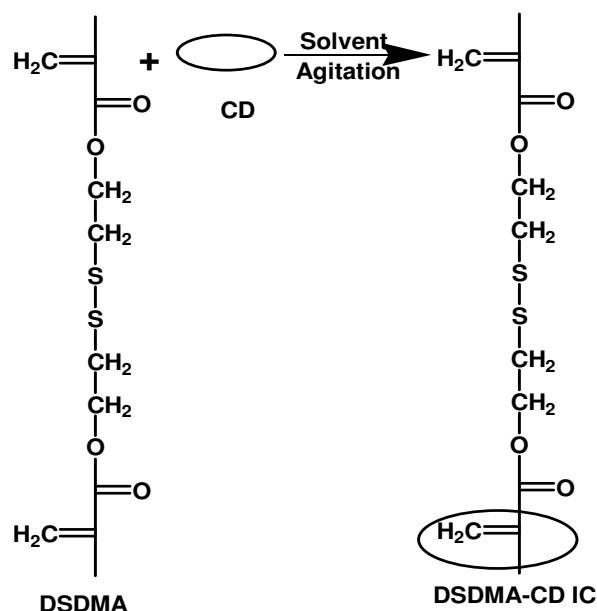
Scheme 6.1 Inclusion complex synthesis

DSDMA-β-cyclodextrin IC by precipitation method

23.5 g (0.0207 moles) β-cyclodextrin (β-CD) was dissolved in 1375 mL distilled water at room temperature. To this, 6 g (0.0207 moles) DSDMA was added and the mixture was stirred using a magnetic stirrer for 48 h at room temperature. Water insoluble IC was obtained (Scheme 6.1). The complex was isolated by filtration and then washed

with petroleum ether and water to remove unreacted monomer and β-cyclodextrin and dried under vacuum at room temperature. The yield was 75%.

6.4 Results and discussion

Methylene bis acryalmide (MBAM) is the most commonly used hydrophilic crosslinkers to form polymer gels. The polymerization in the presence of these crosslinkers leads to the formation of crosslinked network. Due to the interpenetrating network, gels obtained become insoluble in any solvent and also they cannot be processed further. At the same time, removal of the unreacted crosslinker from the gel becomes very difficult due to the entangled network. This disadvantage limits its use in biomedical applications where the presence of traces of crosslinker is unacceptable because of toxicity. Hence, there is a need to obtain the gels without any traces of the crosslinker. We found that, after complexation with cyclodextrin the crosslinker behaves as a vinyl monomer rather than the divinyl monomer. This is due to the encapsulation of one of the vinyl unsaturation of the crosslinker by the cyclodextrin cavity. As a result, when inclusion complex of crosslinker was polymerized a soluble polymer having pendant vinyl unsaturation was obtained. Further, the pendant unsaturation can be used for crosslinking in the subsequent step. Thus, this two stage method can be used either to obtain soluble polymers containing vinyl unsaturation or crosslinked product.

Reduction-sensitive biodegradable polymers are stable in the circulation and in extracellular fluids, whereas they undergo rapid degradation under the reductive environment present in intracellular compartments. The large difference in glutathione concentration between the intracellular and extracellular milieu can be exploited for triggered intracellular delivery of a variety of bioactive molecules (Meng et. al. 2009, Matsusaki et. al. 2007, Aliyar et. al. 2005, Shu et. al. 2002, 2003, Yamauchi et. al. 2001, Cerritelli et. al. 2007, Niu et. al. 2007). These polymers can be synthesized by incorporating disulfide linkage in the main chain, in the side chain or in the cross-linker. Disulfide dimethacrylate (DSDMA) crosslinker having disulfide linkages in the main chain was chosen to synthesize biodegradable nanogels as DSDMA undergoes degradation in reductive environment.

We evaluated the complex formation ability of MBAM with different CD derivatives viz. β–CD, DM-β–CD, HP-β–CD and α-CD using solvent evaporation method. DSDMA i.e. degradable crosslinker was complexed with β–CD by precipitation method. The complexation was confirmed by NMR, FTIR and molecular modeling. MBAM-β–CD and DSDMA-β–CD inclusion complexes were polymerized further with N-vinyl pyrrolidone (NVP) to obtain water soluble polymers comprising pendant unsaturation. These polymers were dispersed in hexane in the presence of macromolecular drugs and crosslinked to yield nanogels. The naogels obtained were demonstrated for the sustained or burst release of drug as discussed in the next chapter.

6.4.1 Synthesis and characterization of inclusion complexes

MBAM and DSDMA are symmetrical molecules. Both the molecules behave in a similar way while forming the inclusion complexes. Hence, herein the detailed characterization of only MBAM molecule is discussed in detail and FTIR and NMR analysis of DSDMA is shown in the following section.

6.4.1.1 DSDMA synthesis

Disulfide dimethacrylate (DSDMA) was synthesized as per the procedure described by Li et. al. (2005) and its structure was confirmed by ^{1}H NMR (figure 6.8). Inclusion complexes comprising MBAM-β-CD and DSDMA-β-CD were prepared by solvent evaporation and precipitation technique respectively. The complex formation and its stoichiometry were confirmed by FTIR and ^{1}H NMR analysis.
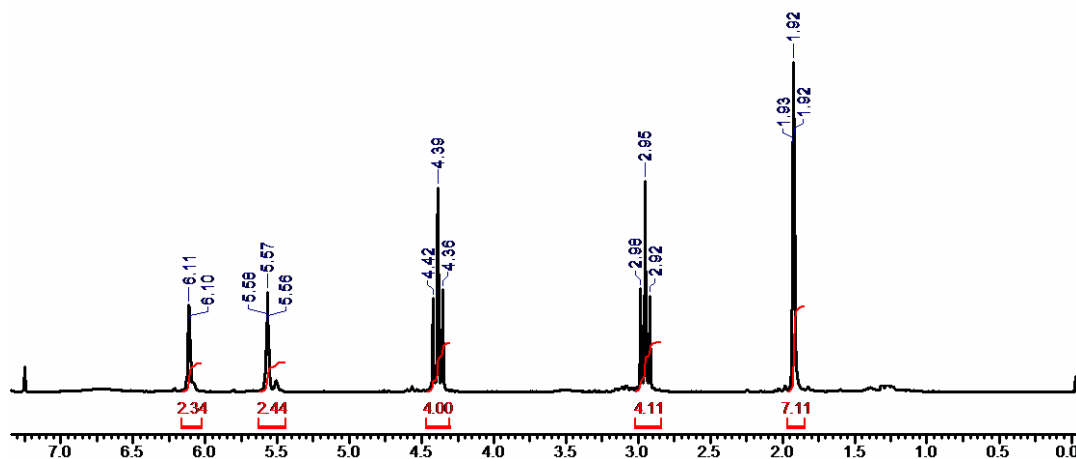
Figure 6.8 ^{1}H NMR of DSDMA monomer

6.4.1.2 FTIR analysis

In FTIR spectrum of CD, the most distinct peak is due to the OH stretching of the glucose ring and appears at 3370 cm^{-1}. This peak showed a shift of -62 cm^{-1} (3308 cm^{-1}) in MBAM-β-CD IC (figure 6.9) and -35 cm^{-1} (3335 cm^{-1}) in DSDMA-β-CD IC (figure 6.11) indicating disruption of intramolecular hydrogen bonding in native β-CD (C$_2$-OH group of one glucopyranoside unit forms a hydrogen bond with C$_3$-OH group of adjacent glucopyranose unit) due to complex formation with the crosslinker (Bratu 1998). In the past, shift of -59 cm^{-1} for OH stretching band of β-CD (3370 cm^{-1} to 3311 cm^{-1}) for trimethylol propane trimethacryalte -β-CD IC was reported by Satav et. al. (2007). The weaker shifts 3413 cm^{-1} (-9.8) in case of MBAM-DM-β–CD IC (figure 6.10) can be attributed to the dominant hydrophobic interactions over hydrogen bonding.
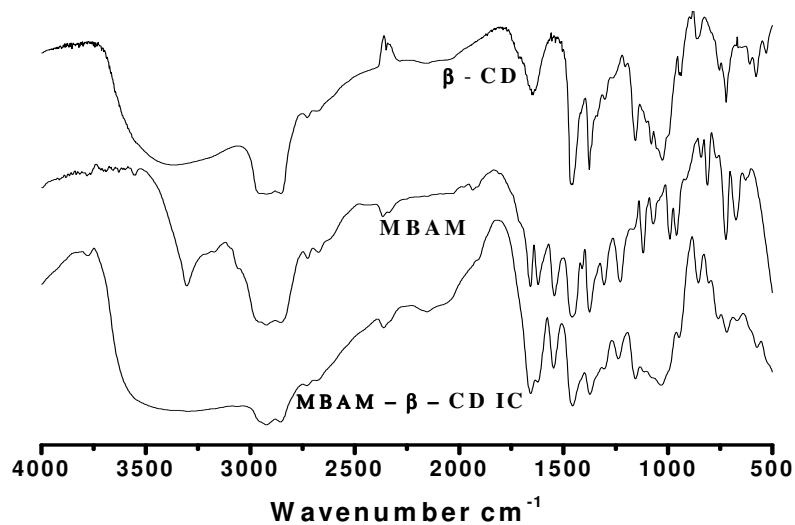
Figure 6.9 FTIR of MBAM, β-CD and its inclusion complex
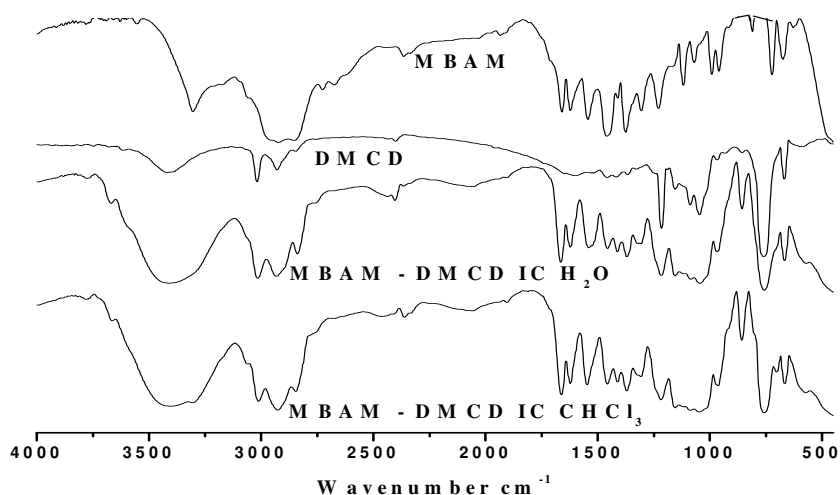
Figure 6.10 FTIR spectrum of MBAM, DM-β-CD and its inclusion complex
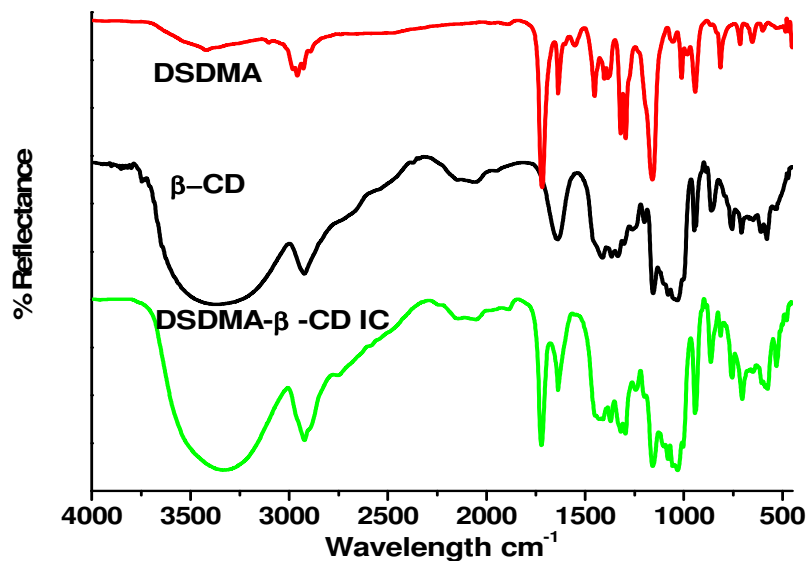
Figure 6.11 FTIR of DSDMA and its inclusion complex

6.4.1.3 ^{1}H NMR analysis

The stoichiometry of DSDMA-β-CD IC was established by integrating the methyl protons of DSDMA at 1.87 δ for 6 protons and C_1 protons of β-CD at 4.82 δ for 7 protons. (figure 6.12). The stoichiometry of MBAM-β-CD IC was established by integrating the vinyl protons of MBAM at 6.15 δ for 4 protons and C_1 protons of β-CD at 4.82 δ for 7 protons (figure 6.13). The integration confirmed 1:1 stoichiometry for both complexes. The same stoichiometry was reported by Satav et. al. (2006) for the inclusion complex comprising ethylene glycol dimethacrylate and β-CD.
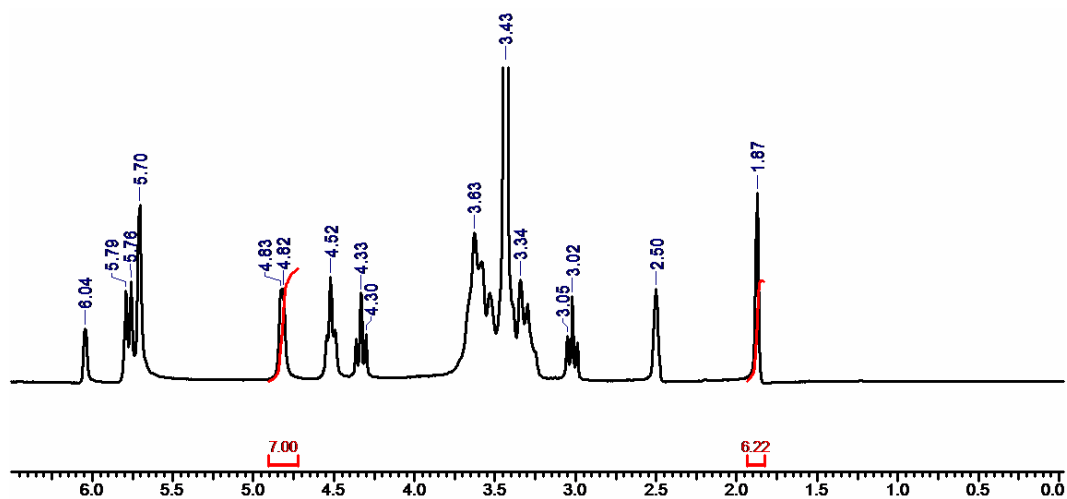
Figure 6.12 ^{1}H NMR of DSDMA-β-CD inclusion complex
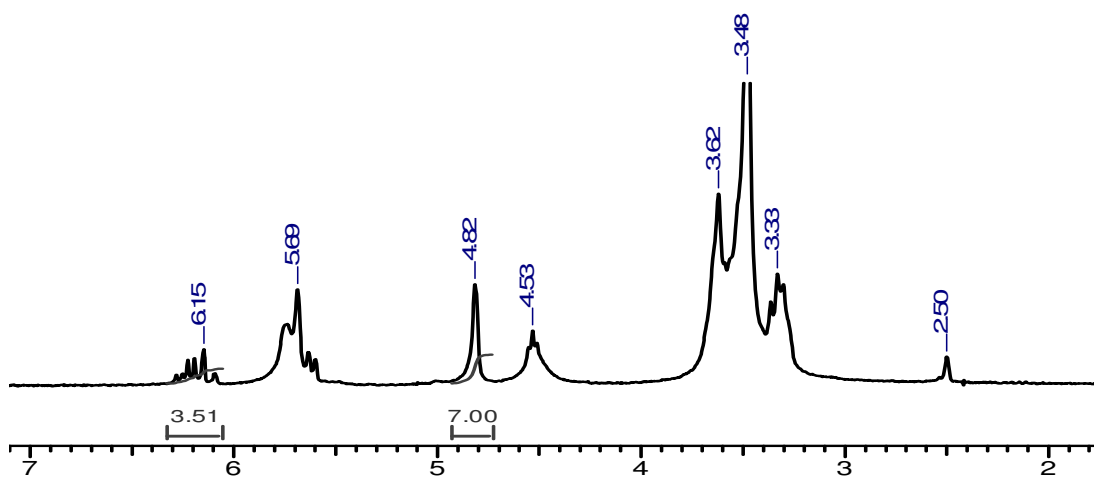
Figure 6.13 ^{1}H NMR of MBAM-β-CD inclusion complex
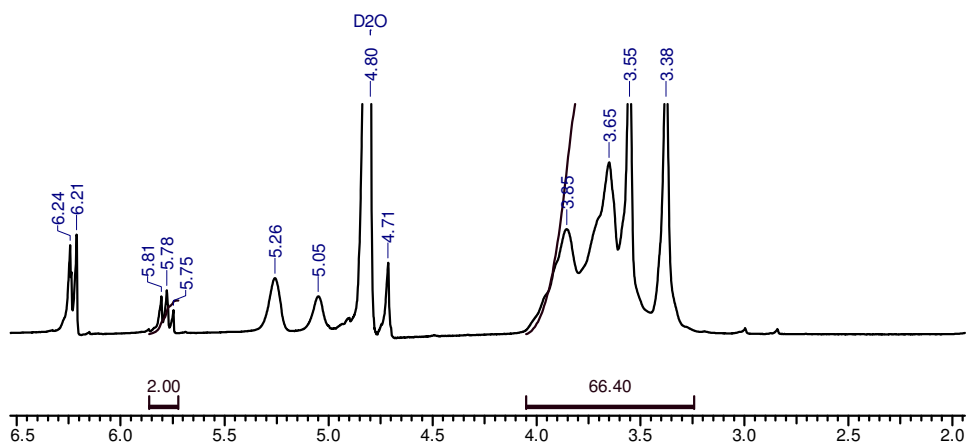
Figure 6.14 ^{1}H NMR of MBAM-DM-β-CD inclusion complex

150

The stoichiometry of MBAM-DM-β-CD IC was established by integrating the vinyl protons of MBAM at 5.75 δ for 2 protons and $C_{1,2,3,4,7,8}$ protons of DM-β-CD at 3.38-3.86 δ for 77 protons. The integration confirmed 1:1 stoichiometry of the complex (figure 6.14). MBAM-α-CD and MBAM-HP-β-CD IC also showed 1:1 stoichiometry.

1:1 stoichiometry for all ICs leads to conclude that only one double bond of the crosslinker is encapsulated by the CD cavity which was also confirmed by the molecular modeling analysis discussed in further section.

MBAM-β-CD IC

^{1}H NMR (DMSOd₆): 3.33-3.62 δ $C_{2, 3, 4, 5, 6}$ H of β-CD, 4.53 δ CH_2 of MBAM and C_6 OH of β-CD, 4.82 δ C_1 of β-CD, 5.69 δ $=CH_2$ and $C_{2, 3}$ OH of β-CD, 6.15 δ $=CH$ of MBAM.

MBAM-DM-β-CD IC

^{1}H NMR (D₂O): 3.38 δ $C_{7, 8}$ CH_3 of DM-β-CD, 3.55-3.85 δ $C_{2, 3, 4, 6}$ H of DM-β-CD, 4.71 δ CH_2 of MBAM, 5.05, 5.28 C_1 proton of DM-β-CD, 5.75 δ $=CH$ and 6.21 δ $=CH_2$ of MBAM.

DSDMA-β-CD IC

^{1}H NMR (DMSOd₆): 3.33-3.62 δ $C_{2, 3, 4, 5, 6}$ H of β-CD and C_6 OH of β-CD, 1.87 δ CH_3 of DSDMA, 4.82 δ C_1 of β-CD, 5.79 δ $=CH_2$ of DSDMA, 5.7, 5.78 δ $C_{2, 3}$ OH of β-CD, 6.04 δ $=CH$ of DSDMA.

6.4.1.4 ^{13}C CP / MASS NMR Spectrum

Cross polarization and magic angle spinning (CP/MAS) solid state ^{13}C NMR spectroscopy provides a powerful approach to the molecular analysis of starch related structures. This technique is based on the investigation of structure at molecular level and therefore complements the information on long range ordering obtained from X–ray diffraction.
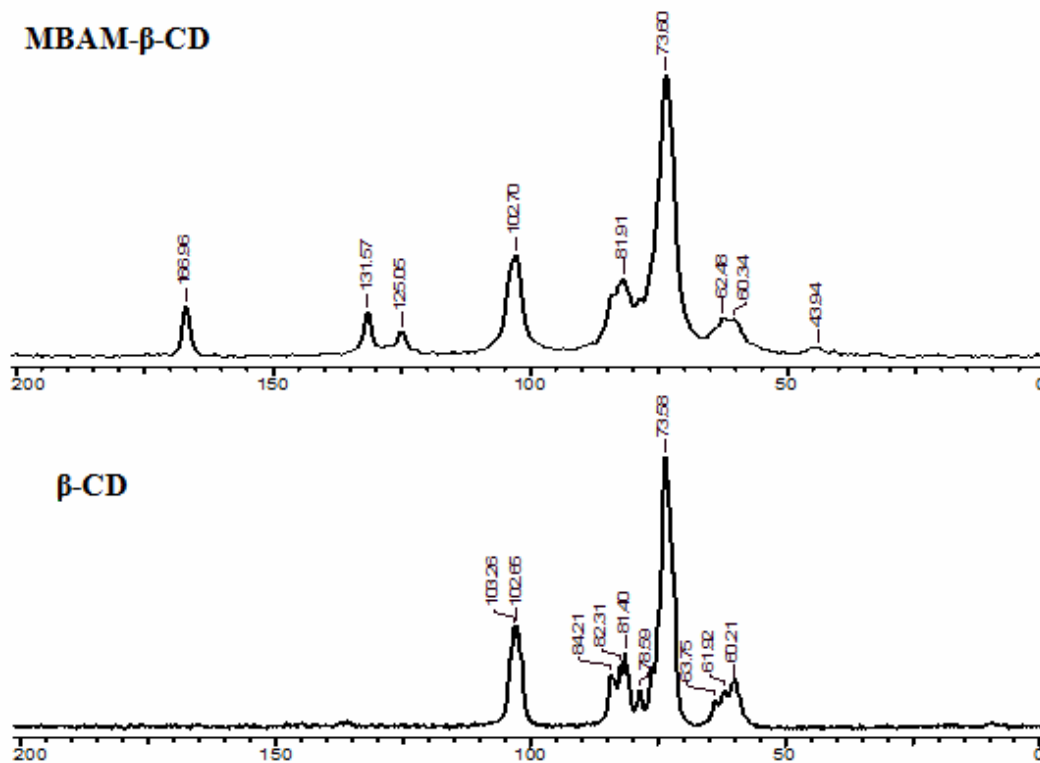
Figure 6.15 ¹³C CP/MAS NMR spectra of β-CD, MBAM-β-CD inclusion complex
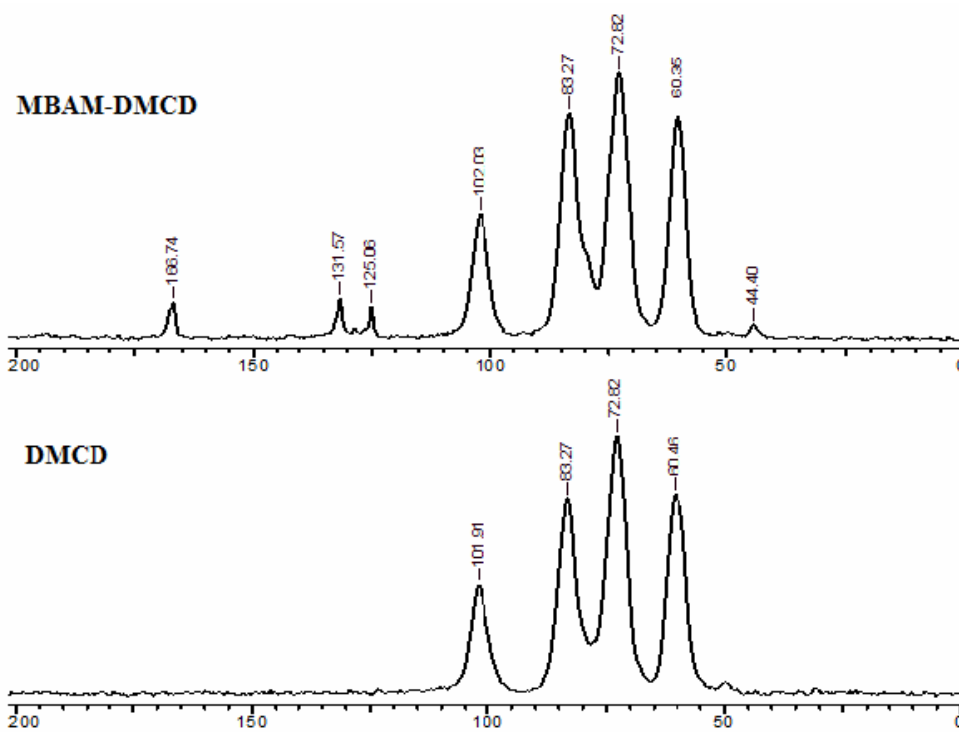
Figure 6.16 ¹³C CP/MAS NMR spectra of DMCD and MBAM-DMCD IC

CP/MAS solid state ^{13}C NMR spectrum of MBAM-β-CD IC displayed well resolved, single peaks for each carbon of all glucose units. The peaks at 78.6 ppm corresponding to C_4 (figure 6.15), adjacent to conformationaly strained glycosidic linkage disappeared. The C_1 peak at 102.66 ppm is shifted to 104.27 ppm for MBAM-β-CD IC respectively. This indicates symmetrical conformation of glycosidic linkage due to the inclusion of MBAM within the cavity of β-CD.

The solid state ^{13}C resonances of C_1 and C_4 of CD elucidate the conformation of glycosidic linkages and the packing state (Okada et. al. 1999). In case of free DMCD (figure 6.16), C_1 peak at 101.91 ppm is broad indicating that DMCD is asymmetric. After forming an inclusion complex it becomes symmetric and shifts to 102.03 ppm in case of MBAM-DMCD respectively. However, multiplicity is not affected. These results are consistent with those reported by Hall et. al. (1986).

6.4.1.5 X – ray diffraction spectroscopy (XRD)

XRD helps to establish the crystalline nature of the ICs. Saenger (1980) and Szejtli (1996) reported that if the diffraction pattern does not correspond to those of the pure compounds i.e. CD and guest a true IC may exist. The structures of the ICs of CD with low molecular weight guest compounds were reported and classified into two groups as one is 'cage type' and the other is 'channel' type (McMullan et. al. 1973).
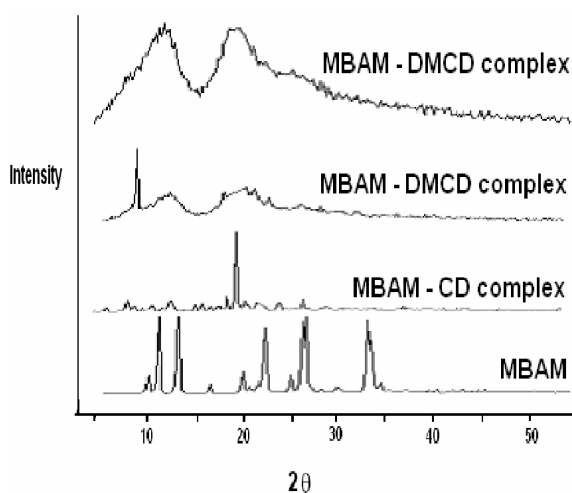
Figure 6.17 XRD of MBAM and its inclusion complexes

The diffractograms of the crosslinker and its ICs are shown in the figure 6.17. In XRD spectrum of MBAM-β-CD complex, the peaks at $2\theta = 15.37^0$, 18.73^0, 19.55^0 and 22.62^0 which are the characteristic peaks of β-CD disappeared. Both diffractograms i.e. MBAM-β-CD IC, MBAM–DMCD IC showed the absence of peaks at $2\theta = 20^0$ and 7.6^0 which are indicative of the channel type structures. (Rusa et. al. 2002). Thus, the ICs formed are cage type structure. The ICs obtained were found to be amorphous. In case of MBAM–DMCD IC, the amorphous nature of the complex is greater when they are prepared in chloroform than in water.

6.4.1.6 Molecular modeling

Conformational analysis

Conformational analysis was performed for MBAM molecule using MCMM method implemented in Schrödinger (Macro Model 9.0) program with the MM2* force field. Two conformations were chosen which have minimum and maximum end-end distances. These conformations are optimized at various force fields and also calculated at DFT (B3LYP/6-31G) level of theory (figure 6.18). Energies were given in kJ/mol and distances are given in Å (Table 6.1).
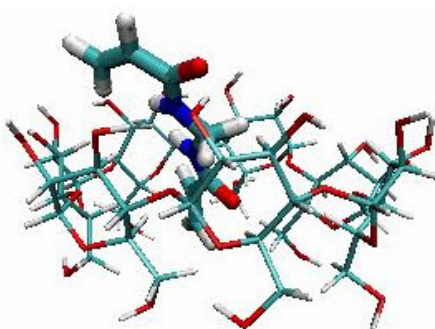
Figure 6.18 Lowest energy conformation of MBAM obtained through molecular dynamics simulations

Table 6.1 Conformations of MBAM molecule with various force fields

Force Field	Bent Conformation		Stretched Conformation	
	End to end distance Å	Energy in kJ/mol	End to end distance Å	Energy in kJ/mol
MM2*	6.67	-370.93	8.53	-369.23
MM3*	7.10	-263.35	8.19	-262.70
AMBER*	7.08	-163.95	8.33	-163.74
OPLS	6.62	-171.31	8.46	-170.17
MMFF	7.47	-418.85	8.63	-418.82
OPLS2001	6.77	-103.78	8.78	-102.79
B3LYP/6-31G	7.50	-532.5469135	7.93	-532.5468868

Docking results

Rigid Docking calculations were performed using Lamarckian Genetic algorithm implemented in AUTODOCK 3.0.5 program. Initial conformation of ligand molecule was taken from the optimized geometry obtained at B3LYP/6-31G level of theory.

Docking parameters: Energy evolutions: 1.5×10^6, population size: 50, GA_runs: 30. Conformations of MBAM molecules with one and two β-CDs were given in figure 6.19 and docked energies were given in kcal/mol.

The conformational analyses of MBAM, their complexation with β-CD, and thermodynamics of oligomerization were analyzed by computational studies. The force field and density functional theory, B3LYP/6-31G calculations indicate that the bent conformation is more stable than linear one by 3-5 kJ/mol in case of MBAM. The complexation of the ligands with β-CD was analyzed by docking, quantum chemical and molecular dynamics simulations using Autodock 3.0.5, Gaussian 03 and AMBER 8.0 programs respectively. The lowest energy complex obtained from the Autodock calculation was taken as initial structure for MD simulations. TIP3P water models were used as solvent and equilibration was performed for 500 ps and MD simulation was carried for 2ns. Conformations of these molecules in MD simulation were shown in figure 6.19.

MBAM-bent conformation	MBAM-stretch conformation	MBAM-bent conformation	MBAM-stretch conformation
Docked Energy in kcal/mol: **-4.54**	Docked Energy in kcal/mol: **-4.57**	Docked Energy in kcal/mol: **-5.56**	Docked Energy in kcal/mol: **-5.51**
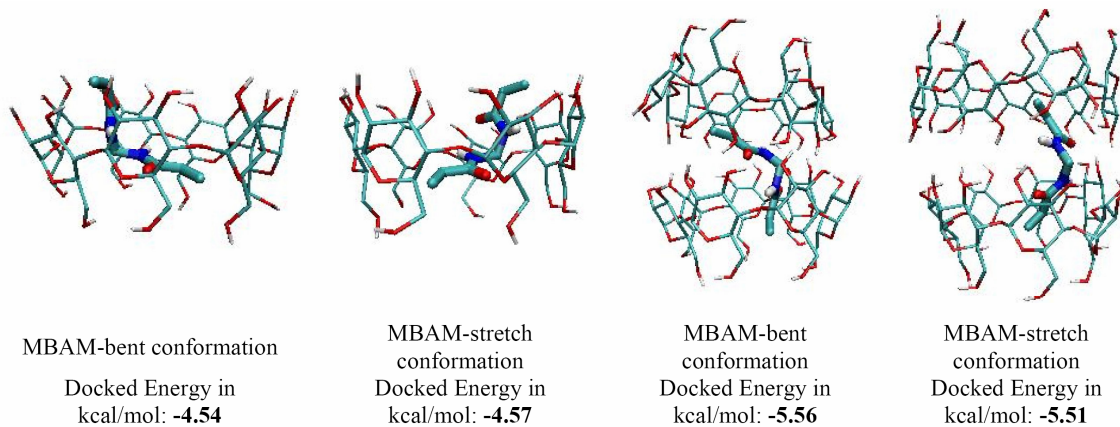
Figure 6.19 Conformation of MBAM with β CD

Computations were also carried out to ascertain if the monomers could bind to second β-CD. In case of MBAM, complexation of ligand with first β-CD has substantial stabilization in the order of 40-50 kJ/mol, while the addition of second β-CD does not provide substantial stabilization.

6.5 Conclusions

Divinyl monomers such as MBAM and DSDMA form 1:1 IC with β-CD as shown by NMR and molecular modeling simulations. FTIR analysis reveals that H-bonding interactions are dominant in β-CD IC as compared to DM-β-CD IC. XRD data give the evidence for the cage type structures of both β-CD and DM-β-CD ICs.

6.6 References

1. Zhu S., Hamielec A. Makromol. Chem., Macromol. Symp. **1993**, 69, 247.

2. (a) Liu J-H., Lin S-H. Shih J-C. J. Appl. Polym. Sci. **2001**, 80, 328. (b) Koo J-S., Smith P., Williams R., Grossel M., Whitcombe M. J. Chem. Mater. **2002**, 14, 5030. (c) Li Z., Day M., Ding J., Faid K. Macromolecules **2005**, 38, 2620. (d) Mecerreyes D., Lee V., Hawker C., Hedrick J., Wursch A., Volksen W., Magbitang T., Huang E., Miller R. Adv. Mater. **2001**, 13, 204. (e) Nagelsdiek R., Mennicken M., Maier B., Keul H., Hocker H. Macromolecules **2004**, 37, 8923.

3. Guan Z. J. Am. Chem. Soc. **2002**, 124, 5616.

4. Fukutomi T., Matsui H., Kakurai T. Kobunshi Ronbunshu **1982**, 39, 499.

5. Matsumoto A., Nishi E., Oiwa M., Ikeda J. Eur. Polym. J. **1991**, 27, 1417.

6. Percec V., Auman B. Makromol. Chem. **1984**, 185, 2319.

7. Neumann W., Peterseim M. React. Polym. **1993**, 20, 189.

8. Farrall M., Alexis M., Trecarten M. Polymer **1983**, 24, 114.

9. Tsuruta T., Makromol. Chem. Suppl. **1985**, 13, 33.

10. Funke J. Oil Col. Chem. Assoc. **1977**, 60, 438.

11. Butler, G. B. Cyclopolymerization and Cyclocopolymerization; Marcel Dekker: New York, **1992**.

12. Butler G. J. Polym. Sci., Part A: Polym. Chem. **2000**, 38, 3451.

13. Kodaira T. Prog. Polym. Sci. **2000**, 25, 627.

14. Takahashi K. Chem. Rev. **1998,** 98, 2013.

15. Breslow R, Campbell P. J. Am. Chem. Soc. **1969**, 91, 3085.

16. Lau W., Rohm and Haas Company: Eur. Pat. Appl., **1996**, Vol. 125, 59402 CA.

17. Chen H., Ishizu K., Fukutomi T., Kakurai T. J. Polym. Sci. Part A : Polym. Chem. **1984**, 22, 2123.

18. Sarvothaman M., Ritter H. Macromol. Rapid Commun. **2004**, 25, 1948.

19. Tabatabai M., Ritter H. Prog. Polym. Sci. **2002,** 27, 1713.

20. Glockner P., Ritter H. Macromol. Rap. Comm. **1999**, 20, 602.

21. Satav S., Karmalkar R., Kulkarni M., Nagaraju M., Sastry N. J. Am. Chem. Soc. **2006**, 128, 7752.

22. Satav, S. S.; Karmalkar, R. N.; Kulkarni, M. G.; Nagaraju, M.; Sastry. G. N. Macromolecules **2007**, 40, 1824.

23. Hoffmann M. Makromol. Chem. **1974**, 175, 613.

24. Obrecht W., Seitz U., Funke W. Makromol. Chem. **1974**, 175, 3587.

25. Obrecht W., Seitz U., Funke W. Makromol. Chem. **1975**, 176, 2771.

26. Obrecht W., Seitz U., Funke W. Makromol. Chem. **1976**, 177, 1877.

27. Frechet J., Schuerch C. J. Am. Chem. Sot. **1971**, 1971, 492.

28. Yamamizu T., Akiyama M., Takeda K. React. Polym. **1985**, 3, 173.

29. Nagasaki Y., Ito H., Tsuruta T. Makromol. Chem. **1986**, 187, 23.

30. Hasegawa H., Higashimura T. Macromolecules **1980**, 13, 1350.

31. Kumar A., Eichinger B. Makromol. Chem. Rap. Commun. **1992**, 13, 311.

32. Okubo M., Nakagawa T. Colloid Polym. Sci. **1982**, 270, 853.

33. Jin X., Zhang Z., Li H., He B., Wang P., Lizi Jiaohuan Yu Xifu **1992**, 8, 508 (in Chinese)

34. Fukuda W., Nakao M., Okumura K., Kakiuchi H. J. Polym. Sci. Part A-1 **1972**, 10, 237.

35. Kawaguchi, Y.; Moroishi, H.; Inoue, T.; Nakano, A. JP Patent JP2004339266, Dec12, **2004**.

36. Takahashi, E. JP Patent JP2007100075, Apr 19, **2007**.

37. Lu, Z.; Lee, S. Y.; Goh, S. H. Polymer **1997**, 38, 5893–5895.

38. Li Z., Day M., Ding J. Faid K. Macromolecules **2005**, 38, 2620.

39. Liu J-H., Lin S-H., Shih J-C. J. Appl. Polym. Sci. **2001**, 80, 328.

40. Koo J-S., Smith P., Williams R., Grossel M., Whitcombe M., J. Chem. Mater. **2002**, 14, 5030.

41. Mecerreyes D., Lee V., Hawker C., Hedrick J., Wursch A., Volksen W., Miekeley A. Ber. Dtsch. Chem. Ges. **1932**, 65, 69.

42. Jiang J., Thayumanavan S. Macromlecules **2005**, 38, 5886.

43. Li Z., Day M., Ding J., Faid K. Macromolecules **2005**, 38, 2620.

44. Chen L., Zhu X., Yan D., Chen Y., Chen Q., Yao Y. Angew. Chem., Int. Ed. **2006**, 45, 87.

45. Nagelsdiek R., Mennicken M., Maier B., Keul H., Hocker H. Macromolecules**, 2004**, 37, 8923.

46. Isaure F., Cormack P., Graham S., Sherrington D., Armes S., Butun V. Chem. Commun. **2004**, 1138.

47. Sato T., Hashimoto M., Seno M., Hirano T. Eur. Polym. J. **2004**, 40, 273.

48. Sato T., Ihara H., Hirano T., Seno M. Polymer **2004,** 45, 7491**.**

49. Meng F., Hennink W., Zhong Z. Biomaterials **2009**, 30, 2180.

50. Matsusaki M., Yoshida H., Akashi M. Biomaterials **2007**, 28, 2729.

51. Aliyar H., Hamilton P., Ravi N. Biomacromolecules **2005**, 6, 204.

52. Shu X., Liu Y., Luo Y., Roberts M., Prestwich G. Biomaterials **2002**, 3, 1304.

53. Shu X., Liu Y., Palumbo F., Prestwich G. Biomaterials **2003**, 24, 3825.

54. Yamauchi K., Takeuchi N., Kurimoto A., Tanabe T. Biomaterials **2001**, 22, 855.

55. Cerritelli S., Velluto D., Hubbell J. Biomacromolecules **2007**, 8, 1966.

56. Niu J., Shi F., Liu Z., Wang Z., Zhang X. Langmuir **2007**, 23, 6377.

57. Li T., Armes S. Macromolecules **2005**, 38, 8155.

58. Bratu I., Astilean S., Ionesc C., Indrea E., Huvenne J., Legrand P. Spectrochimica Acta Part A **1998**, 54, 191.

59. Bojinova T., Coppel Y., Viguerie N., Milius A., Rico-lattes I., Lattes A., Langmuir **2003**, 19, 5233.

60. Ficarra R., Ficarra P., Bella M., Raneri D., Tommasini S., Calabro M., Gamberini M., Rustichelli C., J. Pharm. Biomed. Anal. **2000**, 23, 33.

61. Okada M., Kamachi M., Harada A. Macromolecules **1999**, 32 (21), 7202.

62. Hall D., Lim K. J. Am. Chem. Soc. **1986**, 108 (10), 2503.

63. Saenger W. Angew. Chem. Int. Ed. Engl. **1980,** 19, 344.

64. Szejtli J., Osa T., Eds. Comprehensive Supramolecular Chemistry, Pergamon: Oxford, **1996**, Vol. 3 (Cyclodextrins), 693.

65. McMullan R., Saenger W., Fayos J., Mootz D**.,** Carbohydrate Research **1973**, 31, 37.

66. Rusa C., Bullions T., Fox J., Porbeni F., Wang X., Tonelli A. Langmuir **2002**, 18, 10016.

Chapter 7

Biodegradable Nanogels for Sustained and Targeted Release of Macromolecular Drugs

7.1 Introduction

Stimuli-responsive polymers, which undergo dissolution / degradation in response to environmental changes, have been extensively investigated for biomedical applications especially in drug delivery. The stimulus could be change in pH, (Hruby et. al. 2005, Lang et. al. 2006) UV light irradiation frequency, (Ozlem et. al. 2004) temperature, (Junya et. al. 2005) or reducing agent concentration (Zelikin et. al. 2006, Kakizawa et. al. 2001).

Biodegradable polymers in general and hydrogels in particular are widely used in a wide variety of therapeutic applications including tissue engineering (Langer and Vacanti 1993, Cohen 1993) and pharmaceutical applications such as controlled drug release.(Kwon et. al. 2007, Peppas et. al. 1999, Vinogradov et. al. 2002) Gels can be degraded when crosslinked with degradable agents. The disulfide bonded matrices play a special role in biological systems for both therapeutic (Matsusaki et. al. 2007, Aliyar et. al. 2005, Shu et. al. 2002, Shu et. al. 2003, Yamauchi et. al. 2001) and pharmaceutical applications (Cerritelli et. al. 2007, Niu et. al. 2007) due to their stability under oxidizing conditions and their degradation under reducing conditions. It is well known that disulfide crosslinked hydrogels can be degraded by cleaving the disulfide cross-linkage (–S–S–) to thiol groups (–SH HS–) with various reductants such as dithiothreitol (DTT), glutathione (GSH), L-cysteine (Cys) and so on. (Kakizawa Y. et. al. 1999, Li et. al. 2006, Lees et. al. 1993, Hisano et. al. 1998)

The disulfide group is an example of biodegradable group, which can be cleaved in the presence of reducing agents (Jocelyn 1987, Gilbert 1997) nucleophiles, electrophiles (Parker and Kharasch 1959, Kice 1968) or photochemically (Sonntag and Schuchmann 1980, Bookwalter 1995) Since the redox potential of the disulfide (R-S-S-R') /thiol couple depends on the nature of the substituents R and R' and the reaction medium composition (solvent polarity, pH, presence of complex forming ions, etc.), (Gilbert 1997, Capozzi and Modena 1974) a polymeric disulfide can be designed in such a way that the reductive scission of the sulfur-sulfur bridge will occur at sufficient rate only in a given environment. The disulfide/thiol interchange has been extensively investigated (Gilbert 1997, Houk 1987, Singh and Whitesides 1993) in view of its relevance to various phenomena occurring in living cells including protein structure stabilization,

(Creighton 1984) enzyme catalytic activity and redox cycles (Gilbert 1997, Jocelyn 1972, Gilbert 1984). Of special interest is the fact that tumors are often hypoxic and polymeric materials that degrade in reductive environment can be envisioned to degrade therein, releasing a preliminarily incorporated drug, which provides an opportunity for cancer tissue-selective therapy.(Brown 2004)
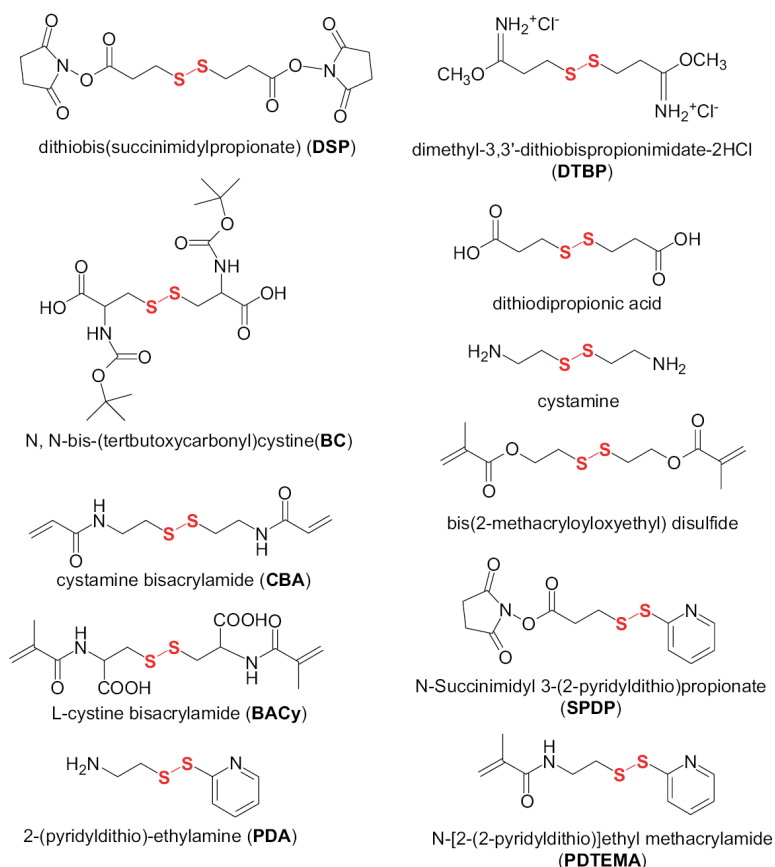
Figure 7.1 Chemical structures containing disulfide bonds

The reduction-sensitive polymers generally involve disulfide linkages in the main chain, at the side chain or in the crosslinker. Disulfide groups can be introduced in a polymer using an appropriate initiator, monomer or a crosslinker (figure 7.1). Crosslinked polymers containing disulfide linkages have been investigated by Matyjaszewski's (Tsarevsky and Matyjaszewski 2005, Oh et. al. 2007, Oh et. al. 2007) and Armes's groups (Li and Armes 2005) to generate drug carriers that readily react in a reducing environment, consequently breaking down crosslinks between chains. Disulfide crosslinked hydrogels can be degraded by various reductants such as dithiothreitol

(DTT), glutathione (GSH), L-cysteine (Cys) and so on. (Kakizawa et. al. 1999, Li et. al. 2006, Lees and Whitesides 1993, Hisano et. al. 1998).

Reduction-sensitive biodegradable polymers are characterized by an excellent stability in the circulation and in extracellular fluids, whereas they undergo rapid degradation under a reductive environment present in intracellular compartments (figure 7.2). The large difference in glutathione concentration between the intracellular and extracellular milieu can be exploited for triggered intracellular delivery of a variety of bioactive molecules.
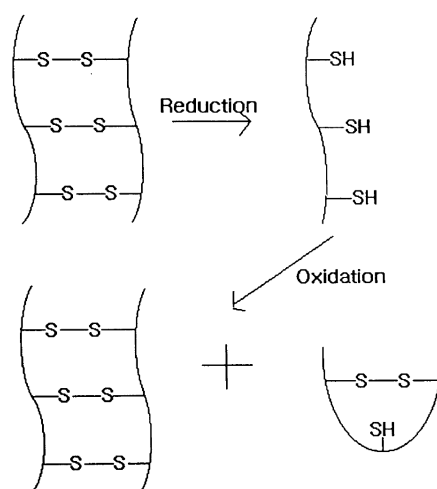
Figure 7.2 Schematic representation of reduction/oxidation induced cleavage/crosslinking of gel containing disulfide bridges (Lee and Park 1998)

Glutathione tripeptide (g-glutamyl-cysteinyl-glycine; GSH) is the most abundant low-molecular-weight biological thiol and GSH/glutathione disulfide (GSSG) is the major redox couple in animal cells (Wu et. al. 2004). GSH/GSSG is maintained at distinct, non-equilibrium potentials in mitochondria, cytoplasm, nuclei, the secretory pathway and the extracellular space (Go and Jones 2008). In body fluids (e.g. blood) and in extracellular matrices and on the cell surface, the proteins are rich in stabilizing disulfides as a result of a relatively high redox potential due to a low concentration of GSH (approximately 2–20 µM). In contrast, inside cells the concentration of GSH is 0.5–10 mM that is kept reduced by NADPH and glutathione reductase, maintaining a highly reducing environment inside cells (Wu et. al. 2004). The large difference in reducing potential between the intracellular and extracellular milieu can be exploited for triggered intracellular delivery of a variety of bioactive molecules including DNA, siRNA, antisense oligonucleotide (asODN), proteins and low molecular weight drugs

(Saito 2003). Furthermore, also of particular interest is that tumor tissues are highly reducing and hypoxic compared with normal tissues (Kuppusamy 1998), with at least 4-fold higher concentrations of GSH in the tumor tissues over normal tissues (Kuppusamy 2002), rendering the reducible bioconjugates valuable for tumor-specific drug and gene delivery.

Bu$_3$P transforms disulfides to thiols very rapidly and has been widely used in the study of proteins (Ruegg and Rudinger 1977). Its major advantages (as opposed to DTT) are relative stability toward autooxidation and high affinity to disulfide groups, meaning that large excess of this reagent is not needed for complete reduction (Jocelyn 1987). Moreover, Bu$_3$P does not interfere with reagents typically used to bind to the formed thiol groups, which is especially important in protein analysis. It can be used, for instance, in conjunction with 1, 3-propane sultone (Ruegg 1979) or o-toluene sultone, (Ruegg 1979) which trap very effectively the formed thiol groups by alkylation, thus preventing back oxidation to disulfide after exposure to air. However, Bu$_3$P is hydrophobic and toxic to cells and hence cannot be used as a reducing agent in vitro. (Oh et. al. 2007).
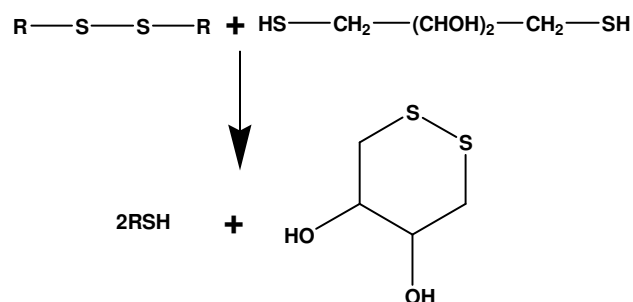
Figure 7.3 Reduction of disulfide by DTT

Dithiothreitol (2, 3- dihydroxy-1, 4-butanethiol, DTT) was selected for the purposes of this study for several reasons. First, disulfide reductions by DTT are rather efficient, due to its low redox potential, which has been explained by the stability of the six-membered cyclic disulfide formed after the oxidation of this dithiol (figure 7.3) (Cleland 1964, Konigsberg 1972, Houk and Whitesides 1987). In addition, DTT is very soluble in a range of solvents including those that dissolve Poly(Styrene) such as THF and DMF.

Water-soluble drugs, especially proteins and nucleic acids, often undergo degradation during their passage through the body before reaching the target site and hence need to

be protected until they reach the site of uptake. The loading efficiency of these drugs in liposomes is very low. Emulsion polymerization leads to nanogels of 100 nm diameter which are highly polydisperse (Allerman et. al. 1993, Davis et. al. 1988, Curt et. al. 1989, Davis 1997). This size is quite large compared to the histology of the endothelial barrier, where fenestrations are around 50–60 nm in diameter. In the case of vasculature in solid tumor sinusoids these could be upto 100 nm in diameter (Mayerson et. al. 1959). Polymeric micelles less than 100 nm diameter are preferred for targeting drugs, particularly to solid tumors (Kataoka et. al. 1993, Kwon and Okano 1996). However, the hydrophobic cores can efficiently dissolve only hydrophobic drugs and are not ideally suited for the encapsulation of water-soluble drugs. The residence time of these particles in the blood is short as these are usually taken up by the RES of the body, mainly the Kupffer cells in the liver. Encapsulation by amphiphilic polymeric surfactants significantly increases the blood circulation time but does not eliminate the RES uptake (Stolnik et. al. 1995, Torchilin and Trubetskoy 1995, Gref et. al. 1995). Thus, the delivery of hydrophilic drugs by targeting nanogels to sites other than RES remains a challenge.

Oh et. al. (2007) and Semyor et. al. (1987) used hydrophilic polymers based on ethylene oxide monomethyl ether methacrylate nanogels in the presence of disulfide dimethacrylate which prevent nanoparticle uptake by RES.

7.1 Disulfide containing polymer : Prior approaches and their limitations

Bharali et. al. (1999) described synthesis of N-vinylpyrrolidone (NVP) - methylene bis acrylamide (MBAM) nanogels less than 100 nm diameter (figure 7.4). These nanogels evade RES uptake, have long circulation times in blood and hence were considered ideal for transendothelial passage. However, the yield of the nanogels was only 25% and the drug loaded nanoparticles were not biodegradable. Further, unreacted monomers and crosslinker cannot be easily removed without extensive leaching of the encapsulated drug.
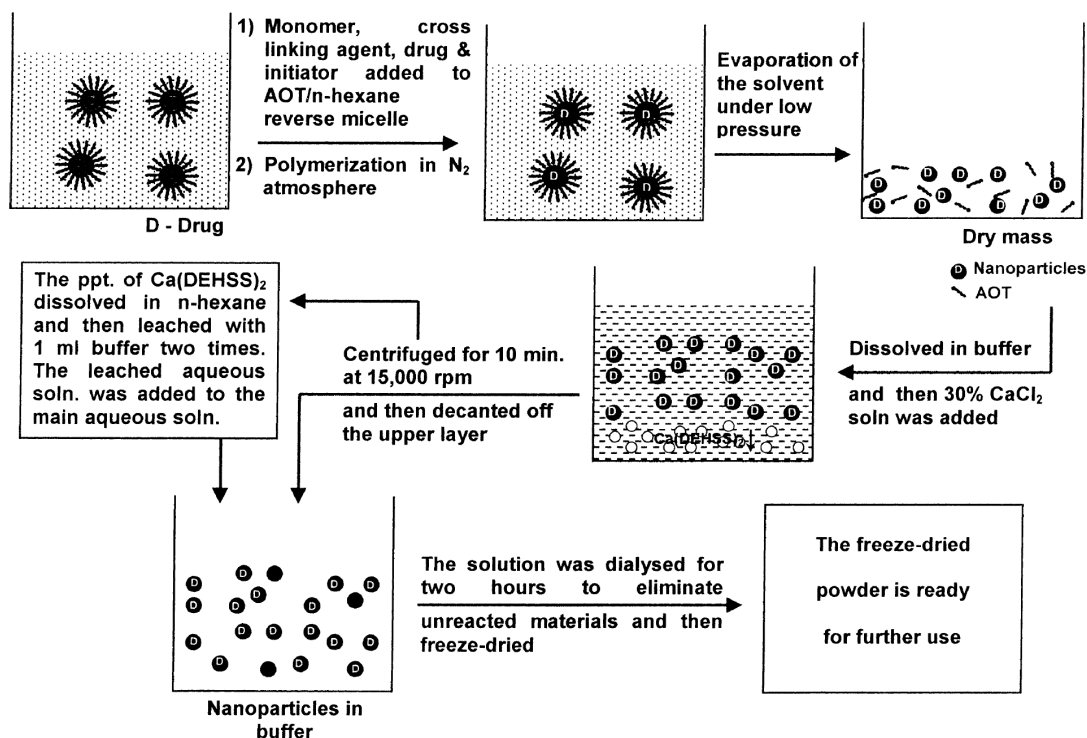
Figure 7.4 Preparation of PVP micelles through reverse micelles (Bharali et. al. 1999)

Lee and Park (1998) synthesized a hydrogel containing N-isopropyl acrylamide with N, N' cystamine bis acrylamide which contain a disulfide linkage between two vinyl groups. The disulfide bond can be reduced to two thiol groups. The cleavage of crosslink points was used for the experimental determination of the polymer molecular weight and the amount of free thiol concentration in the polymer backbone. This was used further for the calculation of an average molecular weight between crosslinks (M_c) which was theoretically predicted by a Flory-Rehner equation based on either swelling or tensile experiments.

Tsarevsky and Matyjaszewski (2005) employed Bis[2-(2-bromoisobutyryloxy)ethyl] disulfide initiator for the ATRP of methyl, tert-butyl and benzyl methacrylate which was catalyzed by CuBr/2, 2'-bipyridine to yield linear polymers with internal disulfide bond (figure 7.5).
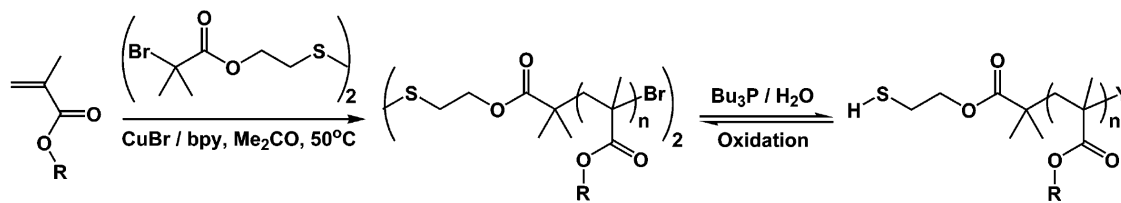
Figure 7.5 Synthesis and reductive degradation of Polymethacrylates with internal disulfide bond (Tsarevsky and Matyjaszewski, 2005)

Plunkett et. al. (2003) synthesized hydrogels of 2-hydroxyethyl methacrylate, acrylic acid (AA) crosslinked with N, N' cystamine bisacrylamide using in situ photopolymerization to form pH/chemically responsive hydrogel (figure 7.6 and 7.7). The crosslink density of the hydrogel network decreased due to the reduction of the disulfide bonds with dithiothreitol which lead to the swelling of the hydrogel. The combination of a decrease in crosslink density and a deprotonation of acrylic acid led to a fast swelling of the hydrogel. The relationship between the hydrogel swelling rate and the rate of crosslink cleavage was linear which would be useful as a quantitative chemical sensor.
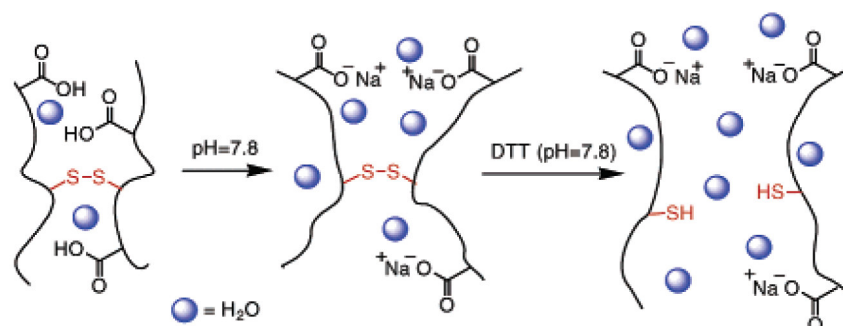
Figure 7.6 Schematic representation of disulfide crosslinked pH responsive hydrogel of HEMA, AA and N, N' cystamine bisacrylamide I) Disulfide crosslinked pH responsive hydrogel II) Hydrogel after it has reached equillibriun swelling, where the hydrogel expanded moderately due to the deprotonation of the pendent pH-sensitive carboxylic acid groups III) Hydrogel after disulfide cross-links were cleaved by exposure to a solution of 10 mM DTT (Plunkett et. al. 2003)
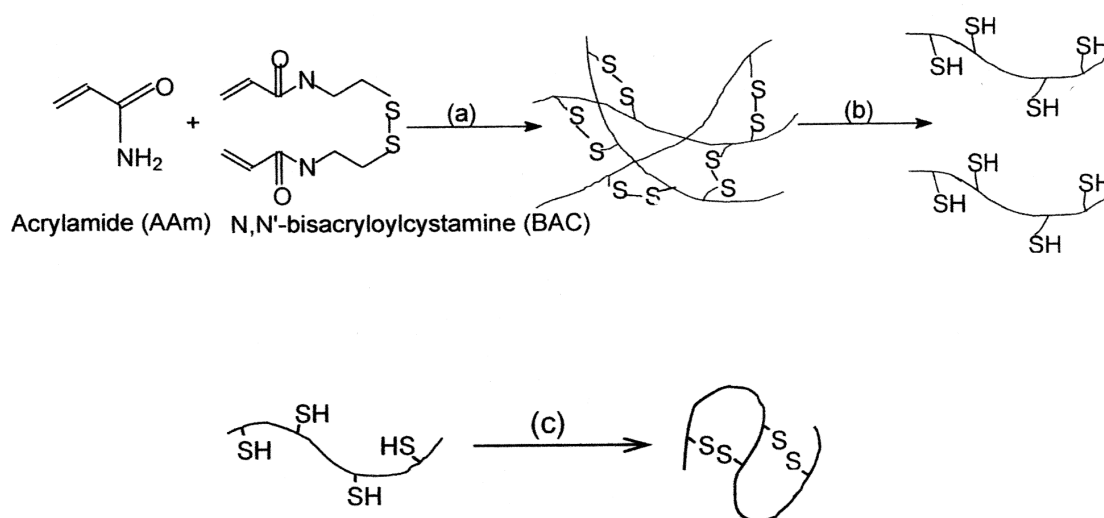
Figure 7.7 Synthesis and degradation of nanogels of AM with N, N' – bisacryloyl cystamine (a) Copolymerization using APS and TEMED at RT (b) Reductive liquefaction of the gel followed by precipitation in methanol, filtration and vacuum drying to get copolymer. (c) Redissolution at dilute concentration in nitrogen-saturated water at pH 4 followed by pH adjustment to 7.5 and bubbling with air to form the nanogels (Plunkett et. al. 2003)

Oh et. al. (2007) synthesized (oligo(ethylene oxide) monomethyl ether methacrylate) (OEOMA) nanogels in the presence of disulfide dimethacrylate by ATRP using inverse miniemulsion technique at 30^0C. The nanogels were loaded with rhodamine B isothiocyanate-dextran (RITC-Dx) and degraded into soluble polymers in a reducing environment to release the encapsulated drug. The released drug interacted specifically with proteins and lectins such as ConA in water which reveal that the drug could bind to pathogens based on lectins.

A chemically cleavable disulfide based dimethacrylate branching agent was used to gain insight into the nature of branched vinyl polymers by Li et. al. (2005). The polymer was obtained by methanolic ATRP of 2-hydroxypropyl methacrylate in the presence of DSDMA under mild condition (figure 7.8). The disulfide bond in the DSDMA branching agent was readily cleaved using either dithiothreitol or benzoyl peroxide. The final polydispersity of the degraded branched polymer was comparable to that of linear poly(2-hydroxypropyl methacrylate) prepared in the absence of any disulfide based

dimethacrylate branching agent. This indicated that the branched copolymer was reduced to its near monodisperse primary chains.
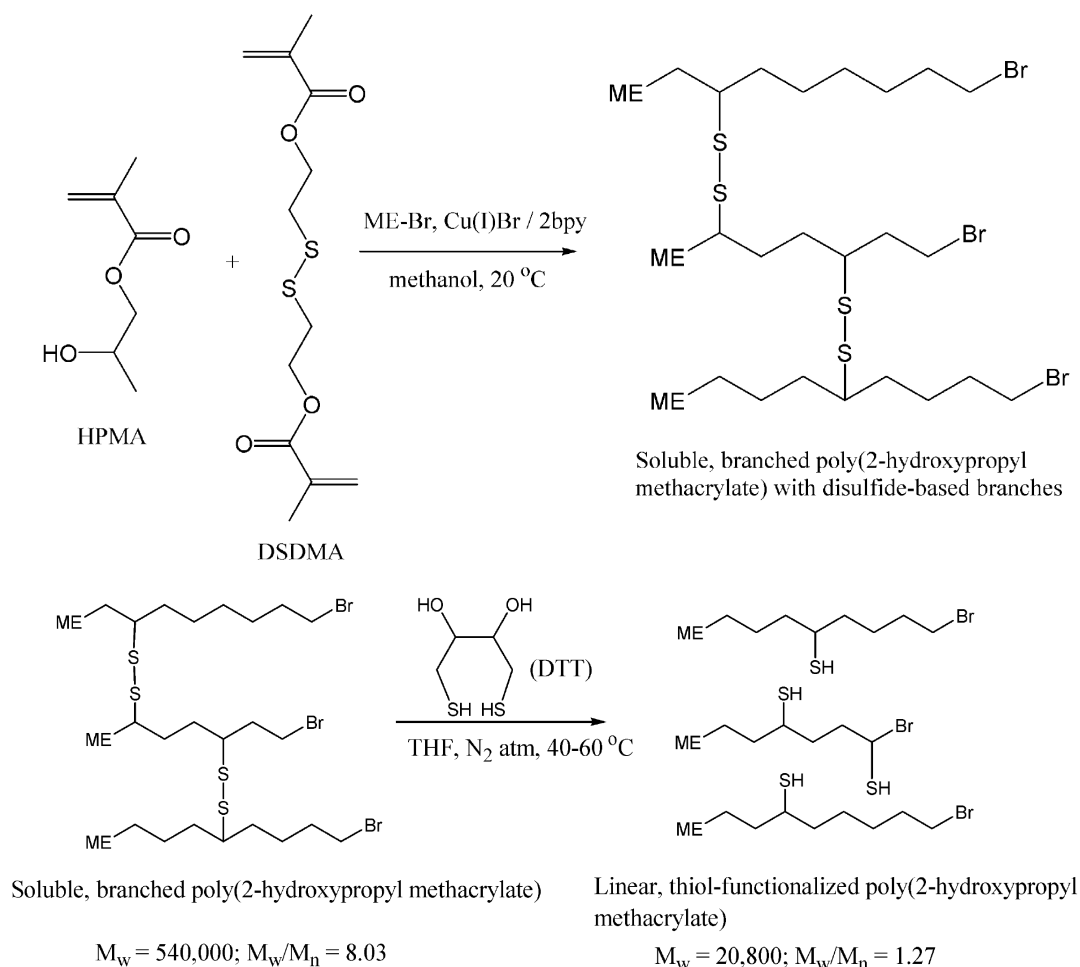
Figure 7.8 Synthesis of branched poly(2-hydroxypropyl methacrylate) with disulfide branches and its degradation to linear thiol functionalized poly(2-hydroxypropyl methacrylate) (Li et. al. 2005)

Zhang et. al. (2008) synthesized a nucleoside containing block copolymer, poly(polyethylene glycol methyl ether methacrylate)-block- poly(5'-O-methacryloyluridine) (PPEGMEMA-b-PMAU). The block copolymer was crosslinked via RAFT polymerization using disulfide dimethacrylate crosslinker to give core crosslinked micelles having PPEGMEMA corona and a polynucleotide core (figure 7.9). These micelles readily hydrolyzed into free block copolymers in the presence of dithiothreitol (DTT) in less than 1 h, depending on the concentration of the reducing agent and the amount of crosslinker in the micelle. Vitamin B_2 was loaded into the

micelles. The release was reached 60-70 % after 7 h in the presence of DTT whereas the crosslinked micelles in the absence of DTT showed only a delayed drug release.

Figure 7.9 Synthesis and degradation of PPEGMEMA-b-PMAU (Zhang et. al. 2008)

In order to overcome the disadvantage of cytotoxicity, multistep synthesis we synthesized water soluble polymer containing biodegradable crosslinker by forming an inclusion complex of crosslinker with cyclodextrin. This approach allowed selective polymerization of the crosslinker leading to water soluble polymer comprising pendant

unsaturation in the first stage. In the second stage, the pendant unsaturation was crosslinked to obtain drug loaded nanogels having low polydispersity. Thus, unreacted monomer and crosslinker can be removed after polymerization and prior to the synthesis of nanogels, yields of drug loaded nanogels are enhanced and the release profile can be manipulated by the concentration of the reducing agent.

In this chapter, we describe a method for the synthesis of water soluble polymers containing biodegradable crosslinker from its inclusion complex with cyclodextrin. This approach allows selective polymerization of the crosslinker leading to water soluble polymer comprising pendant unsaturation in the first stage. In the second stage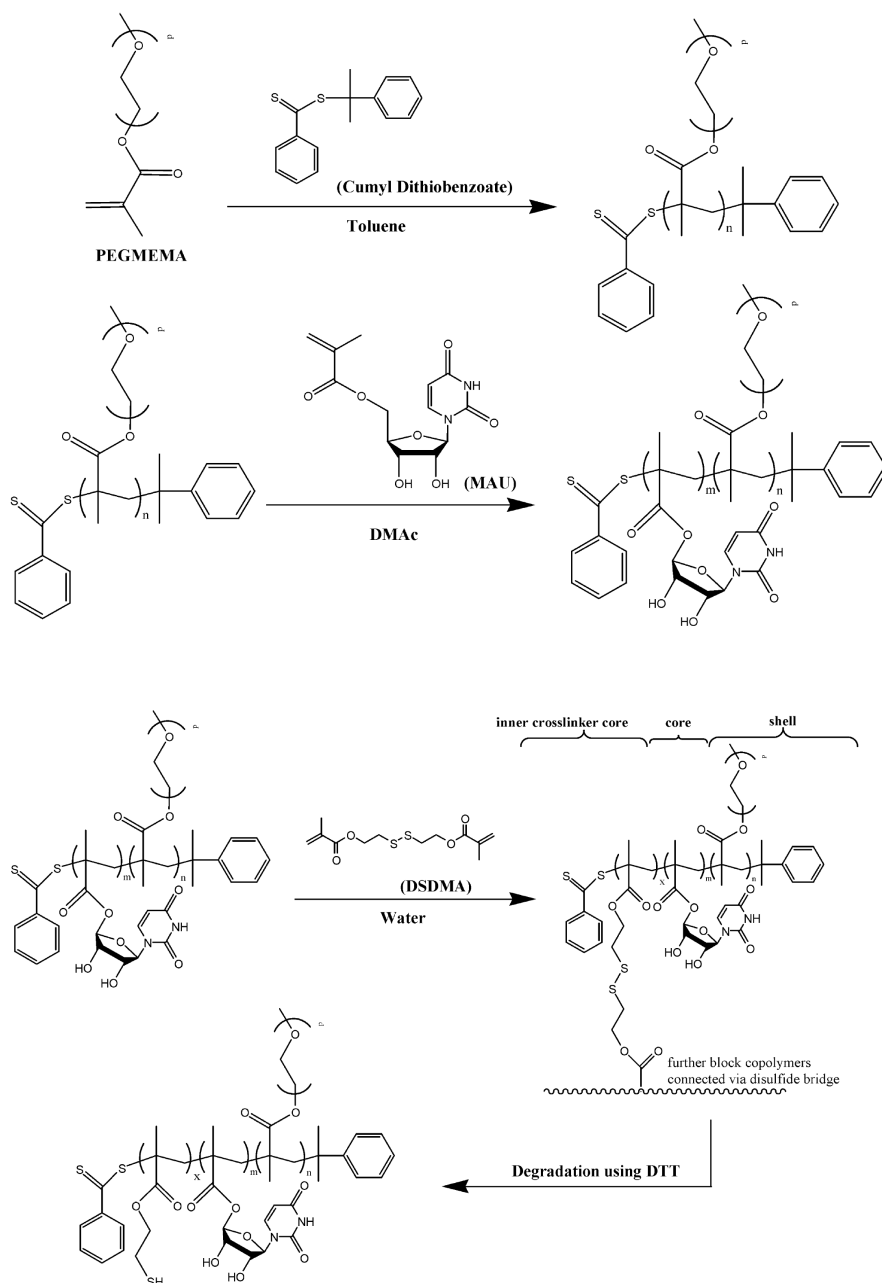, the pendant unsaturation was crosslinked to obtain drug loaded nanogels. As the copolymers used for crosslinking are free from any unreacted monomer and crosslinker, the monomer and crosslinker toxicity can be avoided. Yields of drug loaded nanogels are enhanced and the release profile can be manipulated by the concentration of the crosslinker and reducing agent.

7.2. Experimental

7.2.1 Materials

Aerosol OT, i.e. AOT (sodium bis-2-ethylhexylsulfosuccinate) (purity > 99%), N, N, N', N'' tetramethyl ethylenediamine (TEMED), N, N' methylene bis acrylamide (MBAM) were purchased from Aldrich. 2, 3 dihydroxy 1, 4-butanethiol (Dithiothreitol, DTT) and fluorescein isothiocyanate conjugated to dextran (FITC–Dx) were products of Sigma, USA. n-Hexane (99%), N, N' dimethyl formamide (DMF), 2, 2' azo bis isobutyro nitrile (AIBN), ammonium persulfate (APS), sodium nitrate, sodium monohydrogen phosphate and dihydrogen phosphate were procured from s. d. fine (India). N-Vinyl pyrrolidone (NVP) was purchased from Aldrich and was distilled before use. Deionized water from the Millipore was used for all experiments.

7.2.2 Methods

FTIR spectra were recorded on Perkin–Elmer spectrum one. Polymer and nanogels were mixed with KBr and the spectra were recorded at frequencies from 4000 to 450 cm^{-1} using diffused reflectance spectroscopy (DRS) mode. The resolution was 4 cm^{-1}. The nuclear magnetic resonance spectra of the polymer and nanogels were recorded in

D_2O on Bruker AV 200. Molecular weights of copolymer before and after degradation were determined at 25 °C using aqueous size exclusion chromatography equipped with TSK-GEL columns using 0.2 M $NaNO_3$ at a flow rate 1 mL min^{-1}. The columns were calibrated using Poly(AM) standards. Molecular weights of the copolymer before and after degradation were also determined in methanol using Knauer vapour pressure osmometer (VPO) K – 7000 at 30^0C. Benzil was used as standard for the calibration of the instrument. The particle size of the nanogels was measured using submicron particle sizer NICOMP 380. The solutions used for particle size analysis experiments were sonicated and filtered through a Millipore filter of pore size 0.2 μm to remove any dust impurities. All measurements were made at 25^0C.

Polymer degradation study

An oxygen free DTT solution containing 0.2 M $NaNO_3$ was prepared by purging nitrogen gas for about 30 min. 5 mg Poly(DSDMA-co-NVP) was added in 0.1, 0.01, 0.0025 mM and 5 μM DTT solution containing 0.2 M $NaNO_3$. The solubility of the polymer was checked at different intervals of time. The degradation leads to the complete dissolution of the polymer.

Loading and release study

Fluorescein isothiocyanate conjugated dextran (FITC-Dx) having molecular weight 4,000 and 150,000 were used as a model drug. Poly(DSDMA-co-NVP) having DSDMA content 1.9, 4, 8.8, 16, 37 and 57 mole % and Poly(MBAM-co-NVP) having MBAM content 17, 41 and 63 mole % were used as a drug carrier. Poly(DSDMA-co-NVP) and Poly(MBAM-co-NVP) were crosslinked at 37^0C by dispersion polymerization in the presence of FITC-Dx to obtain drug loaded nanogels.

To measure the loading efficiency, the freeze dried nanogels (25 mg) were suspended in 5 ml pH 7.4 buffer and maintained at 37^0C in a shaker bath for 6 days. The solution was centrifuged and the absorbance of the supernatant solution was recorded on a spectrophotometer. The loading efficiency was calculated as follows.

Loading efficiency = (Loaded FITC-Dx / Total FITC-Dx) X 100

Freeze dried FITC-Dx encapsulated Poly(DSDMA-co-NVP) nanogels were suspended in 5 ml pH 7.4 buffer, centrifuged and its absorbance was recorded. The nanogels were washed with buffer 2-3 times with pH 7.4 buffer so as to remove the free FITC-Dx

which was also confirmed by UV spectroscopy till it gives zero absorbance at 495 nm, dried and then used for release study. The obtained nanogels (25 mg) were suspended in 5 ml pH 7.4 buffer and kept at 37^0C in a shaker bath. 500 μl solution was taken out at predetermined intervals of time, centrifuged and the absorbance of the supernatant solution was recorded on a spectrophotometer at 495 nm.

The percentage release was determined from the equation

% Release = $[FITC–Dx]_{f,t}/[FITC– Dx]_0 \times 100$,

where ($[FITC–Dx]_{f,t}$) is the concentration of FITC–Dx in the filtrate at time t.

The release kinetics of FITC–Dx from nanogels having different degree of cross-linking i.e. Poly(DSDMA-co-NVP) having DSDMA constant 1.9, 4, 8.8, 16, 37 and 57 mole % and Poly(MBAM-co-NVP) having MBAM content 17, 41 and 63 mole % and different molecular weight of drug (FITC-Dx 4,000 and 150,000) was also studied.
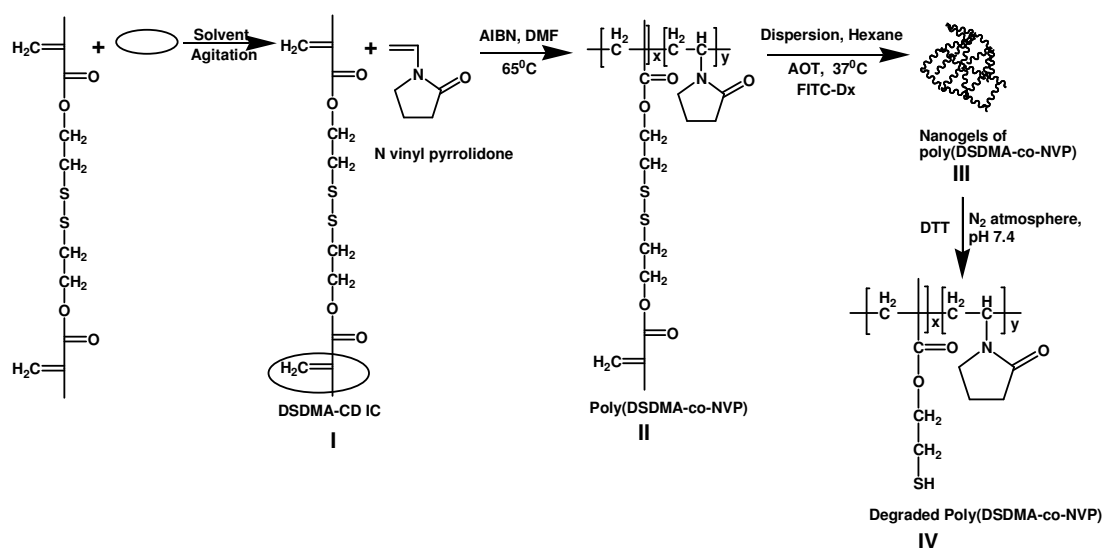
Scheme 7.1 Synthesis of Poly(DSDMA-co-NVP) nanogels
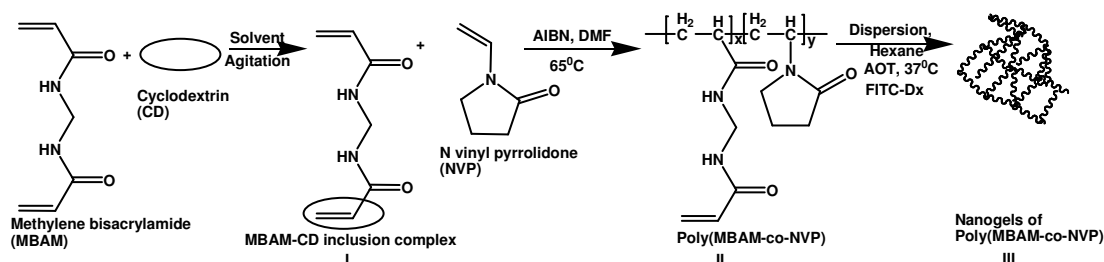
Scheme 7.2 Synthesis of Poly(MBAM-co-NVP) nanogels

7.2.3 Synthesis of Poly(MBAM-co-NVP) and Poly(DSDMA-co-NVP) containing pendant unsaturation

MBAM-β-CD or DSDMA-β-CD IC, N-vinyl pyrrolidone (NVP) and AIBN were dissolved in DMF. Nitrogen gas was purged through the reaction mixture and reaction was continued for 10 h at 65^0C. The reaction mixture obtained was concentrated on rota-vapour and dissolved in methanol so that polymer dissolves and CD gets precipitated. CD was isolated by filtration. The filtrate obtained was concentrated on rota-vapour and then the solid polymer obtained was washed with acetone to remove unreacted monomer and crosslinker (Scheme 1 and 2 II), dried under vacuum at room temperature.

7.2.4   Synthesis of FITC-Dx 4,000 and 150,000 loaded crosslinked nanogels

The crosslinked nanogels were synthesized using the method similar to that described before (Bharali et. al. 2003). Briefly, 0.3048 g of AOT was dissolved in 25 ml hexane and to that 100 mg of Poly(MBAM-co-NVP) or Poly(DSDMA-co-NVP), 1 mg FITC-Dx 4,000 / 150,000, 15μl of APS (20% w/v) and 20 μl of TEMED were added. The crosslinking was carried out at 37^0C for 5 h with continuous stirring at 1500 rpm. After the completion of reaction, hexane was evaporated on a rota-vapour and the solid obtained was suspended in 5 ml water by sonication using a probe sonicator. Then, 400 μl of 30% w/v calcium chloride solution was added drop by drop with continuous stirring so that AOT precipitates as calcium salt of bis-(2-ethylhexyl) sulfosuccinate, $Ca(DEHSS)_2$. The precipitate was dialyzed for 2 h and then separated by centrifugation at 10,000 rpm for 15 min. FITC-Dx loaded nanogels absorbed on $Ca(DEHSS)_2$ were removed by redissolving it in hexane and then washing with water and collecting the phase separated aqueous layer in the previously obtained nanogels. The aqueous solution of FITC-Dx loaded Poly(DSDMA-co-NVP) and Poly(MBAM-co-NVP) nanogels (Scheme 1, 2 III) were freeze dried and further used for the release study.

7.3 Results and discussion

Reduction-sensitive biodegradable polymers are stable in the circulation and in extracellular fluids, whereas they undergo rapid degradation under the reductive environment present in intracellular compartments. The large difference in glutathione

concentration between the intracellular and extracellular milieu can be exploited for triggered intracellular delivery of a variety of bioactive molecules. These polymers can be synthesized by incorporating disulfide linkage in the main chain, in the side chain or in the cross-linker. Hydrophobic polymers can efficiently dissolve only hydrophobic drugs and are not ideally suitable for the encapsulation of water-soluble drugs. The residence time of these particles in the blood is short as these are usually taken up by the reticulo endothelial system (RES) of the body. Encapsulation by amphiphilic polymeric surfactants significantly increases the blood circulation time but does not eliminate the RES uptake. (Stolnik et. al. 1995, Torchilin and Trubetskoy 1995, Gref et. al. 1995). Oh et. al. (2007) and Semyor et. al. (1987) used hydrophilic polymers based on ethylene oxide monomethyl ether methacrylate nanogels in the presence of disulfide dimethacrylate which prevent nanoparticle uptake by RES.

Bharali et. al. (1999) described synthesis of N-vinylpyrrolidone (NVP) - methylene bis acrylamide (MBAM) nanogels less than 100 nm diameter. These nanogels were expected to evade RES uptake, have long circulation times in blood and hence were considered ideal for transendothelial passage. However, the yield of the nanogels was only 25 % and the drug loaded nanoparticles were not biodegradable. Further, unreacted monomers and crosslinker cannot be easily removed without extensive leaching of the encapsulated drug. In order to overcome these limitations a polymer from which the unreacted monomer / crosslinker can be completely stripped off prior to crosslinking is needed. Aliyar et. al. (2005) reported thiol functional polymers obtained by the reduction of acrylamide / bisacryloyl cystamine copolymer which could be crosslinked again in an oxidizing environment. However the storage of such solutions and nanogel synthesis could pose problems apart from the reaction between the thiol groups and other functionalities in protein drugs. We synthesized water soluble polymer containing biodegradable crosslinker by forming an inclusion complex of crosslinker with cyclodextrin. This approach allowed selective polymerization of the crosslinker leading to water soluble polymer comprising pendant unsaturation in the first stage. In the second stage, the pendant unsaturation was crosslinked to obtain drug loaded nanogels having low polydispersity. Thus, unreacted monomer and crosslinker could be removed after polymerization and prior to the synthesis of nanogels. Yields of drug loaded

nanogels were enhanced and the release profiles were a function of the concentration of the crosslinker and the reducing agent.

DSDMA and NVP were chosen to synthesize biodegradable nanogels because DSDMA undergoes degradation in reductive environment. NVP is biocompatible and nonantigenic and hence safe for biomedical applications. (Roninson et. al. 1990) Surfactant AOT was selected since it forms aggregates in oil in the absence of a cosurfactant and the reverse micellar solution can dissolve a large amount of hydrophilic monomer. Further, it can be separated from the aqueous system as calcium salt. (De and Maitra 1995).

Copolymers of NVP containing two crosslinkers *viz.* MBAM and DSDMA were synthesized. The latter degraded in the presence of the reducing agent dithiothreitol (DTT). The release of FITC-Dx from Poly(MBAM-co-NVP) and Poly(DSDMA-co-NVP) in absence of DTT was sustained over 30-40 h. Poly(DSDMA-co-NVP) nanogels containing disulfide bonds released FITC-Dx rapidly at dithiothreitol (DTT) concentrations prevailing in intracellular environment. The release rate was very slow at (DTT) concentrations prevailing in extracellular environment. These nanogels thus can be exploited for intracellular delivery of proteins and peptides as will be shown later.

7.3.1 Synthesis of Poly(DSDMA-co-NVP) and Poly(MBAM-co-NVP) containing pendant unsaturation

The presence of pendant unsaturation in both copolymers was confirmed by FTIR and ^{1}H NMR analysis. FTIR data (figure 7.15) showed the presence of the vinyl unsaturation peak at 1620 cm^{-1} for Poly (DSDMA-co-NVP) and 1623 cm^{-1} for Poly (MBAM-co-NVP) respectively. ^{1}H NMR analysis showed the presence of vinyl unsaturation peaks at 5.69 δ and 6.15 δ for Poly (MBAM-co-NVP) and 5.5, 6.1 δ ppm for Poly (DSDMA-co-NVP).

This polymer was further crosslinked in the presence of FITC-Dx so as to yield FITC-Dx loaded nanogels. The crosslinking was carried out using ammonium persulphate and TEMED by dispersing droplets of aqueous solution of polymers and FITC-Dx in n-hexane at 37[0]C. The surfactant AOT in nanogels was recovered by precipitating with calcium chloride and the nanogels obtained were recovered by centrifugation and dried.
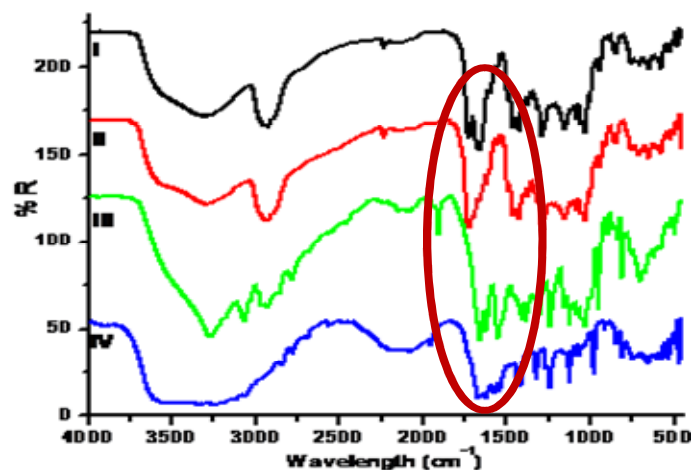
Figure 7.10 FTIR of Poly(DSDMA-co-NVP) and Poly(MBAM-co-NVP) before and after crosslinking I Poly(DSDMA-co-NVP) before crosslinking II Poly(DSDMA-co-NVP) after crosslinking III Poly(MBAM-co-NVP) before crosslinking IV Poly(MBAM-co-NVP) after crosslinking

The absence of any unreacted monomer and crosslinker in the nanogels was confirmed by FTIR and NMR analysis. FTIR data showed the absence of vinyl unsaturation peak at 1620 cm^{-1} for Poly(DSDMA-co-NVP) and 1626 cm^{-1} for Poly(MBAM-co-NVP) (figure 7.15). No peak in the region 5.5-6.2 δ was seen in ^{1}H NMR spectra which confirms the absence of any unreacted monomer and crosslinker. (figure 7.16)
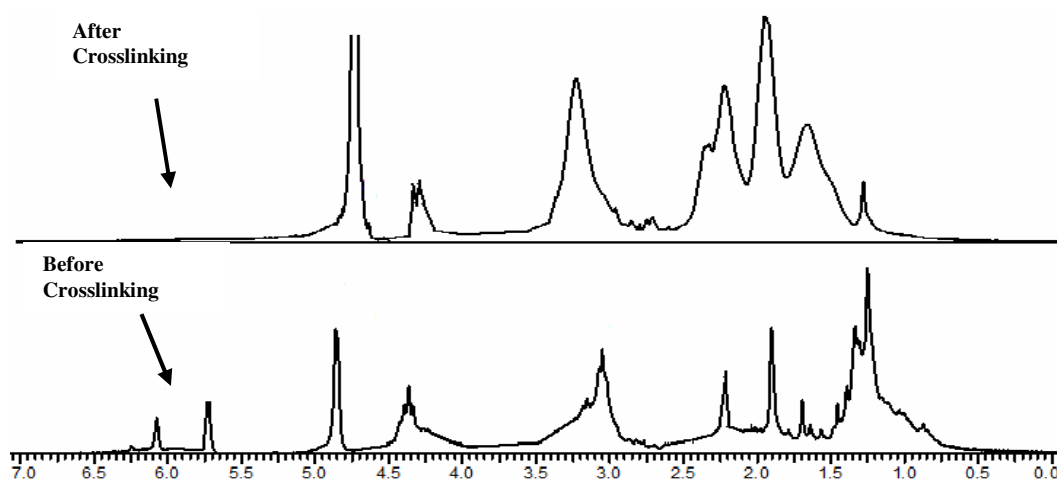
Figure 7.11 ^{1}H NMR of Poly(DSDMA-co-NVP) before and after crosslinking

When DSDMA content in the feed was increased, the copolymer yield decreased since DSDMA also acts as a chain transfer agent (Barner 2007, Chong 1999). At 57 mole %

DSDMA, the polymer yield was as low as 30%. In case of MBAM the yield of the copolymer was above 75 % at all compositions.

7.3.2 Synthesis of FITC-Dx containing nanogels

The synthesis of the prepolymer in the first stage as described in section 3.1 and subsequent crosslinking in the second stage allows complete removal of the unreacted monomer and crosslinker from the polymer prior to the synthesis of nanogel. The crosslinking of the polymer containing pendant unsaturation was carried out by dispersion polymerization using ammonium persulphate / TEMED system at 37^0C. The yield of the FITC-Dx loaded crosslinked nanogels increased with the crosslinker content. The yield of the nanogels containing DSDMA in the range 1.9 mole % to 57 mole %, ranged between 90-98 % whereas in case of MBAM the yield was 94-98 %. The maximum yield of nanogels containing MBAM and NVP synthesized by the dispersion polymerization technique reported in the literature was 25% (Bharali 2003). The higher yield observed in the present case is because of complete removal of monomer and crosslinker from the polymer prior to crosslinking. Also the homopolymer formed if any, would be washed off during the purification procedure.

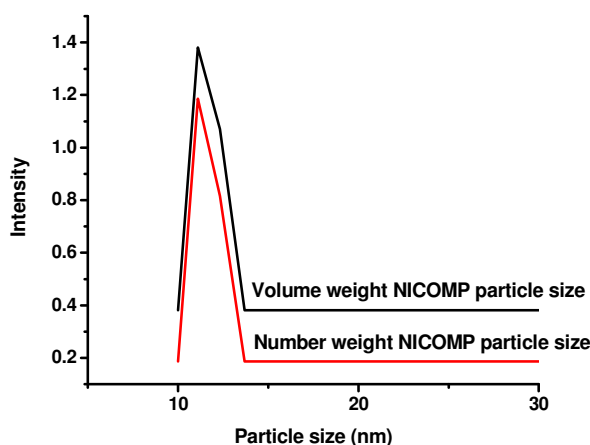### 7.3.3 Particle size and distribution measurements

Figure 7.12 Particle size distribution for Poly (DSDMA-co-NVP) containing 57 mole % DSDMA

The size of the FITC-Dx loaded nanogels was measured by the particle size analyzer NICOMP 380. The solutions used for particle size analysis were sonicated and filtered through a Millipore filter of pore size 0.2 μm to remove any dust impurities. The size of

the nanogels was determined from the diffusion of the particles using the Stokes–Einstein equation. A representative size distribution spectrum is shown in figure 7.17.

The particle size for Poly (DSDMA-co-NVP) was in the range 11-117 nm whereas for Poly (MBAM-co-NVP) it was 42-59 nm. For both polymers, the particle size of FITC-Dx 150,000 loaded nanogels was greater than that for FITC-Dx 4,000 loaded particles. This could be attributed to the difference in molecular weights of the FITC-Dx. The polydispersity of the nanogels in the range 0.3-0.4 suggests that the particles are monodisperse. The decrease in the size of nanogels with the increase in crosslinking density (Table 7.1) indicated that there was no inter chain crosslinking between the particles (Bharali et. al. 2003). The dilute polymer solution used favored intramolecular disulfide crosslinking in the polymer chain, resulting primarily in a single chain nanogel. (Aliyar et.al. 2005).

Table 7.1 Particle size : Poly(DSDMA-co-NVP) nanogels

DSDMA Mole %	Particle size nm	
	FITC-Dx 4,000	FITC-Dx 1,50,000
1.9	59.6	117.1
4	56.4	59.8
8.8	52.3	56.9
16	51.1	53.1
37	42.2	47.8
57	11.1	11.6

The particle size for Poly (MBAM-co-NVP) nanogels decreased from 52.3 to 42.2 nm as MBAM content in the polymer increased from 17 to 63 mole % (Table 7.2). In case of Poly(DSDMA-co-NVP), the particles size decreased from 59.6 to 11.1 nm as DSDMA content increased from 1.9 to 57 mole %. Bharali et. al. (2003) obtained the particle size of 50 nm when the content of crosslinker MBAM was 0.6 %. However, we could not explain why in the case of polymer containing 1.9 Mole % DSDMA, the particle size was higher for dextran of mol. wt. 150,000 except to add that the results were always reproducible.

Table 7.2 Particle size : Poly(MBAM-co-NVP) nanogels

Sr. No.	MBAM Mole %	Particle size nm	
		FITC-Dx 4,000	FITC Dx 150,000
1.	17	52.3	59
2.	41	51.1	56.4
3.	63	42.2	47.8

7.3.4 Determination of FITC-Dx loading in the nanogels

FITC-Dx 4,000 and 150,000 were loaded in Poly (MBAM-co-NVP) and Poly (DSDMA-co-NVP) as described earlier. To measure the loading efficiency, the freeze dried nanogels (25 mg) were suspended in 5 ml pH 7.4 buffer and maintained at 37^0C in a shaker bath for 3 days. The solution was centrifuged and the absorbance of the supernatant solution was recorded on a spectrophotometer. The loading efficiency was calculated as follows.

Loading efficiency = (Loaded FITC-Dx / Total FITC-Dx) X 100

The highest FITC-Dx loading in case of Poly(DSDMA-co-NVP) containing 37 and 57 mole % DSDMA was 93 and 94 %. This could be attributed to the high crosslink density which entraps the FITC-Dx molecule more effectively. In case of Poly (MBAM-co-NVP), the FITC-Dx loading increased from 88 to 94 % when MBAM content was increased from 17 to 63 mole %. Oh et. al. (Biomacromolecules 2007) obtained loading efficiency of 84 % for rhodamine B isothiocyanate-dextran (RITC-Dx) encapsulated nanogels made from oligo (ethylene oxide) monomethyl ether methacrylate and DSDMA.

7.3.5 Degradation of Poly(DSDMA-co-NVP)

It is well known that disulfide crosslinked hydrogels are degraded as a result of cleavage of the disulfide bridge (–S–S–) to thiol groups (–SH HS–) in the presence of various reductants such as dithiothreitol (DTT), glutathione (GSH) and L-cysteine (Cys). (Kakizawa et. al. 1999, Li et. al. 2006, Lees and Whitesides 1993, Hisano et. al. 1998) Dithiothreitol (2, 3- dihydroxy-1, 4-butanethiol, DTT) was used for the degradation of the hydrogels. Cerritelli et. al. (2007) reported that the degradation results with DTT and cysteine were similar. Disulfide reduction by DTT is efficient because of its low redox potential. This has been attributed to the stability of the six-

membered cyclic disulfide ring formed after the oxidation of this dithiol. (Cleland 1964, Konigsberg 1972, Houk and Whitesides 1987)

In extracellular matrices and on the cell surfaces, reducing agent concentration is in the range 2-20 µm. In contrast, within the cells the concentration is 0.5-10 mM and is maintained by NADPH and glutathione reductase. (Wu et. al. 2004) To study the degradation of nanogels, DTT concentration was chosen as to simulate both environments. The degraded nanogels were soluble in water whereas nondegraded nanogels remained insoluble. The rate of degradation of nanogels increased with the concentration of DTT and decreased with increase in the concentration of the crosslinker (Table 7.3). Poly(DSDMA-co-NVP) containing 8.8 mole % of DSDMA did not degrade at any concentrations of DTT. Copolymer containing 4 mole % cross linker remained stable at 5 µM DTT concentration i.e. under extracellular environment but completely degraded at concentrations greater than 2.5 mM i.e. under intracellular environment. The copolymer containing 1.9 mole % DSDMA degraded at concentrations prevalent in intracellular as well as extracellular environment. The rate of degradation at 5 µM DTT concentration which represents intracellular concentration was slow and the dissolution time was 9 h. The degradation rate was drastically enhanced at intracellular concentration of 10 mM and the dissolution time was 2 h.

Table 7.3 Degradation of Poly (DSDMA-co-NVP)

DSDMA Mole % in the polymer	Degradation time in h at DTT concentration			
	100 mM	10 mM	2.5 mM	5µM
1.9	1	2	3	9
4	2	4.5	6	Not degraded
8.8	Not degraded	Not degraded	Not degraded	Not degraded

Table 7.4 Molecular weights of Poly(DSDMA-co-NVP)

DSDMA Mole %	Mol. Wt. of polymer before crosslinking		Mol. Wt. of Nanogels					
			Before degradation		After degradation			
					10 mM DTT		2.5 mM DTT	
	GPC	VPO	GPC	VPO	GPC	VPO	GPC	VPO
1.9	29583	29305	23567	28502	22602	23895	22257	23625
4	27677	27880	19772	26979	18876	20665	18520	20899

The molecular weights of the polymer were studied before and after degradation (Table 7.4). It is interesting to note that the molecular weights of the polymers containing 1.9 and 4 % crosslinker estimated by GPC and VPO are in good agreement. The formation of the nanogels by intra chain crosslinking would be expected to result in a decrease in the hydrodynamic volume and hence a longer residence time on the column which would be interpreted as lower molecular weight. The molecular weights determined by VPO did not show the decrease as it is based on vapor pressure and not on the hydrodynamic volume. The molecular weights after degradation estimated by GPC and VPO are also in good agreement. This is because after degradation the crosslinked chains splitted at disulfide bond and behave as a linear molecule. There is no significant difference between the molecular weights before and after degradation because a very small molecule is separated from the main chain. Aliyar et. al. (2005) concluded that the intrinsic viscosity and radius of gyration of the nanogels (0.284 dL/g, 19.4 nm) was less than that of the polymer (0.511 dL/g, 21 nm) from which the nanogels were synthesized. This further confirms that crosslinking between thiol groups has resulted in an overall decrease in the size and also molecular weight of the resulting polymer chain.

7.3.6 Release study

The dissolution time of nanogels of Poly (DSDMA-co-NVP) was dramatically reduced on increasing DTT concentration. This could be exploited to trigger the release of the encapsulated FITC-Dx in the intracellular environment, with minimal loss during the transit. To demonstrate this, water soluble FITC-Dx of molecular weight 4,000 and 150,000 were selected as model hydrophilic drug. The release of FITC-Dx loaded nanoparticles was monitored at pH 7.4. Oh et. al. (2007) demonstrated that nanogels of oligo (ethylene oxide) monomethyl ether methacrylate with DSDMA degraded in 3 h when 16 wt. % glutathione was used. This is far greater than the intracellular glutathione concentration. We used DTT concentrations which represent intracellular (0.5-10 mM) and extracellular (2-20 μm) glutathione concentrations for the release from Poly(DSDMA-co-NVP) nanogels. The tumor tissues are highly reducing and hypoxic compared to normal tissues wherein the reducing agent concentration in tumor tissues is at least 4 fold higher compared to that in normal tissues (Kuppusamy et. al. 1998 and 2002). Carlisle et. al. (2004) reported that complete release of DNA could be

accomplished by the addition of 20 mM of DTT. Hence, the release was also carried out at higher DTT concentration *viz.* 100 mM. The Poly(DSDMA-co-NVP) nanogels selected for the release of FITC-Dx contained 1.9 and 4 mole % DSDMA since only these copolymer compositions were degradable as shown earlier and supported by Lee and Park (1998).

Poly (DSDMA-co-NVP) nanogels showed practically no release in first 2.5-3 h in absence of DTT. This was also the case with Poly (MBAM-co-NVP) nanogels. FITC-Dx being large in size, its diffusional release from the polymer matrix is difficult unless the matrix is swollen or eroded in aqueous medium. In case of Poly(MBAM-co-NVP) erosion through cleavage can take place through the amide bond of the crosslinker leading to the formation of the loose crosslinked network. However, Torchilin et. al. (1977) reported the very slow cleavage of amide bonds of MBAM when MBAM content is above 1 %. Hence, the release of FITC-Dx from Poly(MBAM-co-NVP) is believed to be diffusion controlled through swollen nanogels as it is well known that Poly(vinyl pyrrolidone) swells in water. Bharali et. al. described the release of FITC-Dx through Poly(MBAM-co-NVP) is diffusion controlled at pH 7. At DSDMA content in the range 16 - 57 mole %, upto 45-50 % FITC-Dx 4,000 was released in 24 h whereas upto 40-46 % FITC-Dx 150,000 was released. Although the release of FITC-Dx 150,000 is marginally slower, the decrease in release rate is not significantly affected by increase in molecular weight.

For nanogels containing 17 - 63 % MBAM, 50% of FITC-Dx 4,000 was released in 12-14 h whereas for FITC-Dx 150,000 the time required was 24-26 h. In these composition ranges, DSDMA was not readily degraded and hence the release in both cases was controlled by diffusion and was not complete in the time duration monitored.

In the presence of DTT, the dissolution time of Poly (DSDMA-co-NVP) nanogels containing lower degrees of crosslinking, was a function of DSDMA concentration (Figure 7.18 and 7.19). Poly (DSDMA-co-NVP) nanogels containing 1.9 mole % DSDMA, released FITC-Dx 4,000 and 1,50,000 as a burst in 1-3 h at DTT concentration of 100 – 2.5 mM. At 5 μM DTT concentration, a sustained release up to 9 h was observed. (figure 7.18). At 4 mole % DSDMA content, the nanogels released FITC-Dx completely in 2 h at 100 mM DTT concentrations (figure 7.19). However, the

copolymer released about 23 % FITC-Dx at 5 µM in 12 h. Cerritelli et. al. (2007) reported almost complete release of calcein in 80 min. when 0.7 mM cysteine was added 5 times in a small amount. The calcein molecule is very small as compared to FITC-Dx. Hence, even at low concentration of cysteine, the calceine molecule releases fast.

Shu et. al. (2002) described the complete release of blue dextran from hydrogels of thiol modified hyaluronic acid in 60-100 min. at DTT concentration of 10-50 mM. These results are comparable with the release of FITC-Dx 4,000 from Poly(DSDMA-co-NVP) containing 1.9 mole % DSDMA. Shu et. al. (2002) described the reversible oxidation reduction chemistry of the disulfide groups for the formation of gel which is more tedious as compared to the approach described in this communication. Further, the removal of the unreacted monomer and crosslinker from the gel remains unanswered and the release of blue dextran in extracellular environment i.e. at 2-20 µm DTT.

Bharali et. al. (1999) demonstrated the synthesis of Poly(MBAM-co-NVP) nanogels by dispersing the droplets of aqueous polymer solution in oil phase which can give the sustained release of macromolecular drugs. The prior literature reveals that there is a need of the delivery systems which can trigger the release of drugs from their carriers within the endosome prior to lysosomal fusion and will also cause the disruption of the endosomal membrane. However, the approach described by Bharali et. al. may lead to lysosomal fusion and has to be avoided by the burst release of macromolecular drugs inside the cells. The two stage crosslinking approach described herein results in the burst release of the macromolecular drugs in the presence of reducing agent minimizing the lysosomal fusion and also gives the nanogels without any residual monomer and crosslinker. The two stage crosslinked nanogel can thus be used as a glutathione sensitive delivery system for the intracellular release of proteins and peptides.
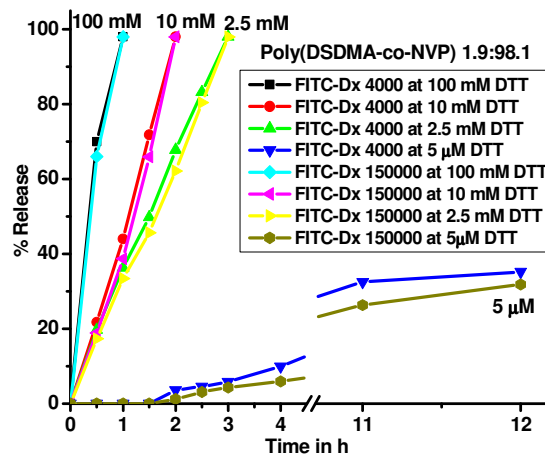
Figure 7.13 Burst release of FITC-Dx from Poly(DSDMA-co-NVP) containing 1.9 mole % DSDMA in presence of different concentration of DTT
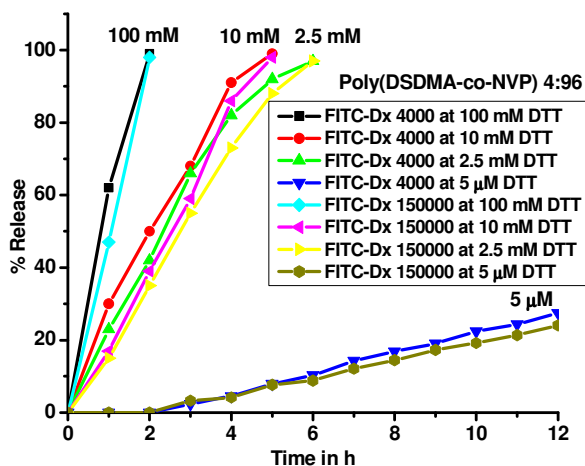

Figure 7.14 Burst release of FITC-Dx from Poly(DSDMA-co-NVP) containing 4 mole % DSDMA in presence of different concentration of DTT

7.4 Conclusions

The inclusion complex approach yields water soluble polymers containing pendant unsaturation even at higher concentration of the crosslinker and enables removal of the unreacted monomer and crosslinker before formation of gel. The two stage crosslinking method gives high yield of FITC-Dx loaded nanogels since unreacted monomers and crosslinker are removed before crosslinking step. This also results in higher drug loading efficiency as compared to the conventional methods. Poly(MBAM-co-NVP) and Poly(DSDMA-co-NVP) nanogels released FITC-Dx in a sustained manner over 30-

40 h. At higher concentrations of reducing agent, DTT Poly(DSDMA-co-NVP) nanogels exhibited burst release due to the reduction of disulfide to thiol groups.

7.5 References

1) Hruby M., Konak C., Ulbrich K. J. Controlled Release **2005**, 103, 137.

2) Lang Y., Li M., Pan S., Zheng Y. J. Drug Delivery Sci. Tech. **2006**, 16, 65.

3) Ozlem C., Vasif H. J. Controlled Release **2004**, 96, 85.

4) Junya F., Yasuo Y., Etsuo Y., Katsuhide T. J. Controlled Release **2005**, 102, 49.

5) Zelikin N., Quinn F., Caruso F. Biomacromolecules **2006**, 7, 27.

6) Kakizawa Y., Harada A., Kataoka K. Biomacromolecules **2001**, 2, 491.

7) Langer R., Vacanti P., Science **1993**, 260, 920.

8) Cohen S., Bano C., Linda G., Cima G., Allcock R., Vacanti P., Vacanti A., Langer R., Clin. Mater. **1993**, 13, 3.

9) Kwon J., Siegwart D., Lee H., Sherwood G., Peteanu L., Hollinger J., Kataoka K., Matyjaszewski K., J. Am. Chem. Soc. **2007**, 129, 5939.

10) Peppas N., Keys K., Torres-Lugo M., Lowman A., J. Controlled Release **1999**, 62, 81.

11) Vinogradov S., Bronich T., Kabanov A., Adv. Drug Deliv. Rev. **2002**, 54, 135.

12) Allerman E., Gurny R., Doelken E., Eur. J. Pharm. Biopharm. **1993**, 39, 173.

13) Davis S., Illum L., in: G. Gregoriadis, G. Poste (Eds.), Targeting of Drugs, Anatomical and Physiological Considerations, Plenum Press, New York, **1988**, 177.

14) Curt T., in: M. Rosott (Ed.), Controlled Release of Drugs: Polymers and Aggregated Systems, VCH, New York, **1989**.

15) Davis S., TIBTECH **1997**, 15, 217.

16) Mayerson H., Wolfram C., Shirby H., Wasserman K., Am. J. Physiol. **1959**, 198, 155.

17) Kataoka K., Kwon G., Yokoyama M., Okano T., Sakurai Y., J. Controlled Release **1993**, 24, 119.

18) Kwon G., Okano T., Adv. Drug Deliv. Rev. **1996**, 21, 107.

19) Stolnik S., Illum L., Davis S., Adv. Drug Deliv. Rev. **1995**, 16, 195.

20) Torchilin V., Trubetskoy V., Adv. Drug Deliv. Rev. **1995**, 16, 141.

21) Gref R., Domb A., Quelle P., Blunk T., Muller R., Verbatz J., Langer R., Adv. Drug Deliv. Rev. **1995**, 16, 215.

22) Tan J., Butterfield D., Voychek C., Caldwell K., Li J. Biomaterials **1993**, 14, 823.

23) Porter C., Mognimi S., Illum L., Davis S. FEBS Lett. **1992**, 305, 62.

24) Bharali J., Sahoo K., Mozumdar S., Maitra A. Journal of Colloid and Interface Science **2003**, 258, 415.

25) Roninson B., Sullivan F., Borzelleca J., Schwartz S., PVP, A Critical Review of the Kinetics and Toxicology of Polyvinyl Pyrrolidone (Povidone), Lewis Publishers, Michigan, **1990**.

26) De T., Maitra A., Adv. Colloid Interface Sci. **1995**, 59, 95.

27) Tsarevsky V., Matyjaszewski K. Macromolecules **2005**, 38, 3087.

28) Oh K., Siegwart J., Matyjaszewski K. Biomacromolecules **2007**, 8, 3326.

29) Oh K., Siegwart J., Lee H., Sherwood G., Peteanu L., Hollinger O., Kataoka K., Matyjaszewski K. J. Am. Chem. Soc. **2007**, 129, 5939.

30) Li T., Armes S. Macromolecules **2005**, 38, 8155.

31) Chirila, T. J. Cataract Refract. Surg. **1994**, *20*, 675.

32) Meng F., Hennink W., Zhong Z. Biomaterials **2009**, 30, 2180.

33) Matsusaki M., Yoshida H., Akashi M. Biomaterials **2007**, 28, 2729.

34) Aliyar H., Hamilton P., Ravi N. Biomacromolecules **2005**, 6, 204.

35) Shu X., Liu Y., Luo Y., Roberts M., Prestwich G. Biomaterials **2002**, 3, 1304.

36) Shu X., Liu Y., Palumbo F., Prestwich G. Biomaterials **2003**, 24, 3825.

37) Yamauchi K., Takeuchi N., Kurimoto A., Tanabe T. Biomaterials **2001**, 22, 855.

38) Cerritelli S., Velluto D., Hubbell J. Biomacromolecules **2007**, 8, 1966.

39) Niu J., Shi F., Liu Z., Wang Z., Zhang X. Langmuir **2007**, 23, 6377.

40) Kakizawa Y., Harada A., Kataoka K. J. Am. Chem. Soc. **1999**, 121, 11247.

41) Li C., Madsen J., Armes S., Lewis A. Angew. Chem. Int. Ed. **2006**, 45, 3510.

42) Lees W., Whitesides G. J. Org. Chem. **1993**, 58, 642.

43) Hisano N., Morikawa N., Iwata H., Ikada Y. J. Biomed. Mater. Res. **1998**, 40, 115.

44) Barner L., Davis T., Stenzel M., Barner-Kowollik C. Macromol. Rapid Commun. **2007**, 28, 539.

45) Chong Y., Tam P., Moad G., Rizzardo E., Thang H. Macromolecules **1999**, 32, 2071.

46) Bratu I. Astilean S., Ionesc C., Indrea E., Huvenne J., Legrand P. Spectrochimica Acta Part A **1998**, 54 (1), 191.

47) Satav S., Karmalkar R., Kulkarni M., Mulpuri N., Sastry N. Macromolecules **2007**, 40 (6), 1824.

48) Cleland W. Biochemistry **1964**, 3, 480.

49) Konigsberg W. Methods Enzymol. **1972**, 25B, 185.

50) Houk J. and Whitesides G. J. Am. Chem. Soc. **1987**, 109, 6825.

51) Wu G., Fang Y-Z, Yang S., Lupton R., Turner D. J. Nutr. **2004,** 134(3), 489.

52) Lee H. and Park T. Polymer journal **1998**, 30(12), 976.

53) Kuppusamy P., Afeworki M., Shankar R., Coffin D., Krishna M., Hahn S. Cancer Res **1998**, 58(7), 1562.

54) Kuppusamy P., Li H., Ilangovan G., Cardounel A., Zweier J., Yamada K. Cancer Res **2002**, 62(1), 307.

55) Carlisle R., Etrych T., Briggs S., Preece J., Ulbrich K., Seymour L. J. Gene Med **2004**, 6(3), 337.

Chapter 8

Conclusions and Recommendations for Further Work

8.1 Introduction

The research work was explored to synthesize graft copolymers from terminally unsaturated macromonomers and water soluble copolymers comprising pendant unsaturation exploiting supramolecular chemistry of CD. Inclusion complexation of addition fragmentation chain transfer agent increases the steric hindrance and hence affects its addition fragmentation mechanism. The complexation helps to yield the macromonomers having functionality close to unity. Inclusion complexation of the multivinyl monomers allows their selective polymerization and yield water soluble polymers containing pendant unsaturation. This work further demonstrates the application of these polymers in the field of sustained / burst delivery of macromolecular drugs and enzyme immobilization.

8.2 Significant findings

Significant findings of the present research work are as follows

1. AMSD forms 1:1 inclusion complex with both β-CD and DMCD (Chapter 3)

2. Computational analysis of IC of AFCT agent confirmed that the allylic group of AMSD is deeply inserted in the cavity in AMSD-β-CD whereas it remains at periphery of cavity in AMSD-DMCD

3. Inclusion complex of AFCT agent controls its reactivity. In AMSD-β-CD allylic group of AMSD is deeply buried in the CD cavity whereas in AMSD-DMCD it remains at the periphery of the cavity and hence CTC are in the order of AMSD-DMCD> AMSD- β-CD (Chapter 4)

4. The steric hindrance due to inclusion complexation helps to obtain macromonomers with functionality close to unity. It can be manipulated by AMSD- β-CD and AMSD-DMCD concentration (Chapter 4)

5. Inclusion complexation allows the use of hydrophobic AMSD to obtain water soluble macromonomers comprising terminal unsaturation (Chapter 5)

6. The functionality (Close to unity) of the water soluble macromonomers can be manipulated by the AFCT agent concentration and temperature (Chapter 5)

7. The macromonomers can be polymerized further with different vinyl monomers to yield water soluble or swellable graft copolymers by RAFT (Chapter 4 and 5)

8. Stiochiometric inclusion complexation of degradable and nondegradable crosslinkers (Chapter 6)

9. A polymerization technique for selective reaction of the crosslinker to obtain degradable and nondegradable water soluble polymers containing pendant unsaturation (Chapter 7)

10. The pendant vinyl groups of polymer can be subsequently cross-linked by intermolecular or intramolecular cross-linking reactions.

11. A process for the synthesis of drug loaded degradable nanogels having size < 60 nm from soluble polymers containing pendant unsaturation by dispersion polymerization (Chapter 7)

12. Nondegradable Poly(MBAM-co-NVP) results in sustained release of macromolecular drugs (Chapter 7)

13. Degradable Poly(DSDMA-co-NVP) results in burst release of macromolecular drugs in the presence of reducing agent. The release can be manipulated by the concentration of the crosslinker and reducing agent (Chapter 7)

14. Glucose oxidase enzyme was entrapped by the two stage crosslinking approach (Chapter 7)

15. The entrapment of the enzyme depends on the parameters like substrate concentration, pH of the buffer, crosslinking density and irradiation time (Chapter 7)

8.3 Recommendation for further work

The results obtained in this work can be further exploited as follows.

1. Synthesis of drug loaded micelles using molecular imprinting approach (MIP) from the graft copolymers prepared through macromonomer approach

2. Extending the concept demonstrated in this work for the synthesis of specific hydrophilic, hydrophobic or amphiphilic graft copolymers for tailored applications

3. The synthesis of hydrogels through inclusion complexation of the crosslinker and detailed evaluation of their application in enzyme immobilization, microlithography and controlled drug delivery

4. Synthesis of biodegradable functional micelles and binding them with the drug

5. Synthesis of gold nanoparticles using two stage inclusion complex approach

List of Publications and Patents

I. Patents

Grant Patent

1. **US 7,560,522**

   Prerana M. Patil and Mohan G. Kulkarni **"**Inclusion complexes of unsaturated monomers, their polymers and process for preparation thereof".

Published Patent Applications

1. **US 20070265365/ WO2006046254**

   Prerana M. Patil and Mohan G. Kulkarni **"**Water-soluble polymers containing vinyl unsaturation, their crosslinking and process for preparation thereof".

2. **US 20090221729/ WO 2007110882**

   Prerana M. Patil and Mohan G. Kulkarni **"**Water-soluble macromonomers having terminal unsaturation and the process for preparation thereof".

II. Communications

(Manuscript Submitted)

1. **Prerana M. Patil** and Mohan G. Kulkarni **(Macromolecular Rapid Communications)**

   "Tailored water-soluble macromonomers via inclusion complex mediated addition fragmentation chain transfer."

2. **Prerana M. Patil**, P. R. Rajamohanan, Mohan G. Kulkarni, Nagraju Mulpuri, G. Narhari Sastry **(Macromolecular Rapid Communications)**

   *"*Addition Fragmentation Chain Transfer by AMSD Inclusion Complex : Implications for Macromonomer Synthesis."

(Manuscript in preparation)

3. **Prerana M. Patil** and Mohan G. Kulkarni

   "Biodegradable nanogels for sustained and targeted release of macromolecular drugs."